INFORMATION TO USERS

This manuscript has been reproduced from the microfilm master. UMI films the text directly from the original or copy submitted. Thus, some thesis and dissertation copies are in typewriter face, while others may be from any type of computer printer.

The quality of this reproduction is dependent upon the quality of the copy submitted. Broken or indistinct print, colored or poor quality illustrations and photographs, print bleedthrough, substandard margins, and improper alignment can adversely affect reproduction.

In the unlikely event that the author did not send UMI a complete manuscript and there are missing pages, these will be noted. Also, if unauthorized copyright material had to be removed, a note will indicate the deletion.

Oversize materials (e.g., maps, drawings, charts) are reproduced by sectioning the original, beginning at the upper left-hand corner and continuing from left to right in equal sections with small overlaps. Each original is also photographed in one exposure and is included in reduced form at the back of the book.

Photographs included in the original manuscript have been reproduced xerographically in this copy. Higher quality 6" x 9" black and white photographic prints are available for any photographs or illustrations appearing in this copy for an additional charge. Contact UMI directly to order.

UMI®

Bell & Howell Information and Learning
300 North Zeeb Road, Ann Arbor, MI 48106-1346 USA
800-521-0600

Removal of Nickel and Lead from Natural Clay Soil through the Introduction of EDTA and Coupling Ion Exchange Processes with Electrokinetic Methodology

By Asif Choudhury

A Thesis
In
The School for Building
Department of Civil Engineering

Presented in Partial Fulfillment of the Requirements
for the
Degree of Master of Applied Science at
Concordia University
Montreal, Quebec, Canada

May 1998

ABSTRACT

Removal of Nickel and Lead from Natural Clayey Soil through the Introduction of EDTA and Coupling Ion Exchange Processes with Electrokinetic Methodology

Asif Choudhury

In clay soils having low initial pH values, electrokinetic transport of heavy metals has proven to be effective. The transport of these metals is predicated on maintaining a low pH throughout the cell, which in turn keeps the metals in the pore water phase, where they are accessible to EK transport. Development of high pH gradients in the cathode region due to the formation of OH^-, from the dissociation of water, produces unfavorable conditions for the transport of heavy metals, namely precipitation. Standard electrokinetic methods have not been employed to a great extent in natural clayey soil. These soils tend to magnify the problems mentioned above and pose several unique problems related to remediation that currently used techniques cannot overcome. Most natural clayey soils have inherently high pH values. The use of EDTA, EK methodology and ion exchange textiles is a new hybrid technique for the enhanced solubilization, transport and localization of Pb and Ni respectively in natural clayey soils. A four-point examination of many of the important system properties related to this hybrid technique, and the effect of the textiles on these properties forms the subject of this thesis. Electrical parameters, system chemistry, enhanced solubilization and transport of EDTA and EK methods only, and the overall localization and removal efficiency of EDTA-EK-Textile experimentation. EDTA–EK methods, without textiles, produced enhanced solubility and transport of lead and nickel. Using all three techniques, solubility was enhanced and the localization and removal achieved was in the range of 90-95 % of lead and nickel ions localized within 10% of the cell. This represents a significant improvement over standard EK methods (which typically have been applied only to low pH soil) and represents a viable remediation technique in natural clayey soil.

"The critical distinction between scientists and engineers is that scientists study that which is, while engineers create that which has never been."

Theodore von Karman

ACKNOWLEDGEMENTS

I would wish to express my sincere gratitude to my supervisor, Dr. Maria Elektorowicz, whose guidance, advice and critical contribution of idea was instrumental to this research effort. Special appreciation is also warranted to the members of the committee for their ideas and constructive criticisms. In addition, I would like to thank Dr. Rosalia Chifrina for her commitment and valued input.

The author would like to also thank L'Institut des Textiles de la France, for their donation of textile samples that were used in this research endeavour. In addition, I would like to thank the Natural Sciences and Engineering Research Council (NSERC) for their financial support.

Finally, I wish to express my deepest appreciation to my parents, my sisters and closest friends for their undying support and encouragement.

TABLE OF CONTENTS

LIST OF TABLES

LIST OF FIGURES

Appendix B Figures:

Appendix D Figures:

NOMENCLATURE

A	=	cross-sectional area [L^2]
C	=	concentration of chemical in solution [mass/volume]
C_{avg}	=	average ion concentration [mass/volume]
c_i	=	solution concentration of the i^{th} contaminant [mass/volume]
C_i	=	concentration of contaminant in 3-D space [mass/volume]
C_{eq}	=	ion concentration at equilibrium [mass/volume]
C_o	=	initial ion concentration [mass/volume]
D	=	diffusion coefficient of the ion at infinite dilution [Length^2/time]
D_h	=	hydrodynamic dispersion/diffusion coefficient [Length^2/time]
D^*	=	effective diffusion coefficient [Length^2/time]
F	=	Faraday's constant [96 487 coulombs/g-equiv.]
$\nabla(-h)$	=	hydraulic gradient
I	=	applied current [Amperes]
i_e	=	potential gradient [Volt/Length]
J	=	flux density [mass/L·Length^2]
J_i	=	flux density of i^{th} contaminant [mass/L·Length^2]
k_e	=	coefficient of EO permeability [Length^2/Volt·time]
k_i	=	coefficient of water transport efficiency [Length^3/Amp·time]
K_h	=	hydraulic conductivity [Length/time]
n	=	porosity
q_e	=	EO flow rate [Length^3/time]
ΣQ_i	=	summation of all contributions - summation of sinks

r	=	resistance [Ohms]
R	=	universal gas constant [8.314 J/mol·K]
R^2	=	correlation factor
t	=	time
T	=	absolute temperature [K]
u^*	=	effective ion mobility
v	=	advection velocity [Length/time]
x	=	distance from a specified origin [Length]
z	=	valence of the ion
θ	=	soil moisture content
ρ	=	soil density [mass/volume]
τ	=	tortuosity factor
Γ_i	=	mass removed from solution by retardation

1. INTRODUCTION

1.1. Scope of the Problem

Metals play an important role in the environment. They are necessary for many biological processes, but are also a major source of environmental contamination. Heavy metal contamination typically originates from: 1) accidental spills, 2) extensive strip mining, 3) fume emission and 4) electroplating operations. They cause toxicity of the soil and readily threaten the country's water supply. Metals are ubiquitous and can easily spread throughout the food chain, where they cause the toxicity of plants and humans.

Present in-situ remediation techniques (e.g. soil washing and chemical precipitation) either cannot be applied to clay or are expensive from a standpoint of capital costs or operational costs. Natural clay soils pose several problems related to remediation that currently used techniques cannot overcome:

1. The high cation exchange capacity (CEC) of natural clay soils promotes the exchange of heavy metals from the liquid phase to the soil, due to their high valence and atomic size.

2. Natural clay soils having inherently high pHs that promote the precipitation of some forms of heavy metals. This results in a tendency for heavy metal contamination to remain sorbed on the solid phase, thereby preventing their dissolution, transport and subsequent removal at desired locations.

3. The low permeability of clay soils results in low flow rates which renders remediation techniques that depend upon hydraulic gradients unfeasible.

Electrokinetic (EK) soil remediation, has proven to be effective on a pilot scale for the remediation of lead-spiked Georgia Kaolinite (Acar and Alshawabkeh, (1996)). The transport of pore water and ionic species between anode and cathode, via

electroosmosis and electrolytic migration respectively is much more efficient than standard hydraulic gradients (Hamed *et al.*, (1991)).

Despite the enhanced transport that existing electrokinetics provide, there are some limitations that this technology presents. Reduction at the cathode produces OH^- ions which readily increases the pH. This creates a precipitation barrier in this region and prevents the transport of heavy metals to desired locations. Therefore, localization and recovery, and subsequent reuse of heavy metals are impossible. In addition, the use of pure clay (i.e. kaolinite), in previously performed tests, presents a simplified case of electrokinetic techniques, since kaolinite has an inherently low pH (5.0-5.5) and low CEC (Acar and Alshawabkeh, (1993)). This low pH facilitates the mobilization of heavy metals from the soil to the pore water. Natural clay soil does not facilitate easy mobilization and therefore may not allow for effective electrokinetic transport. This situation requires a dramatic improvement to existing electrokinetic methodology.

The proposed hybrid method, which consists of an ion-selective textile placed just before the high pH barrier, coupled with electrokinetic phenomena, allows for heavy metals to be transported and localized respectively. The localization of metals allows for their recovery, which results in cost savings. The use of an ion-exchange textile alleviates the problem associated with the development of high pH values in the cathode region and not being able to localize the target metals, as was observed in the previous research pertaining to electrokinetic applications. The use of ion exchange textiles has proven to be effective in the transport, and localization of nickel and lead contamination in natural clay soil (Elektorowicz, (1997)).

1.2. Objective

As a direct result of the problem scope, this thesis attempts to develop a hybrid approach for the remediation of natural clay soil, contaminated with heavy metals, specifically lead and nickel. This hybrid approach attempts to alleviate the problems of classical electrokinetics through the utilization of ion exchange textiles and a chelation agent (Ethylenediaminetetraacetic acid), in combination with electrokinetic transport.

1.3. Scope of the Thesis

Figure 1 summarizes the remediation process that formulates the subject of this thesis. The development of this hybrid method creates an environment that is optimized for transport of heavy metals, since they will be solubilized into the mobile phase. Secondly, through the use of ion exchange textiles (IET), placed strategically within the electrokinetic cell (e.g. in the cathode region, in front of the high pH zone), the heavy metals can be removed before they form precipitates, thereby allowing for localization on the textile, removal and subsequent recovery from the textile. In addition, the behaviour of the process as a whole will be dealt with particularly from the standpoints concerning the behaviour, applicability and overall mobilization effectiveness of EDTA in a clay soil environment. In addition, the behaviour and overall removal efficiency of the ion exchange textiles will be dealt with in order to determine its field applicability for localization and removal of heavy metals. Finally, the behaviour of electrokinetic processes (electrical parameters, transport efficiency) and the effects of the EDTA and IET on the process will be dealt with. In summary, the behaviour of the hybrid process from each sub-process will be experimented in order to gain an understanding of the overall hybrid process and to determine its effectiveness as an in-situ remediation

technique, for the transport, localization, removal and recovery of heavy metals from natural clay soil.

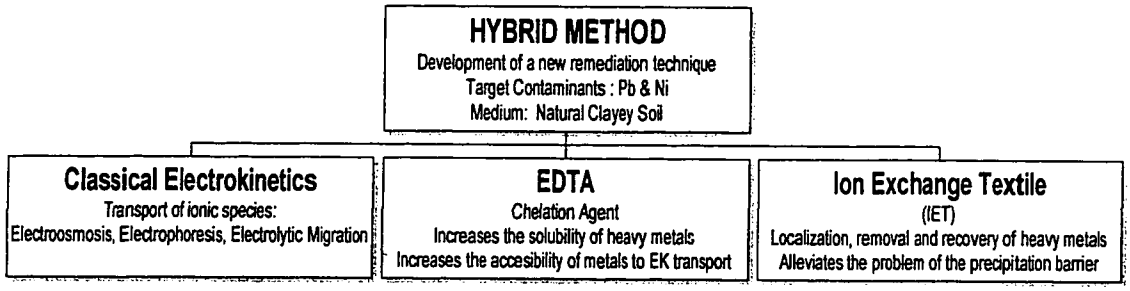

Figure 1 Summary of the hybrid method development: thesis topic

This method represents an innovation to the field of problematic soil remediation. This thesis focuses on a practical approach to this hybrid method. It should represent a significant improvement over standard EK methods (which typically have been applied only to low pH soil). This is done by enhancing mobilization (use of EDTA), transport of ionic species in natural clay soil (use of electrokinetic methods) and enhanced localization and removal (use of ion exchange textiles). The successful development of this hybrid method depends on several factors: 1) Proper recognition of the natural soil environment, 2) knowledge related to the behaviour of metals in soil, 3) ion exchange theory and membrane processes, 4) application and characteristics of EDTA, and 5) electrokinetic phenomena. The overall effectiveness of this methodology will be based on several steps, including the measurement and analysis of: 1) Electrical parameters

(current, potential and resistance), 2) system chemistry and its control (soil pH, soil metal concentration and cathode liquid quality), 3) enhanced mobilization and transport of EDTA by using the EK method only, and the 4) verification of the overall localization and removal efficiency of EDTA-EK-IET system.

2. BEHAVIOUR OF NATURAL CLAY SOIL COMPONENTS

From an environmental engineering standpoint, natural soil presents a medium that is complex in structure, physico-chemical properties and general behaviour. Geo-environmental engineering and the field of soil remediation are particularly concerned with the lithosphere, which consists of the outer mantle and the crust. Through a myriad of erosion processes, the earth's crust is continually undergoing various metamorphic processes, which in turn result in a wide variety of components within this layer. These components are generally subdivided into inorganic matter (rocks and minerals) and varying amounts of organic matter, which can in turn be subdivided into separate categories (Hamblin, (1992)).

Typically, there exists a definite transition for the upper surface of the soil down to the fresh bedrock, known as the *soil profile*. This profile shows a rather consistent sequence of horizons, which small variances with location. The horizons that comprise the soil profile are summarized in Table 1.

Knowledge of the soil horizon forms the initial foundation for the study of soil composition. The efficiency of any remediation effort is predicated on a knowledge of soil composition, since this presents an idea related to the fate (transport, transformation and retardation) of contaminant(s).

2.1. Principal Soil Components

As stated previously, soil consists of a myriad of components that can be subdivided based on their physical structure and their chemical behaviour related to contaminant fate. The subsurface can be subdivided into the solid phase (soil matrix), liquid phase (pore water) and the gaseous phase (i.e. air, VOCs). The solid phase is

composed of a variety of constituents that must be discussed in this chapter. Using this criterion, the constituents of natural soil, excluding pore water and gases, can be subdivided as shown in Figure 2.

Table 1 Typical Soil Horizons (Hamblin, (1992))

Soil Horizon	*General Description*	*Components*
O	• High organic matter content due to varying levels of decomposition	• Several distinct layers; different designations are used
A	• The A horizon as a whole is a topsoil layer that is high in organic matter. • Humified organic matter mixed with mineral soil.	• A_0: thin surface layer of organic matter • A_1: humus rich, dark color • A_2: light, bleached layer, lower organic matter content
E	• Loss of organic matter • Presence of iron and aluminum oxides and clay	• No definite layers are present within this horizon.
B	• Subsoil, contains primarily inorganic substances (fine clays) and colloids from the A horizon • Accumulation of clay, development of distinct structure	• There are no discernible layers. The properties and physical features remain constant throughout this horizon
C	• Zone of partly disintegrated rock and decomposed bedrock • Individual rock fragments are heavily weathered.	• No definite layers are present within this horizon. • Degree of weathering increases with depth.

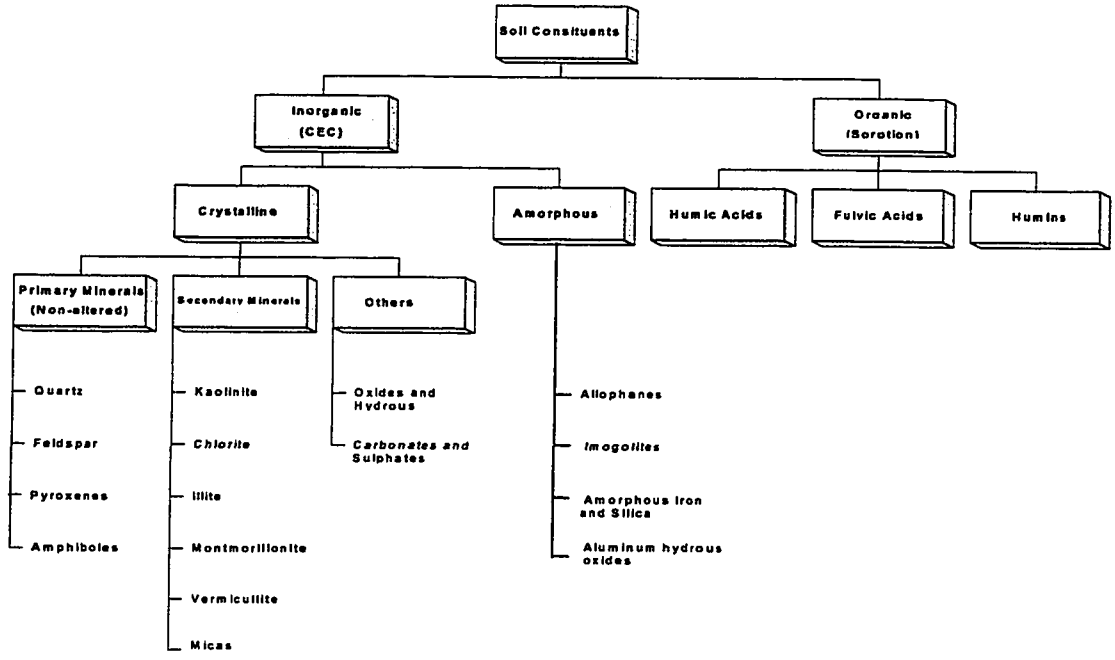

Figure 2 Natural soil constituents and typical examples (Elektorowicz, (1993))

2.1.1. Crystalline Inorganic Components of Soil

Inorganic matter typically constitutes the majority of the soil's composition. The inorganic portion of soil consists largely of aluminosilicates. Typically, feldspar minerals comprise 60 % of an average inorganic rock (Hamblin, (1992)). The inorganic components are subdivided into crystalline and amorphous types. Most clay minerals are weakly crystalline, as a result of their smaller crystal sizes and an increased tendency for ionic substitution.

Inorganic minerals are typically subdivided into primary and secondary groups. Primary minerals are defined as those deRived in unaltered form from a parent rock through physical weathering processes. Typical examples are quartz, feldspar,

amphiboles, and pyroxenes (see Figure 2). These minerals are not significant to geo-environmental engineering, specifically contamination and attenuation processes, due to their low cation exchange capacities, low specific surface areas and high particle sizes. Their importance to geo-environmental engineering and geotechnical engineering lies in their ability to be weathered and chemically transformed into secondary minerals.

Clay minerals are those derived from the previously mentioned primary counterparts. They typically consist of varying structures with silica tetrahedral and alumina octahedral as the basic structural groups (Figure 3). Secondary minerals are characterized by a high specific surface area, a small particle size, and a high surface charge which makes this group significant in influencing contaminant transport and attenuation. The principal layer silicates that comprise this group are kaolinites, chlorites, vermiculites, micas, and montmorillonites (Yong, *et al.*, (1992)). Table 2 summarizes the basic properties of secondary minerals found in natural soils.

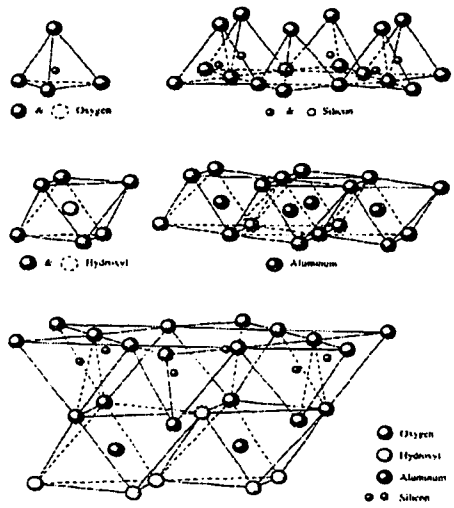

Figure 3 Silica tetrahedral and alumina octahedral (Das, (1994))

Table 2 Structure of Typical Clay Minerals (Yong, *et al.*, (1992))

Secondary Mineral Group	*Minerals*	*Structural Composition*	*Population of Octohedral Sheet*	*Isomorphous Substitution*
Kaolinites	Kaolinite Dickite Halloysite	Silica:Alumina 1:1 (7.2 A thick)	Dioctahedral 2/3 of positions filled with Al	--
Chlorites	Chlorite	Silica:Alumina 2:2 (14.0 A thick)	Dioctahedral, Trioctahedral or Mixed	Al for Si Al for Mg
Micas	Illite Glauconite	Silica:Alumina 2:1 (10 A thick)	Octahedral	Al for Si
Vermiculites	Vermiculite	Silica:Alumina 2:1 (10 A thick)	Dioctahedral	Al for Si
Montmorillonites	Montmorillonite Beldellite Nontronite	Silica:Alumina 2:1 (10 A thick)	Trioctahedral	Al for Si Mg for Al Fe for Al

2.1.1.1. Kaolinites

Kaolinites consist of alternating layers of silica tetrahedral and alumina octahedral, each sharing a layer of oxygen atoms between them. The basic configuration of the kaolinite minerals is shown schematically in Figure 4. Electron microscopy reveals that a silica-alumina layer is three oxygen atoms thick (including the shared oxygen atoms). The layers are bound by strong hydrogen bonds between hydroxyls from the alumina sheet on one face, and oxygen from the silica sheet on the opposite face of each

layer. This allows kaolinite minerals to maintain a relatively strong and stable structure and therefore prevent hydration between subsequent layers. The exception to this is regarding halloysite which can occur in a hydrated from, with a layer of water between each layer of the kaolinite structure. Kaolinite crystals generally range between 70-100 layers thick (Yong, *et al.*, (1992)).

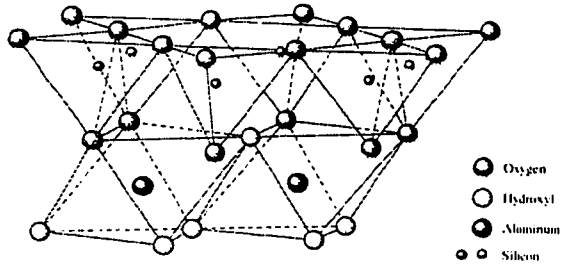

Figure 4 Schematic diagram of a typical kaolinite structure (Das, (1994))

Due to its tight structure, there is relatively little isomorphous substitution in the crystal lattice of kaolinite. The specific surface area of kaolinite is in the range of 10-20 m^2/g and its cation exchange capacity (CEC) is 5-15 cmol/kg, which is attributable to the edges of the particles and the pH dependence of the particle charge. Kaolinite has a point of zero charge (the pH at which the particle surface charge is negligible) of 4.5, and as a result charge reversal is common (Elektorowicz, (1996)). The various views of the kaolinite structure are shown in Figure 5.

It should be noted that Figure 5 shows that the clay crystal lattice is continuous in both directions, but the edges show that broken bonds exist between oxygen and silicon and between oxygen and aluminum. This results in broken bond charges and subsequent

hydrogen ions at the surface. These hydrogen ions can be readily exchanged with other cations (i.e., heavy metal contaminants) with higher valences and larger atomic diameters.

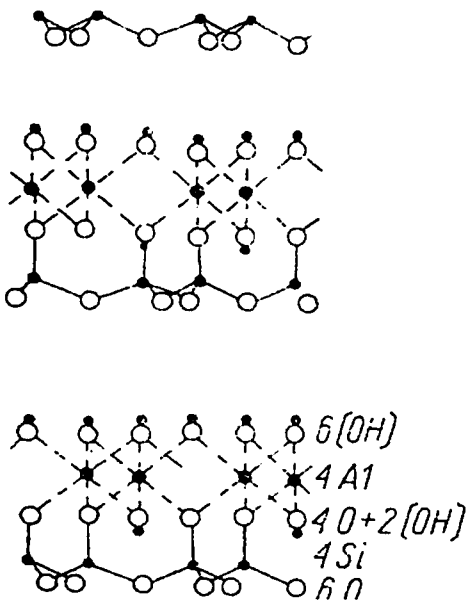

Figure 5 Kaolinite structure: 2-D views

2.1.1.2. Chlorites

Like kaolinite, chlorite minerals are composed of alternating silica and alumina sheets. The principal structural difference is that the sheets are formed in a 2:2 ratio of silica and alumina, as shown in Figure 6 (Elektorowicz, (1993)). Extensive substitution of other cations for silicon and aluminum occurs within chlorite minerals. Typically, the silica sheet is subjected to the substitution of trivalent aluminum for tetravalent silicon, resulting a net negative charge. This charge is counterbalanced by the substitution of

trivalent aluminum for divalent magnesium. The CEC of chlorite is 10-40 cmol/kg with a specific surface area of 70-150 m^2/g (Yong, *et al.*, (1992)).

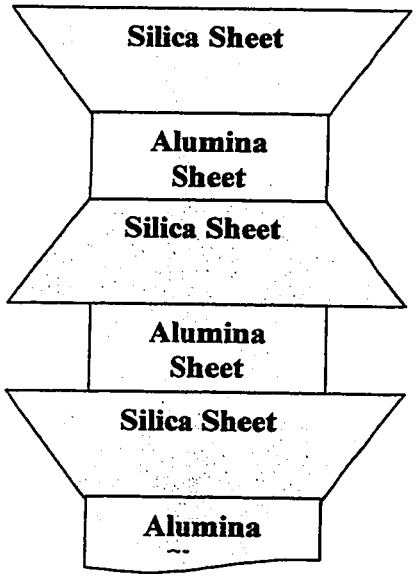

Figure 6 Schematic drawing of chlorite structure

2.1.1.3. Illites

Illites consist of repeated layers of alumina sheets between two silica sheets (2:1, silica to alumina), with oxygen atoms shared. As shown in Figure 7, each layer is bonded by potassium ions which fit exactly into the hexagonal gaps provided by the silica sheets. As a result of the presence of these potassium ions, a positive charge results, which is dissipated by the substitution of aluminum for silicon.

The structure and physical properties of illite are favorable to the retardation of chemicals, particularly heavy metals. Illite is characterized by a small particle diameter, less substitution of aluminum for silicon, and more sites for exchangeable cations than kaolinite and chlorite. The CEC and specific surface area for illite are 25 cmol/kg and 80 m^2/g respectively (Yong, *et al.*, (1992))

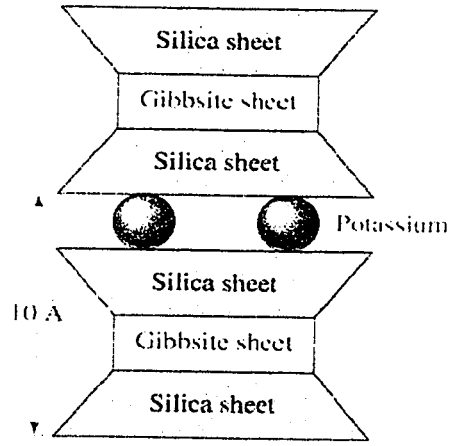

Figure 7 Structure of illite (Das, (1994))

2.1.1.4. Montmorillonites

Montmorillonite (smectite) consists of the same silica-alumina layers and in the same ratio as illite. However, the following structural and behavioral differences exist:

1. Isomorphous substitution occurs mainly in the alumina sheet.
2. There is an absence of potassium ions to bond the repeated layers of silica and alumina. As a result, hydration occurs readily. Figure 8 shows the structure of montmorillonite.

3. Montmorillonites have a higher activity and liquid limit than illites (Das, (1994)).

As a result of the ability of montmorillonite clays being able to incorporate several layers of water, its swelling potential is high. Typically, the water separating the layers is 0.9 nm thick. The specific surface area ranges from 600-800 m^2/g with a CEC of 80-120 cmol/kg. As a result of its high CEC, specific surface area and swelling potential, montmorillonite is highly effective for the retardation of inorganic chemicals (i.e. heavy metals). In addition, it is a constituent in landfill liner design for the retardation of leachate. It is used only in small amounts due to a high swelling potential.

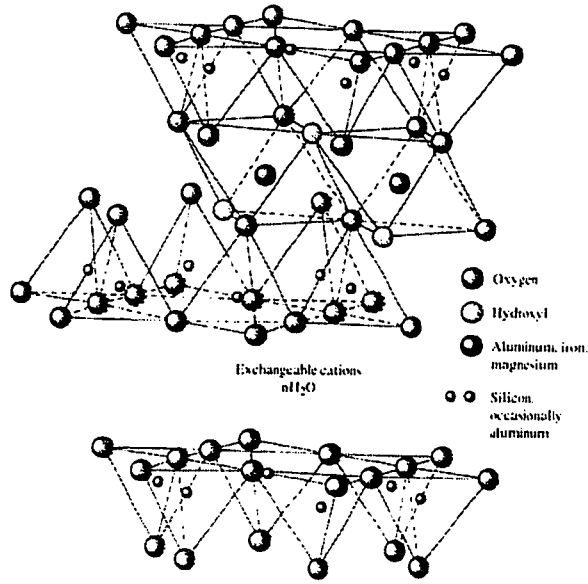

Figure 8 Schematic representation of montmorillonite (Das, (1994))

2.1.1.5. A Comparison of Clay Minerals in Natural Soils

In order to discuss clay minerals adequately, a comparison of properties provides an accurate and relative scale of properties. Table 3 displays a summary of the

environmentally pertinent properties of the secondary minerals discussed in the previous sections. Natural clay soil consists of a mixture of the clay minerals shown in Table 3.

Table 3 Comparison of Properties Related to Clay Minerals (Elektorowicz, (1993))

Mineral	*CEC [cmol/kg]*	*Specific Surface Area [m^2/g]*	*Swelling Potential*	*Plasticity*
Kaolinite	5-15	10-20	Very Low	Very Low
Chlorite	10-40	70-150	Low	Low
Illite	25	80	Moderate	Moderate
Montmorillonite	80-120	600-800	Very High	Very High
Vermiculite	120-150	600-800	Moderate	High

2.1.2. Non-Primary and Non-Secondary Crystalline Inorganics

Broken bonds at the surface characterize non-primary and non-secondary crystalline inorganics. They contain negligible cation exchange capacities and commonly encompass the following groups:

1. Oxides and Hydrous Oxides
2. Carbonates and Sulphates

The following sections deal with a discussion of these aforementioned groups.

2.1.2.1. Oxides and Hydrous Oxides

The oxides and hydrous oxides include hydroxides and oxyhydroxides of iron, aluminum, manganese, titanium and silicon. They are generally derived from the weathering of tropical soils. Typical examples of oxides and hydrous oxides are as follows (Yong *et al.*, (1992)) : 1) Haematite, 2) Goethite, 3) Gibbsite, 4) Anatase and 5) Boehmite. Typically, the surfaces of the aforementioned oxides and hydrous oxides consist of broken bonds, which are satisfied by hydroxyl groups originating from the dissociation of water. It should be noted that the surface charges of these soil materials

are pH dependent and typically have a point of zero charge of 4.0-5.0. The presence of primary minerals with these compounds can dramatically alter the properties of the soil and its sorption tendencies.

2.1.2.2. Carbonates and Sulphates

Carbonates and sulphates are characterized by high water solubilities (relative to the secondary minerals and amorphous oxides), low CECs and low specific surface areas. They include compounds containing carbonate, sulphate and bicarbonate in combination with one or more metallic ions (typically Ca, Mg, and Na). Calcite ($CaCO_3$), magnesite ($MgCO_3$), dolomite ($CaMg(CO_3)_2$), and nahcolite ($NaHCO_3$) are common examples of carbonate minerals. Gypsum ($CaSO_4 \cdot 2H_2O$) is the most abundant of the sulphate minerals found in soil (Yong, *et al.*, (1992)).

2.1.3. Amorphous Inorganics

Amorphous inorganics do not possess a definite structure and generally encompass allophanes, imoglites, amorphous silica, amorphous iron and aluminum hydrous oxides. Allophanes consist of random arrangements of silica tetrahedral and metallic cations (calcium, magnesium, potassium, titanium and sodium). They possess high specific surface areas (300-700 m^2/g) and high CECs (150 cmol//kg), which are comparable to montmorillonite and vermiculite (Yong, *et al.*, (1992)). However, secondary minerals are in much greater abundance than amorphous inorganics and therefore have a larger influence on contaminant fate and environmental engineering.

2.1.4. Organic Soil Components

Organic matter is typically found in wide a variety of soils. It comprises 0.5-5.0% (by weight) of most mineral surface soils, with the exception of peat, which can attain

100% organic matter. Despite this low proportion, organic soil matter plays a significant role in contaminant fate and in any remediation effort due to its ability to adsorb organic compounds, thereby causing immobilization. Organic matter originates from the transformation and decay of vegetation and animal remains. As a result, the classification of organic matter can be based on the degree of degradation as discussed above. In addition, another classification is based on humic and non-humic organic material, specifically, their solubility in acid (Yong, *et al.*, (1992)). Classifications of organic material based on the degree of degradation and on acid solubility are shown in Figure 9 and Figure 10 respectively.

Humic acids are essentially polymers with molecular weights ranging from 100-100000. These high molecular weights combined with high specific surface areas and high CECs allow the molecules to develop van der Waals forces with other soil constituents and/or chemical contaminants. In addition they have high interactive and complexation tendencies. They contain basic carbon and hydrogen constituents, along with oxygen, nitrogen and small amounts of sulphur. The degree of aromaticity, as tested by nuclear magnetic resonance (NMR) methods ranges from 35-92%. The principal functional groups that comprise humic acids are alcoholic OH groups, carboxyls, phenolic OH groups, quinones and ketonic groups (Yong, *et al.*, (1992)). The chemical composition and functional groups are displayed in Table 4 and Table 5 respectively, located at the end of this section in order to provide a means of comparing the composition functional groups (and their proportions) of each organic material type. Fulvic acids are distinguished from humic acids based on their solubility in both acidic and basic solutions. They generally have molecular weights in the range of 1000-2000.

They contain appreciably more sulphur and oxygen than humic acids, but less carbon hydrogen and nitrogen (see Table 4). The major functional groups significant to this group are: carboxyls, phenolic OH, alcoholic OH, carbonyl, quinones and ketones. Humins are generally composed mainly of carbon with small amounts of nitrogen.

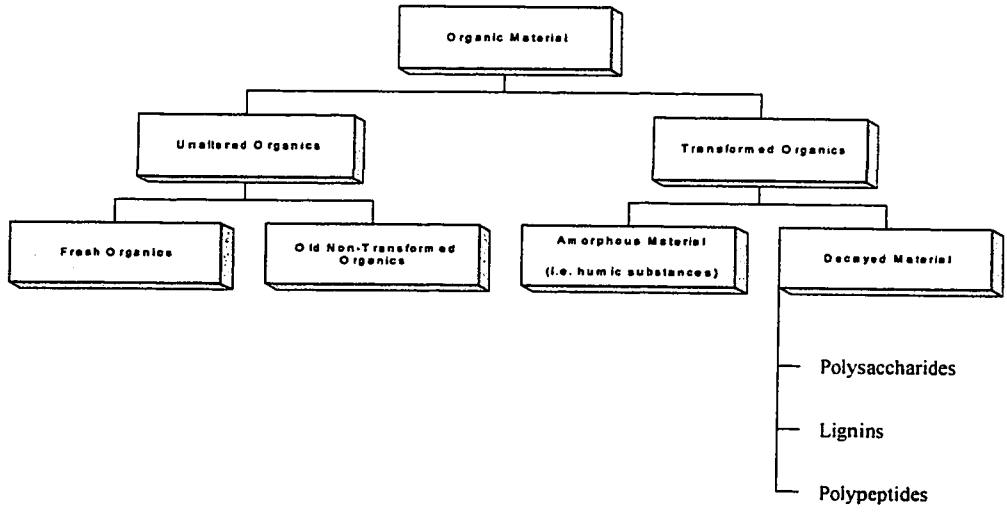

Figure 9 Classification of organic matter according to the degree of degradation

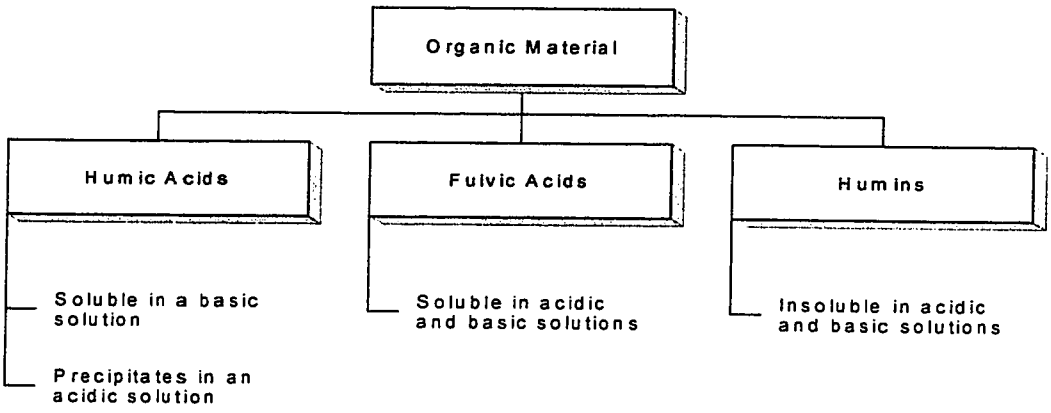

Figure 10 Classification of organic matter by acid solubility (Yong, *et al.*, (1992)).

Table 4 Chemical Composition of Humic and Fulvic Acids (Yong, *et al.*, (1992))

Element	*Humic Acids*	*Fulvic Acids*
Carbon	50-60%	40-50%
Oxygen	30-40%	40-50%
Hydrogen	3-6%	4-7%
Nitrogen	0.5-6%	1-3%
Sulphur	0-2%	1-4%

Table 5 Functional Groups in Humic and Fulvic Acids (Yong, *et al.*, (1992))

Element	*Humic Acids*	*Fulvic Acids*
Carboxyl	3-10%	1.5-6%
Phenolic OH	2-5%	2-6%
Alcoholic OH	0-2%	2.5-4%
Quinones	1-2%	2-2.5%
Carbonyls	0.5-4	0.3-5%
Ketones	1-4%	1.5-2%

2.2. Influence of Soil Properties on Contaminant Fate and Remediation Alternatives

Soil constituents and the properties that accompany them have a significant influence on the fate of contaminants in the subsurface and on any remediation effort. Secondary minerals and organic material present in soil have the largest influence on contaminant fate and to a lesser extent, remediation engineering due to their ability to exchange cationic contaminants (i.e. heavy metals) and adsorb organic substances

respectively. As a result, emphasis will be placed on these two groups of soil components.

2.2.1. Secondary Minerals

Typically, secondary minerals comprise 90-95% of most soils and their inherent properties can influence contaminant fate. A contaminant present in the subsurface is transported to other locations in the soil, by pore water potential, advection, dispersion and diffusion. In clay soils, molecular diffusion is the typical transport mechanism due to the low permeability of clay. While the contaminant is transported through the media, retardation occurs which aids in removing these contaminants from the liquid phase and onto the solid phase, thereby ceasing their mobility. Mathematically, the entire transportation-retardation (fate) regime of chemicals in porous media is expressed by the following general equation (Elektorowicz, (1993)):

$$\frac{\partial C}{\partial t} = \frac{\partial D_h}{\partial x}\frac{\partial C}{\partial x} - \frac{v\partial C}{\partial x} - \frac{\rho \partial S}{\theta \partial t} + \Sigma Q_i \qquad [2.1]$$

Where:

C	=	concentration of chemical in solution (mass/volume)
t	=	time
x	=	distance from a specified origin
D_h	=	hydrodynamic dispersion/diffusion coefficient
v	=	advection velocity (length/time)
θ	=	soil moisture content
ρ	=	soil density (mass/volume)
ΣQ_i	=	summation of all contributions - summation of sinks

As stated above, the second to last term in the general fate model represents any process acting to retard the transport of chemicals. Due to the high CEC values of secondary minerals, particularly montmorillonite and vermiculite, they can readily

exchange cations with those in solution. This forms a natural mechanism for the removal of metal contamination (i.e. lead, mercury, cadmium and nickel) from the mobile (liquid) phase, onto the soil, thereby preventing any further contamination deeper into the subsurface. Regarding the general transport equation, the CEC of these secondary minerals contributes significantly to the retardation term, particularly in the case of high CEC soils, such as montmorillonite and vermiculite.

Theoretically, secondary mineral exchange cations according to a specified hierarchy which is based on the following properties of the cations in question:

1. Ionic charge (valence)
2. Atomic size
3. Concentration of cations in solution
4. pH of the soil
5. Type and shape of the cations in solution

Typically, as the valence of the ion and the atomic size increases, its ability to exchange increases (with some exceptions). Frequently, the shape of the cation in solution can dictate whether any cations exchange with the soil. For example, potassium has an atomic shape that fits exactly into the gaps of silica sheets. Based on the factors mentioned above, following exchange hierarchy results (LaGrega, *et al.*, (1994)):

$$Li^+ < Na^+ < H^+ < K^+ < NH_4^+ << Mg^{2+} < Ca^{2+} < Ni^{2+} < Pb^{2+} << Al^{3+}$$

It should be noted that this hierarchy is superseded by the concentration of cations in solution. If the concentration of cations in solution is significantly higher than that bound to the soil, exchange will occur regardless of ionic size, shape and valence. This is the basis for the regeneration of ion exchange resins. The order listed above forms the basis for retardation mechanisms in secondary minerals. Kaolinite, montmorillonite,

vermiculite and illite all follow this hierarchy of exchange with varying capacities, as reflected by their respective CECs.

The retardation of cationic substances, particularly metals, by secondary minerals is of particular importance to remediation engineering. In any remediation process, accessibility of metals to transport enhancement methods (i.e. electrokinetics) is paramount. Cation exchange with the soil can result in the removal of these metallic species from the liquid phase and render many remediation techniques ineffective.

2.2.2. Organic Matter

The presence of organic matter in the subsurface, event in small amounts (1-2%) can drastically influence the fate of contaminants in the environment. There exist numerous interactions between the organomineral matrix and organic contamination. Humic substances have shown to have a considerable impact on adsorption phenomena in soils. Cation exchange is also prevalent with organic material as reflected by the high CEC values for humus (180-200 meq/100 g) (Yong, *et al.*, (1992)). In addition, the formation of organomineral complexes in soil is pH dependent and is essential in stabilizing soil organic matter, even the complex structure of humic compounds. As a result of these sorption processes, the presence of organic material can cause extensive retardation of inorganic and organic contaminants and prevent further migration deeper into the subsurface.

Regarding remediation processes, sorptive interactions can also influence the availability of contaminants to the mobile, pore water phase. Electrokinetic processes are dependent on the fact that ionic species (i.e. heavy metals) remain in the liquid phase, so that they can be transported via electrolytic migration, electroosmosis and electrophoresis.

If the sorptive capacity of the soil is high, as with many clay soils, standard electrokinetic processes will be ineffective.

Humic substances are effective at absorbing low molecular-weight organic compounds in their macromolecular matrix. As a result of this phenomenon, these soils have a significant buffering capacity to toxic influences (i.e. by phenols or pesticides). Several studies have shown that organic substances, such as phenols can be adsorbed or even linked into the humic matrix by either abiotic reactions with trivalent iron, tetravalent manganese or through the activity of microbes. It should be noted that although not as significant as organic material present in the soil matrix, the fate of sorbed residues such as organic soil contaminants should also include dissolved organic matter in the liquid phase, as a carrier during leachate and run-off.

2.3. Summary

From the standpoint of geo-environmental engineering, soil and the processes that occur in the subsurface are complex and diverse. The constituents of the soil matrix dictate which processes will be prevalent. These processes can be classified into physical, chemical and biological subdivisions. The soil components that influence contaminant fate and remediation engineering are organic material and secondary minerals.

The presence of organic material coupled with secondary minerals has significant effects on contaminant fate and electrokinetic processes. Organic material in proportions of 1-2% (by weight) can cause the adsorption of organic contaminants, thereby preventing the migration of these contaminants into the groundwater. In addition, humic material also has an inherently high CEC, which can also remove inorganic contamination.

Sorptive interactions can also influence the location of metals in soil by connecting them to solid surfaces.

Secondary minerals play a significant role in the removal of inorganic components from the mobile liquid phase onto the solid soil phase. The CEC of each mineral type dictates the tendency of these soils to exchange cations. Montmorillonite and vermiculite have the highest CEC and specific surface area of the secondary minerals, and are therefore the most effective at removing cationic substances. The high specific surface area allows for the maximization of exchange sites. Due to these properties, montmorillonite has had extensive used in liners for landfill design.

3. METALLIC COMPOUNDS IN THE ENVIRONMENT

Metallic ions are transported via a variety of mechanisms. During this tortuous path, myriads of transformations occur that can have drastic ramifications on both surface and subsurface environments. The behaviour of metals depends on a variety of characteristics related to the metal itself and its spatial location. However, from a broad standpoint these characteristics can be classified into two groups, namely 1) Metal Type (light or heavy) and 2) Environment (surface water or porous subsurface media).

This chapter deals with the properties and behavior of light and heavy metals in an aquatic environment and in the subsurface environment (soil and groundwater). Special emphasis will be placed on factors that have impacts on environmental contamination and toxicity. The metallic ions which have posed problematic contamination conditions, and those metals whose recovery are economically feasible will be dealt with. Therefore, this chapter comprises a description of the following metals on the following metallic ions: 1) Nickel (Ni^{2+}), 2) Lead (Pb^{2+}), 3) Zinc (Zn^{2+}), 4) Cadmium (Cd^{2+}), 5) Chromium (as Cr^{+3} and $Cr_2O_7^{-2}$), and 6) Copper (Cu^{2+}).

The environmentally pertinent properties strictly related to the transportation and transformation of species will be considered in this thesis. Particular focus will be placed on lead and nickel, as these heavy metals comprise the target contaminants for this thesis, and due to their contrasting behaviour in the environment.

3.1. Properties and Behaviour of Metals in Aqueous Media

Metals in an aqueous environment may undergo complexation, precipitation, dissolution, and changes in their oxidation states. They can react with the inorganic and

organic types of ligands in the water phase and/or at the surface of the solid phase (i.e. sediments). This phenomenon can dictate the mobility of a particular metal ion in aqueous media and hence its potential for contamination. Heavy metals have the ability to accumulate in living organisms and can therefore cause toxicity within the food chain. Microorganisms utilize trace concentrations of metals during their metabolic processes. In an electrolytic solution, ions of opposite charge are bound together by electrostatic forces within the critical distance, forming ion pairs. These forces decrease in proportion to $1/r^2$, (where r is the interionic distance). When this ion pair is formed, the metal ion or the ligand retains coordination water, so that one or more water molecules separate the cation and anion. Estimates of stability constants (a reflection of a metallic ion to form and remain in a complexed form) can be made based on the coulombic interactions between the ions in an aqueous solution.

The hydration of cations is directly related to the behaviour of metals in aqueous media. The greater the ionic hydration, the higher the tendency for that metal to remain in solution, and be more mobile. The hydration of an ion in solution has a complex internal structure and its outer boundary is difficult to establish. An ion in solution is typically modeled as being surrounded by two zones. An inner layer is equated to what is termed as the *primary hydration shell*, which consists of dense electrorestricted and immobilized water molecules strongly bound by the coulombic field of the ion. The *secondary hydration shell*, is a region of comparative randomness, of disrupted water organization and of broken structure (Kotz and Purcell, (1987)). Beyond the secondary layer lies normal water molecules within the aqueous media.

Generally speaking, cations (metals) are more hydrated than the anions of the same negative charge. In general, the degree of hydration is dependent on the following properties of the ion(s) in question: 1) Charge on the ion (as atomic charge increases, the higher the degree of hydration, and 2) Atomic radius (the smaller the atomic radius, the heavier the hydration).

These characteristics must be considered when attempting to describe the behaviour of metals in an aqueous environment. In addition, it provides a part of the necessary background theory for the design of any remediation technique and the improvement of various techniques for the removal of metals.

One of the most important properties of heavy metals is related to their complexation tendencies. Complexation of metals, specifically lead and nickel, refers to the formation of aquametallic, typically organometallic substances due to the combination of the metal ion (central ion) itself and the anion, known as a ligand. Complexes may have ramifications on the mobility of metals in aqueous media. The anion can be humic substances or acidic ions present in the aqueous media. Lead and nickel complexation is typically preceded by a dehydration step, where hydration water is exchanged with the ligand. Based on the exchange rate of hydration water and comparing the coordination number of covalent compounds with other ligands than water, it is obvious that the complex formation represents ligand exchange of an equivalent number of water molecules from the hydration shell. Complexation can be classified into two groups, depending on the rate at which cations exchange ligands. These groups are 1) Labile complexes and 2) Inert complexes (Merian, (1991)).

3.1.1. Labile Complexes

Labile complexes are those ions that exchange ligands almost instantaneously. Typically, these complexes are formed through a combination of the cation and an inorganic ligand. In aquatic systems, hard acids (i.e. metal ions), are present as ionic pairs. At low concentrations, the soft and boundary cations such as sodium, potassium, calcium, and magnesium can form labile, mononuclear complexes with OH^-, CO_3^{2-}, HCO_3^-, SO_4^{2-}, Cl^- anions in aqueous media. In addition, metals such as lead, zinc, copper, cadmium and nickel can form labile complexes. Nickel and lead form labile complexes with hydroxide ions shows many forms of chloride complexes. The metals, their typical ligands and the final complex formed are summarized in Table 6.

Table 6 Complexation of Various Pertinent Metals in Aqueous Media (Merian, (1991))

Metal	*Author*	*Ligand*	*Complex Formed*
Lead (Pb^{+2})	Sipos et al. (1980)	OH^- Cl^-	$Pb(OH)^+$ $PbCl^+$
Cadmium (Cd^{+2})	Branica, (1977)	Cl^- CO_3^{2-}	$CdCl^+$ $CdCl_3^-$ $CdCO_3$ (precipitate) $Cd(CO_3)_2^{2-}$
Nickel (Ni^{+2})	Bilinski, (1983)	OH^- Cl^- CO_3^{2-}	$Ni(OH)^+$ $NiCl^+$ $NiCl_3^-$ $NiCO_3$ (precipitate) $Ni(CO_3)_2^{2-}$
Copper (Cu^{+2})	Bilinski, (1983)	CO_3^{2-}	$CuCO_3$ (precipitate) $Cu(CO_3)_2^{2-}$

3.1.2. Inert Complexes

Contrary to labile processes, in inert complexes, the hydration water is exchanged slowly with the added ligand. Inert complexes of metals are typically formed with organic ligands. Chen et al., (1995) showed that heavy metals such as cadmium, lead and zinc have been known to readily combine with organic ligands (acids) such as nitrilotriacetic acid (NTA) and ethylenediaminetetraacetic acid (EDTA). In addition, hydrochloric acid (HCl) and acetic acid (HAc) have been documented as ligands for the formation of complexes with the aforementioned metals.

Knowledge of complexation tendencies can define the mobility of the metallic compound. This is paramount to the characterization of contaminant fate, the design of remediation techniques for contaminant removal, the formation of improvement techniques that eliminate problems, and to the determination of process efficiency.

3.2. Properties and Behaviour of Metals in the Subsurface

The properties and behaviour of metals in the subsurface is more difficult to characterize than in aqueous media due to the fact that the subsurface is a multi-phased zone where complex physical and chemical processes can take place. In addition, within each phase there exists ambiguous sub-zones where diverse processes take place. As a result, many types of metal species exist and they can therefore be present in the subsurface in the following manner:

1. As part of soil parent material or soil minerals of secondary origin;
2. As precipitates with other compounds of the soil;
3. In the sorbed phase, on exchange sites with clay minerals, inorganic non-crystalline forms, and organic matter can serve as exchangers;

4. Dissolved in the pore solution, in aquametallic, ionic/dissociated or complexed forms (with organic or inorganic ligands);

5. Embodied in microorganisms, plants or animals.

The fate of metals in the subsurface, which includes their physical transport, chemical transformation and retardation is of particular importance to the understanding of contamination effects and any eventual remediation technique that is to be employed. It is generally understood that the degree of mobility and activity of metals is influenced by pH, temperature, redox potential, cation exchange capacity of the solid phase, competition with other metal ions, ligation potential (the tendency for a ligand to undergo complexation with a metallic ion), complex metal and soil composition, and concentration in the soil solution. Since the subsurface is heterogeneous and anisotropic, the metal content is subject to spatial variability (Merian, (1991)). It should be noted that most complexation characteristics (tendencies and stability), observed in aquatic medium, can readily be applied to the subsurface.

3.2.1. Redox Potential of Soil

The redox potential is an important property of a soil in relation of environmental engineering remediation techniques. For instance, the effectiveness of any electrokinetic remediation process is dependent on the redox potential of the soil. The water and oxygen content of the soil influence the redox status and the value can vary with short distances.

The status of most metal ions is affected by redox conditions, particularly for Fe, Mn, Cr, Cu, As, Hg, Se, Ni and Pb. The redox potential directly effects the oxidation of

state of metals, which therefore influences their mobility/retardation. For instance, under certain redox conditions, divalent Pb and Ni can be oxidized to the insoluble forms where it will form a hydroxide precipitate, thereby ceasing its ability to migrate though the subsurface. Indirectly, the chemical form of a metal can be changed through an alteration in the oxidation state of a ligand atom such as C, N, O, and S.

3.2.2. Sorption of Metals

Sorption is defined as the retardation of a substance that typically occurs between phases (i.e. at a solid surface). This retardation can be at the surface (adsorption), through the surface (absorption) or through chemical bonding based on the valence of the substance in question (ion exchange). The amount of metal adsorbed to the soil is dependent on the properties of the metal in question and the particular physico-chemical properties of the soil. Table 7 displays the properties of the soil and the metal ion that influences sorption:

Table 7 Pertinent Properties that Affect Sorption (Elektorowicz, (1993))

Properties of the Soil	***Properties of the Metal Ion***
Soil type (Clay = low adsorption, high ion-exchange) (Organic soil = high adsorption)	**Concentration** (directly proportional)
Specific surface area (directly proportional)	**Ionic Charge and size** (directly proportional)
Organic matter content (directly proportional)	**Water solubility** (inversely proportional)
	Polarity (directly proportional)

From these properties, the decreasing sequence of ion exchange can be expressed in the following manner:

$$Cu^{2+} > Pb^{+2} > Zn^{2+} > Co^{+2} > Ni^{2+} > Mn^{2+}$$

In general, the capacity of soils for sorption of most metal ions increases with increasing pH, but the natural mobility of the cations is decreased. For example, the mobility of $PbOH^{+}$ increases with increasing pH. This phenomenon has serious ramifications on any remediation technique. In essence, varying the pH is a compromise between natural mobility and soil sorption. Increasing pore water metal concentration by decreasing the pH decreases the mobility of the cations. As a result, another process (electrokinetics) must be introduced to enhance the mobility in soil for the purposes of decontamination and localization. Relative mobility and its dependence on pH are shown in Table 8.

Table 8 Influence of pH on Relative Mobility of Metal Cations in the Subsurface (Merian, (1991))

pH Range	***Very Mobile***	***Moderately Mobile***	***Slowly Mobile***
4.2 - 6.6	Cd, Hg, Ni, Zn	As, Be, Cr	Cu, Pb, Se
6.7 - 8.8	As, Cr	Be, Cd, Hg, Zn	Cu, Pb, Ni

It should be noted that mobility tests were performed individually for each metal (no multiple contamination). As a result competitive adsorption/mobility was not taken into account. This is of particular importance with Pb^{2+} where lower adsorption was observed in the presence of Ca^{+2} than with a pure Pb^{+2} solution. In addition, Cu^{2+} and Zn^{2+} display a synergistic behaviour.

3.2.3. Diffusion Tendencies of Metals

The diffusion of metals from one phase to another or within a phase is an important fate process that is of particular significance in soil. Cations bound to the surface of minerals can diffuse into the interior of the solid phase. The relative diffusion rates depend on the following characteristics: 1) Ionic diameter of the metal ion 2) pH conditions. As the ionic diameter increases, the rate of diffusion into the interior of the solid phase decreases (i.e. Cd^{2+}(0.97 nm) < Zn^{2+}(0.74 nm) < Ni^{2+}(0.69 nm)). In the interior of the soil, these cations can neutralize the negative charge of the soil and remain fixed in that location for indefinite periods of time (irreversible adsorption). With increasing pH, the affinity of the oxide surface is increased up to the point where the formation of hydrocomplexes inhibits the access to the soil surface.

3.2.4. Complexation of Metals in the Subsurface

As in aqueous media, complexation of metals occurs in the subsurface. Frequently, the metal ions are coordinated to organic substances, mainly humic and fulvic acids forming oligodentate complexes and chelates. Complex formation arises when water ligands are replaced by other molecules. The ramifications of complex and chelate formation are as follows:

1. Metal ions are prevented from being precipitated
2. Complexing agents can act as carriers for metals in the liquid phase
3. The toxicity of the free aqueous form is often reduced by complexation. Mercury complexes are the exception to this rule (Merian, ((1991)).

It should be noted that metal ions and ligands are acids and bases respectively and their reactions to form metal complexes are acid-base reactions. As a result of these reactions, a variety of metal speciation occurs, which is invariably dependent on their complexation tendencies. Table 9 displays principal species of metals in soil.

Table 9 Speciation of Metals in Acidic and Alkaline Soils (Kotz and Purcell, (1987))

Soil Type	*Iron* *Fe (II)*	*Nickel* *Ni (II)*	*Copper* *Cu (II)*	*Zinc* *Zn (II)*	*Cadmium* *Cd (II)*	*Lead* *Pb (II)*
Acidic	Fe^{2+} $FeSO_4^0$ $FeH_2PO_4^+$	Ni^{+2} $NiSO_4^0$ $NiHCO_3^+$ Org.	Org. Cu^{2+}	Zn^{2+} $ZnSO_4^0$ $ZnB(OH)_4^+$	Cd^{2+} $CdSO_4^0$ $CdCl^+$	Pb^{2+} Org. $PbSO_4^0$ $PbHCO_3^+$
Alkaline	$FeCO_3^0$ Fe^{2+} $FeHCO_3^+$ $FeSO_4^0$	$NiCO_3^0$ $NiHCO_3^+$ Ni^{2+} $NiB(OH)_4^+$	$CuCO_3^0$ Org. $CuB(OH)_4^+$	$ZnHCO_3^+$ $ZnCO_3^0$ Zn^{2+} $ZnSO_4^0$ $ZnB(OH)_4^+$	Cd^{2+} $CdCl^+$ $CdSO_4^0$ $CdHCO_3^+$	$PbCO_3^0$ $PbHCO_3^+$ $Pb(CO_3)_2^{2-}$ $PbOH^+$

Org. = Organometallic forms

3.3. Summary of the Properties of Metals and Their Compounds in the Environment

A summary related to the properties of various metals pertinent to environmental engineering is necessary in order to determine their expected behaviour in aqueous and soil media. The knowledge of their behaviour is paramount to the design and improvement of any remediation technique. This section deals with a summary and comparison of the properties of the metals found pertinent to the thesis objectives. Table 10 encompasses these properties.

3.3.1. Nickel in the Environment

Nickel is a silver-white, hard but malleable metal that maintains a high luster and is relatively resistant to corrosion. It has atomic mass of 58.71, a boiling point of 2732°C and a melting point of 1453°C. Chemically, nickel has multiple oxidation states which results in multiple forms of this element. The oxidation states of nickel include -1, 0, +1, +2, +3, and +4 with the most commonly occurring valences being 0 (elemental state) and +2. Typically, complexation with peptides can occur thereby reducing the redox potential of the Ni^{+2}/Ni^{+3} couple from 4.2 V to 0.7-1.0 V and allowing for the formation of Ni^{+3} complexes to from under certain biological conditions. These valence shifts may be responsible for nickel-induced free-radical reactions and lipid peroxidation.

Nickel, particularly when in its +2 oxidation is present in aqueous media in a variety of water-soluble forms. These include nickel compounds of acetate, bromide, chloride, flouride, iodide, nitrate, sulfamate and sulfate salts. Their high solubility increases their mobility in the water thereby spreading contamination quickly. Nickel exists in aqueous solutions primarily as the green hexaquonickel ion, $Ni(H_2O)_6^{+2}$ which is poorly absorbed by most living organisms (Merian, (1991)).

There exist organic, lipid-soluble nickel compounds that can be potentially toxic. Nickel carbonyl ($Ni(CO)_4^{2+}$) is the most important compound in this group. At ambient temperatures, nickel carbonyl is a volatile and colorless liquid that originates from the Mond process for nickel refining and from chemical and petroleum industries. Insoluble nickel compounds are also in great abundance in the aquatic environment. Nickel oxides, nickel hydroxides, nickel sulfides, nickel arsenide, nickel chromate, nickel carbonate,

nickel phosphate, nickel selenide and nickel titanate are compounds that fall into this category.

Table 10 Environmentally Pertinent Properties of Metals (Kotz and Purcell, (1987)), (Rump and Krist, (1988))

Property	*Copper Cu(II)*	*Cadmium Cd(II)*	*Chromium Cr(III)*	*Lead Pb(II)*	*Nickel Ni(II)*	*Zinc Zn(II)*
Sources	Mining	Mining of Zinc Ore Smelting	Mining Electroplating	Mining Smelting Recycling Disposal	Mining Refining Electroplating	Mining Electroplating
Solubility (K_{sp} in parentheses)	CuS (8.7×10^{-36}) $CuCO_3$ (2.5×10^{-10}) $CuBr_2$ (5.3×10^{-9}) $CuCl_2$ (1.9×10^{-7})	CdS (3.6×10^{-29}) $Cd(OH)_2$ (1.2×10^{-14}) $CdCO_3$ (2.5×10^{-14})	$Cr(OH)_3$ (6.7×10^{-31}) $CrPO_4$ (2.4×10^{-23}) $CrAsO_4$ (7.8×10^{-21})	$PbCO_3$ (1.5×10^{-13}) $PbSO_4$ (1.8×10^{-8}) PbF_2 (3.7×10^{-8}) $PbCl_2$ (1.7×10^{-5})	$Ni(CN)_2$ (3.0×10^{-23}) NiS (α) (3.0×10^{-21}) $Ni(OH)_2$ (2.8×10^{-16}) $NiCO_3$ (6.6×10^{-9})	ZnS (1.1×10^{-21}) $Zn(OH)_2$ (4.5×10^{-17}) $Zn(CN)_2$ (8.0×10^{-12}) $ZnCO_3$ (1.5×10^{-11})
pH Effects on Mobility	pH<4.2 (mobile) pH>4.2 (slowly mobile to immobile	pH<6.6 (mobile) pH=6.7-8.8 (fairly mobile) pH>8.8 (immobile)	pH<6.6 (fairly mobile) pH=6.7-8.8 (mobile) pH>8.8 (immobile)	pH<4.2 (mobile) pH>4.2 (slowly mobile to immobile)	pH<6.5 (mobile) pH>6.5 (immobile)	pH<6.6 (mobile) pH=6.7-8.8 (fairly mobile) pH>8.8 (immobile)
Distribution in Aqueous Media	0.08 µg/L to 0.8mg/L	0.5 µg/L **	0.3 µg/L	0.1-10 µg/L	15-20 µg/L	0.003 - 0.6 µg/L
Distribution in Soil	20-30 mg/L	N/A	10-90 mg/kg	10-40 mg/kg	50-100 mg/kg	10-300 mg/kg
Reduction Potential (E^o)	0.337 V	-0.403 V	-0.910 V	-0.126 V	-0.250 V	-0.763 V
Analytical Methods & Extraction	Digestion for soil samples	Digestion for soil samples	Digestion for soil samples	Digestion for soil samples	Digestion for soil samples	Digestion for soil samples
	SFE	SFE	SFE	SFE	SFE	SFE
Measurement	AAS (graphite furnace)	AAS (graphite furnace)	AAS	AAS	AAS	AAS
	Mass Spec.	Mass Spec.	Photometry with methylene blue	X-ray fluorescence		X-ray fluorescence
		Atomic Emission Spectra	Iodometric titration			

Table 11 shows the concentration of nickel, lead and other heavy metals found in typical waste. The retention of nickel is primarily due the presence of organic matter, precipitation (with hydroxide ions) and due to the tendency of nickel for hydrolysis. As with all metals, the solubility of nickel compounds is dependent increases with decreasing pH. Harter, (1983) demonstrated that nickel adsorption in soil primarily follows a Langmuir (L-type) isotherm and is not as strongly nor as quickly adsorbed by a given soil as is lead. At pH values of 8.0 and above, the isotherm behaves as an H-type (high affinity) isotherm. Figure 11 shows adsorption isotherms of nickel versus pH and soil type.

Table 11 Heavy Metal Concentration in Typical Wastes (Legret and Raimbault, (1991))

Type of Waste	*Pb*	*Ni*	*Cu*	*Cd*	*Cr*	*Zn*	*Hg*
Unaltered Sites (mg/kg·mS)	127	24	354	5	23	527	3.5
Spiked Waste Sites (mg/kg·mS)	6 721	1 360	7 200	210	523	14 920	36.7
Interstitial Water (mg/L)	14.9	2.7	21.5	2.2	0.9	262	N/A
Metal Stockpiles (mg)	43 350	8 770	46 440	1 350	3 370	96 230	237
Waste (mg/kg·mS)	273	55.3	293	8.5	21.3	607	1.5

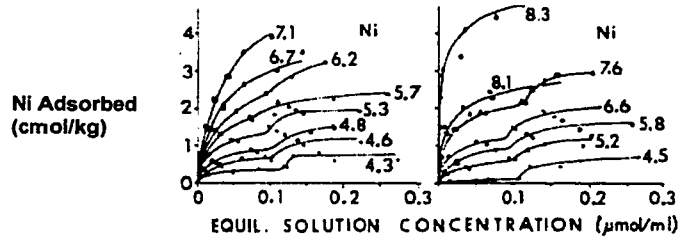

Figure 11 Adsorption isotherms for nickel in Delkalb A and B horizons of soil (Harter, (1983))

At pH values below 6, it can be seen that nickel tends to remain in solution, as dictated by the relatively high equilibrium solution concentration. As the pH increases to neutral and alkaline levels, the solution concentration of nickel adsorbed to the soil three-fold. For remediation purposes, these isotherms indicate that in order to recover nickel from soil for decontamination, nickel ions must be made mobile by decreasing the pH, thereby increasing the concentration of nickel in the mobile/liquid phase.

The degree to which nickel is hydrolyzed also dictates the fate of nickel compounds in the subsurface. It can also have a direct affect on any remediation technique. Once again, the speciation of nickel, as reflected by its degree to undergo hydrolysis, and its variation with pH is shown in Table 12. At all pH values from 4.0 to 8.0, nickel speciation is 99-100% in the form of Ni^{2+}, it would be expected that any nickel compounds that are adsorbed to the soil would be in the form of Ni^{2+}. Nevertheless, the speciation of nickel (99-100% as Ni^{2+}) is an indication of the high mobility of nickel in

the subsurface, 1.5-2.5 times that of lead. This phenomenon shows the potential for nickel recovery in problematic clay soil via solubility enhancement and electrokinetic methods.

Table 12 Percent Speciation of Nickel with pH (Harter, (1983))

Species	*pH=4*	*PH=5*	*pH=6*	*pH=7*	*pH=8*
Ni^{2+}	100	100	100	100	99
$NiOH^{+}$					1

3.3.2. Lead in the Environment

Lead has an atomic number of 82, an atomic mass of 207.19 g/mol. It is a bluish-white, soft metal with a density of 11.34 g/cm^3, a melting point of 327.5°C and a boiling point of 1740°C. In most inorganic compounds, lead has an oxidation state of +2. The salts of Pb(II), lead oxides and lead sulfide are not readily soluble in water, with the exception of lead acetate, lead chlorate and to a lesser degree, lead chloride. Inorganic Pb(IV) compounds are unstable and strong oxidizing agents. The behaviour of lead differs greatly from that of nickel and therefore represents an interesting research approach. The behaviour of lead, as with most metals, is primarily dependent on the environmental medium in which it is located. Although trace concentrations of lead are found in the atmosphere, this section will focus on the behaviour and properties of lead in subsurface (soil and groundwater) and surface water environments.

Table 11 shows the concentration of lead ions within typical waste. Due to the low water solubility of lead compounds, lead is easily adsorbed to all clay soils. Harter, (1983) showed the adsorption tendencies of lead for A and B horizons of Dekalb soils with adjusted pH values. The equilibrium isotherms for lead at specified pH values for theses soil types are shown in Figure 12. These soil types had CEC values in the range of 10.7-18.8 cmol/kg, with an organic matter content of 0.91 to 4.3 % for horizon A and horizon B respectively.

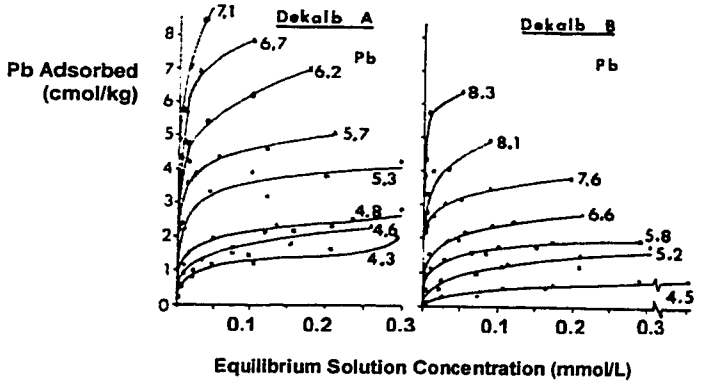

Figure 12 Lead adsorption vs. equilibrium solution concentration at various pH values (Harter, (1983))

Figure 12 clearly shows the adsorption tendencies of lead ions and the variance with pH. At low pH values (<5.0), the concentration of lead adsorbed to Dekalb A and Dekalb B soil is approximately 25% of that absorbed at pH values of 6.2 to 7.1. At all pH values, lead obeys an H-type isotherm (high affinity), with strong adsorption and with a very low equilibrium solution concentration. It is clearly shown that the adsorption of

lead ions strongly depend on pH, with higher pH values promoting the adsorption of lead onto soil surfaces.

Besides pH, other factors influence the adsorption/location of lead in the subsurface. The organic matter content of the soil is a major factor contributing to the retention of lead, particularly for pH-dependent adsorption (Hartman, 1983). Lead tends to form organo-metallic complexes that obey the Irving-Williams series for stabilities of metal-organic complexes. While Irving-Williams studied soluble metal-organic complexes a similar relationship is expected for soil organic matter, provided retention is via complexation rather than metal-organic precipitation. In addition, retention of lead by both insoluble humic and soluble fulvic acid has been reported (Yong, *et al.,* (1992), Harter, (1983)).

The degree to which metals are hydrolyzed is a major factor determining the amount of lead retained at any given pH. If it assumed that hydrolysis characteristics are unaffected by soil colloids, the speciation of lead in solution can be predicted. These values are shown in Table 13. Table 13 reflects the speciation that one might expect at various pH values, and can allow for predicting the speciation of retained lead. In addition, lead also partitions itself between different soil components depending on the CEC and structure. This is typically observed in natural clay soils.

At pH=8.0, 33% in the form of Pb^{2+}, 66% of lead solution species will be in the form of $Pb(OH)^{+}$, and 1% in the form of $Pb(OH)_2^0$. Since, only 1% of $Pb(OH)_2^0$ exists at this pH, retention to the soil in this form might be questioned. At lower pH values, one would not expect to see lead in the form of $Pb(OH)_2^0$ in solution or in soil. Even at

pH=6, the low percentage of $Pb(OH)^+$ would indicate that that the presence of lead in this form in the soil would be questionable.

Table 13 Effect of pH on Probable Solution Speciation of Lead

Species	*pH=4*	*pH=5*	*pH=6*	*PH=7*	*pH=8*
Pb^{2+}	100	100	98	83	33
$Pb(OH)^+$	-	-	2	17	66
$Pb(OH)_2^0$	-	-	-	-	1

Precipitation at high pH is another retention mechanism that causes the removal of lead from the mobile liquid phase. The solubility of potential lead precipitates as a function of pH is shown in Figure 13. Loss of Pb from solution above pH 6.0 can be attributed to precipitation of a separate solid phase. The presence of carbonates, hydroxides and sulphates in soil can promote the precipitation of lead; an already immobile metal. Any remediation technique, particularly those involving mobilization and systems that are pH sensitive, must take this phenomenon into consideration.

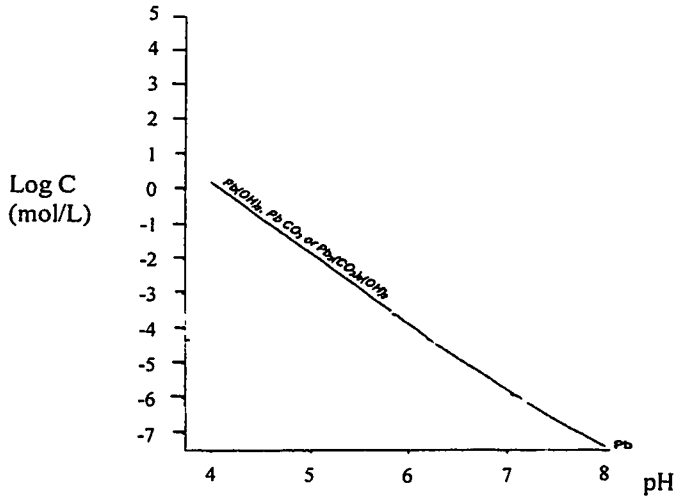

Figure 13 Solubility of lead precipitates versus pH (Harter, (1983))

Lead and its compounds typically enter the environment and originate from mining, smelting, recycling, gasoline stations or disposal processes. Global emissions were about 500000 t/d around 1919, about 2 million t/d around 1940, and about 4.5 million t/d around 1970. Estimates of the dispersal of lead emissions into the environment indicate that the atmosphere is the major initial recipient. However, due to the low water solubility, lead is prevalent in soil (Merian, (1991)).

Mobile and stationary sources of lead emissions tend to be concentrated in areas of high population density, and near smelters. From these emission sources, lead moves through the atmosphere to various components of the environment. It is deposited on soil, surface waters, and plants and thus is incorporated into the food chain of animals and man. Atmospheric lead is also an important component of street dust. Furthermore, lead is inhaled directly from the atmosphere, by humans and animals (Merian, (1991)).

Merian, (1991) stated that the major part of lead found in the atmosphere results from the combustion of leaded gasoline. Organolead emissions may result from the production of trimethyllead (TML) and triethyllead (TEL) and from evaporation and automotive emissions of unburned TML or TEL. Several reports indicate that automobile traffic contributes about 90 % of the total atmospheric lead emissions. In the USA, the annual lead emission from gasoline combustion was estimated to be 34 881 tonnes in 1984 (Merian, (1991)). This corresponds to 89.4% of the total lead emissions in the USA. Other mobile sources, including aviation use of leaded gasoline and diesel and jet fuel combustion contributes insignificantly to lead emissions into the atmosphere.

Organolead compounds, in particular TML and TEL, which are used as additives

in gasoline, are prevalent in urban areas at levels ranging from 5 to 200 $\mu g/m^3$. Since evaporation and automotive emissions of unburned TML or TEL are the main emission sources, the highest concentrations are found in parking garages, gasoline stations, and busy streets in central urban areas. The major part of atmospheric organolead is in the vapor phase. Usually, organolead makes up to 5-10 % of the concentration of particulate lead in urban areas (Merian, (1991)).

Mining, smelting, and refining as well as the manufacturing of lead-containing compounds and goods may also give rise to substantial lead emissions. Particularly smelters of lead ores are well known to create significant pollution problems in local areas. Their effect on the surrounding air and soil depends primarily on the height of the stack, the emission control devices, the topography and other local features. In general, there is a zone of heavy soil pollution around the smelters, which are caused by high levels of lead fall-out resulting from dust emissions from the smelters.

The zone of high lead fall-out and soil pollution usually is extended to 5-10 km from the smelter, depending on prevailing wind conditions, air temperature and climate. The zone of high air lead levels is restricted to a smaller area. In the USA, the annual lead emissions from primary lead smelters were estimated to be 1150 tons in 1984 (Merian, (1991)). Secondary smelters producing lead from scrap are comparatively small but numerous and frequently situated close to human settlements. Several studies showed that pollution in the surroundings of such smelters resulted in an increased lead intake of people living nearby. Further stationary sources of lead emissions are coal-fired power plants, incinerators of solid waste, sewage sludge or waste oil, and the manufacturing of

lead glass, storage batteries, and lead additives for gasoline. The lead emission from coal fired power plants located in the member states of the European Community has been estimated to be in the order of 200 tons per year. In the USA, the lead emission from coal and oil combustion has been estimated at 380 tons per year (Merian, (1991)).

The major fraction of lead in municipal wastewater results from lead-containing dust fall-out, which reaches the drainage system with rain water. Studies show that the concentration of lead, which can be present in the water in dissolved or particulate form, varies greatly. It is dependent on traffic density, industrial emissions and climatic factors. The values are of the magnitiude of 10 to 100 mg/L, and in some areas, several thousand mg/L (Merian, (1991)). In the industrialized Rhine river, about 0.1 mg dissolved Pb per liter and about 50 mg solid Pb per kg suspended particulate matter or sediment have been found.

On a local level, special problems may arise with regard to waste and slag dumps from lead mines and primary lead smelters. These waste materials may contain high lead levels which are detrimental to agricultural and recreational areas. According to Merian (1991), municipal waste contains about 0.3 mg lead per kg. In incineration, lead is typically found in slag. From landfills, lead may be leached out at higher pH values. Windblown dust in fly ashes from these deposits may also significantly contaminate the surroundings including human settlements located there.

From a mass balance point of view, the transport and distribution of lead from stationary and mobile sources into other environmental media is mainly through the atmosphere. Large discharges may also occur directly into natural waters and onto the land, but in such cases lead tends to be localized near the points of discharge because of

the low solubility of the lead compounds that are formed upon contact with soil and water.

Depending on the particle size, airborne suspended particles may have a long residence time in the atmosphere. Studies from remote areas indicate that lead-containing particles are transported over substantial distances, up to thousands of kilometers, by general weather systems. Increased lead levels have been observed in polar ice and glaciers, resulting from long-range transport of lead containing airborne particles. Fergusson, (1990) demonstrated that lead compounds (and some other metal compounds) are enriched in mosses, in podzolic soils, in ombrotropic peat, and in other environmental targets in southernmost Norway from deposition of long-range transported atmospheric pollution (from the European continent).

Lead may be removed from the atmosphere either by dry or wet deposition. In rural areas of Europe and North America the annual deposition rates are typically in the range of 20-80 $\mu g/m^2/day$. This contributes to the contamination of soil , groundwater and surface water bodies. In Greenland and the Antarctic, values below 1 $\mu g/m^2/day$ have been recorded. In large cities the deposition rates are about 1.5-10 times higher than in rural areas. Typical values presently found in German and British cities range from 50-300 $\mu g/m^2/day$. Near busy highways, significantly higher levels have been found. The highest recorded levels of lead deposition occur near primary lead smelters.

According to Merian, (1991), between 15 and 50 mg Pb^{2+}/L rain in Germany, and a wet deposition of about 30 mg $Pb^{2+}/m^2/day$ in rural regions, 50 mg $Pb^{2+}/m^2/day$ in urban areas, and 100-150 mg $Pb^{2+}/m^2/day$ in regions with a metallurgical industry. All values varied with time and had a general decreasing tendency. Regarding deposition on

forests, lead compounds are not concentrated in canopies as other metal compounds, interception is important, lead compounds are introduced by stem-flow, but mobility in litter is very low.

Lead in normal soil ranges from 10-40 mg/kg dry weight. Most values are below 20 mg/kg. In general, soils tend to reflect the composition of their parent materials. Due to deposition, and the lack of mobility of lead, the top layers of soil usually contain higher lead levels than deeper layers. Significantly increased lead concentrations in surface soils have been found particularly in inner city areas, near busy highways and near industries utilizing lead. In Montreal, deeper deposits of lead originate from backfill soil mixed with fly ashes. Concentrations as high as 2000 mg/kg have been reported at contaminated sites in Montreal and the surrounding areas. The lead content of lake and river waters usually is in the range of 0.1-10 μg/L. It is always necessary to distinguish between lead of the dissolved and suspended nature. The lead levels in ground and spring waters may vary over a wide range depending on the particular geochemical conditions. The average lead concentration in surface water depends on emissions and is about 0.01-0.03 mg/L (Merian, (1991)) in deep ocean water it ranges from about 0.001 to 0.004 mg/L. Atmospheric lead levels in remote continental areas fall in the range of 0.1-10 mg/m^3. Marine atmospheres generally contain less lead than continental air. The lowest atmospheric lead concentration measured was 0.046 $\mu g/m^3$ found in the west winds of the North Atlantic. Since the combustion of leaded gasoline represents the major source of atmospheric lead, urban areas have significantly higher air lead concentrations than rural areas. In the 1960s and 1970s the annual mean air lead levels in towns and cities in the USA, Canada, and Europe were found to be in the range of 0.4-4.0 $\mu g/m^3$. In central ur-

ban areas with high traffic density, air lead levels of up to 10 $\mu g/m^3$ were recorded. The reduction of lead in fuel in the mid-1970s and the increasing use of lead-free gasoline led to a substantial decline of atmospheric lead concentrations in urban areas during the last years. The air lead levels presently found in European and North-American cities are in the range of 0.2-0.8 $\mu g/m^3$. In rural areas the air lead levels usually are in the range of 0.05-0.3 $\mu g/m^3$. Due to atmospheric transport of airborne lead, which may range over hundreds and thousands of kilometers, even remote areas show increased air lead concentrations when compared to "baseline" air lead levels.

4. A COMPARISON OF CURRENT SOIL REMEDIATION TECHNIQUES

There exist numerous techniques for the remediation of soil in the environment. In general, these techniques can be classified according to the role that they perform. These roles are as follows:

1. **Extraction:** The removal of the contaminant from the soil-water matrix.
2. **Immobilization:** The removal of the contaminant from the liquid phase of the subsurface.
3. **Degradation:** The biological transformation of an organic contaminant to a less objectionable form.
4. **Attenuation:** Irreversible removal and transformation of contaminants. The process functions as a sink.
5. **Physical separation:** the segregation of species based on differences in physical properties.

A detailed description encompassing all the available soil remediation techniques is beyond the scope of this review. However, in order to compare all of the techniques, a table with judiciously selected criteria is to be formed. Table 14 and Table 15 provides a comparison of the current in-situ and ex-situ soil remediation techniques respectively, their applicability, effectiveness and general advantages and disadvantages. It should be noted that this table solely provides a general comparison of soil remediation techniques. The choice of techniques depends on proper site assessment of the area in question. In addition, the relative effectiveness of each technique is also dependent on site characterization and the chemicals that are present at the site location.

Table 14 Comparison of In-Situ Soil Remediation Techniques

Process or Techniques	*Role*	*Treatable Contaminant Types*	*Effectiveness*	*Modification Requirements*	*Modifiers, Reagents*	*Cost*	*Advantages*	*Disadvantages*
Soil Flushing (Laboratory)	E	Soluble organics and inorganics	variable (dependent on what type of liquid is used and contaminant type)	pH and Temperature	Water, acids, bases and surfactants		• allows for extraction of contaminant from soil • relatively low cost • wide range of applicability	• field applicability is limited • cannot be applied to clay soil • determination of which chemicals can be used for which contaminant is difficult
Soil Mining	E	Soluble organics and inorganics	variable (dependent on what type of liquid is used and contaminant type)	pH and Temperature	Water, acids, bases and surfactants		• allows for extraction of contaminant from soil • wide range of applicability	• field applicability is limited • determination of which chemicals can be used for which contaminant is difficult
Sorption of	I	Heavy metals						

Heavy Metals							
1. Using organics (lab)			effective (desorption can occur and degradation of organics can also occur)	pH	products from agriculture and humic substances	• effective and low cost • applies to a wide variety of heavy metals	• desorption can occur • field applicability is limited • pH sensitive
2. Using activated carbon (lab)			effective (desorption can occur)	pH	activated carbon and lime (for pH control)	• applicable to a wide variety of heavy metals	• limited field applicability • pH sensitive
3. Chelation (lab)			high (depending on choice of ligand)	pH	tetren, lime	• applicable to a wide range of heavy metals • high degree of effectiveness	• limited field applicability • must control pH • unfeasible in clay soil
Ion Exchange	I						
1. With clays (lab)		Organic and inorganic cationic compounds	low to high depending on solubility of various metals and	none	bentonite, vermiculite	• natural process • low cost	• no field tests have been performed • flow rate is low in soil (removal

			CEC of clays					time is long)
Precipitation (lab)	I, A	Heavy metals (Pb, Ni, Cu, Cd, Hg, Zn)	variable	pH (particularly in kaolinite soils where natural pH is acidic)	CaS_2 or NaS_2		• applicable to a wide range of heavy metals • effective because the solubility of most heavy metal compounds are low	• only causes immobilization , not removal from soil • must control pH • difficult to uniformly distribute additives in clay soil
Vitrification (field)	I, De	Organics and inorganics	very high	soil moisture	None	very high	• highly effective • no chance of reversibility	• cannot reuse soil for any purpose • extremely high cost
Solidification	I	Organics and inorganics	very high	none	solidification agents, cement, lime	very high	• highly effective • no chance of reversibility	• cannot reuse soil for any purpose • extremely high cost
Chemical Reduction	D, A	Some heavy metals (Cr, Se, Pb)	high	pH, soil moisture	reducing, oxidizing and liming agents		• highly effective • moderate	• limited applicability

							cost	
Electrokinetics (lab and field)	E	inorganics, organics	high	pH	modifying liquids, mobility enhancers (EDTA, NTA, HNO_3)	Mod erate	• high removal efficiencies for a wide variety of chemicals • allows for extraction of contaminant • is effective in clay soil	• high pH at cathode decreases electroosmotic flow and subsequent removal • low solubility of metals makes it difficult to induce electroosmotic flow

N.B. A = Attenuation, D = Degradation, De = Destruction, E = Extraction, I = Immobilization

Table 15 Comparison of Ex-Situ Soil Remediation Techniques

Process or Techniques	*Role*	*Treatable Contaminant Types*	*Efficiency*	*Modification Requirements*	*Modifiers, Reagents*	*Cost*	*Advantages*	*Disadvantages*
Soil Washing **With acid/base (field)**	E	soluble organics, cyanides, heavy metals	low to medium	pH (must be low to in solution phase)	acids (EDTA, NTA, HNO_3) bases	High	• relatively simple to perform	• acidifies the soil • hydraulic flow is low especially in soils of low permeability
Steam Stripping (lab)	E	volatile organics and inorganics (NH_3, H_2S)	low to medium	none	none	Very High	• vastly improving technique	• difficult to obtain uniform distribution of steam into the soil • no field studies
Gravity Separation (field)	PS	substances with a lower density than the flushing liquid substances which are non-miscible with the flushing liquid	low to medium	none	water or other flushing liquid	High	• cost of chemicals are relatively low	• limited applicability • the flushing liquid most suitable for the contaminants present must be chosen (requires extensive research)

Sedimentation (field)	PS	heavy metals, miscible organics	low to medium	none	water	High	• effective if particle settling times are short • good range of applicability	• not efficient for colloidal material
Sieving	PS					Mode rate		
1. Dry (field)		organics and inorganics with different particle sizes than that of the soil	medium	none	none		• moderate effectiveness • low cost relative to other ex-situ techniques	• limited applicability
2. Wet (field)		organics and inorganics with different particle sizes than that of the soil	medium	none	water		• moderate effectiveness • low cost relative to other ex-situ techniques	• limited applicability
Magnetic Separation (lab)	PS	heavy metals with magnetic properties	medium	none	water	High	• good metal removal efficiencies	• extremely high power costs • cannot separate specific metals for recovery (must remove all metals and then use a separation technique)

								• limited applicability
Thermal Desorption (lab) **direct or indirect heat transfer**	PS	volatile organics, cyanides, sublimable metals	low to medium	temp., soil moisture	hot air or combustion gases	Very High	• where effective, can separate species with temperature controlled thermal desorption	• limited applicability • high costs for combustion gases
Incineration (field)	De	organics, cyanides, metals	medium	temp., soil moisture	combustion gases	Ver High	• effective in the destruction of contaminants • reduces contaminant volume for easy storage	• produces toxic bottom ash and fly ash • produces a concentrated contaminant • destroys the soil
Chemical Oxidation (lab and field)	D	inorganics and organics	medium	pH	oxidizing agents (H_2O_2, O_3, UV light)	High	• wide range of applicability	• non-extracting technique • non-uniform distribution of oxidizing agent
Reduction (lab and field)	D	heavy metals	medium	pH	SO_2^-, SO_3^{2-}, Fe^{2+}, Al^{3+}	High	• wide range of applicability	• non-extracting technique • non-uniform introduction of

								reducing agent
Electrolysis	D	organics, heavy metals	low	none	Electrolyte	Mode rate	• wide range of applicability	• non-extracting technique • non-uniform distribution of reducing agent • low effectiveness

N.B. A = Attenuation, D = Degradation, De = Destruction, E = Extraction, I = Immobilization, PS = Physical Separation

Based on the comparison of available soil remediation techniques presented in the previous chapter, there exists a lack of effective techniques for the decontamination of heavy metals from soil. Generally, there are distinct disadvantages to all of these techniques. These can be summarized as follows:

1. Most soil remediation techniques are non-extracting. With the exception of soil washing and steam stripping (which are expensive) these processes only transform, retard, attenuate or degrade metal contamination. As a result, metal extraction for recovery and recycling is impossible. In addition, some of these processes are reversible which can result in remobilization of contaminants.

2. The effectiveness of these techniques is lacking. Table 14 and Table 15 clearly show that the methods used to remediate soil are still in their infancy. As a result, they are generally costly and/or ineffective.

3. The techniques that are highly effective do not allow for the reuse of the soil. Techniques such as incineration and vitrification are highly effective in decontamination of heavy metals from soil. However, they do not allow for recovery of metals and the reuse of the soil for other purposes.

4. Ex-situ techniques have proven to be expensive. The cost of excavating soil from the site constitutes over 50% of the total remediation costs.

5. These techniques do not allow for localization and subsequent removal. Due to the nature of the soil and the technique applied, the majority of these methods do not allow for localization (thereby minimizing the volume of contaminated soil) and removal.

6. The effectiveness of the aforementioned techniques is drastically reduced or rendered inapplicable for natural clay soil. Natural clay soil presents a medium that makes remediation extremely difficult. Due to its low hydraulic conductivity, high specific surface area, high cation exchange capacity, the above mentioned methods are rendered ineffective or will take years for decontamination to occur below specified limits. This is particularly true for any process relying on transport and if the target contaminants are heavy metals.

Based on an extensive literature review, it has become apparent that the removal of heavy metals using electrokinetics is a promising technique. Lead and copper removal efficiencies of 75-85 % have been documented in laboratory scale tests using kaolinite (inherently low pH) soil. In addition, the use of conditioning liquids and acids injected at the cathode and/or anode have increased the mobilization of metals thereby enhancing electrolytic migration and eventual removal. Electrokinetics has therefore shown promise for the removal and recovery of heavy metals from soil.

Despite the potential effectiveness of electrokinetics for the removal of heavy metals from soil, there are many problems and limitations inherent to this technique and the research accompanying it. These problems are summarized below:

1. The development of high pHs at and near the cathode region. This results in the precipitation of heavy metals in this area, thereby preventing their removal at the cathode. In addition, a precipitation wall develops and prevents electrolytic migration.

2. Limited research diversity. An extensive literature review has revealed that most of the research related to electrokinetics has been performed on kaolinite soil. This type of soil presents the simplest problem for heavy metal removal since kaolinite has a natural pH of 4.5-5.0. This low pH is favorable to the dissolution and mobilization of metals. In Quebec, bentonite, vermicullite and illite soils are abundant and have pHs in the range of 10.5-11.5. This high pH is not favourable to the dissolution of metals. As a result, electrokinetics on these soil types will be more difficult. Research must focus on the use of natural soil rather than strictly kaolinite soil.

3. Electrolytic migration of cations in clay soil is slow. This is due to the low permeability of the soil and the low water solubilities of the heavy metal contaminants (they will tend to be sorbed strongly onto the soil rather than remain in the pore water where they can be transported electrokinetically). Therefore, the mobility of these metal ions must be improved in order to increase the efficiency of the process and reduce decontamination time.

In order to ensure efficient removal of heavy metals from soil using electrokinetics, these problems must be rectified or a combination of techniques must be used. It is proposed that electrokinetics should be coupled with ion-exchange textiles for the removal of heavy metals. These textiles have proven to be very effective in the removal of metals from wastewater. In addition, careful placement of these textile will ensure the removal of metals and alleviate the problem of excessive precipitation in the cathode area. It is certain that this removal is more difficult in soil, however, with the use of electrokinetics, electrolytic migration can be generated using an applied direct current. In addition, this process should be applied to natural, fine-grained soil (non-homogeneous) since this will better simulate field conditions and presents the worse case scenario for electrokinetic flow. As stated previously, the use of kaolinite has been extensive, but this does not simulate field conditions and it also presents an easier medium for heavy metal removal since the inherent pH of kaolinite is acidic.

Since natural soil is being used, the problem of heavy metal mobility becomes more critical. Due to high pH of the soil (pH $\approx$ 11), the mobility of cations is not favorable. As a result, they will tend to bind to the solid phase via sorption mechanisms. Therefore, the pH of the soil must be lowered in order to enhance the mobility of these heavy metals. The addition of a chelating or complexation agent (conditioning liquid) can be used for this purpose. As mentioned previously, EDTA, NTA, HNO_3 and HCl are suitable as conditioning liquid. Experiments related to type, concentration and injection location (anode and/or cathode) for the conditioning liquid should be performed in order to obtain the best configuration.

The following sections deal with electrokinetics and some technologies that can be employed in conjunction with electrokinetics (ion exchange and chelation), in order to form a hybrid method. This hybrid method represents the scope of this thesis and will allow for the enhanced mobilization, transport, localization and removal of heavy metals, from natural clay soils.

5. APPLICATION OF ELECTROKINETICS

Electrokinetic soil processes are founded on the theories of electrochemistry and the flow of fluids in porous media. The reference section of this report clearly displays the pertinent and recent literature related to this topic. In order to represent electrokinetic processes adequately from a theoretical standpoint, the process is subdivided into two general groups as shown in Figure 14:

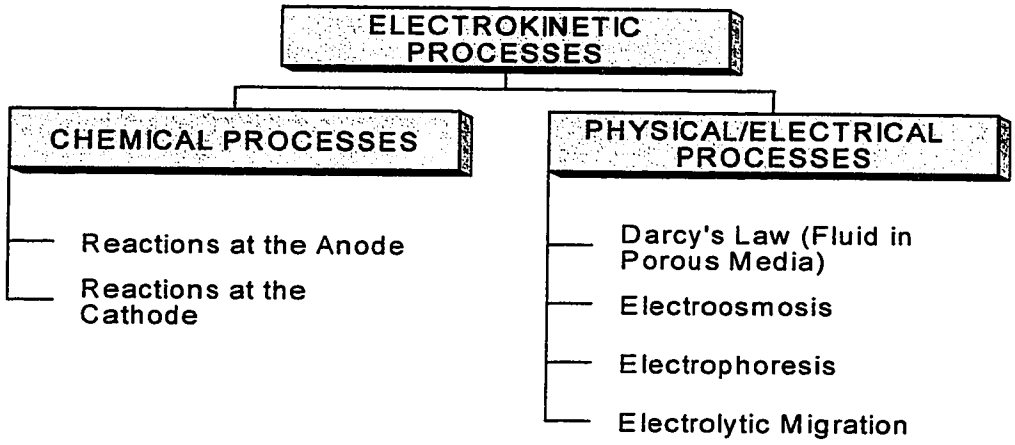

Figure 14 Components of electrokinetics mechanisms in soil

5.1. Principles of Electrokinetic Phenomena in Clay Soil

When an electrical field is applied to a system having charged particles, three general transport phenomena are observed as outlined in Figure 14. Electrolytic migration is the movement of ions within the pore water. Electrophoresis is the movement of charged colloids, while electroosmosis is the movement of the pore water within the subsurface, both in response to the applied electrical field. In essence, electroosmosis can be seen as the dragging of pore water by traveling ions. Within a clay

soil system, typically of low permeability, electrolytic migration and electroosmosis are the dominant mechanisms and therefore comprise the focus for any mathematical model. The term electrokinetics is used to describe the combination of these two transport phenomena, when electrophoresis is deemed to be negligible. Of particular importance are the basic reactions that occur at the anode and cathode of any electrochemical cell. Although simple in nature, these reactions have serious ramifications on the soil that is to be remediated, and therefore affect the removal of heavy metals from the soil matrix via electrokinetic processes.

A system consisting of anode or cathode, a DC power supply and fine particle soil between the electrodes will incite electrokinetic processes such as electroosmosis, electrolytic migration and electrophoresis. With an applied DC current, non-spontaneous oxidation-reduction reactions occur. The DC system continuously "pumps" electrons into the cathode while removing them at the anode. Oxidation and reduction reactions occur at the anode and the cathode respectively in order to maintain electroneutrality. Figure 15 displays a typical electrokinetic process and a schematic diagram respectively.

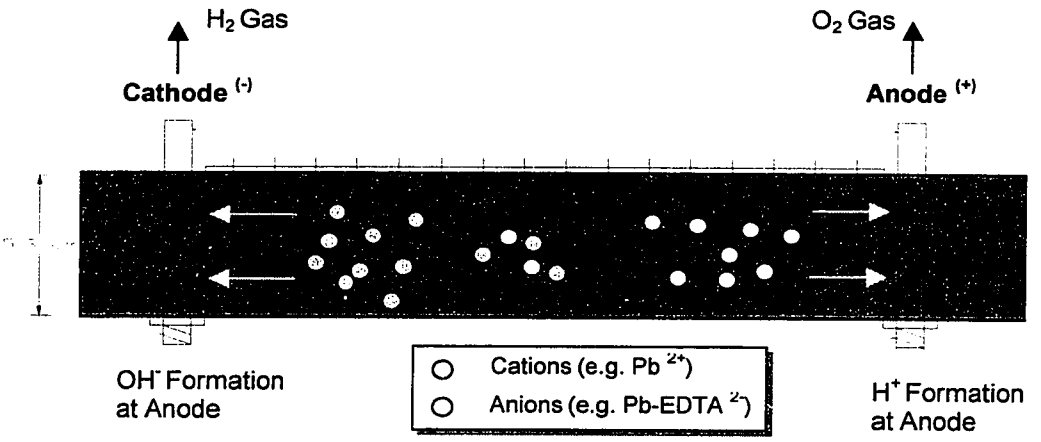

Figure 15 Schematic Diagram of an electrokinetic cell

Standard electrode potentials (E°) for oxidation-reduction half-reactions are a quantitative indication of the relative tendency for a reaction to occur without the application of an external potential. The order of preference for oxidation-reduction reactions are for those that require the least electrical energy. In general, for soil containing pore water, the principal anodic and cathodic reactions are shown in equations [5.1] and [5.2] respectively (Acar and Alshawabkeh, (1993)):

$$\textbf{Anode:}\quad 2H_2O \Rightarrow O_2\uparrow + 4H^+ + 4e^- \qquad [5.1]$$

$$\textbf{Cathode:}\quad 4H_2O + 4e^- \Rightarrow 2H_2\uparrow + 4OH^- \qquad [5.2]$$

Equations [5.1] and [5.2] are chemical representations of the typical response of an electrokinetic cell. If there is an abundance of cationic species in the subsurface between electrodes, electrolytic migration will be from anode to cathode. Therefore, anions will tend to migration to the anode and cations towards the cathode. This results in a deficit of anions and cations in the system, which therefore increases the production of H^+ ions at the anode and OH^- ions at the cathode to maintain electroneutrality within the cell.

Equations [5.1] and [5.2] display the general behaviour of an electrokinetic cell and how the subsurface environment between the electrodes can change with time. In addition, they dictate the measures that must be taken to improve the removal of heavy metals. The oxidation reaction at the anode shows that there is a production of hydrogen ions, which will eventually lower the pH in the area. The constant production of hydrogen ions coupled with the applied electrical field, causes dissolution and transport respectively of these ions from anode to cathode, thereby producing an acid front. The

rate of pH decrease is dependent on the buffering capacity of the soil and the current efficiency of the cell. At the cathode, the formation of hydroxyl ions is prevalent, which increases the pH. This increase promotes the precipitation of heavy metal ions (Pb^{2+} and Ni^{2+}), thereby removing them from the mobile liquid phase to the solid phase, where electrokinetic transport is rendered ineffective. The precipitation "barrier" that forms in the cathode region is the most significant problem in standard electrokinetics and must be overcome in order to achieve a high heavy metals removal efficiency. At first glance, it would appear that the hydrogen and hydroxyl ions would eventually meet at the centre of the cell and neutralize each other. However, hydrogen ions have higher ionic mobility values and will therefore travel farther than their hydroxyl counterpart (Acar and Alshawabkeh, (1993)).

5.2. Mathematical Equations for Classical Electrokinetic Processes

5.2.1. Modelling of Ionic/Electrolytic Migration

As stated previously, when a DC electric current is applied to a soil system, cations move toward the negatively charged cathode and anions move towards the positively charged anode. Mathematical models can be applied to represent this movement and predict how fast this movement will occur. The effective ion mobility is a measure of how fast ions will migrate toward the oppositely-charged electrode. Acar and Alshawabkeh proposed that the effective ion mobility may be expressed by the Townsend-Einstein equation (Acar and Alshabwabkeh, (1996)):

$$u^* = \frac{D^* zF}{RT} \qquad [5.3]$$

Where: u^* = effective ion mobility

D^* = effective diffusion coefficient [cm^2/s]
z = valence of the ion
F = Faraday's constant [96 487 coulombs/g-equiv.]
R = universal gas constant [8.314 J/mol·K]
T = absolute temperature [K]

The effective diffusion coefficient is expressed by the following equation:

$$D^* = D\tau n \qquad [5.4]$$

Where: D = diffusion coefficient of the ion at infinite dilution [cm^2/s]
τ = tortuosity factor
n = porosity

Diffusion, or the transport of ions in response to a concentration gradient, is taken into consideration in equations [5.3] and [5.4]. It does not occur due to the applied electrical field, but nevertheless occurs in clay soil. It should be noted that the diffusion coefficient can be represented by Fick's first law provided a concentration gradient is known:

$$J = - D^* [\partial C_x/\partial x + \partial C_y/\partial y + \partial C_z/\partial z] \qquad [5.5]$$

Where: J = flux density [$g/L \cdot m^2$]
C_i = concentration of contaminant in 3-D space

In order to simplify its determination the length of the electrokinetic cell (or the distance between the anode and the cathode) is taken to be significantly longer than the width and the depth (1-D problem). This equation forms the foundation for representing the effective ionic mobility in response to electrokinetic phenomena. Equation [5.3] could be modified by introducing a potential term to represent the effect of the electrical

field on ionic mobility. It should be noted that the formulae shown above, and those to follow, represent possible mathematical representations of electrokinetic phenomena. They are not governing equations for electrokinetics.

5.2.2. Modeling of Electroosmotic Flow

The most widely accepted theory for electroosmotic flow, is that net water flow results when the transfer of momentum between migrating ions of one sign exceeds that of the ion of the opposite sign. As cations flow to the cathode and anions flow toward the anode, it has been hypothesized that water surrounding the ions is dragged along via frictional forces. It has also been postulated that the dipole structure of water incites this movement. However, a definite theory has yet to be developed. Since there are more cations than anions in the electric double layer (EDL), a net flow of water towards the cathode will occur. Based on this premise, EO flow is modeled using an approach that is analogous to Darcy's Law (Terzaghi, (1930), Eykholt and Daniel, (1994)):

$$\boxed{q_e = k_e i_e A = k_i I} \qquad [5.6]$$

Where:
- q_e = EO flow rate [cm^3/s]
- k_e = coefficient of EO permeability [$cm^2/V \cdot s$]
- i_e = potential gradient [V/cm]
- A = cross-sectional area [cm^2]
- k_i = coefficient of water transport efficiency [$cm^3/A \cdot s$]
- I = applied current [A]

It should be noted that since EO flow is not a direct function of pore size, there can be significant water movement in low-permeability soils. This fact makes electrokinetic processes favorable for the transport of ionic species in clay soils.

5.2.3. Modeling General Contaminant Transport

General contaminant transport that typically occurs within the subsurface can also be mathematically modeled. The complete model takes into account the hydraulic transport mechanisms (advection, dispersion, diffusion) and those transport mechanisms resulting from the applied electrical field. Acar and Alshawabkeh presented the following equations to describe the transport of contaminants in the presence of an electric and hydraulic field (Acar and Alshawabkeh, (1996)):

$$\partial(nc_i) = -\nabla \cdot J_i + n\Gamma_i \qquad [5.7]$$

$$J_i = D_i^* \nabla \cdot (-c_i) + [\,|z_i|/z_i\,]\, c_i u_i^* \nabla \cdot (-V) + c_i k_e \nabla \cdot (-V) + c_i K_h \cdot \nabla(-h) \qquad [5.8]$$

Where:
- J_i = mass flux of i^{th} contaminant
- c_i = solution concentration of the i^{th} contaminant
- $\nabla \cdot (-V)$ = electrical potential gradient
- Γ_i = mass removed from solution by retardation
- K_h = hydraulic conductivity
- $\nabla(-h)$ = hydraulic gradient

The first and fourth terms in equation [5.8] represent diffusion and hydraulically induced advection respectively. The second and third terms represent transport via electrolytic migration and electroosmotic flow respectively. This encompasses the transport of contaminants via hydraulically induced and electrically induced phenomena. The transport mechanism that dominates is dictated by soil permeability, grain size, porosity and the nature of the contaminant.

5.3. Summary of Practical Applications of Classical Electrokinetics

Numerous publications related to experimental and theoretical analyses of electrokinetic processes and their applications to soil decontamination have emerged. The publications, a detailed comparison and a summary of each are dealt with in Table 16. It should be noted that the use electrokinetic technology is relatively new, particularly for transport enhancement and decontamination of soil. It has applications in the field of geo-technical engineering for soil improvement (i.e. increasing shear strength and dewatering), determination of soil properties (coefficient of permeability). However, recent applications and detailed research has focused on the use of electrokinetics for enhanced transport, removal and recovery of heavy metals from soils having low coefficients of permeability. This section provides an extensive review of the major research breakthroughs and findings in the field of electrokinetics, from experimental and theoretical standpoints.

Table 16 Pertinent Publications Related to Electrokinetic Removal of Heavy Metals

Author	*Analysis Type* *Dimension*	*Washing Liquid?* *Modifiers*	*Soil Used and Contaminant Type*	*Cell Configuration and Electrodes Used*	*Summary*
Choudhury and Elektorowicz, (1997)	Laboratory	N/A	Natural clay soil Pb(II) and Ni (II) (1000 mg/L)	Horizontal Length = 16.0 cm from anode to cathode Width = 5.3 cm Depth = 5.3 cm	• Use of electrokinetics and ion-exchange textiles for the localization and removal of lead and nickel from natural clay soils • 75-85% removal of Pb(II) and Ni(II) by the textiles
Acar, Alshwabkeh, (1996)	Analytical, Pilot-Scale Tests 2-D	Tap water No modifier	Kaolinite Moisture content: Cell 1: 44.0% Cell 2: 44.0% Cell 3: 24.6% Contamination: Pb(II)	Horizontal set-up Wood frame Length = 182.9 cm Width = 91.4 cm Height = 91.4 cm Electrode spacing: 70 cm Carbon electrodes	• Pilot scale tests for electrokinetic remediation of lead contaminated kaolinite soil in Georgia • Two-dimensional analysis with large cell dimensions (w = 91.4 cm, h = 91.4 cm, l = 182.9 cm) • cell boundaries were made of wood for electrical insulation and to resist lateral compaction pressure. • carbon electrodes (chemically inert)

					• tungsten wires were used as probe electrodes • current supplied: 1.7 A divided to the two cells (constant current design)
Alshawabkeh, Acar, (1996)	Theoretical 2-D	N/A	N/A	See below (pilot-scale test performed by the same authors)	• Mathematical model for the simulation of electrokinetic remediation using Fick's law for diffusion and Townsend- Einstein relation. • Comparison of pilot-plant studies and the aforementioned mathematical model. • Lead sorption by kaolinite versus pH was obtained (sorption is proportional to pH). • Soil sampling size: D = 10 cm, L = 5 cm
Shang and Dunlap, (1996)	Experimental, Theoretical 2-D	N/A	Soft Clay Soil CEC = 34 meq/100 g Smectite: 30% Quartz: 25% Mica: 20% Kaolinite: 20% Calcite: 2%	Copper electrode pair system (15 cm pair spacing) Cell Height: 32 cm Cell Width: 30 cm AC and DC electrical fields	• theory of high voltage EK methods in clay-water-electrolyte systems • theoretical development of electrophoresis, dielectrophoresis and total electrokinetic force • Conclusions: • High voltage electrokinetics includes both electrophoresis and dielectrophoresis, due

			Other: 3% No Contamination	Potential: in the order of kilovolts	to a non-uniform electrical field • The effect of high-voltage electrokinetics is irreversible • The efficiency of the process increases with treatment time
Yeung *et al.*, (1996)	Experimental 2-D	EDTA (0.004-0.100 mol/l)	Georgia and Millwhite Kaolinite CEC: 29 cmol/100 g Contamination: $Pb((NO_3)_2)$	Graphite electrodes Cell Height: N/A Cell Width: N/A	• New digestion procedure using 8 M HNO_3 was utilized lead extraction • 98.14% lead extraction • Procedure for buffering capacity • Low pH developed at anode, high pH at cathode • Net electroosmotic flow and net electrolytic migration from cathode to anode • Pb-EDTA complexes: anionic form • At 0.004 mol/L: no complexation of sorbed lead • At 0.1 mol/L: significant complexation of sorbed lead • EK-EDTA process decreased the contaminated area by 85%

Elektorowicz, M, and Boeva, (1996)	Laboratory	Nutrients	Natural clay soil	N/A	• Supply of nitrogen nutrients in natural clay soil during bioremediation using electrokinetics
Elektorowicz, M., *et al.*, (1996b)	Laboratory	Surfactant	Natural Clay soil Phenol	Horizontal set-up Length = 16 cm from anode to cathode Width = 5.3 cm Depth = 5.3 cm	• Electrokinetics combined with surfactants for phenol sequestration and transport respectively.
Elektorowicz, *et al.*, (1996a)	Laboratory		Natural clay soil Heavy metals	Horizontal set-up L = 8 cm from anode to cathode w = 5.3 cm, d= 5.3 cm	• Use of ion-exchange textiles in combination with electrokinetics for small cells.
Elektorowicz, M, (1995)	Laboratory	N/A	Natural clay soil Heavy metals Organic contamination	N/A	• Technical requirements for electrokinetic removal of contaminants from soil

Elektorowicz, *et al.*, (1995)	Laboratory	Surfactant	Natural clay soil Diesel fuel	N/A	• Electrokinetics combined with surfactants for phenol sequestration and transport respectively.
Reed *et al.* (1995)	Laboratory 1-D	$NaNO_3$, Electrolyte solution (S=500 µS/cm, used as a blank) HCl at anode (0.1 and 1.0 M), HAc (0.1 M and 1.0 M), EDTA (0.01 M and 0.1 M)	Erie county kaolinite) Moisture content: 25-30 % CEC: 25.6 meq/100 g Pb (soil was already contaminated with 22.8 mg of Pb/kg of soil	Horizontal set-up, cylindrical cell: L = 7.5 cm, D = 3.5 cm. Porous stones and 8 µm filter paper was paced at each end of the specimen. Anode and cathode reservoirs were utilized. Graphite electrodes Spacing: N/A	• Effects of modifiers on the electrokinetic transport of lead in soil. • anode and cathode reservoirs were used to supply the acid modifiers. • 60 V (DC) to ensure a fast experimentation time
Eykholt,	Experiment	Tap water	Georgia	Horizontal,	• Series of electrokinetic experiments using the

Daniel, (1994)	al 1-D	Citrate solution	Kaolinite CEC: 22 meq/100g Moisture content = 43 % Cu and Pb	cylindrical set-up L = 20 cm, D = 5.1 cm (PVC tubes) Graphite electrodes Spacing: 20 cm	following parameters: a. Blank cell with soil b. Cell with soil and copper solution c. Cell with soil, copper solution • And citrate introduced at the • Cathode d. Cell with soil, copper solution, • And citrate solution introduced • in the anode and cathode e. Cell with soil, copper solution • and citrate introduced at the • anode f. Cell with soil, copper solution • citrate introduced at the • anode and citrate initially mixed with soil • Voltage supplied: 5.5 - 5.7 volts (DC) • Assumption of uniform and constant electroosmotic permeability coefficient. • Anode and cathode area consisted of reservoirs for liquid collection. • Passive platinum probe electrodes were used in the vicinity of the anode and the cathode.

					• Stainless steel probe electrodes were placed along the axis of the soil specimen. • Graphite disks were used as the anode and the cathode.
Allen and Chen, (1993)	Laboratory 1-D	EDTA 0.01 mol/L	New Jersey contaminated soil Initial Pb conc.: 1786.2-1946.6 mg/L Initial Cu conc.: 437.1-572.4 mg/L	Copper and Nickel electrodes Cell dimensions: N/A Current Applied: 0.1-1.0 amp	• 73-98% recovery of lead and copper • The liquid stream at the anode was collected and subjected to further electrolysis for separation of metal-EDTA complex; allows for the recycling and reuse of EDTA.
Segall, Bruell (1992)	Laboratory and Theoretical 1-D (Lab) 2-D (Theory)	Tap water No modifiers	Georgia Kaolinite Organic and Inorganic Moisture content = 80 %	Iron and graphite electrodes Vertical columns, Circular cross-section. L = 56 cm, D = 7.6 cm	• Deals with the fluid transport in soil, in one and two dimensions due to an electromotive force. • Applications to organic and inorganic chemical removal coupled with the effects of pH, moisture content, pore water salinity, voltage gradient, and electrode material (iron versus graphite) on electrophoretic mobility and therefore contaminant

			Initial pH: 5.5	Spacing: 80 cm	removal. • Voltage supplied: 22 VDC, (0.4 V/cm) • Repeated experiments with varying voltage gradients (0.20, 0.39, 0.79 V/cm)
Pamukcu, Wittle (1992)	Experimental 1-D	N/A No modifier	Georgia Kaolinite, Na-Montmorillonite Distilled water, humic, simulated groundwater solutions of Cd, Co, Ni, Sr (1000 mg/L)	Vertical, cylindrical set-up (soil column) L = 7.62 cm, D = 3.56 cm Graphite electrodes	• Removal of a variety of selected heavy metals from soil using electrokinetics • Cell configuration unavailable • Anode and cathode areas consist of reservoirs (chambers) for the collection of liquid and the precipitate formed at the cathode. • For metal analysis, an acid is added to solubilize the precipitate. • Voltage supplied 30 Volts (DC)
Hamed, *et al.*, (1991)	Laboratory and Theoretical 1-D	Tap water No modifier	Saturated Georgia Kaolinite Moisture content: 65 % (ends) 92 % (middle)	Horizontal set-up, Dimensions not available. Reservoirs at anode and cathode Graphite electrodes Spacing: approx.	• Kaolinite contaminated initially with $Pb(NO_3)_2$. • Adsorption experiments showed that soil adsorbs 1100 μg/g of dry clay. • Lead was loaded at 110-165 μg/g of dry clay. • Five tests were performed with constant current,

			Pb (II)	Same as cell length.	varying cell lengths (10.2 or 20.3 cm), and varying porosities (0.68-0.76). • Electrical potential, resistance and current measurements were taken versus time and versus distance. • pH profiles and conductivity data was obtained • Current supplied: 3 mA (constant current)
Lageman *et al.*, (1989)	Laboratory Field	N/A	Clay Peat Fine sand Various heavy metals: As, Cd, Cr, Cu, Hg, Ni, Pb, Zn	Anode to Cathode Distance: 3 m	• Laboratory and field tests for electrokinetic remediation in different soil types • High metal concentrations (>5000 ppm in some locations)
O'Brien, (1985)	Theoretical 2-D	N/A	N/A	N/ A	• Mathematical representation and simulation of electroosmosis processes in porous materials. • Smoluchowski formula • Assumptions:

- ions move independently of each other and the electrolyte is dilute everywhere
- particle surfaces are smooth and impermeable
- the fluid adjoining the surface remains on the surface (no-slip condition)

5.4. Conclusions Related to Classical Electrokinetics

Upon extensive review of the aforementioned publications, it is apparent that the use of electrokinetic processes is a promising technique for the removal of heavy metals from soil. Moderately high removal efficiencies have been documented and costs are lower than comparable soil remediation techniques. This leads one to believe that electrokinetic processes are a viable and economically feasible technique for soil remediation, specifically for the removal of heavy metals from soil. However there are numerous problems with this technique that must be overcome in order to increase the efficiency of the metal removal.

5.4.1. Problem Related to High pH Development

High pH development in the cathode region creates a precipitation barrier, which has adverse effects on electrokinetic remediation. In order to maintain electroneutrality, OH^- ions are constantly produced at the cathode. These ions begin migrating towards the anode at a rate that is a function of their ionic mobility.

$$2H_2O + 2e^- \Rightarrow H_2\uparrow + 2OH^- \qquad [5.9]$$

Classical electrokinetics does not allow for complete localization of heavy metals. It performs well with respect to inducing the transport of metals in the mobile phase from anode to cathode. Upon entering the cathode region (an area of high pH), these metals form insoluble or slightly soluble precipitates, thereby ceasing their transport via electrokinetic methods. This allows for the moderate localization of heavy metals to approximately 20-30% of the original contaminated soil. Acar and Alshawabkeh (1996),

performed a pilot-plant study for the electrokinetic remediation of lead-spiked kaolinite (see Table 16). Their study showed that lead can be transported efficiently through the soil close to the cathode compartment. However, it cannot be transported to the cathode, due to the development of a high pH barrier in this area (as a result of OH^- formation at the cathode). As a result, the lead ions were precipitated thereby preventing the efficient localization and collection of lead. The energy expenditure was measured to be 700 kWh/m^2, and was concluded to be dependent upon the chemical equilibria of the targeted species, current density used, enhancement techniques employed, electrode type, geometry and spacing and extraction levels targeted.

The same problem was observed in the research performed by Eykholt, *et al.*, (1994). The effect of system chemistry on electroosmosis in soil contaminated with copper (II) was examined. It was shown that the electrokinetic flow was greatest in cases where the pH in the soil was at its highest, in the case when the kaolinite was free of copper and for the case in which citrate had been added to the kaolinite initially. Adding citrate to the anode had a positive effect on electroosmotic flow. To the contrary, some soil treatments produced a reversal in flow direction. The major problem that occurred was the development of high pH values at the cathode, which decreased the flow and hampered the removal of copper. Pamukcu, *et al.*, (1992) performed detailed experiments related to the removal of various heavy metals using electrokinetic processes. It was concluded that this technology was found to be promising and that kaolinite soil provided the best efficiency for flow due to its low pH (prevents excessive precipitation). The significant transport mechanism was electrolytic migration. In

addition, the significant problem encountered was the inability of heavy metal removal at the cathode due to precipitation at this location.

Elektorowicz, (1995), dealt with the technical requirements related to electrokinetic removal of contaminants from soil. One of the major requirements was lowering the pH in the cathode region in order to allow for increased mobilization and to make heavy metals accessible to electrokinetic transport. This is increasingly difficult in natural clay soil. This is of particular importance in the removal of heavy metals from soil.

5.4.2. Limitations of Classical Electrokinetics in Relation to Soil Type

The type of soil used during electrokinetic extraction affects the overall removal efficiency achieved. The majority of research in classical electrokinetics has focused on kaolinite soils, which have inherently low pH values (4.5-5.5) and lower CEC values than natural clay soils. Acar and Alshawabkeh, (1996), Yeung, *et al.*, (1996), Reed *et al.*, (1995), Eykholt and Daniel, (1994), Segall and Bruell, (1992), Pamukcu and Wittle, (1992), Hamed *et al.*, (1991) all utilized kaolinite soil, which represents a best case condition for maintaining heavy metals in the liquid phase. A low soil pH promotes the mobilization of heavy metals, thereby placing these metals in the mobile, liquid phase. This makes them accessible to electrokinetic transport (electrolytic migration). Natural clay soil, as used for this thesis, presents a more difficult remediation and recovery problem due to increased sorption, higher initial pH, higher CEC, lower concentration in the mobile phase. This renders classical electrokinetics less effective, due to the fact that it can only transport those metals which are in the liquid phase. Therefore, a means by which the mobilization of heavy metals can be augmented, must be developed.

Lageman, (1989) performed a field-scale electrokinetic extraction of numerous heavy metals from natural clay soil. The localization and removal efficiencies were low to moderate, due to the high initial pH of the soil. Choudhury and Elektorowicz, (1997) utilized natural clay soil during electrokinetic experimentation, coupled with IETs. The removal efficiency was moderate. The principal obstacle was maintaining lead and nickel in the pore water phase. This was difficult due to the inherently high pH values of natural clay soil (7.5-7.6). The formation of OH^- ions at the cathode compounded this problem.

5.4.3. Problems Related to Mobilizing Heavy Metals During Electrokinetics

In order for electrokinetics processes to be successful, the heavy metals must remain in ionic form (in the liquid phase) so that they can be transported to desired locations. The low water solubility of lead and nickel, the high pH development in the cathode region and the CEC of the soil, prevents the mobilization of heavy metals. The problem becomes more difficult in the case of natural clay soil where, high CEC values and high initial pH values are observed. As shown in Table 16, Reed *et al.,* (1995) used acetic acid and hydrochloric acid in anode and cathode reservoirs in order to maintain low pH values in the system. Allen and Chen, (1993) used EDTA for recovery of lead and copper from soils during electrokinetic processes.

Despite some research with chelating agents, definitive conclusions related to their effectiveness during electrokinetics are limited. In addition, the use and applicability of chelating agents in natural clay soils has not been examined. This type of soil represents a difficult case for heavy metal mobilization, due to its inherently high pH and CEC. There exists a discrepancy between the effects of various conditioning liquids (acids, chelating agents, etc.) on the efficiency of metal removal. Further research is

required in order to determine the advantages of these conditioning liquids in the field of electrokinetics, specifically in the domain of natural clay soil.

The problems related to classical electrokinetics, as discussed above, display the need for improvements to the existing technology. One of the limitations with classical electrokinetics is that the heavy metals must be accessible to electrokinetic transport (i.e. they must be in ionic form). The use of chelating agents has shown to be effective in mobilizing heavy metals in kaolinite, but their use in natural clay soils is non-existent. In addition, they do note promote the localization of heavy metals. A hybrid technology is required to create optimum mobilization, transport, localization and removal of heavy metals from natural clay soil.

6. ION EXCHANGE TEXTILES AND RESINS

Ion exchange textiles and resins have been widely used for the treatment of wastewater contaminated with polyvalent metallic cations. However, IETs have not been applied to soil for the localization and removal of heavy metals from soil. There exist two broad classifications of ion exchange materials. This classification is as follows:

1. Inorganic ion-exchange materials
2. Organic ion-exchange resins

Inorganic ion-exchange materials are those related to natural clay soils while organic forms are generally formed through the copolymerization procedures of styrene and divinybenzene (Harland, (1994)). This chapter deals with the most significant ion-exchange textiles and resins, their structure, properties and applications. Finally, a detailed comparison of these materials will be dealt with, as this is important to the selection procedure.

6.1. Inorganic Ion-Exchange Materials

Inorganic ion exchange materials were the first widely used type for ion exchange processes. Clay minerals (aluminosilicates) such as kaolinite, illite, montmorillonite, chlorite and vermicullite possess a natural ability to exchange cations which makes them instrumental in the ion exchange process. It is these minerals that comprise the significant inorganic ion exchange materials (Harland, (1994)). The basic structural unit making up the layer lattice silicates if the silica tetrahedron $(SiO_4)^{4-}$. The reader is referred to chapter 2 for a description of clay minerals and their structure.

Double layer lattice silicates display high cation exchange capacities greatly in excess of that attributable to specific surface area, crystal fracture and edge effects. Isomorphous substitution in the octohedral layer, resulting in charge deficiencies in the layer lattice is the principal contributor to the high CEC values. Since isomorphous substitution occurs in the octohedral layer, the resulting positive charge deficiency is relatively delocalized with respect to the inter-lamellar plane (Harland, (1994)).

As a consequence of weak inter-layer bonding, the montmorillonite-type minerals can expand reversibly during the sorption of solvated ions, and are often termed expanding layer lattice silicates. The capability to expand gives montmorillonite-type materials high CEC values. Mica structures are not capable of expanding and therefore have low CEC values, comparable to those of the single layer lattice type. The major contributors to cation exchange for micas are high specific surface areas and low particle sizes. Illites are transitional between kaolinites or micas and montmorillonite, and their exchange capacities are impossible to systematically quantify. Table 17 shows typical cation exchange capacities of some layer lattice silicate minerals. These values are pertinent to the selection of the most suitable inorganic exchange material for a particular ion exchange process. Although this is an important parameter, it does not comprise the only criteria by which the selection is made.

6.2. Organic Ion-Exchange Resins

Organic ion-exchange resins have come to the forefront of membrane technology and continued experimentation is being performed in this area. Organic resins are produced through a specific type of polymerization reaction known as *addition* or *vinyl*

polymerization. This reaction consists of free radical induced polymerization between reactants (monomers) carrying ethenyl (or vinyl) double bonds ($-CH=CH_2$). The actual reaction is shown in Figure 16. It should be noted that the synthesis of the resin is shown as occurring in two stages for easier comprehension. However, the complex polymerization reactions occur simultaneously.

Table 17 Cation Exchange Capacities of Various Silicate Minerals (Yong, *et al.*, 1992)

Structural Type	***Mineral Designation***	***Cation Exchange Capacity (mequiv/kg)***
Single Layer	Kaolinite	30-150
	Halloysite ($2H_2O$)	50-100
	Livesite	400
Double Layer (non-expanding lattice)	Muscovite (mica)	100
	Illite (hydrous mica)	100-400
	Glauconite	110-200
	Pyrophyllite	40
	Talc	10
Double Layer (expanding lattice)	Montmorillonite	700-1000
	Vermicullite	1000-1500
	Nontronite	570-640
	Saponite	690-810
Three-dimensional		
• **Dense Lattice**	Felspar (orthoclase)	20
	Quartz	50
• **Open Lattice**	Zeolites	300-600

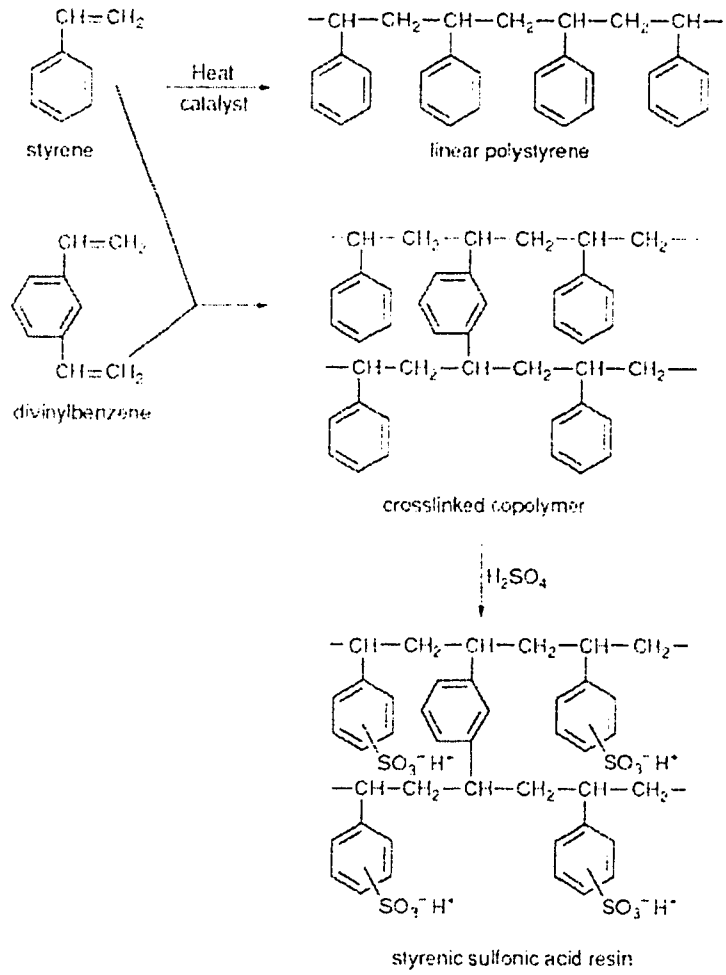

Figure 16 Addition polymerization of a styrene sulfonic acid cation exchange resin (Harland, (1994))

Ion exchange resins are classified according to their composition, function (anion or cation exchanger) and the solution used for the activation of the polymer. As a result, the following classification occurs:

1. Styrenic cation exchange resins (strong and weak acid)
2. Acrylic cation exchange resins (strong and weak acid)
3. Styrenic anion exchange resins (strong and weak base)
4. Acrylic anion exchange resins (strong and weak base)

These types will be discussed briefly in the section to follow.

6.2.1. Styrenic Cation Exchange Resins

Styrenic cation exchange resins are formed through the free radical copolymerization of two miscible monomers, namely ethylbenzene (styrene) and diethylbenzene (divinylbenzene, DVB). The reaction is highly exothermic, and is carried out in an aqueous suspension whereby the mixed monomers are immiscibly dispersed as spherical droplets throughout the reacting medium, thereby resulting in discreet beads of copolymer being formed (Harland, (1994)).

Activation of the copolymer is carried out by sulfonation of the matrix with hot sulfuric acid thereby introducing the sulfonic (fixed, negatively charged ions) functional group onto the matrix. This functional group gives a strongly acidic cation exchange resin. Subsequent treatment of the sulfonic acid resin with brine or sodium hydroxide solution gives, via ion exchange, the sodium sulfonate salt form (RSO_3Na). Therefore, sodium is utilized as the exchangeable cation due to its small atomic size and charge. It should be noted that weakly acidic cation exchange resins of this type can be formed using a carboxylic acid derivative instead of sulfuric acid as the polymer activation agent.

6.2.2. Acrylic Cation Exchange Resins

Acrylic cation exchange resins utilize propenoic (acrylic) monomers instead of ethylbenzene during copolymerization with divinylbenzene (DVB). For example, the methacrylic-divinylbenzene weakly acidic cation exchanger is formed by copolymerization DVB and methylpropenoic acid. Typically, the derived copolymer is further subjected to an acid hydrolysis stage which results in the carboxylic acid functional group (fixed ion) as shown by the following equations (Harland, (1994)), where R and R' are organic radicals (e.g. methyl group):

$$\text{R-C-R}' \text{ (polymer)} + 2H_2O \rightarrow \text{R-COOH (carboxylic acid)} + \text{R''} \qquad [6.1]$$

$$\text{R-COOR'} + H_2O \rightarrow \text{R-COOH} + \text{R'OH} \qquad [6.2]$$

Currently, a bifunctional cation exchange resin displaying strongly acidic and weakly acidic groups simultaneously is being researched. However, they are not in commercial use at present.

6.2.3. Styrenic Anion Exchange Resins

Styrenic anion exchange resins have the same styrene-DVB matrix as their cationic counterparts, but the preformed copolymer is subject to two further synthesis steps:

1. **Chloromethylation.** The reaction between the copolymer and chloromethoxymethane with aluminum chloride as the catalyst introduces chloromethyl groups ($-CH_2Cl$) into the styrene nuclei.

2. **Amination.** Trimethylamine, $(CH_3)_3N$ results in the quartenary benzyltrimethyl-ammonium chloride functional group ($RCH_2N(CH_3)_3^+Cl^-$. This functional group gives the resin its strong base anion exchange characteristic. If methylamine or dimethylamine is employed, the resulting resins are weakly basic.

The range of amine functional group configuration is vast because of the availability of many copolymers and amine derivatives. However, most commercially available styrene based anion exchange resins are bases on weakly based secondary or tertiary amine functional groups or strongly based quartenary ammonium grouping.

6.2.4. Acrylic Anion Exchange Resins

Acrylic anion exchange resins demonstrate beneficial exchange equilibria and kinetics towards large organic ions compared with styrenic structures. The reason for this phenomenon lies with the greater hydrophilic nature of the aliphatic skeletal structure of the acrylic matrix. This in turn forms a weaker van der Waals type attraction between the resin matrix and the hydrocarbon structure of an organic counter ion.

Typically, methyl propenoate is utilized as the monomer for copolymerization with DVB to form the resin matrix. The matrix is relatively flexible due to the fact that it can be used in three ways as described by functionality (Harland, (1994)):

1. **Weak Base Functionality**. Amination with dimethyl aminopropylamine (DMAPA) introduces a tertiary amine functional group.
2. **Strong Base Functionality**. A subsequent quartenization step employing chloromethane (methyl chloride) converts the weak base product to the strongly basic quartenary ammonium resin.
3. **Bifunctionality**. Are obtained by physically mixing weak and strong functional resins.

All three types of acrylic anion exchange resin mentioned above are widely used commercially for the treatment of wastewater, but have not seen any use for soil decontamination. In the future, as the need for soil decontamination becomes urgent, the

applicability of these types of resin could be expanded towards the subsurface domain, namely problematic clay soils.

6.2.5. Specific Ion Exchangers

Specific ion exchangers exhibit the ability to uptake one or not more than a few particular ions. This specificity is typically due to the fact that these ions form strong complexes with, or are precipitated by a certain class of compound. Therefore, ion exchange resins incorporating such class of compound, exhibit a high affinity for such ions. Such an exchanger has a great potential and usefulness in analytical chemistry and forms a foundation for commercial recovery or purification processes.

The chemistry of common heavy metals is characterized by their ability to form coordination complexes and chelates with electron pair donating ligands. Therefore, any resin containing iminodiacetate functional groups or ethylenediaminetetraacetic acid (EDTA) shows strong affinity towards many polyvalent and transitional metal cations. Table 18 displays the commonly used organic ion exchangers, the functional (ionogenic) group that gives them their specificity and metal affinity.

6.3. Characterization of Ion Exchange Materials and Resins

Knowledge related to the characterization of ion exchange resins is important because a data summary or data specification commonly accompanies commercially formed resins. In addition, an understanding of the terminology contained in these summaries is of paramount importance since it encompasses the pertinent properties of the resin in question. Table 19 deals with the main properties of ion exchange resins.

Table 18 Specific Organic Ion Exchangers (Harland, (1994))

Matrix	*Ionogenic Group*	*Specificity*
Styrene-DVB	*Iminodiacetate* $-CH_2-N(CH_2COO^-)_2$	Fe, Ni, Co, Cu, Ca, Mg
Styrene-DVB	*Aminophosphonate* $-CH_2-NH(CH_2PO_3)^{2-}$	Pb, Cu, Zn, Ca, Mg
Styrene-DVB	*Thiol; Thiocarbamide* $-SH$; $-CH_2-SC(NH)NH_2$	Pt, Pd, Au, Hg
Styrene-DVB	*N-methylglucamine* $-CH_2N(CH_3)[(CHOH_4)CH_2OH]$	B, (as boric acid)
Phenol-formaldehyde	*Phenol; Phenol-methylnesulfonate* $-C_6H_3(OH)$; $-C_6H_2(OH)CH_2SO_3^-$	Cs

Table 19 Classification of Properties for Ion Exchange Resins (Harland, (1994))

Property	*Description*
PHYSICAL PROPERTIES	
• Appearance	⇒ color and texture of resin beads
• Particle size	⇒ diameter of resin particles
• Uniformity coefficient	⇒ D_{60}/D_{10}
• Gradation	⇒ particle size distribution
• Density	⇒ mass per unit volume (bulk or resin)
• Shipping weight	⇒ weight of the swollen resin per V_{bulk}
• Percent whole beads	⇒ proportion of unbroken resin beads
• Sphericity	⇒ percent of perfectly spherical beads
CHEMICAL PROPERTIES	
• Matrix (polymer structure)	⇒ styrene-DVB or acrylic-DVB
• % Crosslinking	⇒ as measured by % DVB
• Functional group	⇒ the fixed ion (strong or weak)
• Ionic form	⇒ cation or anion exchanger
• Water content	⇒ W_{water}/W_{resin}
• Ion exchange capacity	⇒ dry weight (eq/kg)or wet vol. cap. (eq/L_{resin})
• Salt splitting capacity	⇒ strongly functional component of a resin's capacity
• pH range	⇒ the range at which the resin is efficient
• Chemical stability	⇒ resistance to degradation due to sustained exposure
• Thermal stability	⇒ maximum allowable temperature
• Reversible swelling	⇒ observable volume changes that occur (hydration)

6.4. Properties and Comparison of Ion Exchange Materials and Resins

A comparison of inorganic and organic ion exchange materials, coupled with a comparison of resins within the organic category is necessary to the selection process. Knowledge of the applicability, lifespan, and various advantages and disadvantages is paramount to the successful selection of the appropriate resin for the particular need. Table 20 deals with a comparison of inorganic and organic ion-exchange materials and resins, while Table 21 and Table 22 display comparisons of the typical and most widely used organic cation exchange and organic anion exchange resins respectively.

6.5. Ion Exchange Theory

In equal concentrations, multivalent cations with large atomic radii and atomic charges, are adsorbed more strongly than sodium. As the water comes into contact with the medium, the following reaction occurs instantaneously (Peavy *et al.*, (1985)), where [R] is the exchange media:

$$Cation^{+n} + Anion^{-n} + 2Na[R] \Rightarrow Cation[R]_n + 2Na^{+} + Anion \qquad [6.3]$$

The engineering requirements for the ion exchange process are summarized in Table 23. A schematic drawing of the ion exchange process is shown in Figure17. The exchange of cations continues until all of the exchange sites on the medium have been filled. At this point, metals become evident in the effluent and the medium must be regenerated. A concentrated NaCl solution (5% to 20%) is used to remove the hardness on the medium by 'reverse' ion exchange. It should be noted that the solution must be of sufficient concentration to overcome the high ionic charge and ionic size of the

multivalent cations on the medium. The medium can then be regenerated with a less concentrated sodium chloride solution.

Table 20 A Comparison of Organic vs. Inorganic Ion-Exchange Materials/Resins (Harland, (1994))

Description	***Inorganic Ion-Exchange Materials***	***Organic Ion Exchange Resins***
Advantages	1. High CEC values for double layer clays. 2. High specific surface area. 3. Excellent thermal stability.	1. Hydrophilic form that is regular and readily reproducible. 2. Increased application flexibility (allow for the introduction of solution that can alter the resin from a cation exchanger to an anion exchanger. 3. High pH flexibility (most resins are efficient in all pH ranges). 4. Can increase the porosity of the resin and make the structure macroporous (decrease organic fouling), by adding a solvent (methylbenzene).
Disadvantages	1. Lack of flexibility (cannot choose the type of exchange (anionic or cationic). 2. Lack of chemical stability toward electrolyte solutions. 3. High pH sensitivity. The exchange of metals onto the surface is highly dependent on pH. 4. Heterogeneous material (results in concentration of ions in locations of high specific surface area).	1. Some degree of heterogeneity due to the copolymerization process. Homogeneity is still better than inorganic ion-exchange materials. 2. Lifespan of the resin is lower due to its susceptibility to microbial degradation. 3. Subject to organic fouling which can make the regeneration process difficult.

Table 21 Properties and Comparison of Organic Cation Exchange Resins (Harland, (1994)), (Murviev et al., (1995))

Property	*Strong Acid Type*	*Weak Acid Type*
Matrix	Styrene-Divinylbenzene	Acrylic-Divinylbenzene
Structure	Gel	Gel
	Macroporous	Macroporous
Functional Group (fixed ion type)	$--SO_3^{2-}$	$--COO^-$
	(both gel and macroporous)	(both gel and macroporous)
Ionic Form (counter ion type)	Na^+ (Gel and Macroporous)	H^+ (gel)
	H^+ (Gel and Macroporous)	H^+ (macroporous)
Wet Volume Capacity (keq/m^3)	Gel: 2.0 (Na), 1.8 (H)	Gel: 4.2
	Macro.: 1.8 (Na), 1.6 (H)	Macroporous: 3.0
pH Range of Applicability	0-14 (Gel)	4-14 (Gel)
	0-14 (Macroporous)	4-14 (Macroporous)
Thermal Stability	120°C	120°C

Macro.= Macroporous

Table 22 Properties and Comparison of Organic Anion Exchange Resins (Harland, (1994))

Property	***Strong Base (Type 1)***	***Strong Base (Type 2)***	***Strong Base (Type 3)***	***Weak Base (Type 1)***	***Weak Base (Type 2)***	***Mixed Base***
Matrix	Styrene-DVB	Styrene-DVB	Acrylic-DVB	Styrene-DVB	Acrylic-DVB	Acrylic-DVB
Structure	Gel Macro.	Gel Macro.	Gel Macro.	Gel Macro.	Gel Macro.	Gel
Functional Group (fixed ion)	$-N(CH_3)_3^+$	$-N(CH_3)_2(CH_2CH_2OH)^+$	$-N(CH_3)_3^+$	$-N(CH_3)_2$	$-N(CH_3)_2$	$--N(CH_3)_3$
Ionic Form (counter ion)	Cl^-	Cl^-	Cl^-	Gel: Cl^- Macro.: Free Base	Free Base	Cl or Free Base
Wet Volume Capacity (keq/m^3)	Gel: 1.30 Macro.: 1.15	Gel: 1.30 Macro.: 1.15	Gel: 1.25 Macro.: 1.20	Gel: 1.20 Macro.: 1.25	Gel: 1.60 Macro.: 1.00	Gel: 1.30 Macro.: 1.30
pH Range	0-14	0-14	0-14	0-9	0-9	0-14
Thermal Stability	80°C	50-60°C	75°C	100°C	60°C	35°C

DVB: Divinylbenzene
Macro.: Macroporous structure

Ion exchange is currently being used as the primary technology in the removal of metals. It has proven to be effective in removing heavy metals such as cadmium, lead mercury and selenium. Its diversity as a softening and heavy metal removal technology has led to its wide use.

Table 23 Engineering Requirements for the Ion Exchange Process (Peavy *et al.*, (1985))

Engineering Requirements	***Amount Required***
Volume of Medium	Depends on inflow and amount of hardness
Tank Diameter	2.0-4.0 m
NaCl or Another Salt	Depends on inflow and amount of hardness
Concentration of Salt for Regeneration	5.0-20.0 %
Mass of Salt Required for Regeneration	80-160 kg/m^3 of medium

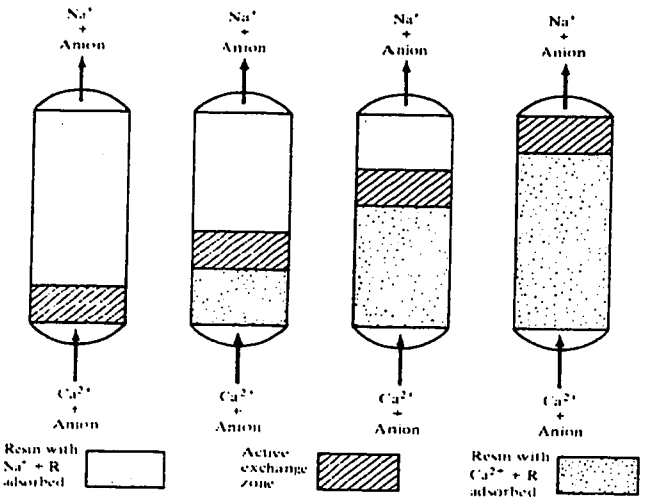

Figure 17 Schematic diagram of the ion exchange process (Peavy *et al.*, (1985))

6.6. Applications to Wastewater and Sludge Treatment

Ion exchange has been extensively applied for the removal of heavy metals with moderate efficiency. Maliou *et al.*, (1992), through various experiments, studied the removal of Pb and Cd (simultaneous contamination) with the use of zeolites, specifically

clinoptilolite as an exchange medium. This mineral has four cation exchange sites which make it highly conducive to ion exchange. Concentrated sodium chloride was used as the exchange liquid. Various conditions related to temperature and grain size were explored in order to determine which ones affect ion exchange efficiency. For Pb ion exchange, temperature caused an increase in the amount of Pb exchanged (0.1-0.2 meq/g), while grain size did not affect the ion exchange efficiency. For Cr ion exchange, the efficiency is augmented at higher temperatures using finer clinoptilolite grains. This is in agreement with basic ion exchange theory as exchange efficiency tends to increase with smaller grain size due to the larger specific surface area provided.

In addition to these condition specific phenomena, the rate of ion exchange was very fast for the early stages of the experiment for both Pb and Cd at temperatures of 25°C and 50°C with grain sizes of 0.6 - 1.0 mm. This indicates that ion exchange is a relatively fast process that enables the removal of heavy metals from wastewater in short periods of time which is a critical criteria in wastewater treatment selection.

D'Avila *et al.* (1992), have displayed the effectiveness of heavy metal removal using activated peat as the exchange resin. Peat has an exchange capacity of 2000 meq/kg and provides a medium for fast exchange of heavy metals thereby removing them from wastewater. Removal efficiencies of 99 %, 97 %, 96 %, and 94.5 % for Cd, Zn, Ni, Cr, and Cu respectively. The most attractive feature of this ion exchange process is the relatively short period of time that this removal takes place. These removal efficiencies were achieved in 7-10 minutes. The kinetics of ion exchange are described by the following equation:

$$\frac{C_{avg} - C_{eq}}{C_o - C_{eq}} = e^{-Kt} \qquad [6.4]$$

Where: C_{eq} = ion concentration at equilibrium
C_o = initial ion concentration
C_{avg} = average ion concentration

Peat is a very effective exchange material that has proven to be efficient in the removal of heavy metals at concentrations of 40-50 g/m^3. The optimum pH for ion exchange with peat was determined to be 5. The speed at which ion exchange takes place makes this method highly desirable.

6.7. Recent Advances and Applications

Recent advances and applications have emerged in the field of ion exchange materials. These advances have resulted in more effective and more flexible ion exchange techniques using resins. Table 24 summarizes the major and most recent applications of ion exchange, which have emerged in recent years. From this table, it should become evident that many innovations have emerged and that the full applicability of this technology has not yet been realized.

Table 24 Applications of Ion Exchange Resins in Water and Wastewater

Author and Date	*Type of Resin*	*Selectivity*	*Results and Conclusions*
McNeff and Carr (1995)	Quarternized Polythylenimine-Coated Zirconia Anion Exchanger	p-alkoxybenzoic acid	• zirconia based resin performed better than silica based resins • chemical stability from pH=1 to 13 • high thermal stability was realized

Muraview, Gonzalo, Valiente (1995)	Iminodiacetic (IDA) and Aminomethylphosphonic (AMP) Resins Cation Exchanger	Cu^{2+}, Zn^{2+}	• ion exchange of IDA resin proceeds faster at higher temperatures (at 80°C rather than 40°C) • temperature did not influence ion exchange rate for AMP resin • exchange of Zn^{2+} proceeds faster the Cu^{2+} for both resins • separation of ions can proceed by a dual temperature fractionation process
Yang, Burban, Cussler (1995)	Cross-linked terpolymers (allyl acetylacetone, 2-hydroxyethyl methacrylate, ethylene glycol dimethacrylate synthesis) Cation Exchanger	Cu^{2+}	• these resins are effective for the selective exchange of cupric ions • exchange is further enhanced by controlling the pH (pH=2.1 using HNO_3) • resins have a low capacity (0.07 meq/g) at 0.1 M Cu^{2+} • the effect of feed concentration on breakthrough is much greater than the effect of changing feed velocity
Li and Schlenoff (1994)	Polystyrene-DVB plastic resin coated with sulfonic acid (SO_3^{2-} fixed ions) Cation Exchanger	Ca^{2+}, Y, Pb^{2+}	• exchange on the resin was achieved using a sulfonation procedure • rate limiting process is diffusion through a

			thin film solution at the surface rather than mass transport through the polymer
Stathakis and Cassidy (1994)	Polystyrene-DVB coated with polyelectolytes: 1. poly (1,1-dimethyl-3,5-dimethylene piperidinium) chromate 2. hexadimethrine chromate 3. poly (1,1-dimethyl-3,5-dimethylenepyrrolidiniu m) chromate Cation Exchanger	Br^-, Cl^-, NO_3^-, NO_2^-, F^-, SO_4^{2-}, PO_4^{3-}	• use of electrophoretic movement and resins for the separation of inorganic ions • the polyelcctrolytes were shown to be capable of reversing the direction of flow • electroosmotic flow was relatively constant (±16%) in pH range 6.5-10.0 with the use of each polyelectrolyte, while a 400% change was observed in the absence of these polyelectrolytes
Guha, Yun, Basu, and Sirkar (1994)	Hollow-fibre liquid membrane Cation Exchanger	Cu^{2+}, Cr^{3+}, Hg^{2+}, Pb^{2+}	• feed concentrations ranged from 90-500 mg/L • successful removal of all metals mentioned previously • copper was removed and concentrated by countertransport • the resistance of the membrane varies inversely to influent flow rate • maximum mass transfer rate is achieved by maximizing the

			interfacial area and minimizing resistance
Sata (1993)	Composite Membranes (polymers) Anion Exchanger	N/A	• testing for membrane resistance during electrodialysis • electrical resistance of the anion-exchange membrane was increased by the formation of polypyrole • the formation of a thin polypyrole matrix in the desalting side of the anion exchange membrane may decrease the resistance
Peasvento, Biesuz, Gallorini, Profumo (1993)	Styrene-DVB polymer coated with iminodiaceteate Cation Exchanger	Ca^{2+}, Cd^{2+}, Cu^{2+}, Ni^{2+}, Zn^{2+}	• strong complexes are formed with copper and nickel • competition between ions occurs and is pH dependent • exchange of zinc and cadmium occurs at higher pH values in seawater than in freshwater (due to higher concentration of competing calcium and magnesium ions in seawater)

6.8. Conclusions Pertaining to Ion Exchange Textiles and Resins

The use of ion exchange resins and textiles in the treatment of water and wastewater containing heavy metals has been extensive and well documented. Table 24 showed numerous research efforts and applications of ion exchange resins with varying degrees of effectiveness. Based on the literature review performed, the sole uses of ion exchange technologies (resins or textiles) for soil remediation is lacking. Elektorowicz, (1995), Elektorowicz, et al., (1996a) and Choudhury and Elektorowicz, (1997) have studied the use of ion exchange textiles (IETs) during electrokinetic methodology for the removal of lead and nickel from natural clay soils. The removal efficiencies obtained indicate the potential application of IETs for soil remediation. The principal drawback related to its use in conjunction with electrokinetic methodology is that heavy metals do not remain in the pore water phase, due to the low water solubility of lead and nickel compounds and the high cation exchange capacity of the soil. As a result, a percentage of the contaminants are not accessible to electrokinetic transport, and therefore never make it to the textile.

This fact presents the need for a hybrid technology, employing electrokinetic methods (for transport), chelation with EDTA (enhanced mobilization) and ion exchange textiles (localization and removal). Using EDTA in conjunction with electrokinetics and IETs increases the solubility of heavy metals and results in more contaminants being located in the pore water phase, thereby making them more accessible to electrokinetic transport. There is a need to choose a textile that complies with the electrokinetic system (e.g. electrical field). In addition, ion-selective textiles can be employed in cases where contamination is limited to a few species of heavy metals.

Some obstacles exist related to the use of IETs in soil. For example, fouling and increased resistance in the soil during electrokinetic treatment are ramifications related to the use of IETs in soil. Nevertheless, its use presents a potentially effective method for localizing and removing heavy metals from clay soils, particularly during a hybrid process (i.e. in combination with electrokinetics and chelation). Research in this domain is required to determine the overall effectiveness of IETs in soil, specifically its use in this new hybrid technology.

7. BEHAVIOUR AND APPLICABILITY OF ETHYLENEDIAMINETETRA-ACETIC ACID (EDTA) FOR THE CHELATION OF HEAVY METALS IN THE SUBSURFACE

7.1. Characterization of EDTA

Ethylenediaminetetraacetic acid (EDTA) is a highly branched and high-molecular weight acidic compound. EDTA has a specific gravity of 0.86, a molecular weight of 292.25 g/mol, is slightly soluble in water and tends to exist as white, odourless crystals. Due to its ability of form strong water soluble chelates with most metals, EDTA has been extensively used to extract heavy metals from contaminated soil, through solubility and mobility enhancement (Yeung and Menon, (1995)). Ethylenediaminetetraacetic acid is a tetraprotic acid that is commonly abbreviated as H_4Y, where Y denotes the $EDTA^{4-}$ ion. As stated previously, it is slightly soluble in water and typically dissociates into a wide variety of species such as: H_3Y^-, H_2Y^{2-}, HY^{3-}, and Y^{4-}. The respective pK_a values are shown in Table 25.

Table 25 EDTA Speciation and pK_a Values (Yeung and Menon, (1995)).

Ionic Species	*pK_a*
H_3Y^-	2.00
H_2Y^{2-}	2.76
HY^{3-}	6.16
Y^{4-}	10.26

[a] pK_a values are at 20°C with the presence of 0.1 M KNO_3

Each EDTA ion can coordinate bond to a metal at six different sites, namely, each of the four acetate sites and the two nitrogen sites, which have free electron pairs available for coordinate bond formation. The structure and configuration of the metal-

EDTA complex is shown in Figure 18. The numerous coordination sites inherent to EDTA ions creates complexes that are highly stable and favourable to chelation technology.

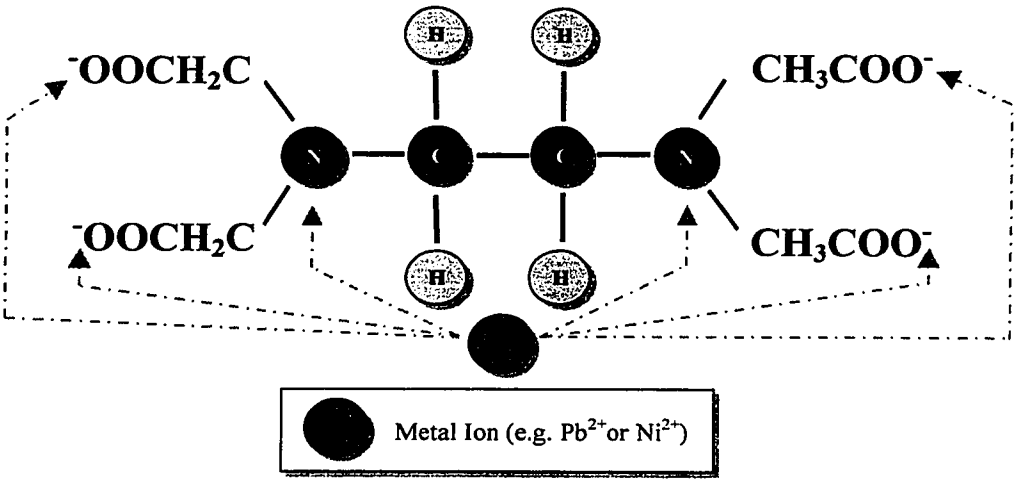

Figure 18 Structure and location of metal-EDTA complexation sites (Yeung and Menon, (1995)).

7.2. Metal-EDTA Complexation Theory

When a metal cation comes into contact with an EDTA (Y) ion, numerous complexes can result. A complex of the form MY, a protonated MHY complex, hydroxo complex $MY(OH)_n$, and a mixed complex MYX can result, where X is a unidentate ligand. The simplified complexation reactions are shown below (Yeung and Menon, (1995)):

$$M^{n+} + Y^{4-} \Leftrightarrow MY^{n-4} \quad [7.1]$$

$$M^{n+} + H^{+} + Y^{4-} \Leftrightarrow MHY^{n-3} \quad [7.2]$$

$$M^{n+} + OH^{-} + Y^{4-} \Leftrightarrow MY(OH)^{n-5} \quad [7.3]$$

The log of the stability constants for the MY^{n-4} and MHY^{n-3} Pb-complexation reactions are 18.0 and 2.8 respectively. MY^{n-4} and MHY^{n-3} stability constants for various metal are shown in Table 26. This gives an indication of the expected speciation of metals complexes and allows the engineer to determine the applicability of EDTA for solubility enhancement and extraction potential.

Table 26 Stability Constants for Metal-EDTA Complexes (Allen and Chen, 1993))

Element	*Cationic Form*	$logK_{MY}$	$LogK_{MHY}$
Cadmium	Cd^{2+}	16.5	2.9
Calcium	Ca^{2+}	10.7	3.1
Chromium	Cr^{2+}	23.0	2.3
Copper	Cu^{2+}	18.8	3.0
Iron	Fe^{2+}	14.3	2.8
	Fe^{3+}	25.1	1.4
Lead	Pb^{2+}	18.0	2.8
Magnesium	Mg^{2+}	8.7	3.9
Manganese	Mn^{2+}	14.0	3.1
Mercury	Hg^{2+}	21.8	3.1
Nickel	Ni^{2+}	18.6	3.2
Zinc	Zn^{2+}	16.5	3.0

These high stability constants, particularly for the MY^{n-4} complex indicate that these complexes will remain in these water soluble forms and that EDTA is potentially useful in enhancing the sequestration and mobilization of lead, nickel and other heavy metals in contaminated soil. In natural clay soil, the use of EDTA has the potential to keep more heavy metals in the solution phase, thereby allowing EK methods to transport an increasingly higher amount of metals. It should be noted that if EK methods are used with EDTA, electrolytic migration will tend toward the anode, due to formation of negative metal-EDTA complexes.

Research pertaining to combining the use of EDTA with electrokinetics to treat natural clay soil is limited, but nevertheless presents an interesting hybrid approach to in-situ mobilization and subsequent transport and recovery of heavy metals from natural clay soil. Based on the stability constants for lead and nickel metallic and hydrometallic complexes, the utilization of EDTA presents a suitable method for the sequestration and solubility enhancement of lead and nickel ions in natural clay soil. In addition, the six possible exchange sites on the EDTA ion enhances the degree of complexation. The use of EDTA coupled with electrokinetic methods presents a technology that results in enhanced mobilization of (via EDTA) and efficient transport of lead and nickel ions in natural clay soil. This would otherwise be difficult without the solubility enhancement created by the utilization of EDTA.

8. ACCOMPLISHMENT OF RESEARCH OBJECTIVES

The problem scope and objectives of this research effort are based on the inherent deficiencies of classical electrokinetics and on the need to develop and analyze the system parameters related to an effective technique for the in-situ remediation of natural clay soils, particularly those sites contaminated with heavy metals. At present, the most effective remediation technique is ex-situ slurry-phase treatment, which is costly and requires full excavation and transport of contaminated soil. The following section encompasses the principal objectives that are to be accomplished. These objectives can be summarized as follows:

1. To analyze and verify the effectiveness of lead and nickel mobilization from natural clay soil using ethylenediaminetetraacetic acid (EDTA) as a chelating agent.
2. To study the electrical parameters (current, potential and resistance) and the effect of EDTA and textiles on the spatial distribution.
3. To study the spatial soil pH distribution in response to EDTA addition, textile utilization and EK methods in comparison to standard EK and combined EK-EDTA methods. This is performed after the completion of the process and is important, as these pH changes dictate removal efficiency.
4. To analyze and verify the effectiveness of lead and nickel removal from natural clay soil using electrokinetic processes, ion selective textiles and enhanced complexation with EDTA.
5. To study the effectiveness of the ion-exchange textile in the removal and localization of lead and nickel. In addition, to study the effect of the textile in alleviating the effects of the high pH zone in the cathode region.
6. To conclude on the overall behaviour and effectiveness of EK methods, ion exchange textiles, and EDTA-chelation for the localization and removal of heavy metals from natural clay soils.

7. To verify the applicability of supercritical fluid extraction (CO_2) for the extraction of lead, nickel, calcium, iron and potassium from soil and textile samples. This extraction technique is to be used as an alternative to acid digestion.

8. To determine the overall applicability of this hybrid process as a possible in-situ field remediation and recovery technique.

9. EXPERIMENTAL METHODOLOGY

The description of the experimental setup and the analytical methods used in all experiments for obtaining experimental data and results was required in order to verify the accuracy and precision of all the parameters measured. To accomplish the objectives outlined in Chapter 9, a series of experiments were performed using a strict methodology. Figure 19 summarizes the methodology that was employed and it encompasses this thesis. This chapter deals with a description of the parameters measured during and after experimentation of both EDTA-EK (Experiment F5) and EDTA-EK-Textile (Experiment F6) experimentation.

9.1. Soil Characterization and Preparation

The proper characterization and preparation of the soil was important in order to ensure that the experimental procedure was accurate. They represented limiting factors for the accuracy and precision of this experiment. Special attention was taken to ensure that the same procedure was used for soil characterization and preparation as was used in previous experiments. This maintained the consistency between experiments and allowed for accurate comparisons and inferences to be made. As a result, a batch of soil (15-20 kg) was prepared in advance or obtained from various agencies. In order to properly characterize the soil, Table 27 displays the tests that were performed before experimentation.

The soil was predominantly fine-grained (passing though the No. 200 sieve) material of clay nature. For experimental purposes and for documentation, the soil was designated as 6-4. A detailed characterization of the soil was performed and a variety of

parameters were obtained. Figure 20 shows the soil mineralogy and Table 28 summarizes the results that comprise this characterization.

Table 27 Tests for the Characterization of Soil

Test	*Parameter Obtained*	*Reason(s) for Performing the Test*
Sieve analysis	Grain size distribution for particles not passing through No. 200 sieve	To separate fine grained and coarse grained material. The coarse grained material can be further crushed to the desired fineness
Hydrometer analysis	Grain size distribution for particle passing through No. 200 sieve	To obtain the fine-grained portion of soil
Supercritical Fluid Extraction and Atomic absorption	Initial metal composition of the soil (K, Ca, Pb, Ni, Fe)	To characterize the mineral composition of the soil. Can dictate the CEC value and how much contaminant will be sorbed by the soil.
Cation Exchange Capacity (CEC)	CEC	Affects the location of metals (on the soil or in the pore water phase)
Sulfate Content	Sulfate concentration	Affects nickel complexation
Carbonate content	Carbonate concentration	Affects precipitation
Organic Matter Content	Percent organic matter	Affects the sorption of substances
Initial pH (Rump and Krist, 1989)	pH of soil	To see how much the pH has changed due to electrokinetic processes and due to the addition of conditioning liquid.

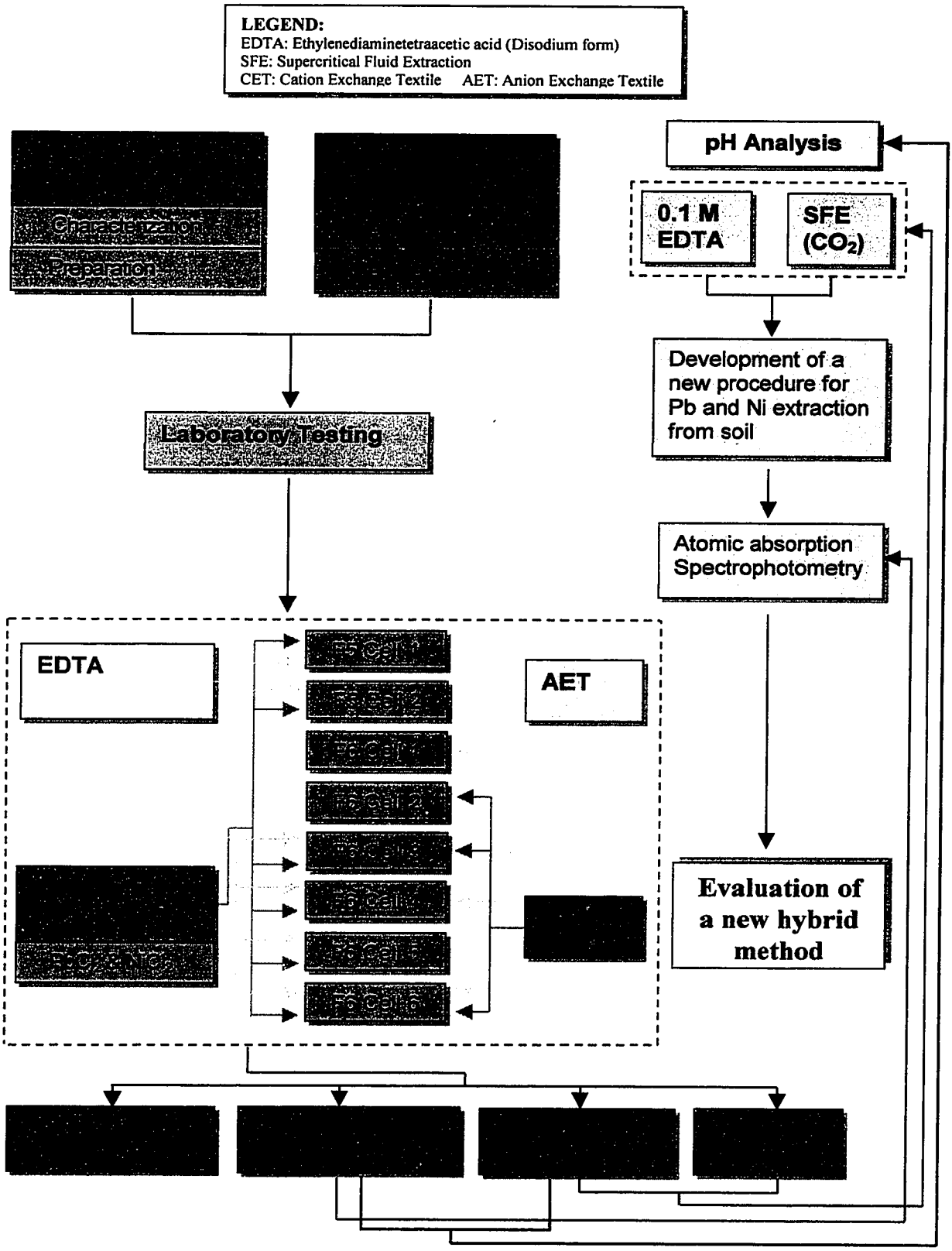

Figure 19 Experimental methodology

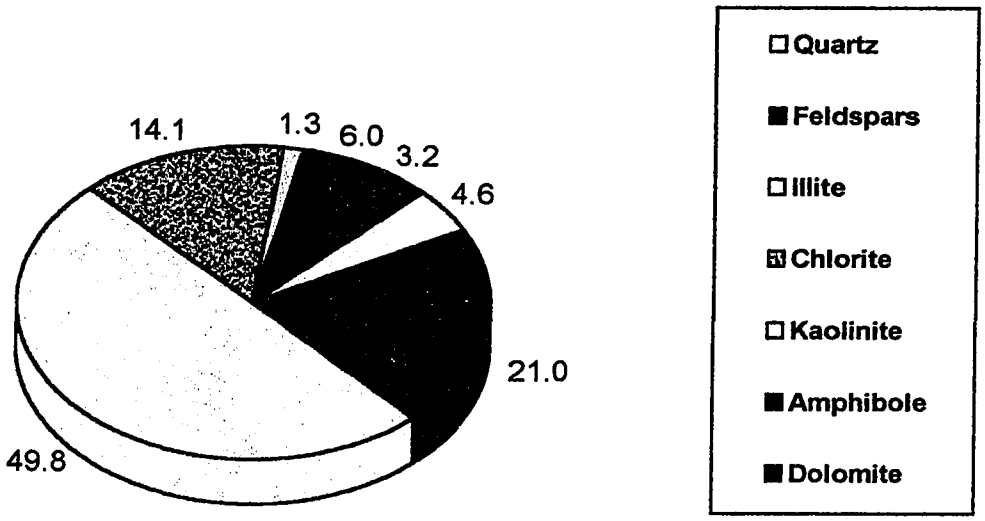

(a)

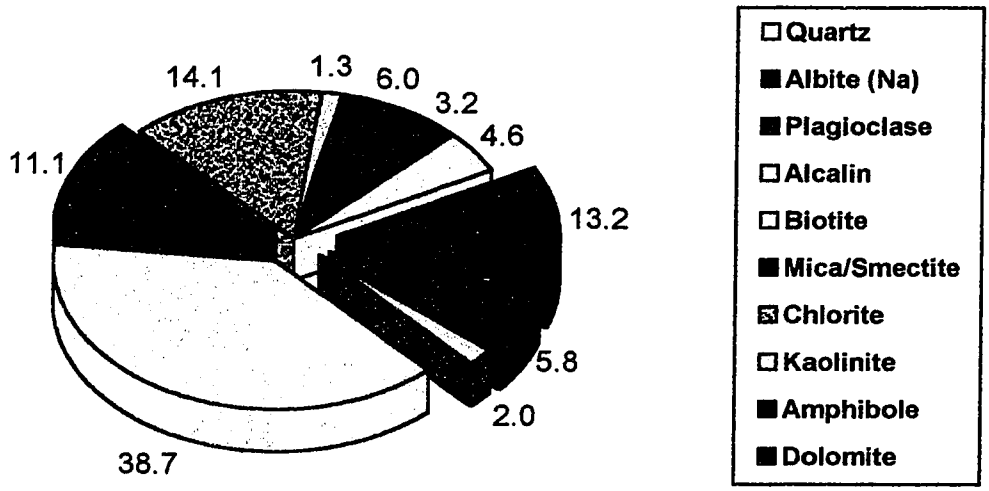

(b)

Figure 20 Normalized soil mineralogy (%): a) General composition, b) Component breakdown

Table 28 Results Pertaining to Soil Characterization for Experiment F6

Parameter Measured	*Value*
Mineral Composition	See Figure 27
Cation Exchange Capacity	21 meq/100g
pH	7.60 ± 0.05
Organic Matter Content	1.3 %
Carbonate Content	4.5 %
Total Kjeldahl Nitrogen (TKN)	0.042 %
Specific Gravity	2.753
Sulfate Test	0.6 ppm as SO_4^{2-}
Metal Content	Fe: 273 mg/kg dry soil K: 176 mg/kg dry soil Ca: 250 mg/kg dry soil Ni: 31 mg/kg dry soil Pb: 9.3 mg/kg dry soil

Following the characterization, the soil was prepared for placing into the experimental cells. The following steps underline the complete preparation of the soil for its implementation into the electrokinetic cells:

1. The soil was shredded and air dried for 96 hours to allow for the removal of pore water.

2. After air drying, the soil was milled and crushed until fine-grained clay material was obtained. Sieves were utilized in order to verify that the soil particles were sufficiently fine. The soil was then weighed.

3. On the same day of the experiment, a 1000 ppm solution of lead chloride and nickel chloride (source of contamination) was added to a known mass of dry soil, to be used on the anode side of the textile so that a 40-45% water content could be obtained. The soil was tamped in-situ to minimize the presence of air bubbles, which can effect the efficiency of the EK process.

4. The soil was then air-dried for 96 hours again, crushed and sieved using the aforementioned procedure. Ethylenediaminetetraacetic acid (0.1 M) was added to the soil so that a 40-45% moisture content was achieved.

5. The soil was then placed into the cells in five layers. Tamping was performed on each layer in order to minimize air pockets. After each cell was filled, all cells were weighed for initial cell mass.

It should be noted that both the characterization and preparation of the soil for all experiments represented standard methods in order to maintain consistency and allow for accurate comparisons between experiments. It was paramount to maintain this consistency because if the soil used is not the same and/or not prepared using the same methods, the entire experimental procedure and subsequent results that follow will be useless for comparison purposes.

9.2. Pertinent Parameters Measured: Experiment F5 and F6

The parameters measured encompass a complete analysis of the electrokinetic process, the processes occurring in the proximity of the textile and those occurring on the textiles themselves. In order to ensure that a detailed analysis of heavy metal removal using this process was achieved, a series of sampling and testing procedures were performed to accurately obtain the required parameters. Table 29 summarizes the parameters measured prior to, during and after experimentation. Each sampling and method of measurement that was utilized will be discussed in detail in the sections to follow. The parameters measured in the EK-EDTA-IET (F6) experiment were similar to those measured in the EK-EDTA (F5) experiment. The principal differences were that potential measurements were made at the textile locations using platinum probe electrodes placed on both sides of each textile. In addition, the metal concentration for

the soil in the proximity of the textile and on the textile itself was measured. Each sampling and method of measurement that was utilized will be discussed in detail in the sections to follow.

Table 29 Summary of the Measured Parameters and Analysis Performed for All Experimentation

Parameter Measured	*Frequency of Measurement*	*Storage Procedures*	*Used in Which Test*	
Initial Soil Moisture Content	Once	N/A	F5 & F6	Prior to Experiment
Soil Characterization • **Grain size distribution** • **Initial pH** • **CEC** • **Carbonates** • **Sulfates** • **Organic Matter Content** • **Metal content (Ca, Fe, Pb, Ni,K)** • **Mineral composition**	Once	N/A	F5 & F6	
Electrical Parameters (current and potential)	Daily	N/A	F5 & F6	During Experiment
pH and volume of the Cathode Liquids	Daily	Each sample (taken daily) was stored in a 20 ml sampling vial and stored at room temperature	F5 & F6	
pH of Soil	Soil was sampled at known distances and analyzed for pH	Samples were stored in a refrigerator at 5°C-7°C	F5 & F6	After Experiment (to end of table)

Metal Content of Soil (Pb^{2+}, Ni^{2+}, Ca^{2+}, Mg^{2+})	Soil was sampled from the cells at known distances. ISCO Supercritical fluid extraction was used and the extract obtained was placed in vials filled with 10 mL of distilled water Atomic absorption was used for obtaining metal content.	All soil samples were stored in a refrigerator at 5°C-7°C	F5 & F6
Metal Content on the Textile	The textile in each cell was cut in six equal segments. ISCO Supercritical fluid extraction; The extract was collected in 10 mL of distilled water Atomic absorption spectrometry metal content	All textile samples were stored in a refrigerator at 5°C-7°C	F6

9.3. Experimental Setup and Cell Configuration

The experimental setup and cell configuration consisted of a cell skeleton made of rigid polyethylene. In all experiments, the cells had the same dimensions (L=23.5 cm, w = 5.3 cm and d= 5.3 cm). Based on previous experiments and on literature previously studied (Elektorowicz, (1995), Elektorowicz, *et al.,* (1996b)), perforated tubes were used (diameter = 1.0 cm) as cathode and anode, fixed to the cell at an edge-to-edge distance of 16.0 cm. The cathodes and anodes were made of stainless steel and although the performance of graphite electrodes is high (Elektorowicz, (1995)) graphite electrodes stainless steel oxidizes more than graphite, stainless steel performance is higher, producing 3-4 times the electrokinetic flow (Acar, et al., (1996)).

The cathode extended through the cell, in order to permit the attachment of a 20 mL sampling vial at the bottom. This facilitated the collection of liquid samples on a daily basis. A reservoir attached to the anode was used where the supply of conditioning liquid was required.

The textile was placed judiciously in order to alleviate the problem of high pH formation at the cathode. Based on experiments performed previously by Elektorowicz *et. al.*, (1996a)), high pHs develop within 3.0-3.5 cm of the cathode for an anode-cathode distance of 16.0 cm. In addition, pH values lower than that of the original soil occur within 3.0-3.5 cm of the anode. Therefore, the ion exchange textiles were placed 3.0-3.5 cm from the edge of the electrodes. It was assumed that the placement of the AET would alleviate the problem of anionic precipitation near the anode and will allow for the localization of anions (i.e. metal-EDTA complexes).

The electrodes extended through the cell, in order to permit the attachment of a 20 mL sampling vial, which was attached to the bottom of the cathode, and/or anode if necessary, in order to facilitate the collection of liquid samples on a daily basis. Silver probe electrodes, 0.10 mm in diameter and spaced 1.0 cm apart were used for potential measurements. For increased sensitivity and due to their chemical inertness, platinum probes (0.05 mm in diameter) were used on both sides of the textile. Potential measurements were obtained every 24 hours, at each probe electrode location for the entire duration of the experiments.

The electrodes were attached to the DC power supply, using silver wires. The ammeter was attached in series to the electrical system. A TES Multimeter was used to measure the voltage gradient within the cell. This allowed for the determination of the resistance distribution and permitted the monitoring of electrokinetic phenomena during the experiments.

9.3.1. EDTA-EK Experiment (Experiment F5)

The experimental setup and cell configuration for the EDTA-EK experiment represented one that was easy to construct and easy to reproduce for future experiments.. Two cells were used in experiment F5 (designated F5C1 and F5C2), and their dimensions were identical. Schematic drawings of cell 1 and cell 2 are shown in Figure 21 and Figure 22, respectively. The cells differed in the mechanism used for the supply of EDTA and the liquids collected. For cell 1, 0.1 M EDTA was supplied directly through the cathode (from the bottom), and therefore liquid was not collected in this area. For cell 2, 0.1 M EDTA was supplied through a porous sand zone of the same cross-sectional dimensions of the cell. The porous quartz sand zone was 1.5 cm in thickness and was

located 1.5 cm from the cathode (edge-to-edge). A perforated plastic PVC tube, 0.5 cm in diameter, was employed in the sand zone in order to supply the EDTA. The PVC tube was similar in shape to the stainless steel electrodes employed for the electrodes. Silver probe electrodes, 0.10 mm in diameter were spaced 1.0 cm apart and were used for potential measurements.

9.3.2. EDTA-EK-Textile Experimentation (Experiment F6)

Similar to experiment F5, the experimental setup and cell configuration for experiment F6 represented one that was easy to construct and easy to reproduce for future experiments. Six cells were used in experiment F6 (designated F6C1 to F6C6, inclusive), and their dimensions were identical. Each cell skeleton was made of rigid plastic with the same dimensions as those cells used in experiment F5. The electrodes, as shown in Figure 23 were made of stainless steel with perforations within the electrode to allow for the supply of additional contaminant for the duration of the experiment. Similar to experiment F5, the electrodes extended through the cell, and a 20 mL sampling vial was attached to the bottom of the cathode in order to facilitate the collection of cathode liquids on a daily basis. Silver probe electrodes, 0.10 mm in diameter were spaced 1.0 cm apart and were used for potential measurements. At the textile location, platinum probes (0.05 mm in diameter) were used instead of silver due to their increased sensitivity. It should be noted that the same soil was employed in both experiment F5 and F6.

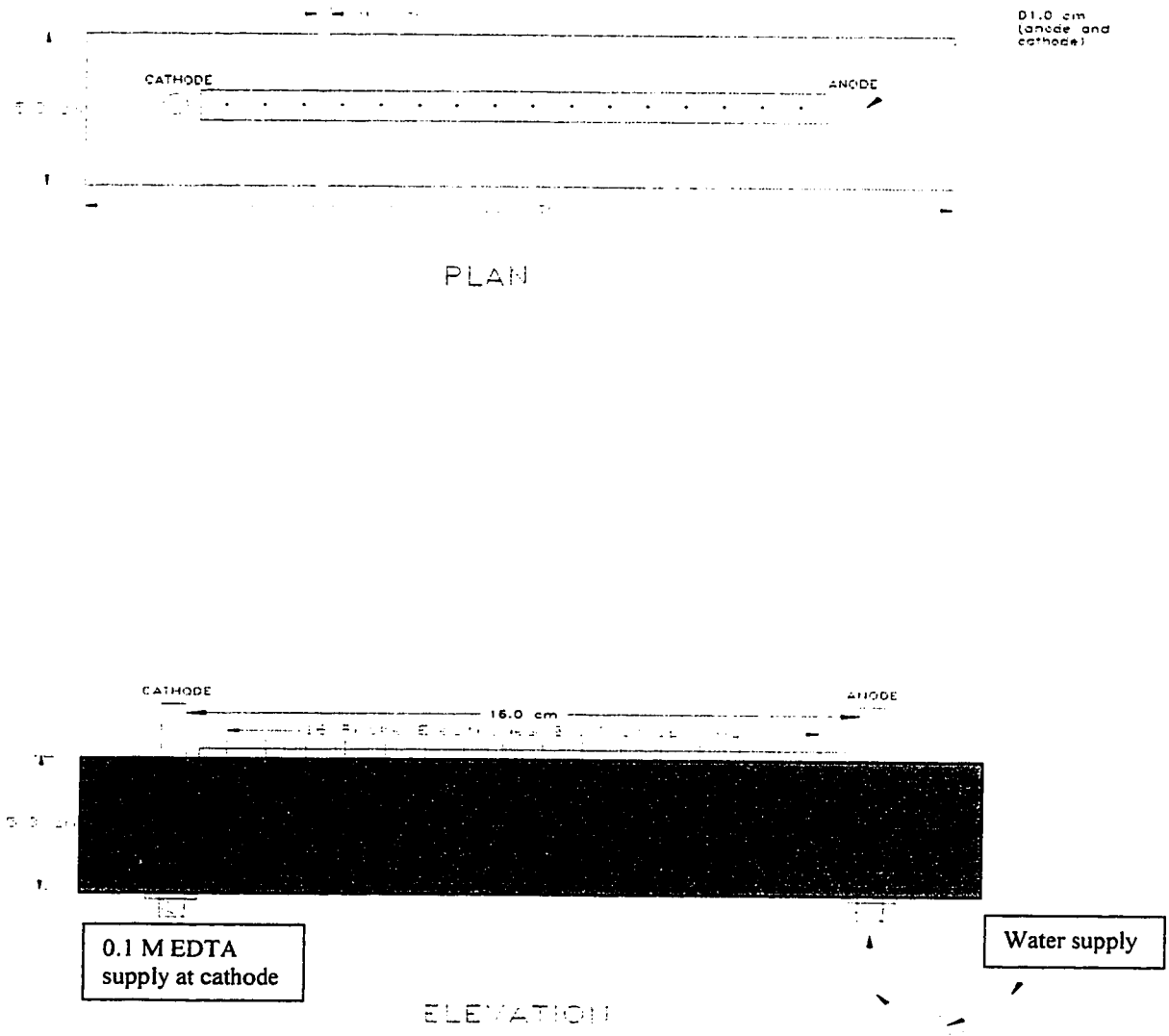

Figure 21 Configuration of Cell 1 (F5C1)

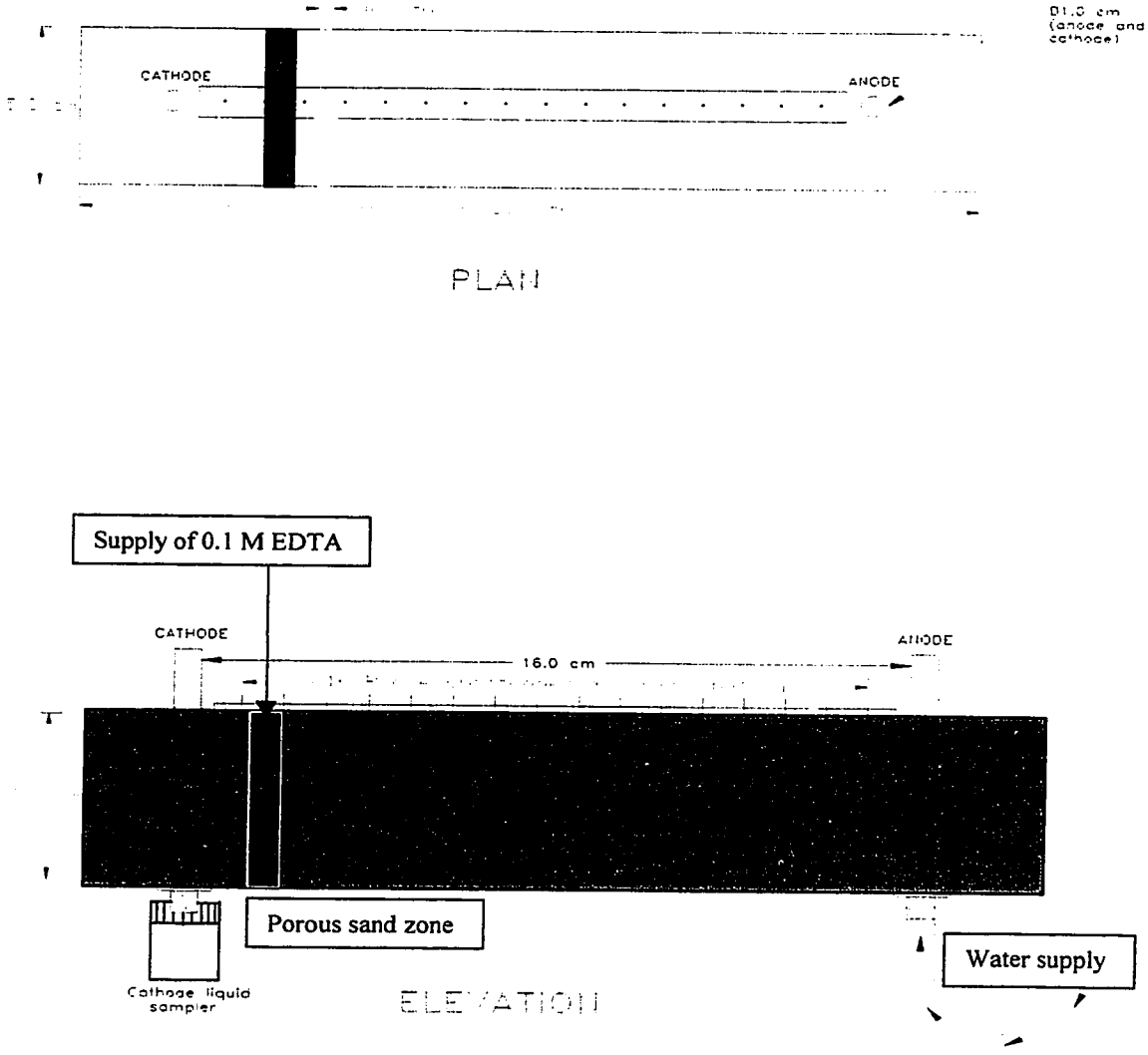

Figure 22 Configuration of Cell 2 (F5C2)

The cells differed in the number, location and type (anion and/or cation exchange) of textile utilized and whether the soil was contaminated or non-contaminated. It should be noted that the textiles were located 3.0 cm from the edge of their respective electrodes (i.e. anion exchange and cation exchange textile were located 3.0 cm from the edge of the anode and cathode respectively). Schematic drawings of cell 1 through to cell 6 are shown in Figure 24 to Figure 29 respectively. Actual photographs of the cells during experimentation are shown in Appendix B (Figure B-1 to Figure B-8) at the end of this thesis. Table C-1 (Appendix C) provides a summary of each cell in Experiment F6, including the type(s) and location(s) of textiles, whether contaminated or non-contaminated soil was present and which cells contained EDTA.

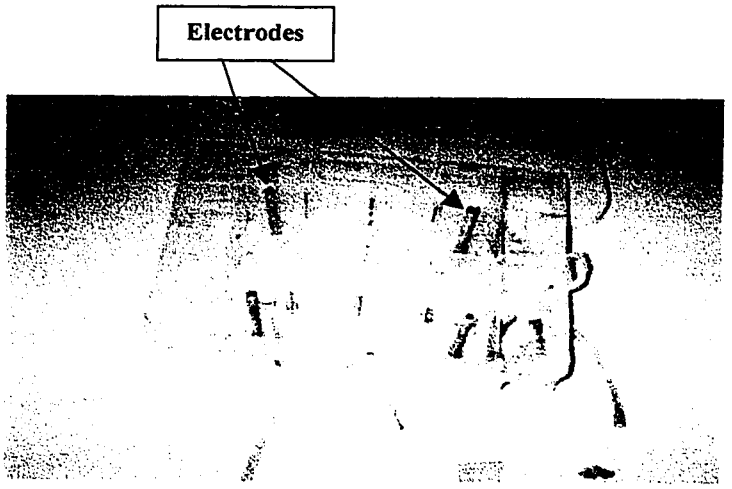

Figure 23 Stainless steel electrodes used in all experimentation

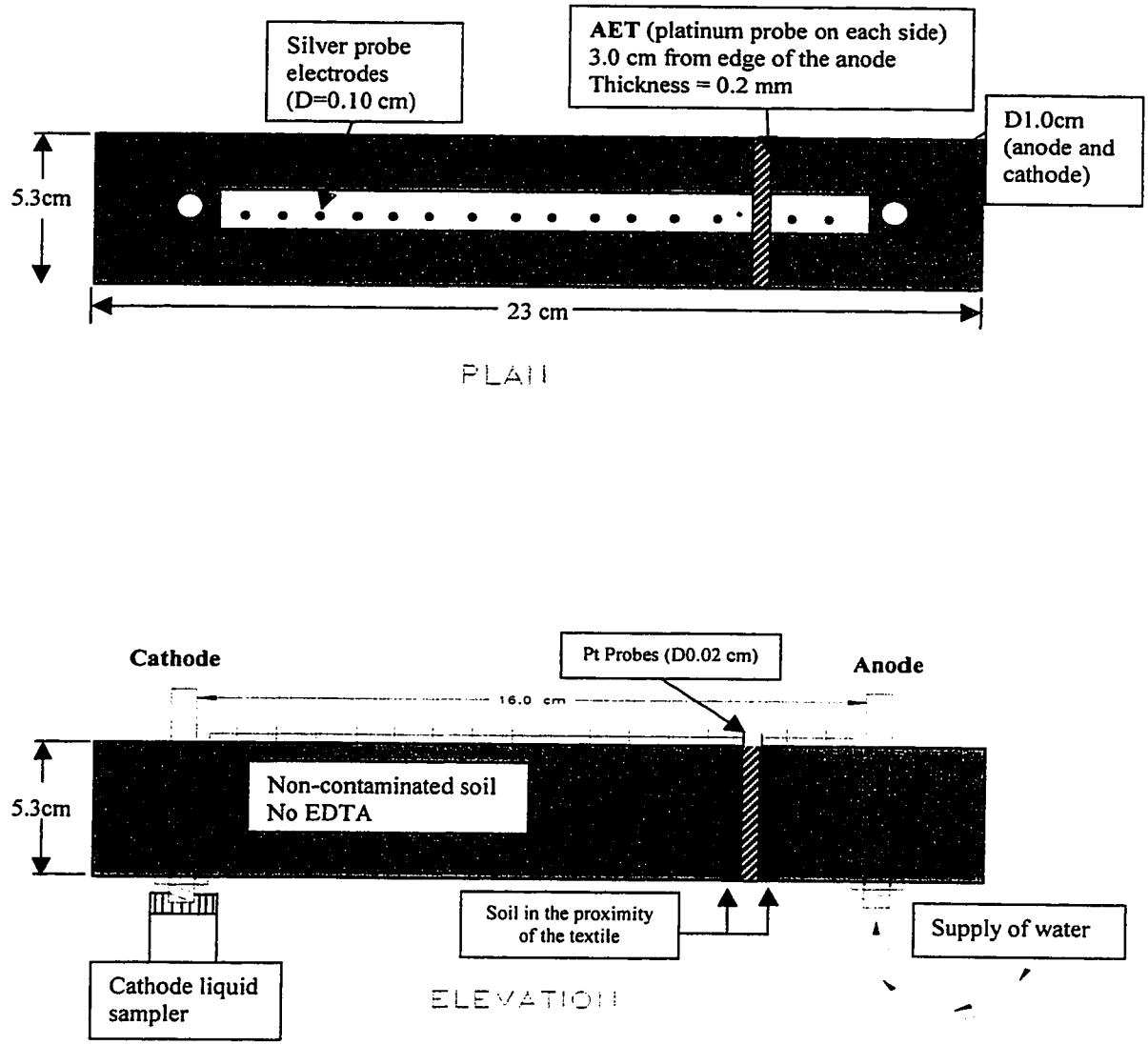

Figure 24 Experiment F6: Configuration of Cell 1 (F6C1)

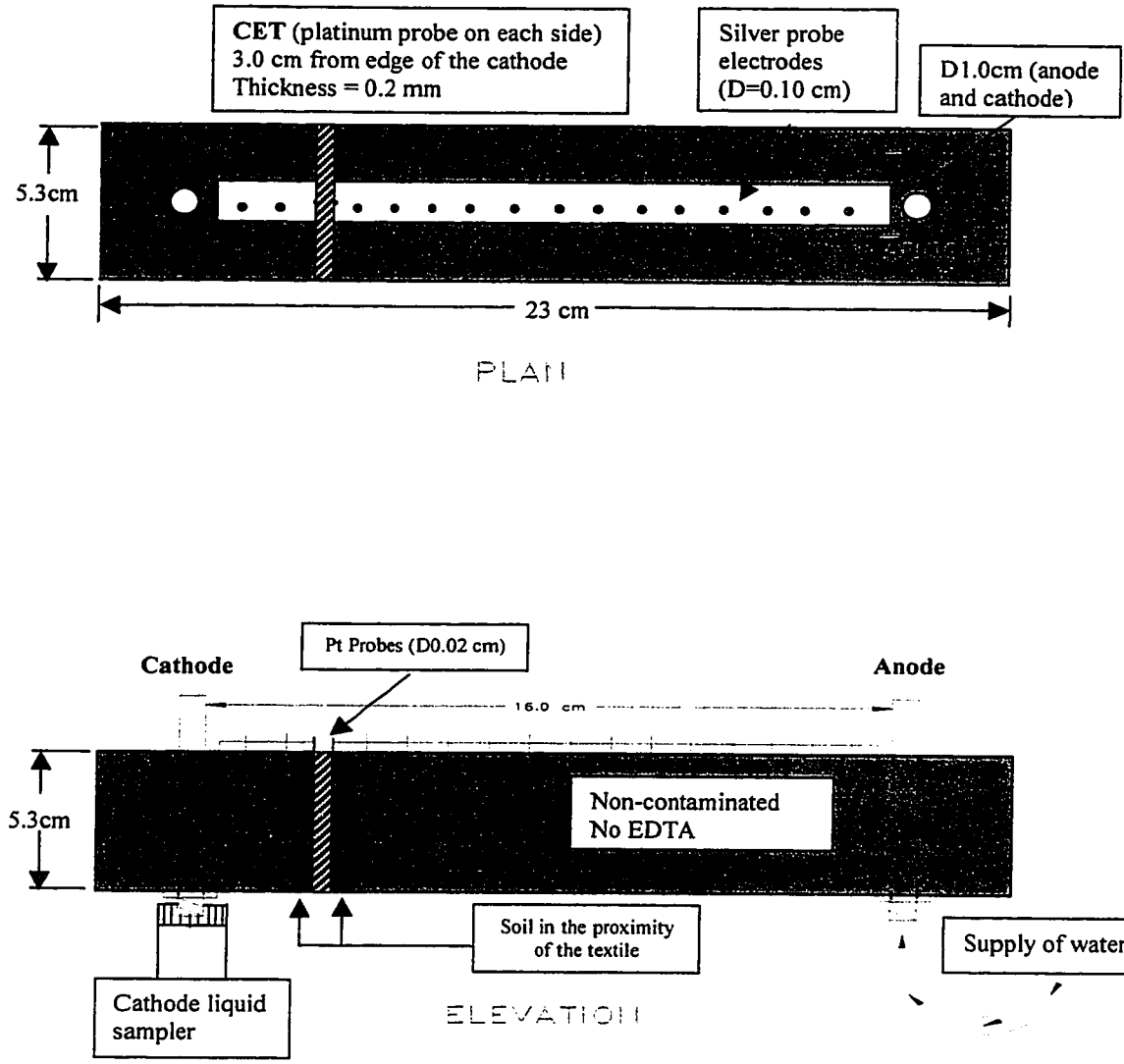

Figure 25 Experiment F6: Configuration of Cell 2 (F6C2)

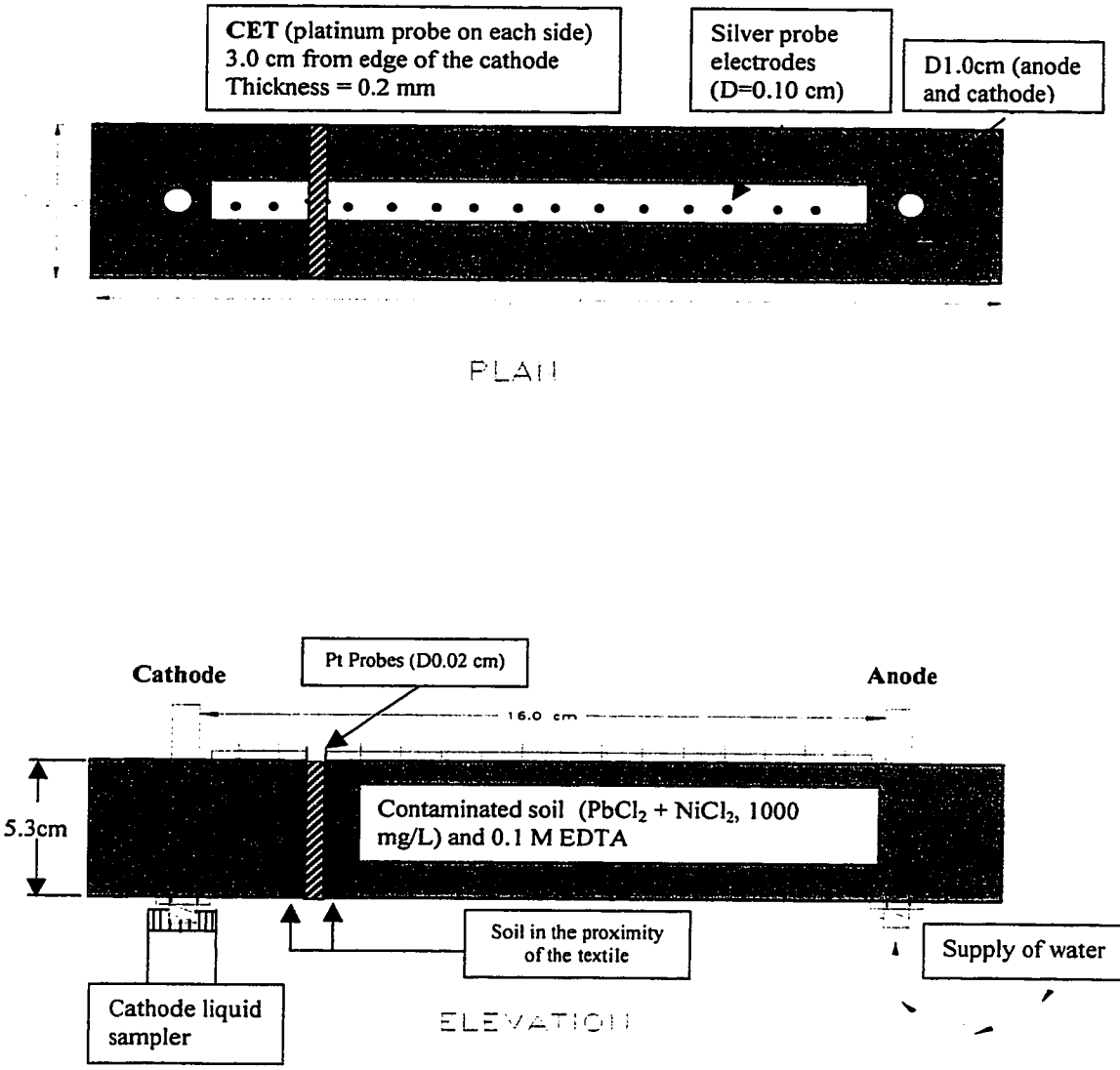

Figure 26 Experiment F6: Configuration of Cell 3 (F6C3)

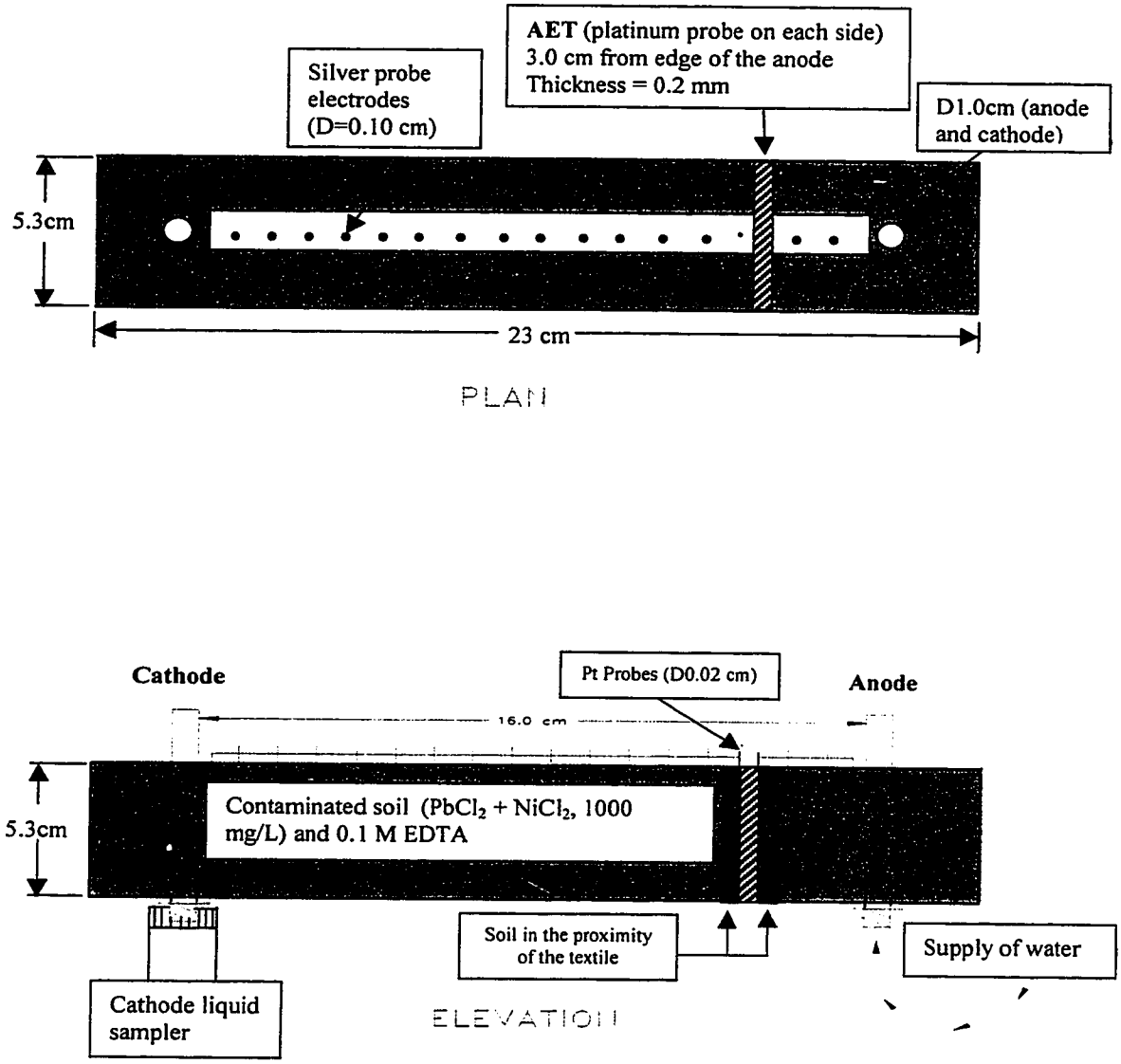

Figure 27 Experiment F6: Configuration of Cell 4 (F6C4)

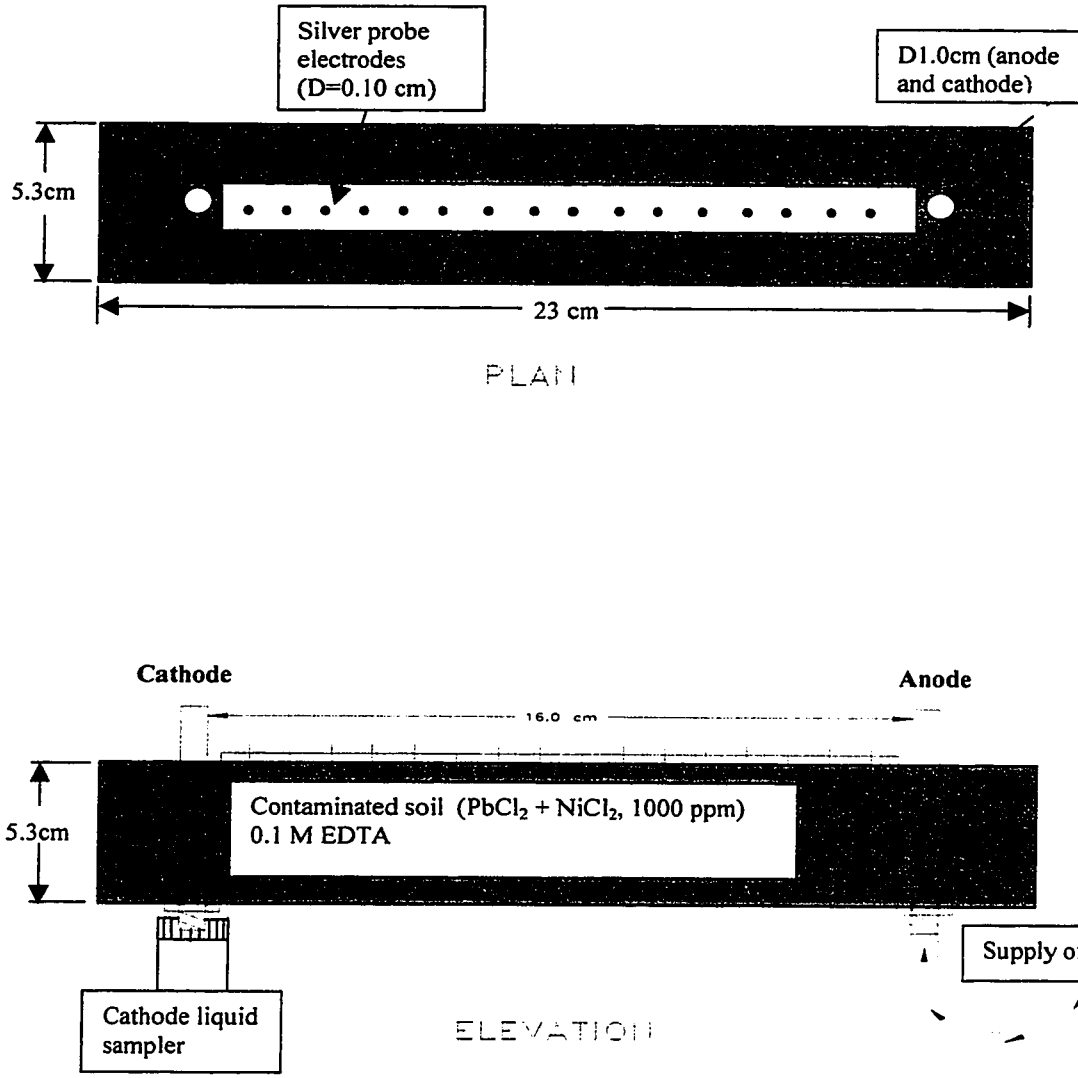

Figure 28 Experiment F6: Configuration of Cell 5 (F6C5)

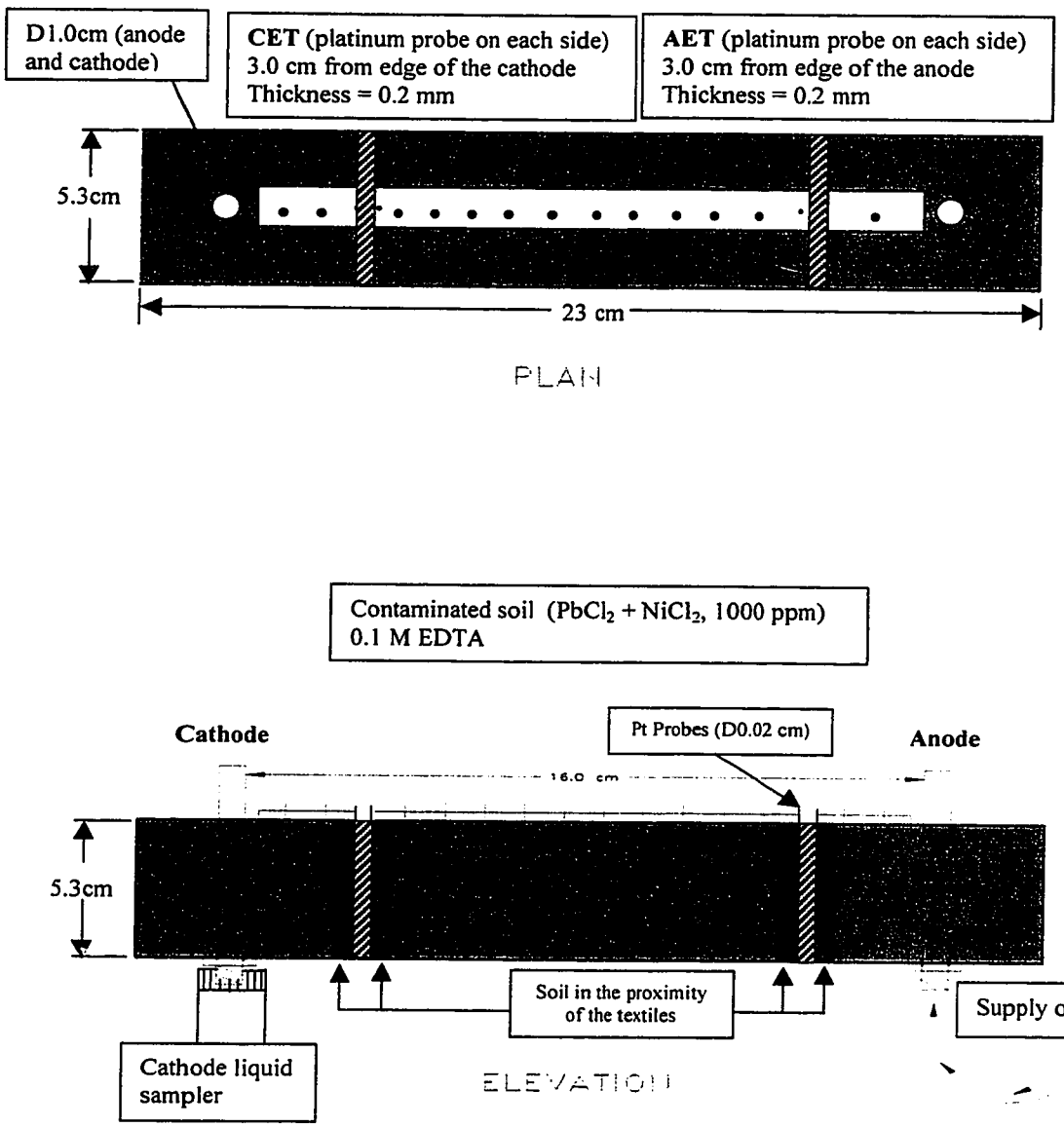

Figure 29 Experiment F6: Configuration of Cell 6 (F6C6)

9.4. Characteristics and Preparation of the Textiles

Both anion and cation exchange textiles were used in Experiment F6. Both textile types were obtained from "L'Institut des Textiles de France" and were artificially constructed of synthetic polymers. The cation exchange textile was of the strong-acid type consisting of a sulfonic group (HSO_3^-) as its primary functional group. The anion exchange textile was a strong base anion exchanger consisting of a quartenary ammonium group as its primary functional group. The properties of the textiles, resembled those discussed in the sections of this thesis pertaining to strong acid cation exchange and strong base anion exchange resins. The reader is referred to Chapter 6 for the characteristics of ion exchange textiles. The principal difference was the material used, in this case a textile rather than a resin.

Each textile was cut into a size that matched the cross section of the cell, which was 5.3 cm x 5.3 cm. No activation was required, except that the textiles were placed in petri dishes filled with distilled water for 5 days before their use. On the day of the experiment's initiation, two platinum probes were inserted on both sides of the textile in order to measure the potential across the textiles. Figure 30 shows a schematic diagram of the textiles used in this research.

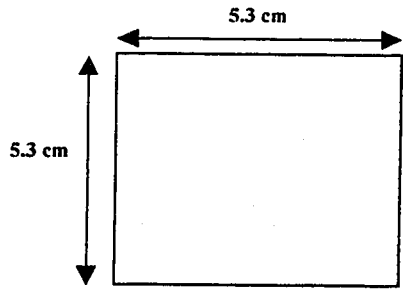

Figure 30 Schematic diagram of the textiles utilized

9.5. Apparatus, Reagents and Equipment

The following section deals with a summary of the significant apparatus and equipment used in this experiment.

9.5.1. Cell Construction and Experimental Setup

- ***Apparatus and Equipment***
  - Four Stainless steel electrodes (D = 1.0 cm (i.d.))
  - 96 Silver probe electrodes (D = 0.10 cm)
  - 12 Platinum Electrodes (D-0.02 cm)
  - 30 ml plastic sampling bottle (sampling of cathode liquids)
  - Flexible plastic tubing (D=1.0-1.5 cm)
  - DC power supply (see Figure B-9)
  - TES Scientific Multimeter (see Figure B-10)
  - EDTA and water supply reservoirs

- ***Reagents***
  - *1000 ppm solution of $PbCl_2$ and $NiCl_2$*
    Prepared from stock of $PbCl_2$ and $NiCl_2 \cdot 6H_2O$
  - *0.1 M EDTA*
    Prepared from Disodium Ethylenediamine Tetraacetate
    Fisher Chem Alert Guide
    M.W. 372.24 g/mol
    Pb (0.005%)
    Iron (0.01%)
    Nitrilotriacetic Acid (0.1%)

9.5.2. pH Measurements

- ***Apparatus and Equipment***
  - Fisher standard multimeter
  - Mechanical shaker
  - 20 ml sample vials
  - 10 ml graduated pipettes

- ***Reagents***
  - Distilled water
  - Buffer solutions (pH=7 and pH=10)

9.5.3. SFE-AAS System for Heavy Metals

- *Apparatus and Equipment*
  - 10 ml reusable plastic cartridges
  - ISCO Two-Chamber SFX 220 Supercritical Fluid Extractor (SFE)
  - Perkin-Elmer Flame Atomic Absorption Spectrophotometer (AAS)

- *Reagents*
  - 1000 ppm solution of $PbCl_2$ and $NiCl_2$
  - 0.1 M EDTA (see section 9.5.1)
  - Standard solutions of Calcium (5 ppm), Iron (5 ppm), Lead (20 ppm), Nickel (5 ppm), and Potassium (2 ppm)

9.6. Measurements, Sampling, Data Retrieval and Analytical Methods: Experiment F5

In order to properly analyze the overall effectiveness of this enhanced technology, a myriad of samples were obtained related to the principal aspects of experiment F5. In addition, standard data retrieval procedures were used during the experiment that continued to be used in future experiments. Table 29 summarized the entire sampling regime along with the data retrieval methods and storage procedures that were used.

9.6.1. Measurement of EDTA Supplied (Experiment F5)

The volume of EDTA supplied was regulated through the use of a supply system connected to graduated cylinders for easy daily measurement. Each cell had a separate reservoir for the supply of the chelation agent. Transparent, flexible rubber tubing was connected from the graduated cylinder to the bottom of the anode (below the cell) for the supply of EDTA. Hydraulic pressure head was used as the driving force for this supply. Initial and final readings were taken from the graduated cylinder in order to obtain the actual volume supplied. This entire configuration allowed for the easy and inexpensive

measurement. In addition, the supply system is modular, thereby allowing for its disconnection and reuse in future experiments.

9.6.2. Soil Sampling Procedures (Experiment F5)

As summarized in Table 29, the soil was sampled in approximately equal thickness and at known distances. Eighteen samples were obtained from cell 1 and cell 2. The soil from both cells were sampled from the middle row and not from the periphery of the cells. The sampling configuration is shown in Figure 31. The large number of samples was necessary in order to obtain an accurate representation of the pH and the metal content of the soil and their variation with distance. In addition, the number of samples are necessary in order to verify the degree of mobility of the heavy metals within the soil and to see if metals were concentrated in any given area, thereby adversely affecting the removal efficiency. The method used for the determination of soil pH and metal content will be discussed later in this report.

M1	M2 •	M3	M4	M5	M6	M7	M8	M9	M10	M11	M12	M13	M14	M15	M16	M17 •	M18
	C															A	

F5C1

M1	M2 •	M3	M4	M5	M6	M7	M8	M9	M10	M11	M12	M13	M14	M15	M16	M17 •	M18
	C															A	

F5C2

Figure 31 Soil sampling configuration for F5C1 and F5C2 (experiment F5)

9.6.3. Determination of Cathode Liquid and Soil pH (Experiment F5)

The determination of pH values for both the cathode liquids and the soil were performed using standard pH tests. The pH meter was periodically standardized using pH=7 and pH=10 buffer solutions. As stated previously, liquid from the cathode was extracted daily and directly measured for pH using a standard multi-electrode pH/voltmeter. A standard Fisher multi-meter was used for these pH measurements. Since these samples were liquid, additional preparation was not necessary.

Additional sample preparation was necessary for the determination of soil pH. As a result, 3.0 g of crushed air-dried soil from each sample was paced in a 20 ml vial. Distilled water (7.5 ml) was added to the soil. The suspensions obtained were shaken for 1 hour and allowed to settle for 0.5 hours. The pH of the supernatant was obtained once the reading became stable. The measurement of each sample took 5-7 minutes.

9.6.4. Supercritical Fluid Extraction and Atomic absorption Spectrophotometry

Supercritical fluid extraction, using 0.1 M EDTA (modifier) and CO_2 (supercritical fluid) was used in the preparation of samples for metal content analysis using atomic absorption spectrophotometry (AAS). It represented a newly formed analysis technique for the extraction of heavy metals from natural clay soil. Extensive preliminary testing was performed, as will be discussed in chapter 10, to determine the viability and applicability of this method. Reusable plastic, 10 mL SFE cartridges were used. The soil samples were oven dried at 105°C and crushed. 1.00±0.01g of soil was placed in each cartridge. 9.0 mL of 0.1 M Na_2EDTA was added to each cartridge and the mixture was shaken for 2 hours at 60 rpm. Each cartridge was extracted, dynamically at

90°C and 5000 psi for 15 min. The extract was collected in 10 ml of distilled water. The distilled water was tested for metal content (using AA spectrophotometry) and used for background correction. The samples were directly subjected to AAS analysis for lead, nickel, iron and calcium concentration. The concentration of lead, nickel, calcium, and iron was determined using flame AAS analysis. A discussion and interpretation related to the results obtained are dealt with in later sections of this report. The results obtained from this analysis give a reflection of the overall effectiveness of this technology.

9.7 Measurements, Sampling, Data Retrieval and Analytical Methods: Experiment F6

In order to analyze the overall effectiveness of this enhanced technology, a myriad of samples were obtained related to the principal aspects of experiment F6. The sampling methods used in experiment F6 were similar to those mentioned in experiment F5 and the reader is referred to Table 29 for a summary. The methods used in experiment F5 and F6 were maintained as similar as possible, in order preserve consistency and proper comparison of results.

9.7.1. Soil Sampling Procedures (Experiment F6)

As summarized in Table 29, the soil was sampled in approximately equal thickness and at known distances. The soil from all cells were sampled from the middle row and not from the periphery. The sampling configuration is shown in Figure 32. The large numbers of samples were necessary in order to obtain an accurate representation of the pH and the metal content of the soil and their variation with distance. In addition, the number of samples are necessary in order to verify the degree of mobility of the heavy metals within the soil and to see if metals were concentrated in any given area, thereby

adversely affecting the removal efficiency. The method used for the determination of soil pH and metal content will be discussed later in this report.

M1	M2 ●	M3	M4	M5	M6	M7	M8	M9	M10	M11	M12	M13	M14	M15	M16	M17 ●	M18
	C															A	

Figure 32 Soil sampling configuration for all cells: Experiment F6 (sample location for the textiles and the soil in the proximity of the textile is not shown)

9.7.2. Sampling of the Soil Near the Textile (Experiment F6)

The sampling from the cells and the division of the soil near the textile are shown in Figure 33. The soil in the proximity of the textile in each cell was of paramount importance to this experiment because the results obtained related to metal content determined the efficiency of the electrokinetic process coupled with the use of the ion exchange textile. If the metal content of this area of soil was high, the electrokinetic force was effective in the mobilization of the heavy metals from anode to cathode. The soil near the textile was removed from each cell with the textile so that enough soil (5.0-10.0 mm thickness) was taken from the anode and cathode side. The textile was therefore covered with soil on both sides. The sample obtained was placed into a plastic petri dish and refrigerated. For analysis purposes, the soil was divided into six parts (approximately

18 mm x 26 mm and placed in plastic bags for storage until extraction procedures were initiated.

9.7.3. Sampling Protocol for the Ion Exchange Textile (Experiment F6)

The sampling of the ion exchange textile in each cell was necessary in order to determine the concentration of metals (lead and nickel in particular) exchanged onto the textile. The concentration of metals on the textile dictated the heavy metal removal efficiency and the degree of localization. After the soil on textile was divided and sampled, the textile itself was divided into six equal parts (26 mm x 18 mm) for each cell as shown in Figure 34. All six samples were subjected to supercritical fluid extraction with CO_2 (to be discussed in Chapter 10) and AA spectrophotometry for lead, nickel, potassium, calcium and iron concentration analysis.

Cathode Side-Top-Left **S-CSTL**	**Cathode Side-Top-Middle** **S-CSTM**	**Cathode Side-Top-Right** **S-CSTR**
Cathode Side-Bottom-Left **S-CSBL**	**Cathode Side-Bottom-Middle** **S-CSBM**	**Cathode Side Bottom-Right** **S-CSBR**

Soil Near the Textile, Facing the Cathode (F6C1 to F6C4, F6C6)

Anode Side-Top-Left **S-ASTL**	**Anode Side-Top-Middle** **S-ASTM**	**Anode Side-Top-Right** **S-ASTR**
Anode Side-Bottom-Left **S-ASBL**	**Anode Side-Bottom-Middle** **S-ASBM**	**Anode Side Bottom-Right** **S-ASBR**

Soil Near the Textile, Facing the Anode (F6C1 to F6C4, F6C6)

Figure 33 Sampling and division of the soil near the textile

Top Left T-TL	Top Middle T-TM	Top Right T-TR
Bottom Left T-BL	Bottom Middle T-BM	Bottom Right T-BR

Figure 34 Division of the textile for F6C1 to F6C4, and F6C6

9.8. Experimental Duration

The EDTA-EK (F5) experiment was executed for a duration of 361 hours. The EDTA-EK-IET experiment (F6) was executed for a duration of 546 hours. The soil and textiles were sampled immediately after disconnecting the power supply. Table 30 shows the initial data for EDTA-EK (F5) and EDTA-EK-IET (F6) experimentation

Table 30 Initial Data Pertaining to Soil use in Electrokinetic Experimentation (Experiment F5 and F6)

Cell	*Mass of Wet Soil in Cell (kg)*	*Initial Moisture Content*
F5C1	1124.8	44.6
F5C2	1153.6	44.9
F6C1	1098.2	43.0
F6C2	1101.6	44.5
F6C3	1107.3	43.8
F6C4	1123.2	43.6
F6C5	1110.3	42.5
F6C6	1134.2	44.6

10. DEVELOPMENT OF A NEW ANALYTICAL METHOD FOR METAL EXTRACTION USING SUPERCRITICAL FLUID EXTRACTION (SFE)

ISCO supercritical fluid extraction (SFE) was examined as an alternative to existing acid digestion techniques for the extraction of heavy metals from clay soil samples. This was to be used for the analysis of heavy metal concentrations after the completion of electrokinetic experimentation. Fundamentally, SFE is advantageous over acid digestion from numerous standpoints:

1. SFE is safer than acid digestion. SFE requires supercritical CO_2 and a modifier if desired, which do not pose a serious health threat. Acid digestion requires the use of high concentrations of nitric acid, hydrochloric acid, sulfuric acid and 30% hydrogen peroxide. These chemicals are highly reactive, dangerous and require the use of neoprene gloves and facial shield.

2. SFE is faster. Each SFE sample can be obtained in 15-30 minutes, while acid digestion samples are typically obtained in 3-6 hours.

3. In most cases for heavy metal extraction, SFE does not require the use of a fume hood. Therefore, a supercritical fluid extraction apparatus can be placed in areas not equipped with a fume hood.

10.1. Literature Review and Current Research

Supercritical fluid extraction (SFE) of metals from soil has been performed extensively in research. It has been used for the extraction of metals from clayey soil. Coupled with atomic absorption spectrophotometry, it is useful for the extraction and analysis of metal concentrations in solid-phase or slurry-phase media. Laintz *et al.*, (1992), and Lin *et al.*, (1993) extracted metals from liquid and solid materials using lithium bis-triflouroethyl-dithiocarbamate (FDDC) as a modifier. Using this modifier, the metal-FDDC complexes showed high solubilities in supercritical CO_2. Laintz *et al.*

(1992), performed the extraction at pressures in the range of 69.0-79.3 bars, and at a temperature of 35°C. Removal efficiency for copper was 90 % to 95 % at a CO_2 density of 0.35 g/cm^3. Lin *et al.*, (1993) used a pressure of 150 atm and 60°C and obtained extraction efficiencies for La^{3+}, Eu^{3+} and Lu^{3+} of 91 %, 96 % and 99 % respectively.

Wang and Marshall, (1994), performed a series of SFE tests in order to obtain speciate metals within soil samples. Tetrabutylammonium dibutyldithiocarbamate (TBADB-DTC) was used as a modifier, in order to improve the metal solubility in supercritical CO_2. The metal complexes had a lower solubility in CO_2 than those in the experiments performed by Laintz *et al.* (1992). Fluorinated compounds tend to form complexes that are more soluble in supercritical CO_2, than their non-fluorinated counterparts. Using on-line atomic absorption spectrophotometry, metal speciation was achieved. Wenzel, *et al.*, (1993), extracted nickel (II), copper (II), zinc (II) and lanthanum (III) using supercritical CO_2 and bis-β-diketonate compounds as modifiers.

10.2. Supercritical Fluid Extraction versus Acid Digestion: Experiments

In order to determine the extraction efficiency and feasibility of SFE techniques versus acid digestion, the concentration of various metals measured in the extract of SFE samples and acid digestion samples was compared. The soil used consisted the initially prepared soil that was used for all experiments discussed in this thesis. For the SFE test, 2.5 mL cartridges were used consisting of 1.00 g of soil and 1.5 mL of 0.1 M EDTA. The samples were shaken for 30 minutes and placed into the supercritical fluid extractor for a 15 minute dynamic extraction at 90°C and 5000 psi. The restrictor temperatures were also maintained at 90°C. The acid digestion procedure that was employed was EPA

Method 3050 ("Acid Digestion of Soil, Sediments and Sludges"). A summary of results for various metals is shown in Table 31.

Table 31 Comparison of SFE Technique Versus Acid Digestion

Metal Type	*Concentration of Metals in Extract: SFE Technique (ppm)*	*Concentration of Metals in Extract: Acid Digestion (ppm)*	*% Increase from Acid Digestion*
Lead	9.3	Below detectable limits	-
Nickel	31.1	Below detectable limits	-
Calcium	249.8	56.0	346 %
Potassium	61.8	63.8	-3.1 %

Table 31 shows that the utilization of SFE techniques with EDTA was significantly higher in the extraction of lead, nickel and calcium. The extract from acid digestion produced lead and nickel concentrations that were below detectable limits during atomic absorption spectrophotometry. Appreciable lead and nickel concentrations were detected in the extract from SFE procedures. The calcium concentration in the SFE extract was 346 % higher than that of the acid digestion extract. Therefore, supercritical fluid extraction with EDTA represents a viable and more efficient method for analyzing metals in clay soils, as is the case in the analysis of soil after the termination of electrokinetic treatment.

10.3. Supercritical Fluid Extraction Tests: Obtaining Optimum Shaking Time

Once it was established that SFE extraction with EDTA was more efficient in the extraction of heavy metals, particularly lead and nickel, the establishment of the optimum

shaking time was necessary. This optimum shaking time was used for all future analysis for soil samples obtained from the enhanced EK soil treatment. Sample preparation consisted of the use of 1.00 g of soil with the addition of 9.0 mL of 0.1 M EDTA directly into the cartridge. The samples were then shaken at 60 rpm at 30 minute, 1 hour, 2 hour, 4 hour and 8 hour time intervals using an AROS orbital shaker. When required, the samples were extracted dynamically for 15 minutes at 90°C and 5000 psi. It should be noted that four samples for each shaking time were used:

1. A control sample using 9.0 mL 0.1 M EDTA, 1.00 g of soil and shaking, with no extraction (a control sample for extraction). This allows for the determination of the extraction effect of EDTA on its own. The samples were allowed to settle for 1 hour and the supernatant was filtered using Whatman Filter Paper No. 41 to remove colloidal particles.

2. A second control sample using 9.0 mL of distilled water, 1.00 g of soil, shaking and extraction (a control sample for EDTA).

3. Actual samples consisting of 9.0 mL of 0.1 M EDTA, 1.00 g of soil, shaking and extraction. Table 32 summarizes the testing profile and sample designation.

10.4. Results of Supercritical Fluid Extraction Tests

The results of supercritical tests for the determination of the optimum shaking time are shown in Figure 35. The five metals (calcium, iron, lead, nickel and potassium) which were analyzed are shown versus shaking time, for samples employing 1) EDTA and extraction (SFE) and 2) EDTA without supercritical fluid extraction. All metals show a significant improvement in extract concentration when SFE is employed, independent of shaking time, due to the enhanced solubility of metal-EDTA complexes in supercritical CO_2. Table 33 shows the average percent increase in metal extracted when SFE is employed.

Table 32 Description of Sample Preparation in SFE Extraction Heavy Metal Analysis

Sample No.	*Mass of soil Used (g)*	*Volume of 0.1 M EDTA (mL)*	*Shaking time (hrs)*	*SFE Extraction?*
SW-SFE 0.5	1.0	0.0 (9.0 mL of distilled water)	0.5	Y
SE 0.5	1.0	9.0	0.5	N
SE-SFE 0.5 A	1.0	9.0	0.5	Y
SE-SFE 0.5 B	1.0	9.0	0.5	Y
SW-SFE 1.0	1.0	0.0 (9.0 mL of distilled water)	1.0	Y
SE 1.0	1.0	9.0	1.0	N
SE-SFE 1.0 A	1.0	9.0	1.0	Y
SE-SFE 1.0 B	1.0	9.0	1.0	Y
SW-SFE 2.0	1.0	0.0 (9.0 mL of distilled water)	2.0	Y
SE 2.0	1.0	9.0	2.0	N
SE-SFE 2.0 A	1.0	9.0	2.0	Y
SE-SFE 2.0 B	1.0	9.0	2.0	Y
SW-SFE 4.0	1.0	0.0 (9.0 mL of distilled water)	4.0	Y
SE 4.0	1.0	9.0	4.0	N
SE-SFE 4.0 A	1.0	9.0	4.0	Y
SE-SFE 4.0 B	1.0	9.0	4.0	Y
SW-SFE 8.0	1.0	0.0 (9.0 mL of distilled water)	8.0	Y
SE 8.0	1.0	9.0	8.0	N
SE-SFE 8.0 A	1.0	9.0	8.0	Y
SE-SFE 8.0 B	1.0	9.0	8.0	Y

Samples Designation:
S = soil, E = EDTA, W = distilled water, SFE = Supercritical Fluid Extraction, Numbers = shaking times
A, B = denote sample designation

Table 33 Average Percent Increase in Extracted Metals (SFE versus No SFE)

Metal	*% Increase in Metal Extracted when Utilizing SFE Technique*
Calcium	144 %
Iron	24 %
Lead	213 %
Nickel	117 %
Potassium	124 %

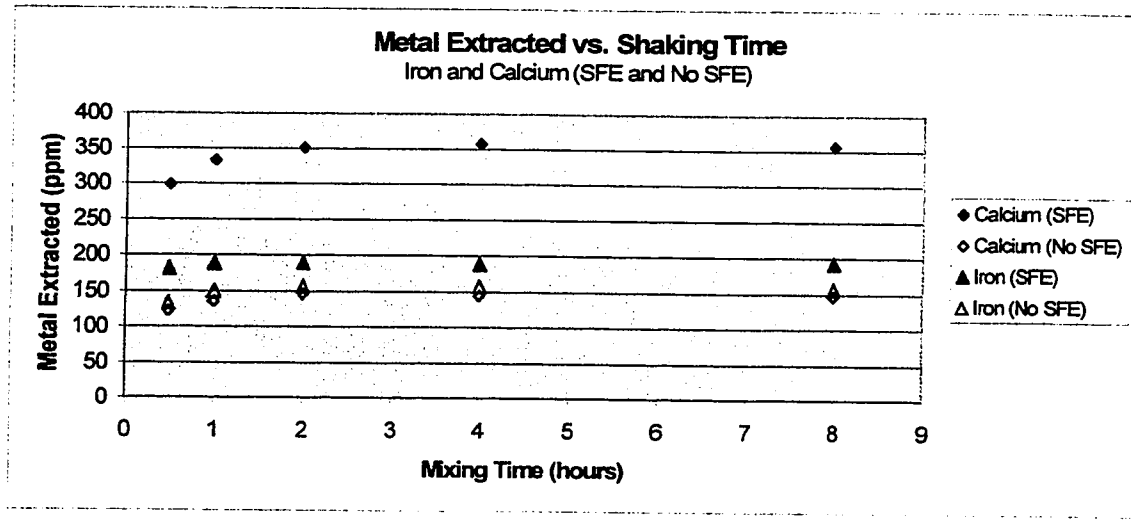

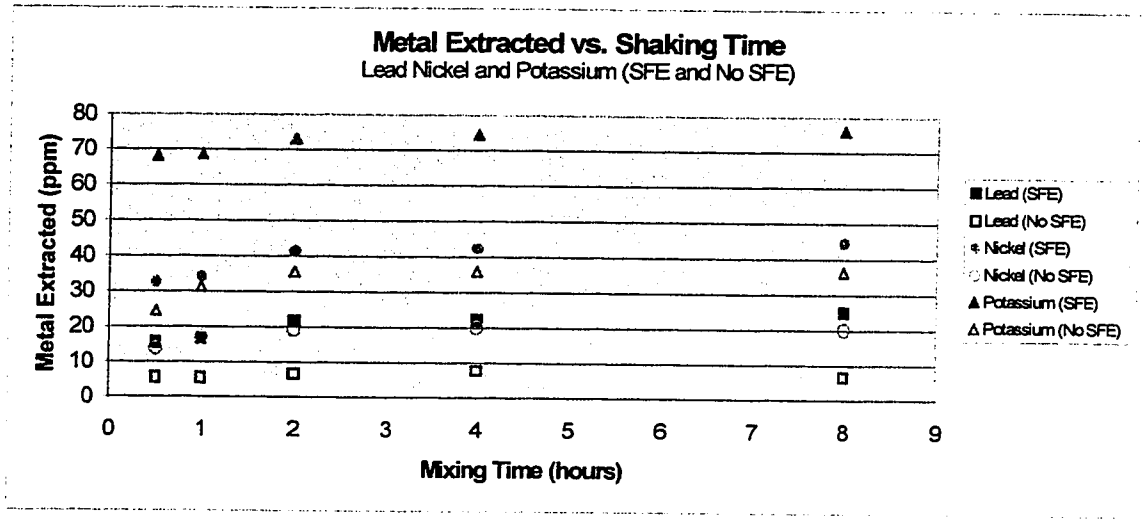

Figure 35 Metal extracted versus shaking time (supercritical fluid extraction analysis)

All metals show a significant percent increase with the exception of iron. Nevertheless, it can be seen from Table 39 that the use of SFE methods provides an appreciable improvement in the concentration of metal extracted, and therefore warrants its use.

Figure 35 shows a general increasing trend in metal concentration versus shaking time, for all metals. The highest percent increases occur from 0.5 to 2.0 hours of shaking. After 2.0 hours, the concentration of metals in the extract does not increase appreciably. Table 34 shows the percent increase in metals extracted within each time interval.

Table 34 Metal Extraction: Percent Increase versus Shaking Time

Metal	***Shaking Interval 1*** ***0.5 – 1.0 hrs.***	***Shaking Interval 1*** ***1.0 – 2.0 hrs.***	***Shaking Interval 1*** ***2.0 – 4.0 hrs.***	***Shaking Interval 1*** ***4.0 – 8.0 hrs.***
Calcium	10.3 %	5.2 %	1.7 %	-0.1 %
Iron	3.5 %	1.0 %	-1.0 %	2.2 %
Lead	6.7 %	23.1 %	2.5 %	11.1 %
Nickel	4.3 %	17.6 %	2.2 %	4.9 %
Potassium	0.7 %	6.2 %	1.7 %	2.3 %

For all metals with the exception of iron, the most significant extraction increases are observed when the shaking time is increased from 1.0 hours to 2.0 hours. After 2.0 hours the metal concentration in the extract does not increase drastically. Based on the results shown, 2.0 hours is the optimum and most practical shaking time. The small improvement in metal extraction, when the mixing time is increased from 2.0 to 4.0 hours, does not warrant its use from a practical standpoint.

10.5. Conclusions and Finalized SFE Procedure

Based on the results obtained, supercritical fluid extraction is a viable alternative to acid digestion. The following conclusions can be made with respect to the use and overall applicability of supercritical fluid extraction techniques for the extractions studied in this chapter:

1. SFE techniques, with the use of EDTA as a modifier, had a higher extraction efficiency than acid digestion for all metals tested, except for iron.
2. Using SFE techniques with EDTA and mixing showed an appreciable improvement in extraction over standard EDTA addition and mixing (without SFE). Therefore, the improvement is due to the use of SFE with CO_2.
3. The optimum and most practical shaking time for the extraction of Pb, Ni, Ca, Fe, and K was 2 hours. Increasing the shaking time to 4 hours or 8 hours did not improve the extraction enough to warrant its use.

The results obtained and presented in this chapter show that SFE is a viable alternative to acid digestion and it can be applied to any porous medium. Based on these results, this technique was used in combination with flame atomic absorption spectrometry for the extraction and analysis of Ca, Fe, K, Ni, and Pb from soil and textiles. The results pertaining to metal extraction and concentration analysis, presented throughout this thesis will utilize this technique, with a shaking time of 2.0 hours.

Based on an analysis of the results obtained, the following represents the finalized procedure that is to be used for the extraction of metals from soil and textile samples using SFE techniques with EDTA:

1. Weigh 1.00 g of each soil sample to be extracted and place it in 10 mL reusable SFE cartridge. If a textile is to be extracted, place a cut sample of the textile into the cartridge.

2. Add 9.0 mL of 0.1 M EDTA to each cartridge. Shake for 2 hours at room temperature at 60 rpm.

3. Set SFE restrictor and chamber temperature to 90°C. Extract dynamically for 15 minutes, at 5000 psi.

4. Collect extract in 10 mL of distilled water and analyze for metal concentration using AAS procedures.

It should be noted that textile samples typically have soil particles adhered to their surface (physical process), which have not actually exchanged via chemical methods. As a result, textiles must be prepared before they are placed into the cartridges for extraction. Each textile sample is placed into a 125 mL Erlenmeyer flask with 30 mL of distilled water. The solution is shaken for 20 minutes and the liquid collected in 20 mL vials. The procedure is repeated until the liquid is visibly clear and the textile retains its original color upon visual inspection. Each liquid sample is collected until this occurs. Once the liquid is visibly clear, the textile sample is ready to be subjected to SFE techniques and the procedure discussed above is used.

11. EXPERIMENT F5: RESULTS AND DISCUSSION

Based on the experimental and sampling protocols, as outlined in chapter 9, results related to electrical and chemical parameters were obtained. In addition, pertinent chemical properties such as pH and metal concentration were also obtained. These results allowed for accurate conclusions to be made related to the performance of the developed technology for the imposed conditions. This section deals with the presentation and discussion of results acquired from experiment F5 (EDTA-EK).

11.1. Electrical Parameters

11.1.1. Potential Distribution

Measurements related to potential at each probe and current supplied in each cell were performed. The potential and its variance with the distance from the cathode is displayed graphically in Figure 36 and Figure 37 for cell F5C1 and cell F5C2 respectively. Maximum and minimum potential values obtained in cell F5C1 were 4.55 V (probe 16, at 17 and 23 hours) and 0.75 V (probe 1, at 313 hours) respectively. As for cell F5C2, maximum and minimum values observed were 4.64 V (probe 16, at 23 hours) and 0.80 V (probe 1, at 147 hours) respectively. The current in each cell varied daily with maximum and minimum values for cell F5C1 from 8.17 mA (0 hours) to 3.00 mA (361 hours) respectively. For cell F5C2, maximum and minimum current supplied to the soil was from 7.44 mA (0 hours) to 2.51 mA (361 hours) respectively.

The potential distributions for cell F5C1 and cell F5C2 showed similar trends in the first 47 hours of EK execution. A general linear trend was observed from cathode to anode with a voltage gradient of 0.20 V/cm during this time interval. As the experiment

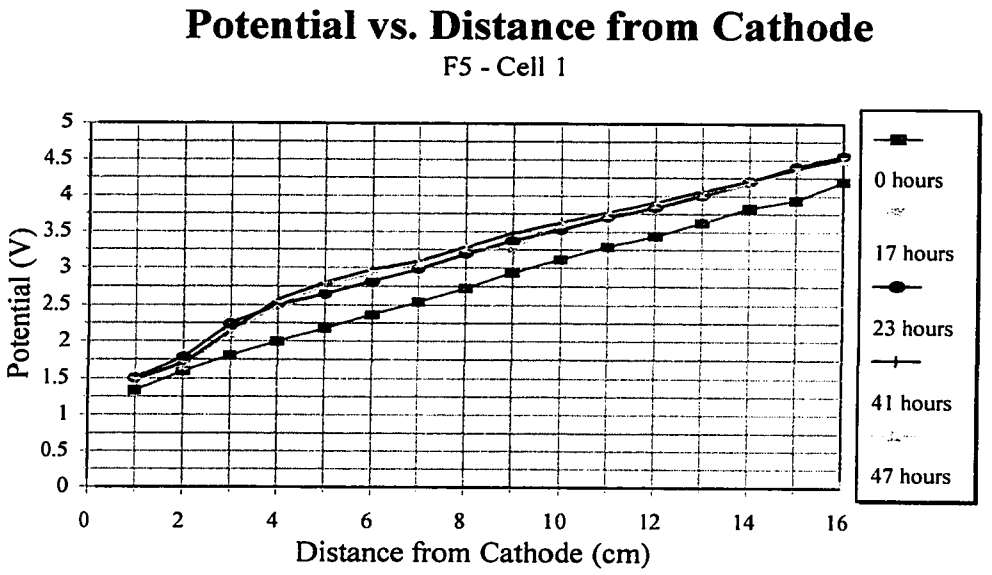

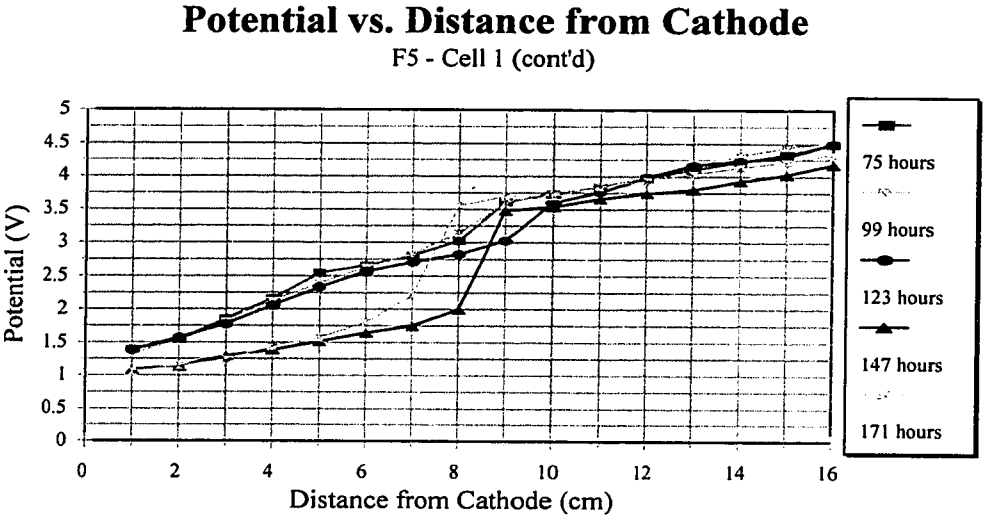

Figure 36 Potential distribution versus distance from the cathode (F5C1)

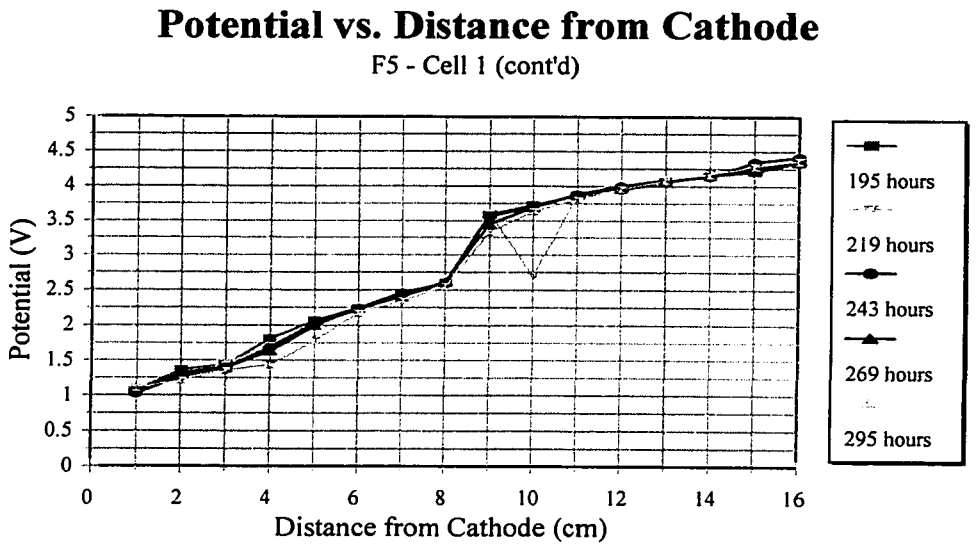

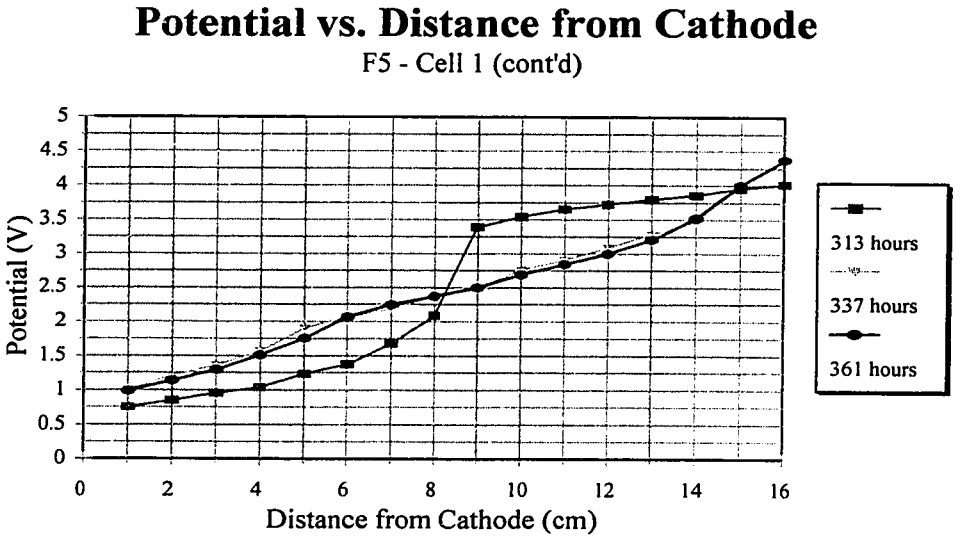

Figure 36 Potential distribution versus distance from the cathode (F5C1) (cont'd)

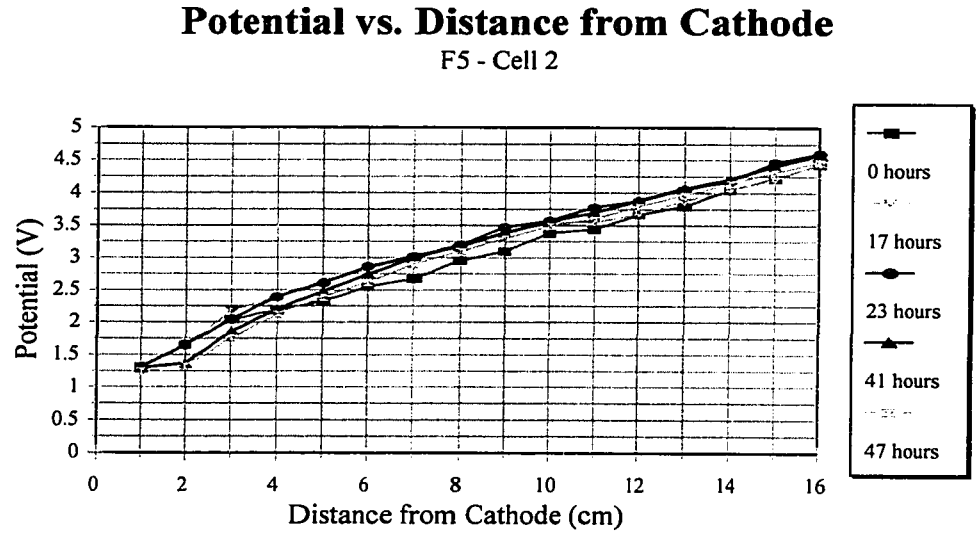

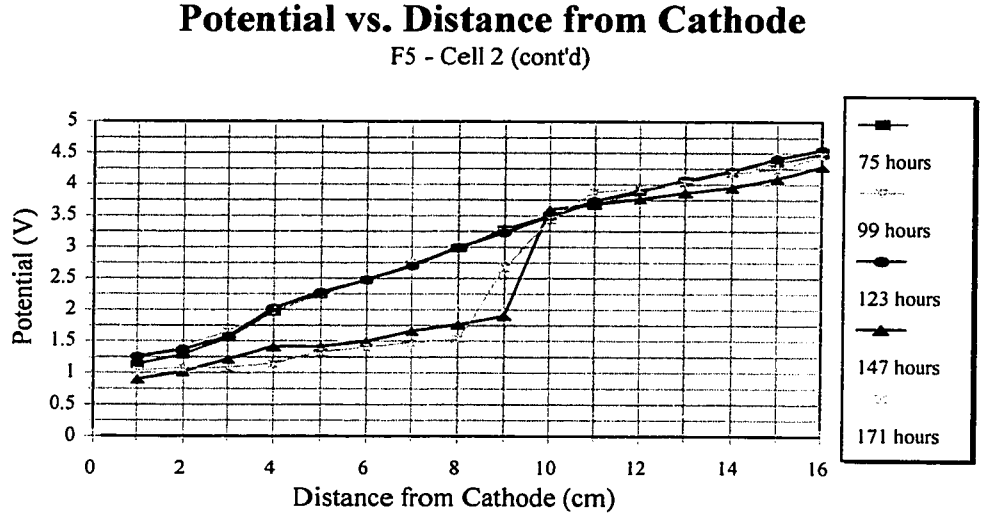

Figure 37 Potential distribution versus distance from the cathode (F5C2)

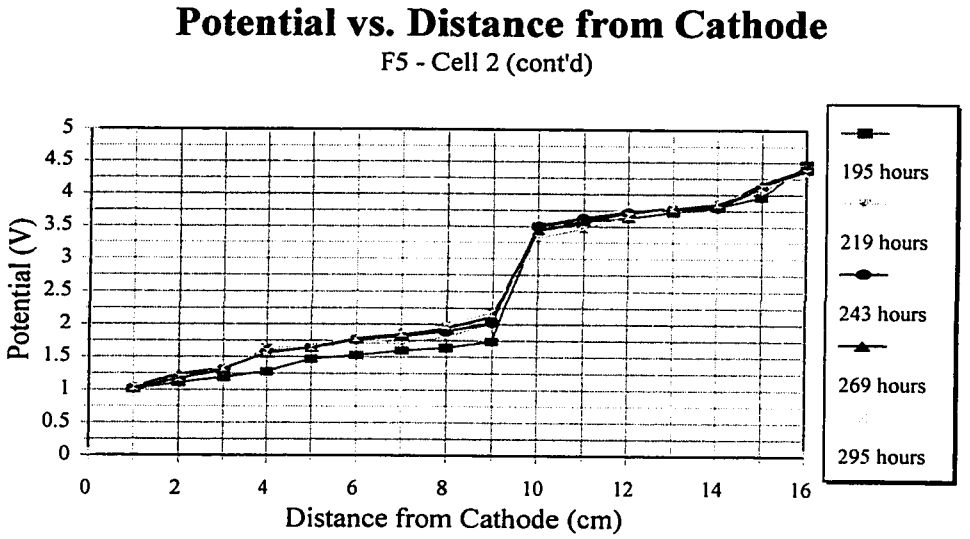

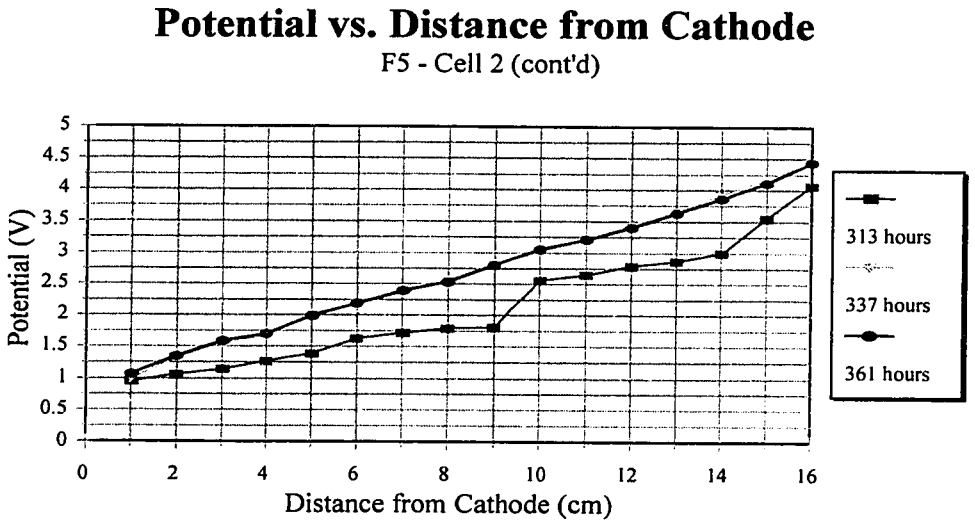

Figure 37 Potential distribution versus distance from the cathode (F5C2) (cont'd)

progressed (75 hours to 171 hours), instabilities became prevalent in both cells, with gradients developing in the central region of each cell. In cell F5C1, a voltage gradient of 0.88 V/cm was observed in the region located from 7.0 to 9.0 cm from the cathode. This corresponded to the location of cracking, which became apparent after 75 hours. A similar gradient of 1.0 V/cm was observed in F5C2, located 8.0 to 10.0 cm from the cathode. This can be attributed to crack propagation within cell F5C2. From 195 to 295 hours, the gradient in cell F5C1 dissipated. This can be attributed to the introduction of water at the anode, which in turn minimized the presence of cracking within the cell. In addition, electrolytic migration of metallic complexes from cathode to anode created a homogeneous soil-water medium, thereby decreasing the gradient that was previously prevalent. Although a gradient of 1.3 V/cm was present after 313 hours, the resistance distribution within cell F5C1 stabilized for the remaining duration of the experiment, due to the addition of water in the anode.

A comparison of cells F5C1 and F5C2 shows that the presence of a sand barrier for the supply of EDTA in cell F5C2 did not affect the potential distribution. This is indicated through a comparison of Figure 36 and Figure 37. Cell F5C1 (absence of a sand barrier) and cell F5C2 show similar distributions, particularly 0 to 1.5 cm from the cathode (from the cathode to the sand barrier in cell F5C2). The sand barrier therefore did not influence potential distribution.

11.1.2. Resistance Distribution

The resistance distributions for cell F5C1 and cell F5C2, as calculated from Ohm's law (V=iR) are also shown graphically versus distance and versus time elapsed, in

Figures 38 to 39 and Figures 40 to 41 respectively. Maximum and minimum resistance obtained in cell F5C1 was 1470 Ohms (probe 16, at 361 hours) and 180 Ohms (probe 1, at 0 and 17 hours) respectively. In cell F5C2, maximum and minimum resistance achieved was 1790 Ohms (probe 16, at 361 hours) and 190 Ohms (probe 1, at 0 hours) respectively. It should be noted that the cathode and the anode are located at 0 cm and 16 cm respectively on the graph.

Similar resistance distributions are observed for cell F5C1 and cell F5C2 with time and with distance. The overall resistance of cell F5C2 was consistently 30 Ohms higher than comparative values in cell F5C1. Both cells are characterized by constant resistance gradients for the first 47 hours. The resistance gradients that were observed in cell F5C1 and cell F5C2 were 26.3 Ohms/cm and 31.9 Ohms/cm respectively. The increases are relatively constant from location to location, as dictated by the constant resistance gradient. As time progressed, the resistance in both cells increased accordingly, due to the electroosmotic flow from anode to cathode thereby decreasing the conductivity of the soil in the anode region. With time, the resistance in the cathode region of cell F5C1 increased from 180 Ohms at the beginning of the experiment to 320 Ohms at the end. In cell F5C2, the corresponding resistance in the cathode region increased from 190 Ohms to 420 Ohms. This increase can be attributed to the formation of OH^- ions at the cathodes. This increased the pH and promoted the precipitation of cations, thereby increasing the resistance and resistivity of the soil.

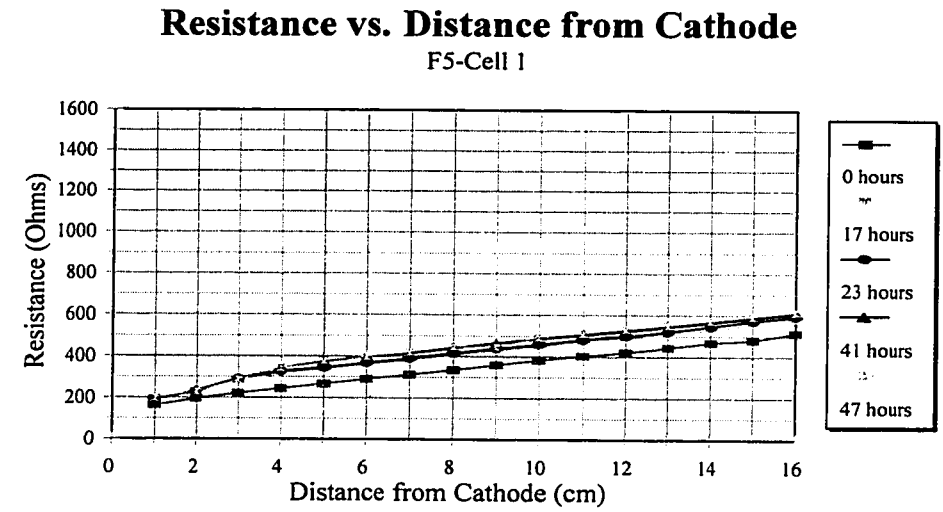

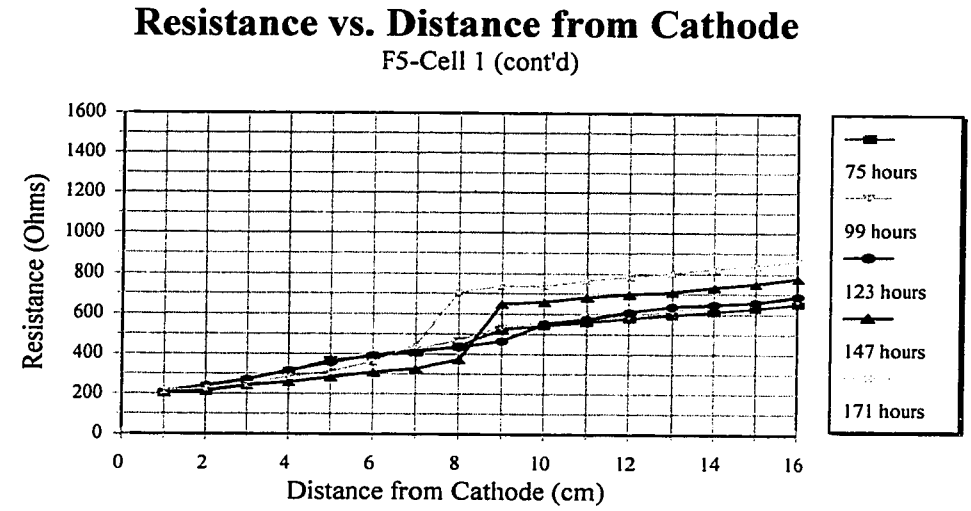

Figure 38 Resistance distribution versus distance from the cathode (F5C1)

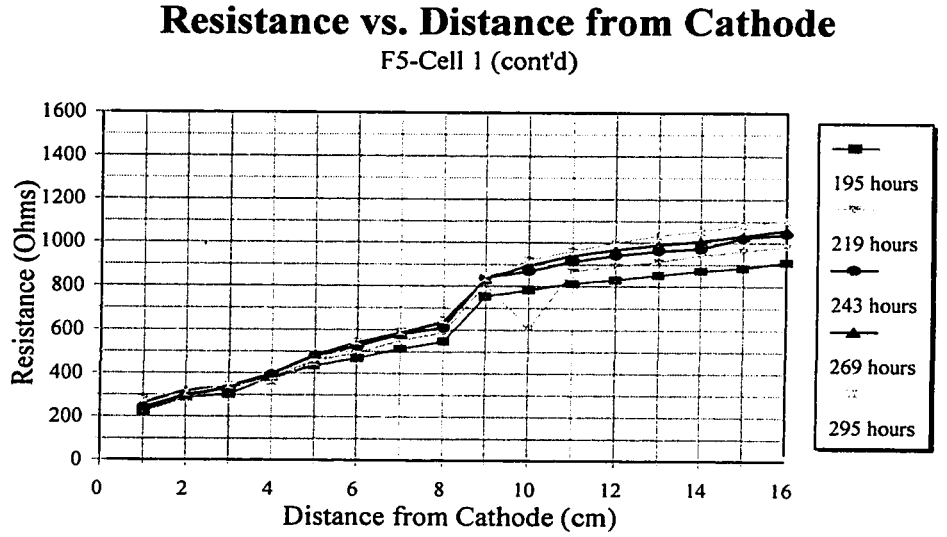

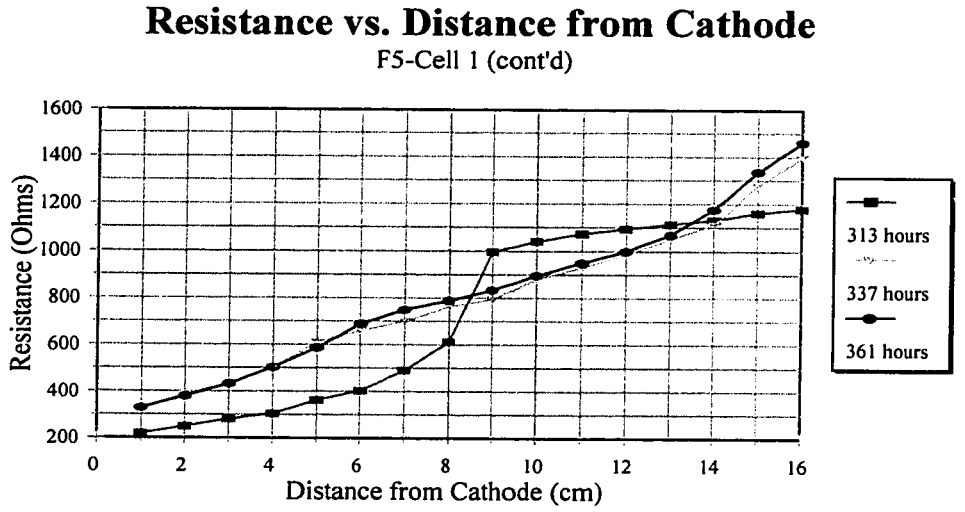

Figure 38 Resistance distribution versus distance from the cathode (F5C1) (cont'd)

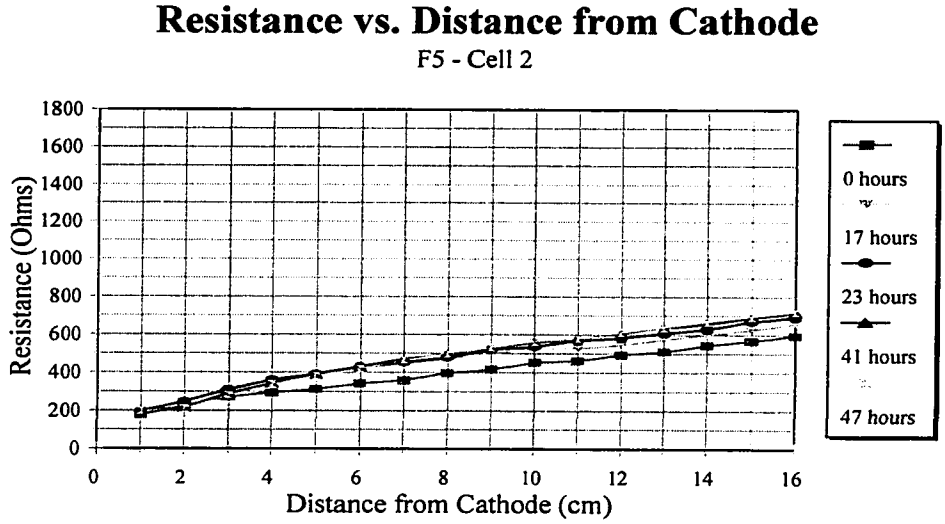

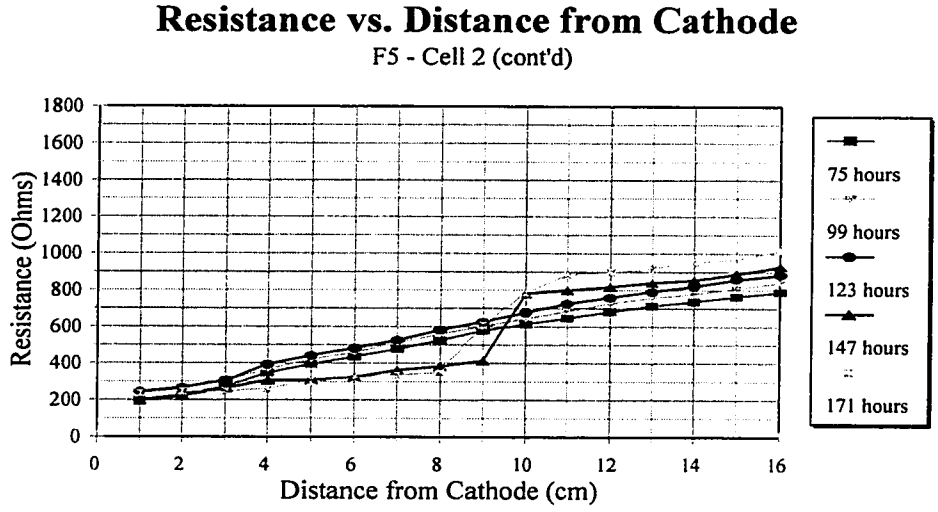

Figure 39 Resistance distribution versus distance from the cathode (F5C2)

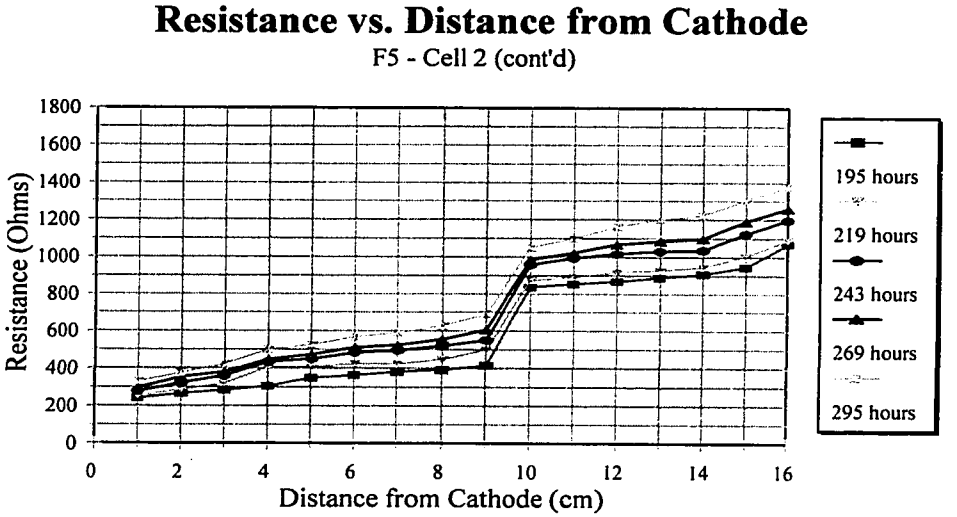

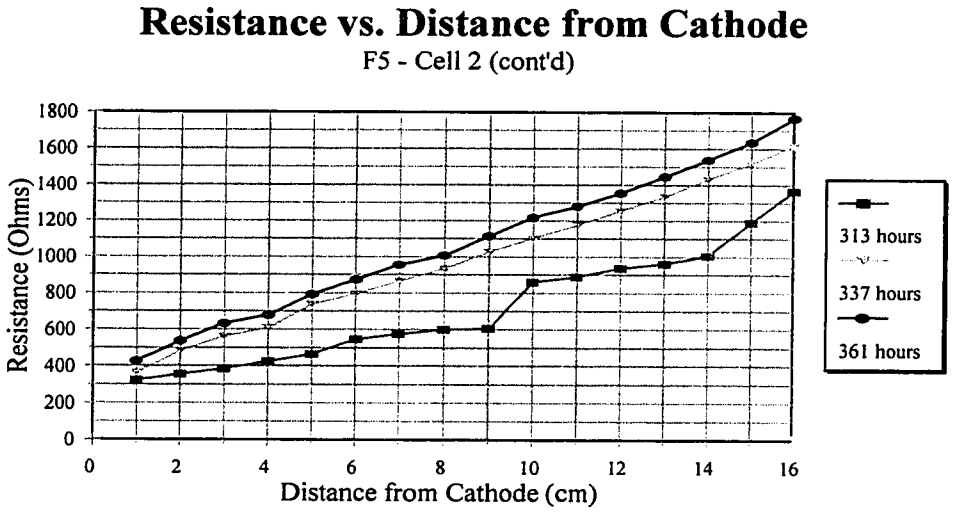

Figure 39 Resistance distribution versus distance from the cathode (F5C2) (cont'd)

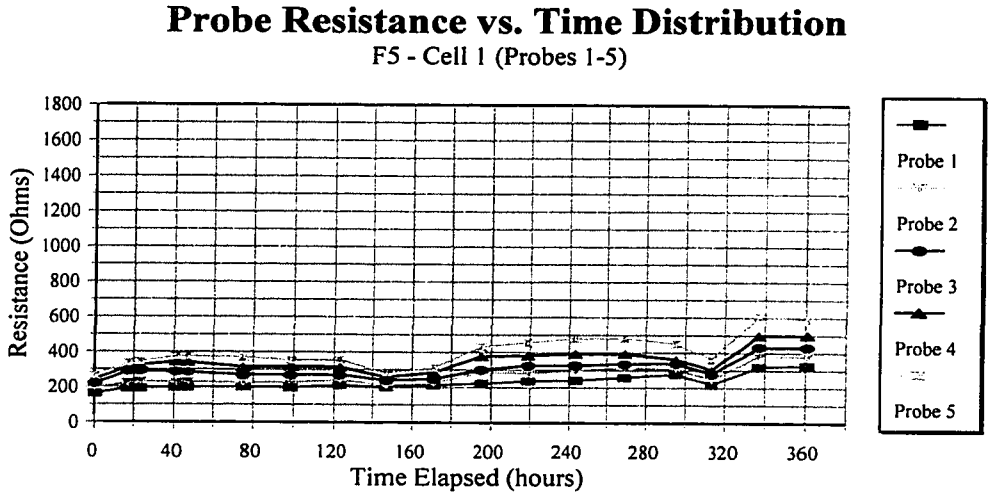

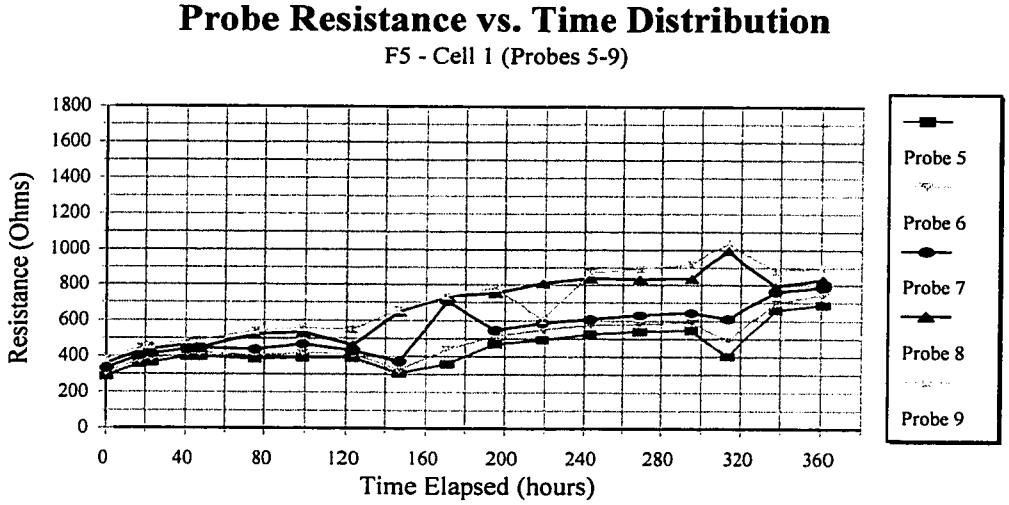

Figure 40 Probe resistance versus time elapsed (F5C1)

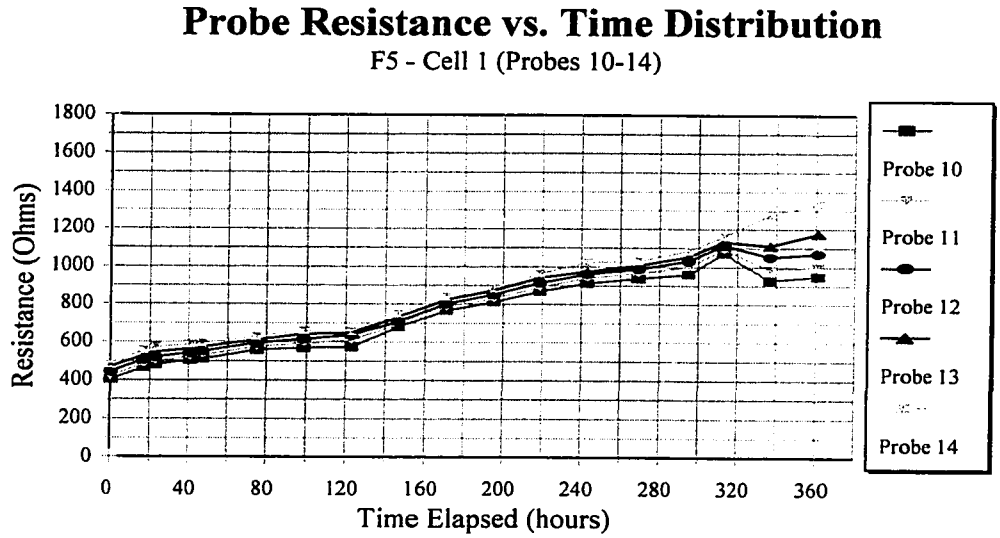

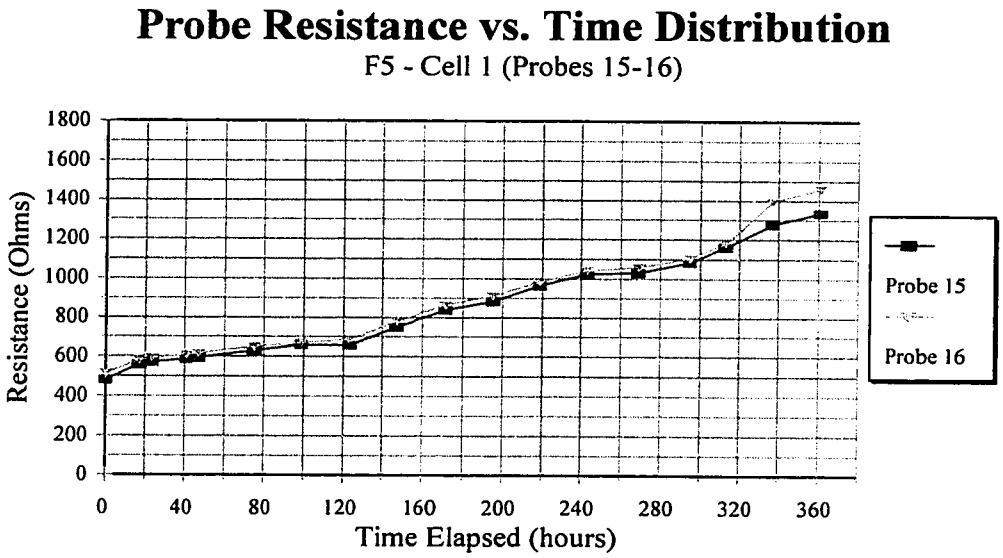

Figure 40 Probe resistance versus time elapsed (F5C1) (cont'd)

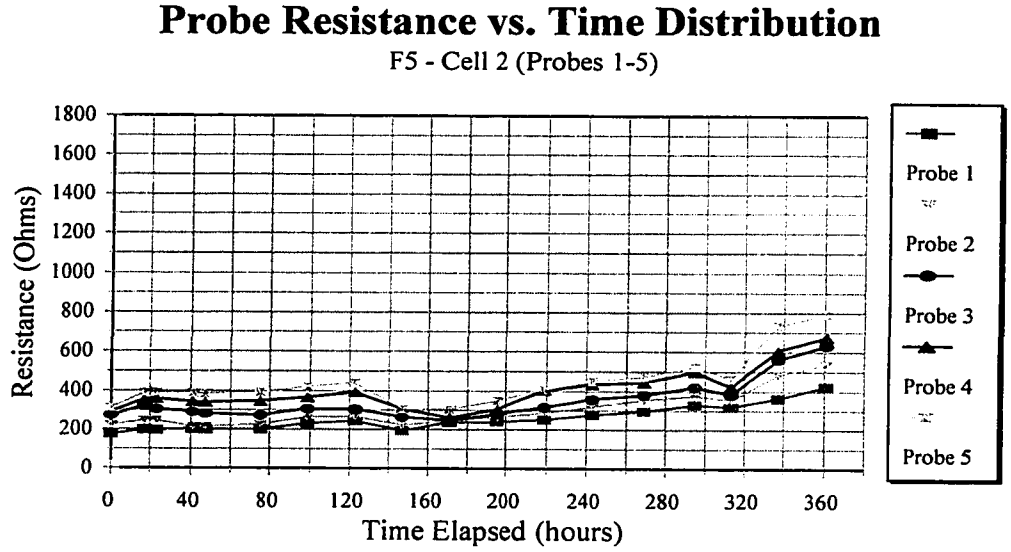

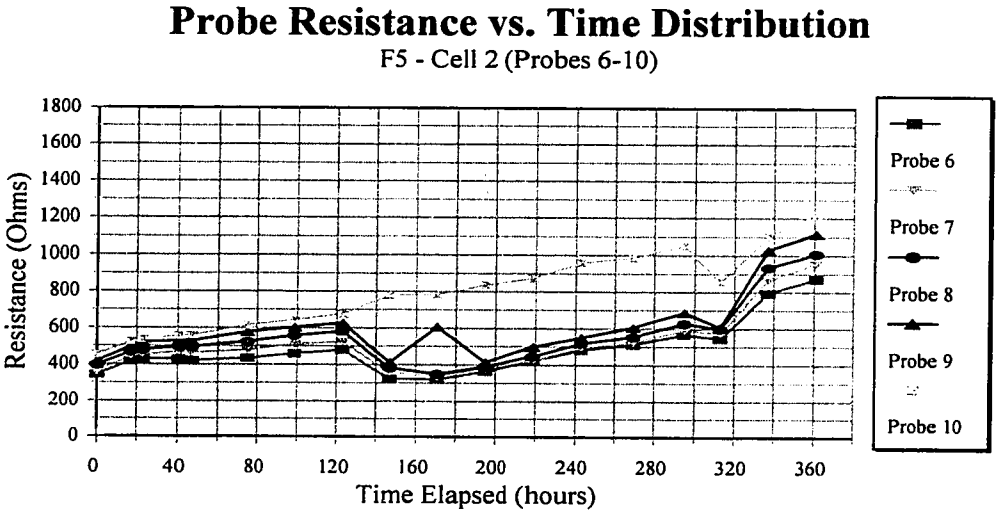

Figure 41 Probe resistance versus time elapsed (F5C2)

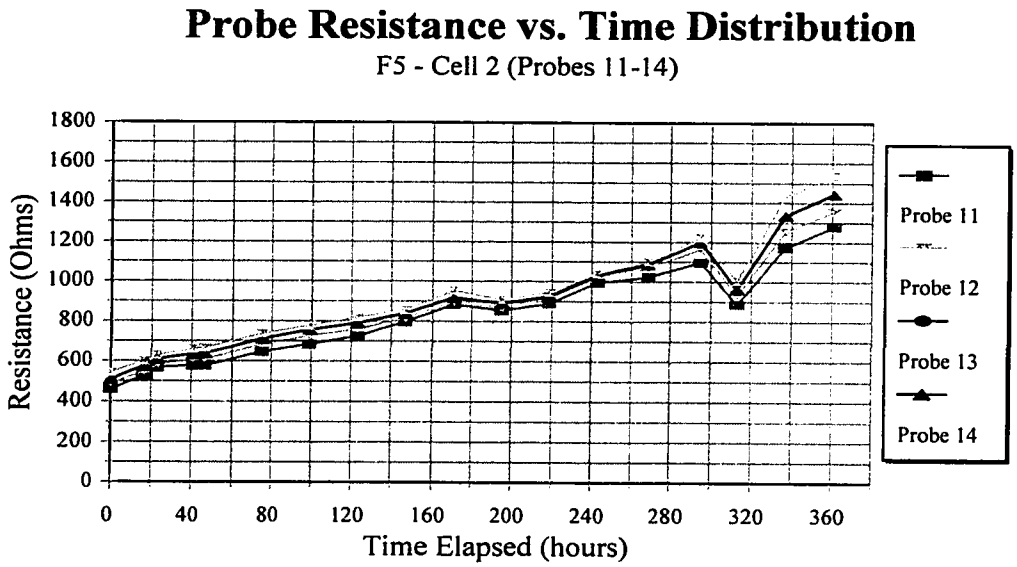

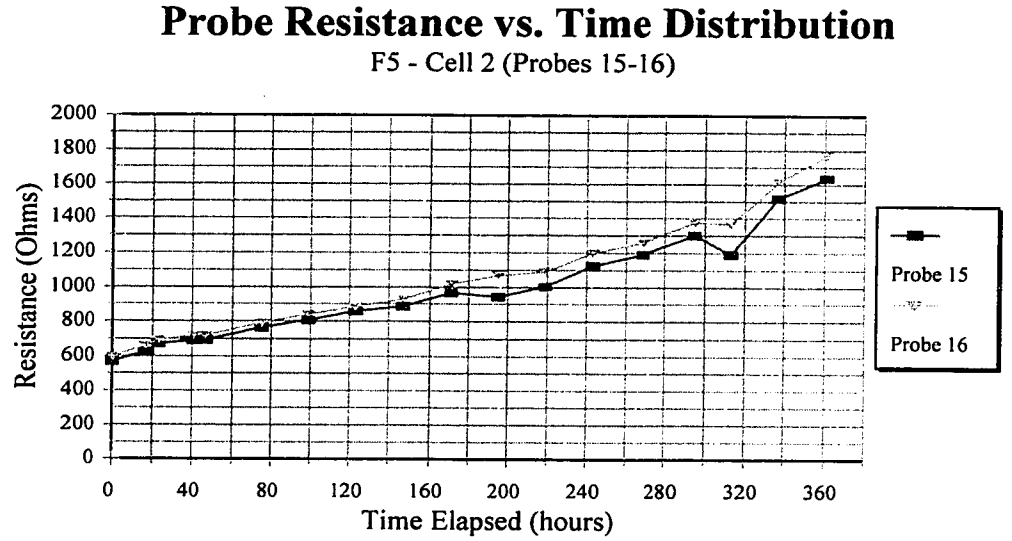

Figure 41 Probe resistance versus time elapsed (F5C2) (cont'd)

Distinct time intervals existed where the gradients remained relatively constant. In both cells four time intervals were observed. These intervals and their respective resistance gradients are summarized in Table 35. These intervals correspond to the consistent decrease in current supplied, the production of OH^- ions and the extensive precipitation that occurred in the cathode region. As stated previously, cracking occurred in both cells, thereby resulting in abnormally higher resistance gradients.

Similar to the potential distributions, a comparison of resistance distributions in F5C1 and F5C2 showed similar trends, particularly in the proximity of the cathodes (0 to 2.0 cm from the cathode of each cell). This indicates that the presence of the sand barrier, for the supply of EDTA did not effect the resistance distribution within the soil. This fact presents favorable conditions for field scale remediation, since a supply barrier can be introduced without adversely affecting the electrical distribution.

Table 35 Resistance Gradients Observed in F5C1 and F5C2

Time Interval (hours)	***Resistance Gradient Cell F5C1 (Ohms/cm)***	***Resistance Gradient Cell F5C2 (Ohms/cm)***
0 – 17	26.3	31.9
47 – 171	41.9 (Sharp gradient of 170 Ohms/cm from 7.0-9.0 cm)	50.0 (Sharp gradient of 390 Ohms/cm from 9.0-10.0 cm)
195 – 295	50.6 (Dissipation of sharp gradient)	59.4 (Sharp gradient of 430 Ohms/cm from 9.0-10.0 cm)
295 - 361	67.5	87.5

11.2. Results Pertaining to Cathode Liquids

11.2.1. pH of the Cathode Liquids

The pH of the liquids extracted from the cathode in cell F5C2 on a daily basis is displayed in Figure 42. Since EDTA was supplied directly into the cathode of cell F5C1, liquid samples could not be obtained. For cell F5C2, the maximum and minimum pH values observed were 12.2 (41 and 123 hours) and 10.4 (219 and 243 hours).

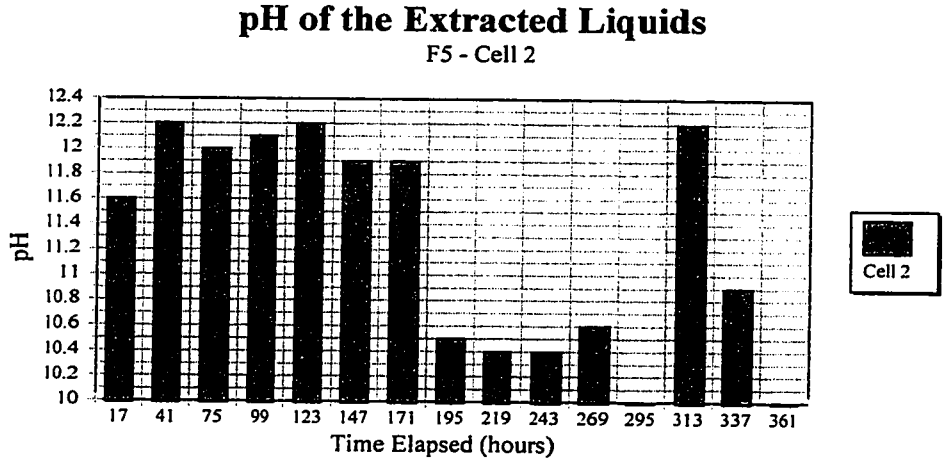

Figure 42 pH of the extracted liquids (F5C2)

The pH of cathode liquids observed in cell F5C2, displayed two distinctive zones as time progressed. The first zone consisted of high pH values (11.6 to 12.2) from 17 hours to 171 hours. This phenomenon is typical for an electrokinetic cell, as the high pH is indicative of extensive OH^- formation in the cathode region. The second zone is characterized by lower pH values ranging from 10.4 to 10.5 (195 hours to 337 hours). These significant pH decreases (1.5 - 2.0 pH units) observed in cell F5C2 as the time elapsed increased are due to the addition of EDTA in this zone, combined with the

dilution effect of supplying a solution of EDTA. This magnitude of this phenomenon is influenced primarily by the buffering capacity of the soil and secondarily by the hydraulic conductivity of the soil.

The large pH decreases can also be attributed to the introduction of EDTA into the system. As stated previously, 0.1 M EDTA was introduced into cell F5C2 through a porous sand zone, located 1.5 cm from the cathode. The dissociation of Na_2EDTA in solution, created hydrogen ions, which decreased the pH within the system. It is therefore speculated that the presence of EDTA in the cathode region, coupled with the movement of the acid front, reduced the pH of the extracted liquids. It would be impossible to observe lower pH values (i.e. 10.5-11.0) in the early stages of the experiment since EDTA complexation and the movement of the acid front are time-dependent processes. However, the sharp pH decrease from 171 hours to 195 hours indicates that the combined effect of acid front movement and the presence of EDTA was effective in decreasing the pH in the cathode area.

11.2.2. Volume of the Cathode Liquids

The fluctuation of the volume of the liquids extracted daily through the cathode of cell F5C2 is shown in Figure 48. A sharp decrease was observed during the time period from 195 hours to 269 hours. This time period corresponds directly to the time period observed for low pH values, as shown in Figure 43. The volume extracted from cell F5C2 for the entire duration of the experiment was 92.8 mL. Maximum and minimum daily volumes were 20.4 mL (t = 361 hours) and 4.0 mL respectively. It is speculated that this is due to the fact that high species flow during this time period was from cathode

to anode, due to the presence of more anions than cations within the system. This anion predominance was due to the formation of EDTA complexes with heavy metals.

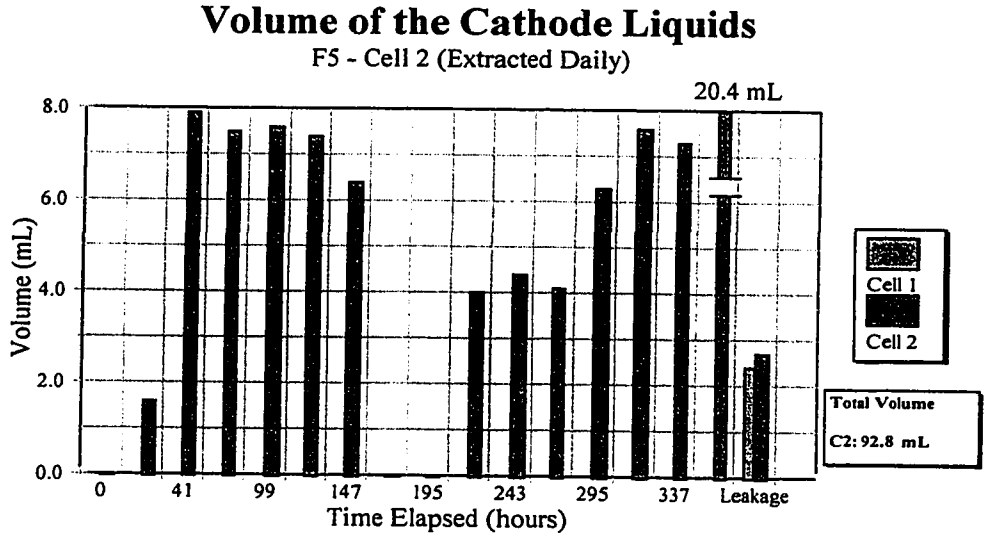

Figure 43 Volume of extracted liquids (F5C2)

As the experiment progressed, the volume of liquid extracted at the cathode increased accordingly, indicating a net electroosmotic and electrolytic flow from anode to cathode. The supply of water in the sixth day of the experiment, introduced in the anode area, competed with the electrolytic migration of EDTA complexes.

11.2.3. Concentration of Metals in the Cathode Liquids

The concentration of heavy metals in the cathode liquids (collected daily) for cell F5C2 is shown in Figure 44. The concentration of metals in the extracted liquids is important because it gives an indication related to the movement of ionic species within

the cell. Table 36 shows a summary of the maximum and minimum metal concentration and the corresponding time elapsed for each metal analyzed.

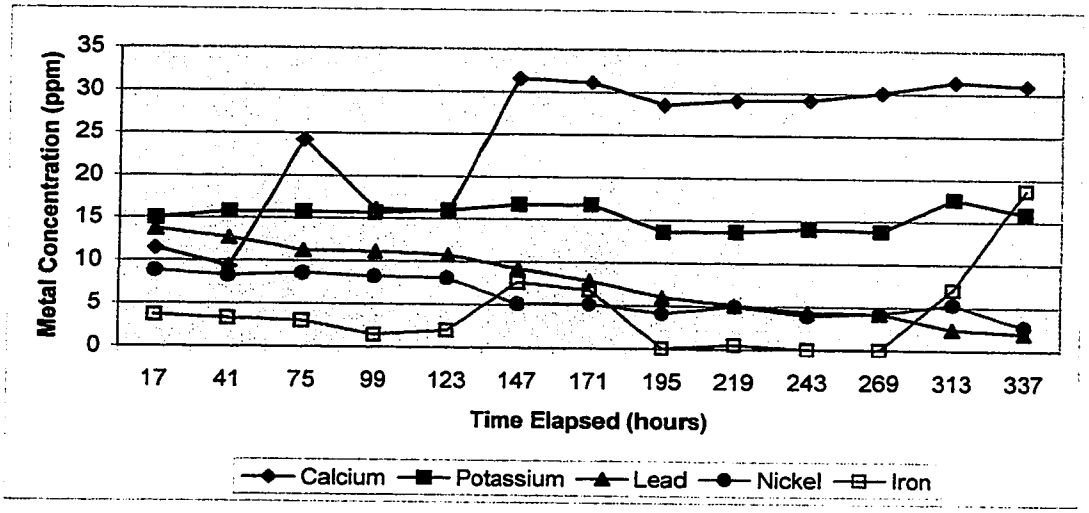

Figure 44 Metal concentration of extracted liquids (F5C2)

Table 36 Maximum and Minimum Metal Concentrations for Extracted Liquids

Metal	*Maximum Metal Concentration (ppm)*	*Minimum Metal Concentration (ppm)*
Calcium	31.4 (313 hours)	9.4 (41 hours)
Iron	18.7 (337 hours)	0.0 (243 hours)
Potassium	17.6 (313 hours)	13.8 (269 hours)
Lead	13.7 (17 hours)	2.0 (337 hours)
Nickel	8.8 (17 hours)	2.7 (337 hours)

The calcium concentration consistently increased from 17 hours to 147 hours. After this time, the calcium concentration remained relatively constant. The constant

production of hydroxide ions at the cathode, increased the pH and therefore increased the presence of calcium in this area, until a threshold was achieved. In addition, the precipitation at the cathode is typically of the calcium form. It is possible that some calcium ions were released into solution and into the extracted liquid. It is speculated that after 147 hours, the EDTA penetrated into the cathode region, thereby decreasing the pH and countering the OH production and precipitation in this area. As a result, the calcium concentration in the extracted liquids remained relatively constant.

It can be seen from Figure 49 that both lead and nickel concentrations in the extracted liquid decreased as time progressed. Maximum lead and nickel concentrations occurred after 17 hours (first sample taken), and minimum concentrations occurred at the end of the experiment. This phenomenon can be attributed to the electrokinetic processes and the supply of EDTA. Specifically, the following can be observed:

1. The highest lead and nickel concentration was observed at the beginning of the experiment (17 hours). After 17 hours of the experiment, only 17 mL of EDTA was supplied which was not sufficient enough to cause a high degree of complexation. As a result, there was still an abundance of cations within the pore water. Therefore, uncomplexed lead and nickel (cationic species) were transported to the cathode region and subsequently appeared in the cathode liquids.

2. As the experiment progressed, the concentration of lead and nickel found in the extracted liquids decreased to 14 % of the initial lead and 31% of the initial nickel. This indicates the presence and influence of EDTA on the system. As the cumulative volume of EDTA supplied increased and became well distributed, an increased amount of metal-EDTA complexes (anionic species) formed. This resulted in the transport of anionic species within the cell. Therefore, as the experiment progressed, an increased amount of anionic Pb-EDTA and Ni-EDTA complexes were transported to the anode region. In addition, a decreased amount of Pb and Ni were in cationic form. The final soil metal concentrations (Figure 50 and Figure 51) support this observation,

as can be seen by the higher concentrations of lead and nickel in the anode region.

It should be noted that out of the five metals analyzed, only lead and nickel showed this consistent decreasing trend as time progressed. This could be an indication of EDTA selectivity for lead and nickel. The other metals analyzed showed no decreasing trend and therefore may not have been complexed and transported to the anode.

11.3. Volume of EDTA Supplied

As stated previously, 0.1 M Na_2EDTA was continuously added to each cell and the daily volume was measured. Table 37 summarizes the maximum, minimum and average values of 0.1 M EDTA supplied. A comparison of the volume of 0.1 M EDTA solution supplied to cell F5C1 and cell F5C2 is shown in Figure 45. It can be seen that the values were fairly close, despite the use of different supply configurations. Total volumes supplied to cell F5C1 and cell F5C2 was 146.1 ml and 171.3 ml respectively.

Table 37 Results Pertaining to Volume of 0.1 M EDTA Supplied

Cell No.	*Maximum Daily Volume Supplied (ml)*	*Minimum Daily Volume Supplied (ml)*	*Average Daily Volume Supplied (ml)*
1	30.9	0.0	9.74
2	48.9	0.0	11.42

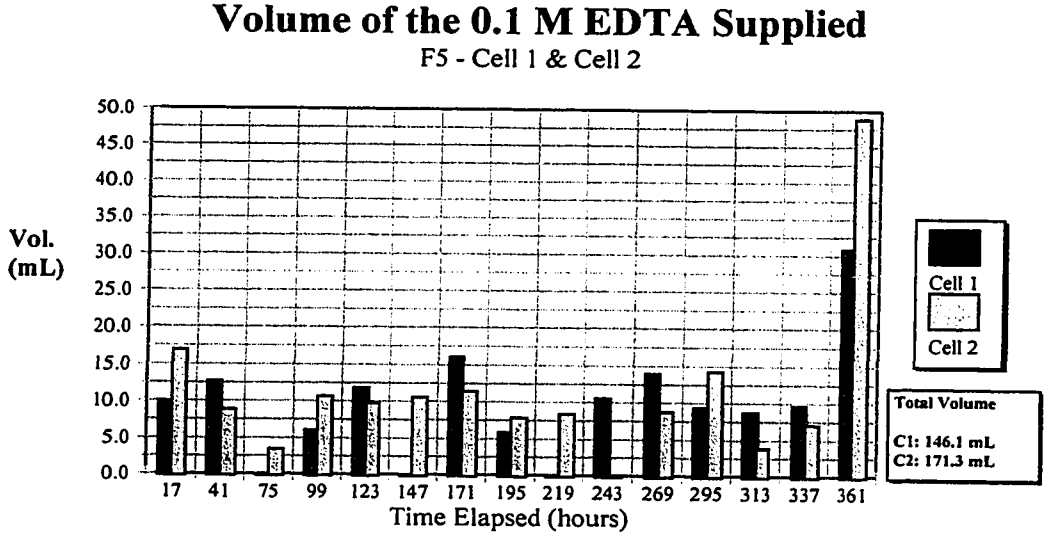

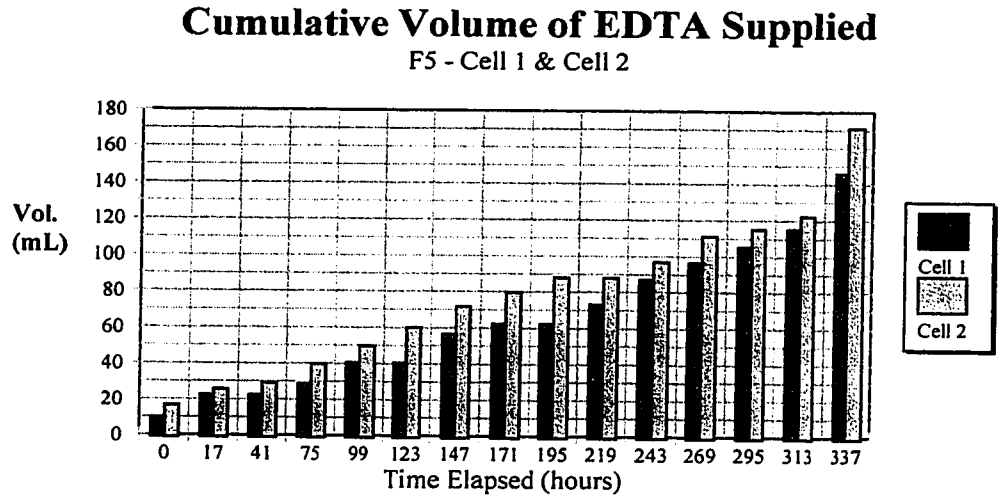

Figure 45 Daily and Cumulative Volumes of 0.1 M EDTA supplied

11.4. Soil Samples

11.4.1. pH of the Soil

Sampling of the soil for the purpose of analysis was described in chapter 9. The pH analysis of these soil samples and its variance with the distance from the cathode for cell F5C1 and cell F5C2 are shown in Figure 46 and Figure 47, respectively. The locations of the anode, the cathode and the porous sand supply zone are superimposed onto this graph in order to give an accurate representation of each cell. Maximum and minimum soil pH values observed in cell F5C1 were 10.21 (2.0 cm from the cathode), and 6.97. For cell F5C2, maximum and minimum values observed were 10.42 (at the cathode) and 7.16 (at the anode). As expected, there was a general increase from anode to cathode.

The pH of the soil versus the distance from the cathode for cell F5C1 and cell F5C2 showed a typical distribution from cathode to anode. The initial pH of the soil was 7.6 as shown in Figures 46 and 47, and the formation of hydrogen ions at the anode lowered the soil pH to 6.97 and 7.16 in both cell F5C1 and cell F5C2 respectively. The small reduction was due to the supply of water directly into the anode. This caused a dilution effect on the hydrogen ion concentration, thereby offsetting the constant formation of hydrogen ions in the anode area and maintaining the pH near the initial value.

Zones are observed in cell F5C1, the pH gradient from the anode to 6.2 cm from the cathode was 0.137 pH units/cm, which indicated that there existed migration of EDTA complexes and the acid front, which mitigated the migration of OH^- ions. A sharp

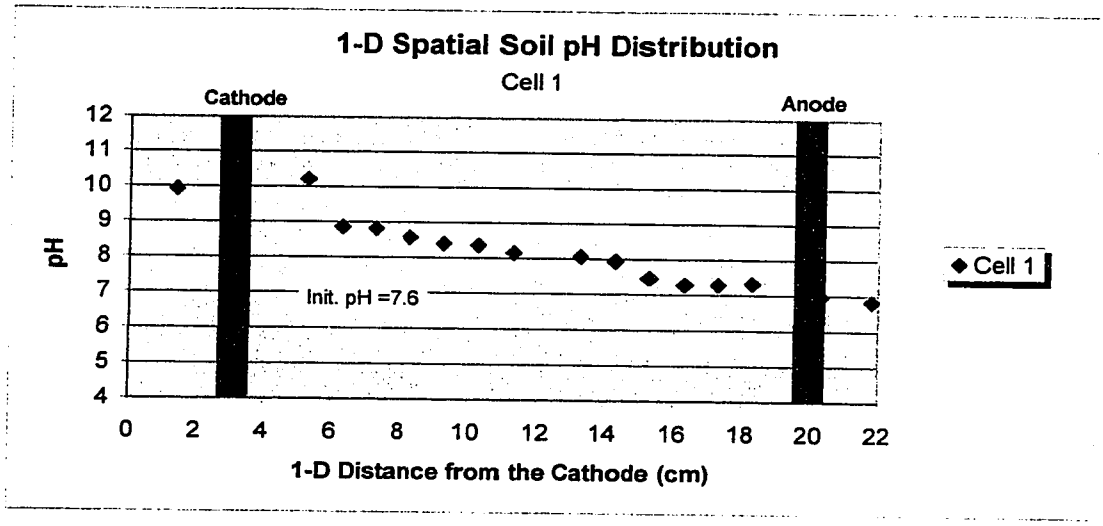

Figure 46 pH of the soil versus distance (F5C1)

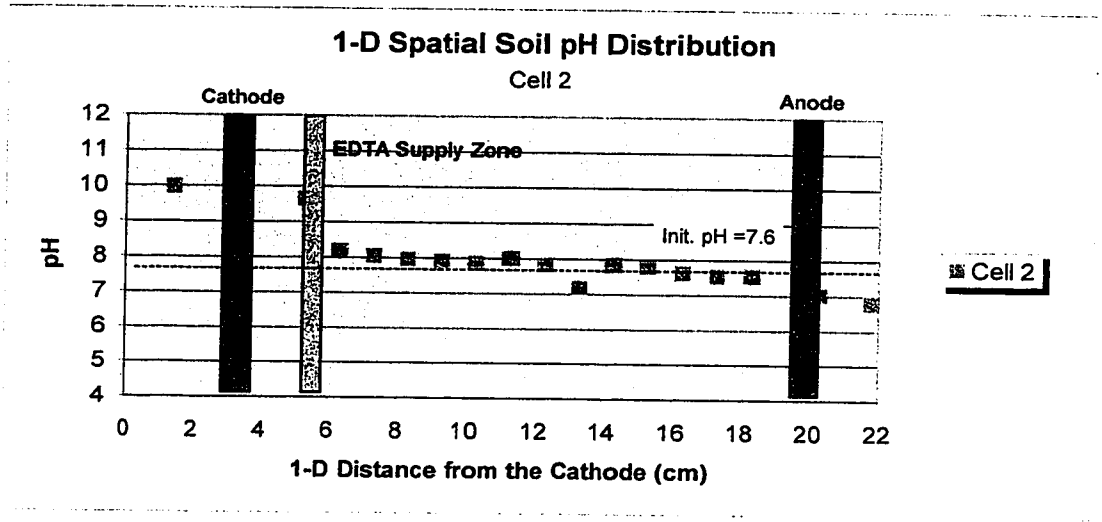

Figure 47 pH of the soil versus distance (F5C2)

pH gradient was evident from 6.2 cm from the cathode to the cathode itself, with a value of 0.54 pH units/cm. This increase was due to the formation of OH^- ions in the cathode region. The formation of EDTA complexes and their subsequent transport to the anode, via electrolytic migration, resulted in a deficit of negatively charged ions within the system. In order to maintain electroneutrality, hydroxide ions were produced by the decomposition of water molecules. However, the pH in the cathode region was lower than in previous experiments and in literature, which is an indication that EDTA had an effect in lowering the pH, and that this supply counteracted the effect of hydroxide ion formation. Typically, it is expected that the pH of the soil in the cathode region would be closer to 11.00, but the formation of hydroxide precipitates removed some hydroxide ions from solution thereby lowering the pH slightly.

It should be noted that there was one anomaly with the pH distribution in cell F5C1. A distinct pH drop occurred 12.2 cm from the cathode. This corresponds with the location of a crack within the soil that occurred during the experiment's progression. This resulted in a concentration of EDTA solution within this area, thereby decreasing the pH. A more significant decrease was mitigated by the high buffering capacity of the soil.

Cell F5C2 displayed a similar soil pH distribution as cell F5C1 with the exception of the fact that lower pH values were observed throughout the transition from the anode to 6.2 cm from the cathode. The gradient in this area was 0.096 pH units/cm, which was significantly lower than cell F5C1. This is due to the better distribution and transport of EDTA and their complexes, thus decreasing the pH. The better formation and transport of complexes lead to higher pH values and gradients (1.12 pH units/cm) in the cathode

region of cell F5C2 than in cell F5C1, due to an increased driving force (a larger anionic deficit within the cell). The pH of the soil decreased below the initial value, in the range of 6.79-7.01 in the anode region. Once again, the pH was kept relatively low due to slow but consistent migration of the acid front originating from the H^+ formation at the anode. In the cathode area, the pH rose sharply, peaking at 10.42, at the cathode. The minimum value obtained in cell F5C2 was 6.79, 18.3 cm from the cathode. It should be noted that the maximum pH in cell F5C2 was 0.21 pH units higher than the maximum soil pH in cell F5C1.

In general, both cells displayed similar soil pH distributions. The migration of the acid front was not significant, as indicated by the small pH decrease (relative to the initial), in areas outside the cathode region. The supply of EDTA to both cells played a significant role in minimizing severe pH increases in the cathode region. However, even lower pH values in this area could not be achieved due to the transport of EDTA complexes from cathode to anode. This caused a deficit of anions within the system, thereby forcing the formation of hydroxide ions at the cathodes. Atomic absorption analysis will indicate the transport and distribution of heavy metals achieved through electrokinetics and chelation. The acid front did not penetrate the cathode region as evidenced by the high pH values in that area.

11.4.2. Metal Concentration in the Soil

The concentration of lead, nickel, iron and calcium in the soil was measured using the SFE-AAS methods outlined in chapter 9 and 10. This section deals with a discussion of the metal concentration in the soil, and its spatial distribution.

11.4.2.1. Calcium Concentration

11.4.2.1.1 Cell 1 (F5C1)

The distribution of calcium in the soil for F5C1 is shown in Figure 48. Maximum and minimum calcium concentrations were 120.6 mg/kg and 15.2 mg/kg respectively. Concentrations were significantly higher in the cathode region as was expected due to hydroxide formation, and calcium precipitation. The development of high pHs is magnified due to the addition of EDTA. It is speculated that the abundance of negatively charged complexes and their subsequent transport to the anode, created a deficit of anions in the cathode region. In order to preserve electroneutrality, hydroxide formation resulted. Superimposing soil pH and calcium concentration in the soil for cell F5C1 shows typical relationships of calcium solubility and pH. In the cathode area, the pH of the soil was approximately 9.0-10.5, the calcium concentration in this area increased substantially from 55 mg/kg to 125 mg/kg. At these high pH values calcium formed insoluble precipitates, particularly $Ca(OH)_2$ and $CaCO_3$. The precipitation barrier formed in the cathode area did not have a substantial effect on the localization of the target heavy metals, namely lead and nickel. Although the distribution of calcium within the soil was typical, the overall concentration of calcium in the soil was lower than expected.

11.4.2.1.2. Cell 2 (F5C2)

The calcium distribution for cell F5C2 is shown in Figure 49. Maximum and minimum soil calcium concentrations were 96 mg/kg and 3.5 mg/kg respectively. As with cell F5C1, the highest calcium concentrations were observed in the cathode region. These values were 25-30 % lower than comparative values in cell F5C1. The use of the

porous sand zone in F5C2 for the supply of EDTA allowed for better distribution, resulting in lower pH values (see Figure 46), and therefore contributed to the lower calcium concentration.

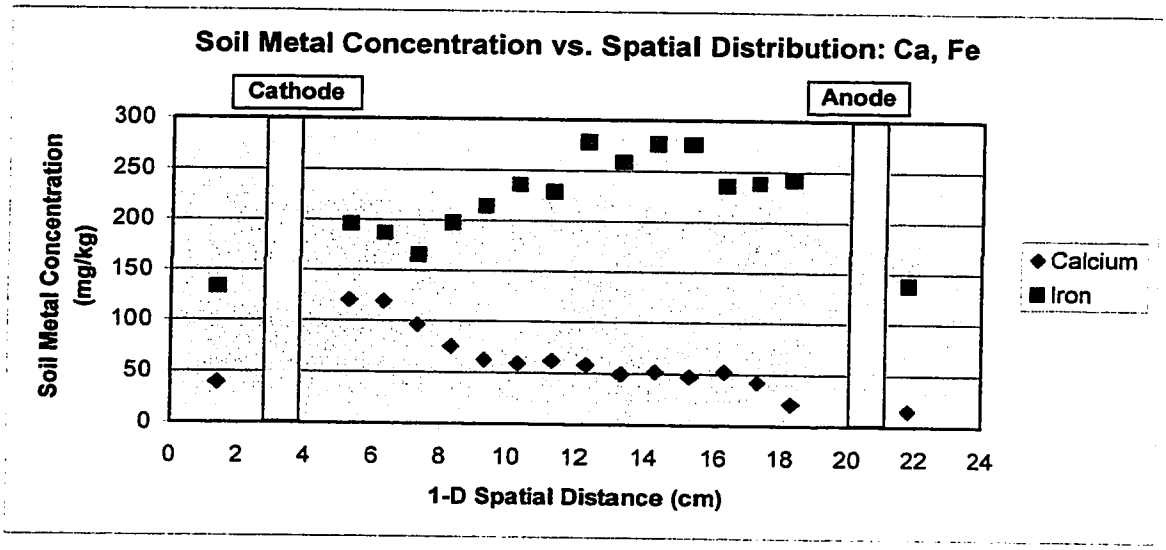

Figure 48 Ca and Fe concentration in soil for EDTA enhanced EK (F5C1)

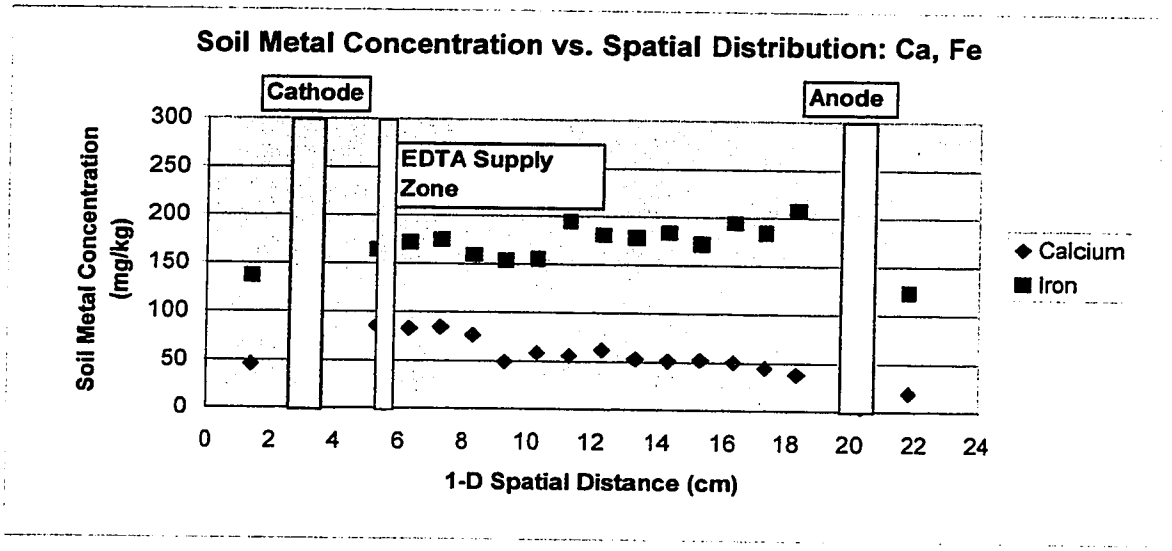

Figure 49 Ca and Fe concentration in soil for EDTA enhanced EK (F5C2)

The calcium distribution was directly related and similar to the pH distribution. Progressing from anode to cathode resulted in an increase in pH, with the sharpest gradient occurring in the cathode area. Atomic absorption analysis revealed that the highest calcium concentration (96.1 mg/kg) occurred in the cathode region, specifically at the cathode, where the highest pH was achieved. The sharp gradient in the pH did not correspond to a similar concentration gradient, but an increase of 35 mg/kg was achieved. Nevertheless, the concentration distribution obtained for cell F5C2 was as expected based on the pH distribution. The high concentration of OH^- ions produced at the cathode caused extensive precipitation of calcium in the soil, with an average of 87 ppm in the cathode region. As with cell F5C1, the calcium concentration did not play a significant role in affecting the localization of lead and nickel.

11.4.2.2. Iron Concentration

11.4.2.2.1. Cell 1 (F5C1)

Figure 48 shows the spatial variation of iron for cell F5C1. High concentrations were observed in cell F5C1. The iron concentrations in cell F5C1 represented the highest metal concentration of the any metal analyzed. Maximum and minimum values observed were 278.3 mg/kg and 132.8 mg/kg respectively. High iron concentrations were expected and can be attributed to the following phenomena:

1. The iron oxides present in the soil matrix. This is the primary source of high iron concentrations in the soil.
2. The oxidation of the anode during electrokinetic treatment. Stainless steel electrodes were used in order to minimize oxidation, but some iron was oxidized and released into the soil. The iron that was bound to the soil was

most likely of the trivalent type (oxidation of Fe^{2+} to Fe^{3+}), which is characterized by low water solubility.

There was no distinct area where iron ions were concentrated. However, some general locations within the cell displayed some tendencies. The iron concentration was approximately 20-30 % higher in the location from 6.5 cm to 12.5 cm from the cathode edge. The iron concentrations were approximately 20 % higher in the anode region than in the cathode region. This can be attributed to the oxidation of the anode and subsequent release of iron ions in solution. From Figure 48, it can be seen that some transport of iron did occur, but it did not reach the cathode area. In addition, the use of different supply systems in F5C1 and F5C2 did not affect the transport of iron species.

11.4.2.2.2. Cell 2 (F5C2)

The iron distribution in the soil for cell F5C2 is shown in Figure 49. Maximum and minimum values observed were 207.6 mg/kg and 122.8 mg/kg respectively. The iron concentrations were significantly lower in cell F5C2 than in cell F5C1. This can be attributed to the lower daily current measured in this cell. A lower current, resulted in a lower degree of oxidation. Therefore less ferric ions were released into the soil, which resulted in a lower concentration. Unlike cell F5C1, the maximum iron concentration was observed at the anode, as would be expected, due to the constant oxidation of the anode. Using the porous sand supply zone as opposed to the supplying EDTA directly into the cathode may have had an effect on minimizing the concentration of iron in the soil. By ensuring a better distribution of EDTA, thereby increasing the amount of iron complexes and allowing for their transport to the anode, this might be expected, but the high concentration of iron at the anode is most likely due to oxidation.

To summarize, both cell F5C1 and cell F5C2 showed appreciably high and constant concentrations with an average of 217 mg/kg and 171 mg/kg for cell F5C1 and cell F5C2 respectively. The high concentration was due to the extensive oxidation of the anode. It should be noted that, the iron ions introduced from the oxidation of the anode tended to remain in that area. The presence of iron within the soil, and the fact that iron forms highly stable complexes with EDTA, created competition for EDTA between iron and the target heavy metals. This caused problems related to the amount of nickel and lead complexed by EDTA. This was and is probably the most important factor influencing the mobilization of the target heavy metals. It is difficult to alleviate, due to the high inherent iron concentration in clay soils, particularly in Québec. The soil within Montréal has shown particularly high concentrations of iron.

Overall, the iron concentrations within the soil were 2.0-2.5 times higher than comparable calcium concentrations. This can be attributed to the presence of iron in the soil, originating from the iron oxides already present in the soil and from the oxidation of the anode. Having a lower solubility than calcium in this pH range, iron readily formed precipitates before calcium. The formation of $Fe(OH)_3$ used up many hydroxide ions produced at the cathode, thereby leaving a substantial amount of calcium ions in solution.

11.4.2.3. Nickel Concentration

11.4.2.3.1. Cell 1 (F5C1)

The nickel concentration in the soil samples and its variance with distance, between the cathode and anode, for cell F5C1 is shown in Figure 50. Cell F5C1 displays high nickel concentrations in the anode area, which is indicative of significant electrolytic migration from cathode to anode. This is due to the addition of EDTA, which caused the

formation of negative complexes. The abundance of negative complexes within the system resulted in an increased migration of anionic species from cathode to anode. Maximum and minimum nickel concentrations in cell F5C1 were 81.0 mg/kg and undetectable respectively. Approximately 79 % of nickel ions were concentrated in $1/6^{th}$ of the cell and 89 % was concentrated in $1/4^{th}$ of cell F5C1 after the EDTA-EK process. This is an indication that EDTA increased the mobilization of nickel ions thereby making them accessible to EK transport (electrolytic migration and electroosmosis). The stability of Ni-EDTA complexes, as represented by stability constants prevents their exchange onto soil particles, effectively increasing their tendency to remain in the pore water. The majority of nickel was located at the anode to about 4.0 cm from the anode, with significantly lower amounts observed in the remaining portion of the cell. This indicates that significant migration of nickel-EDTA complexes (negatively charged) occurred from cathode to anode in response to the electrical gradient. This migration continued until the anode area was reached and precipitation of these complexes occurred. In essence, a barrier was established in the anode zone, where the pH ranged from 7.1-7.8. Despite this fact, significant mobilization, by EDTA, and transport, by EK methods resulted.

11.4.2.3.2. Cell 2 (F5C2)

The distribution of nickel in the soil for cell F5C2 is shown in Figure 51. A trend similar to that of F5C1 is observed. A high concentration was achieved in the anode area (86.1 mg/kg). The localization of nickel within cell F5C2 was lower than that of cell F5C1, with 76 % of nickel ions localized within $1/6^{th}$ of the cell and 82 % localized within $1/4^{th}$ of the cell. The use of a porous sand supply zone did not ensure a better initial spatial distribution of EDTA than supplying directly to the cathode, as performed

in cell F5C1. This fact can be explained by the increased resistance in the area of the porous sand zone, which prevented some transport of metal-EDTA complexes to the anode region. Comparing cell F5C1 and cell F5C2 reveals that in both cells, significant movement transport of nickel was achieved. Both cells showed precipitation of Ni-EDTA complexes close to the anode. Significant localization of nickel ions was achieved in both cells.

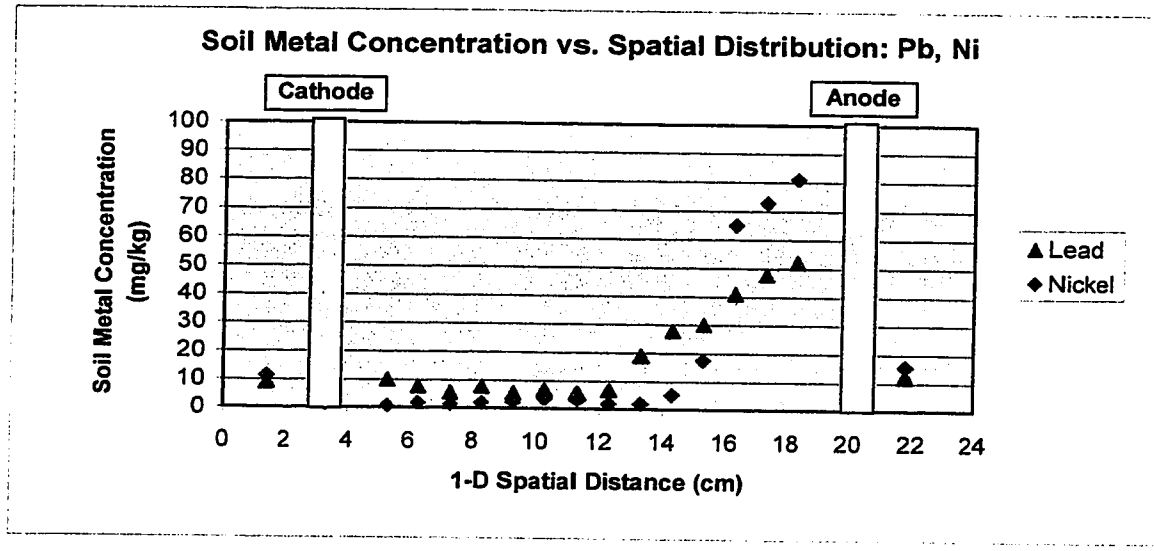

Figure 50 Pb and Ni concentration in soil for EDTA enhanced EK: (F5C1)

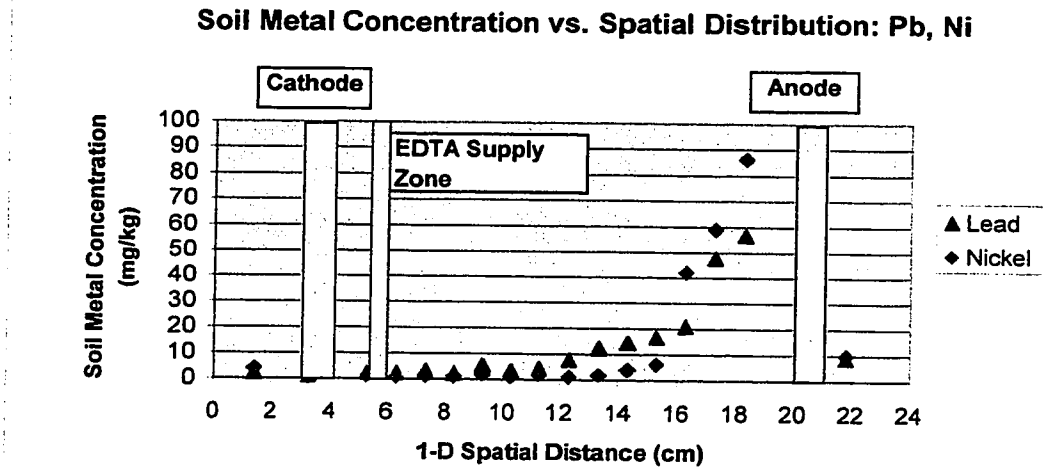

Figure 51 Pb and Ni concentration in soil for EDTA enhanced EK: (F5C2)

11.4.2.4. Lead Concentration

11.4.2.4.1. Cell 1 (F5C1)

The distribution of lead in the soil for cell F5C1 is shown in Figure 50. Electrolytic migration from cathode to anode was observed. Maximum (52.2 mg/kg) and minimum (5.22 mg/kg) values were the result of an abundance of negatively charged lead species in the system, created by the complexation of heavy metals with EDTA. The presence of the majority of lead ions in the anode area is directly related to this phenomenon and provides an indicator as to the effectiveness of EDTA in the mobilization of lead.

Approximately 72 % of lead ions were localized in $1/3^{rd}$ of the cell. This decreased localization (when compared to nickel) can be attributed to low solubility of lead compounds and the competition with nickel for EDTA. Lead has a strong affinity

for clay soil and has higher power of exchange with soils, than other heavy metals. It is assumed that many lead ions preferred to remain sorbed rather than be complexed by EDTA. Although the localization of lead that was achieved was not as high as that of nickel, significant mobilization and localization did occur. It should be noted that the pH distribution provides an indication related to the relative concentration of heavy metal complexes within the soil. Observing the soil pH distribution in F5C1 (Figure 45) in comparison with the soil lead/nickel distribution (Figure 50), it can be seen that the higher the pH, the lower the concentration of negatively charged Pb-EDTA complexes. Where the pH was lower, as in the anode region, the concentration of Pb-EDTA complexes was significantly higher. Therefore, the pH distribution can help in the prediction of the spatial distribution of heavy metals complexes (specifically lead and nickel) within an electrokinetic cell.

11.4.2.4.2. Cell 2 (F5C2)

The spatial distribution of lead within the soil at the end of enhanced EK treatment, for F5C2, is shown in Figure 51. Maximum and minimum values for lead concentration in cell F5C2 were 56.7 mg/kg and 1.11 mg/kg respectively. The lead distribution was similar to that of cell F5C1 and consequently, the method of EDTA supply probably did not play a role in lead transport. After 15 days of treatment, lead was localized to an efficiency of 78 % within $1/3^{rd}$ of the cell, which was slightly better to that achieved in cell F5C1. The degree of electrolytic migration, as reflected by the localization, seemed to be influenced by the nature of lead ions and lead complexation rather than the method of EDTA supply utilized. As with cell F5C1, the degree of lead localization was lower than nickel in cell F5C2. Nevertheless, the localization of lead

that was achieved though the use of EDTA coupled with EK processes was significant considering the fact that natural clayey soil was used.

11.5. Conclusions and Recommendations

An enhanced electrokinetic experiment, consisting of standard EK methods coupled with the use of a chelating agent, ethylenediaminetetraacetic acid (EDTA), was conducted in order to study the principles of transport, mobilization and localization and removal of lead and nickel contamination. The enhanced electrokinetic cells were effective in the transport and localization of lead and nickel. For both cells, 81 % of nickel ions were localized within $1/6^{th}$ of the cell and 85 % were localized within $1/4^{th}$ of the cell. For lead, an average of 79 % of lead contamination was localized within $1/3^{rd}$ of the cell. Significant electrolytic migration was observed for both cells as indicated by this localization. It has been observed, based on the results from experiment F5 and previous work (Elektorowicz *et al.*, (1996a)), the enhanced hybrid method used represented an improvement over standard electrokinetic methods from the following aspects:

1. The use of EDTA throughout the cell volume enhanced the mobilization of lead and nickel. The increased solubility of lead and nickel allowed more ions to become accessible to electrokinetic transport. Typically, nickel and particularly lead compounds have low water solubilities. With the use of EDTA, stable Ni-EDTA and Pb-EDTA complexes formed and remained in solution.

2. The use of EDTA tended to decrease the overall pH. With standard electrokinetics, using natural clay soil, high pH gradients develop in the cathode and anode areas (pH=12.0 at the cathode and pH=7.5 at the anode). The supply of EDTA in the cathode region, using either supply system, decreased the pH between 1.5 to 2.0 pH units.

3. Localization of nickel and lead was enhanced with the use of EDTA. Literature has shown that significant localization of lead and nickel using standard EK methods is difficult, even in pure kaolinite soils (pH=4.5-5.5). Based on the results obtained in this test, the use of EDTA in natural clay soils is effective.

4. During the early stages of the experiment, the EDTA supplied was not significant enough to promote substantial heavy metal complexation. This is indicated by the concentration of heavy metals in the extracted liquid for cell F5C2. As a result, the highest lead and nickel concentrations were obtained in the cathode liquid. As the supply and distribution of EDTA increased, the lead and nickel concentrations obtained in the cathode liquid decreased to 15% and 30% of the initial concentrations respectively. As the EDTA became well distributed, the amount of negatively charged metal-EDTA complexes increased, thereby resulting in an abundance of transported anionic species within the soil.

Table 38 summarizes the problems and inefficiencies with this experiment and the solutions that have been proposed for use in future experiments. Despite some inefficiency with the use of EDTA for improved mobilization of nickel and lead during EK methodology, the following conclusions can be made:

1. The use of EDTA is effective in mobilizing bound heavy metals, specifically lead and nickel. The formation of complexes allows for the transport, of Pb-EDTA and Ni-EDTA complexes to desired locations, thereby allowing for moderate to very good localization.

2. The use of EDTA in soil decreases the overall pH of the soil, particularly in the cathode region. This is due to supplying the EDTA in the cathode region.

3. The method of supplying EDTA directly through the cathode (F5C1), or through a porous sand zone (F5C2) did not show a significant difference in localization efficiency for lead. Slightly better nickel localization was achieved in F5C1 than F5C2.

4. The use of a porous supply zone increases the potential and therefore the resistance of the soil. Since the overall localization efficiency for both tests were similar, the use of a porous supply zone is not required. Where direct supply to the cathode is impossible, the supply zone method is a viable alternative. Regarding pilot-scale and field studies, the use of a porous sand zone would increase costs due to the need for a more complex EDTA supply system and excavation.

Table 38 Problematic Conditions during the use of EDTA in EK Processes

Problem	*Reason and Associated Problems*	*Proposed Solution*
Higher resistance in Cell F5C2	• The implementation of a porous sand barrier used for the supply of EDTA	• Direct contact of EDTA with the soil before EK processes • Implementing a supply configuration similar to that of Cell F5C1
Full distribution of EDTA in each cell was not achieved	• High resistivity of the soil • Countercurrent flows: water supplied at the anode and EDTA supplied at the cathode	• Directly contact of EDTA with the soil before EK processes to ensure proper distribution
High iron concentrations were observed in the soil	• High oxidation of the anode in both cells • Presence of high initial concentrations of iron in the soil • Creates competition for EDTA complexes • Potential of competition for ion exchange textiles)	• Change anode material • Apply this EDTA-EK methodology in soils with low initial iron content
Localization of lead and nickel was only moderately high	• Precipitation of metal-EDTA complexes in the anode region • Affinity of lead and nickel for the soil • Low water solubility of lead and nickel	• Employ ion exchange textiles (IET) to allow for the exchange of target heavy metals. • The IET will improve localization and facilitate simpler removal of lead and nickel.

The advantages with the use of the textile cannot be underestimated, since they can alleviate the inherent problems of standard EK methods. The next experiment attempts other EK enhancement methods, to improve the localization and overall removal efficiency of nickel and lead, through the use of ion exchange textiles (the second enhancement method). This method examines a new hybrid system (EDTA-EK-IET) that combines the use of ion exchange textiles with EDTA-EK methods.

12. EXPERIMENT F6: RESULTS AND DISCUSSION

Results were obtained following the methodology of measurements and sampling described in chapter 9. Electrical parameters, and physico-chemical parameters of the soil and liquids were obtained. These results allow for accurate discussions and conclusions to be made related to the performance of the EK-EDTA-IET technology for the imposed conditions. This section deals with the presentation of results acquired from experiment F6 (cell F6C1 to cell F6C6).

12.1. Electrical Parameters

The variance of resistance with the distance from the cathode for cell F6C1 to cell F6C6 is displayed graphically in Figure 52 (F6C1), Figure 53 (F6C2), Figure 56 (F6C3), Figure 57 (F6C4), Figure 60 (F6C5) and Figure 61 (F6C6). This section deals with a discussion and comparison of cells with respect to the resistance distribution.

12.1.1. Cell 1 (F6C1) and Cell 2 (F6C2): Resistance in Soil

The resistance distributions between electrodes for cell F6C1 (EK-AET) and cell F6C2 (EK-CET), as shown in Figure 52 and Figure 53 respectively, are characterized by a general increasing trend in the anode direction with time and distance. The use of IETs in each cell created sharp resistance gradients, particularly in cell F6C2. The resistance gradients observed in cell F6C1 and F6C2, at the beginning of the experiment, were 32 ohms/cm and 20 ohms/cm respectively. After 281 hours of the experiment, the gradients increased to 42 ohms/cm and 27 ohms/cm respectively. At the end of the experiment (546 hours), the resistance gradients were 53 ohms/cm and 32 ohms/cm respectively.

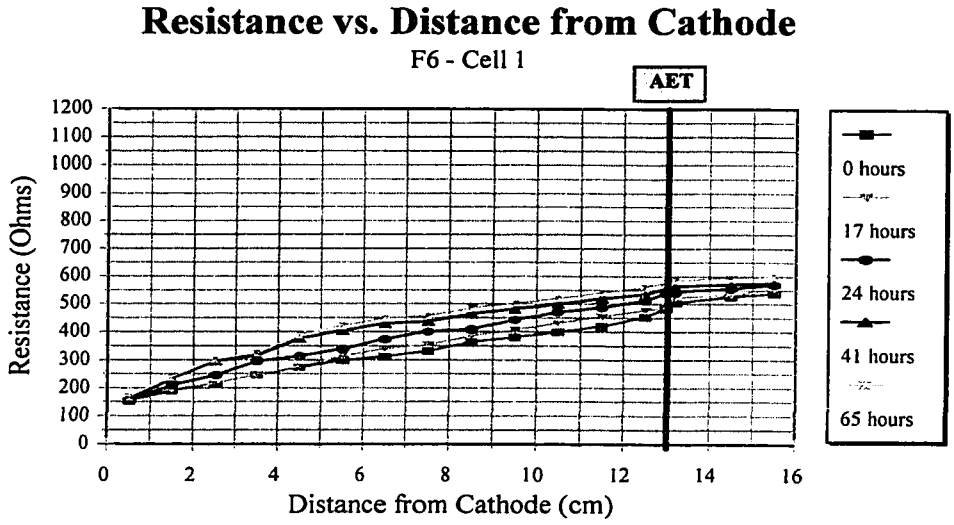

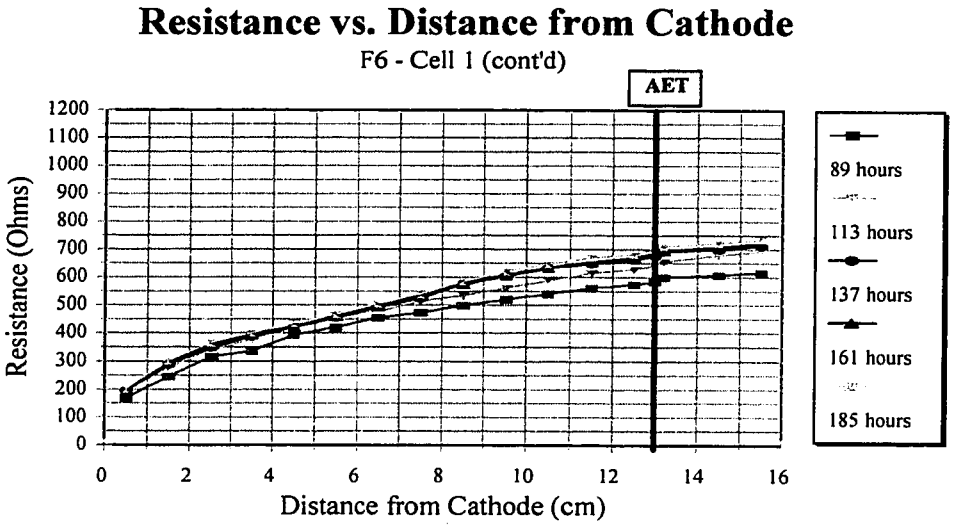

Figure 52 Resistance distribution versus distance from the cathode (F6C1)

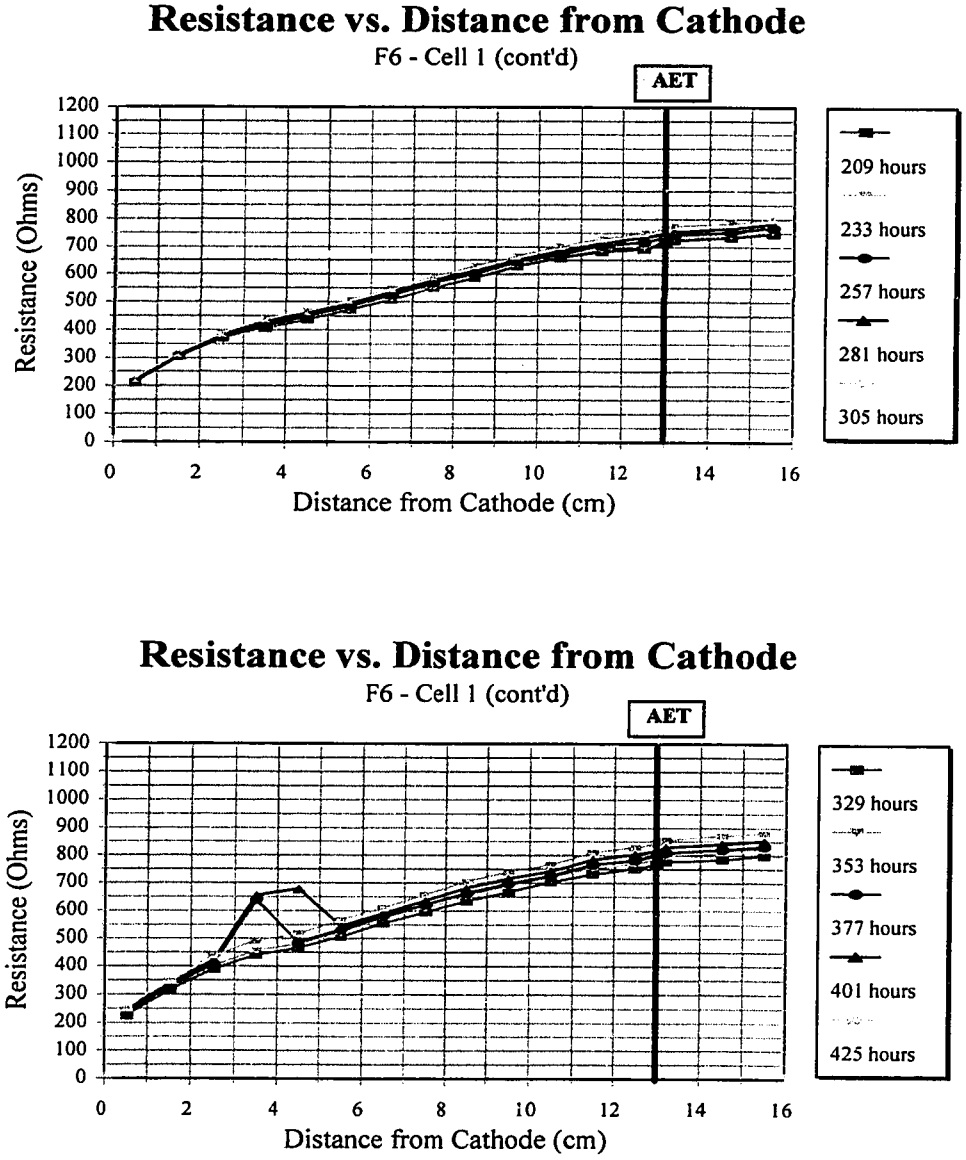

Figure 52 Resistance distribution versus distance from the cathode (F6C1) (cont'd)

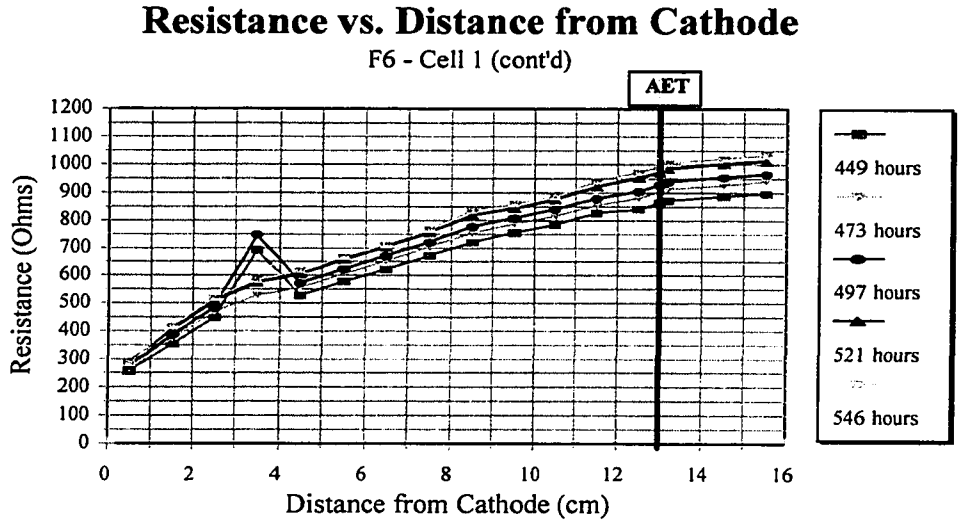

Figure 52 Resistance distribution versus distance from the cathode (F6C1) (cont'd)

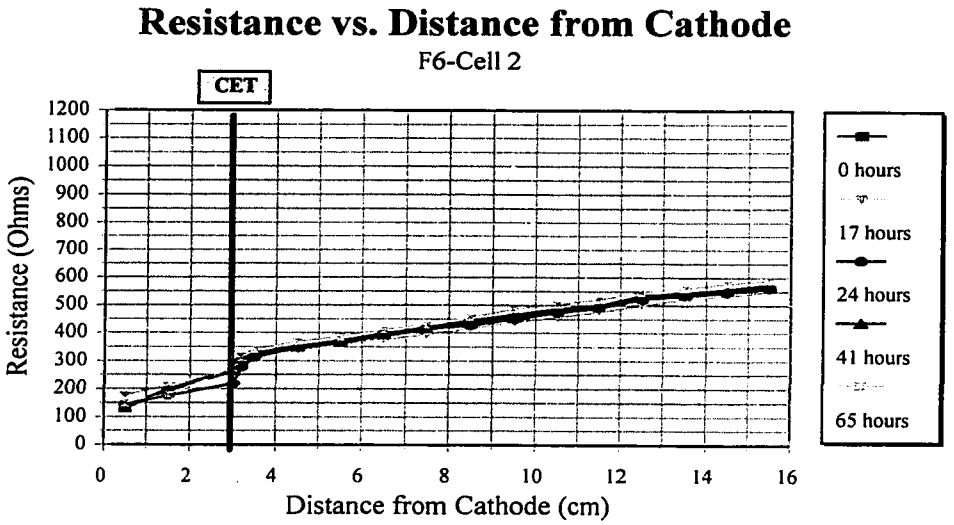

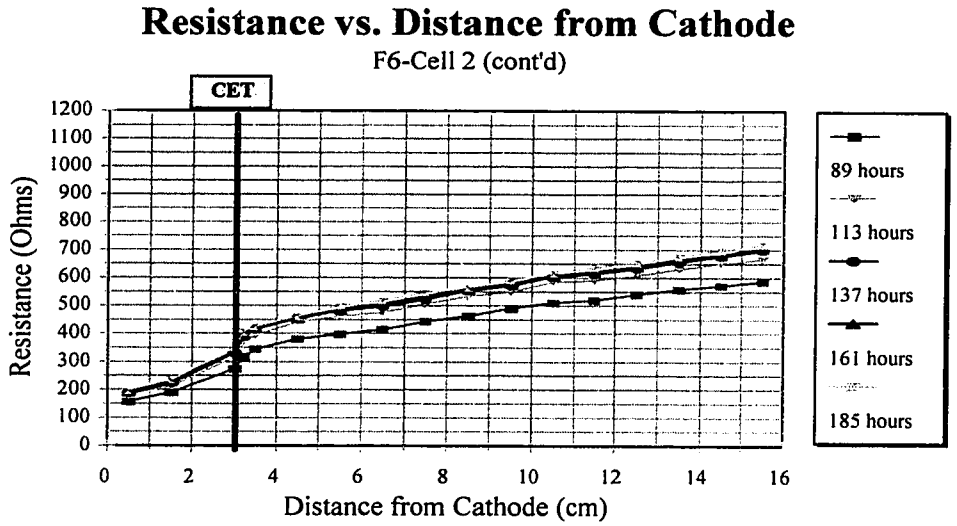

Figure 52 Resistance distribution versus distance from the cathode (F6C2)

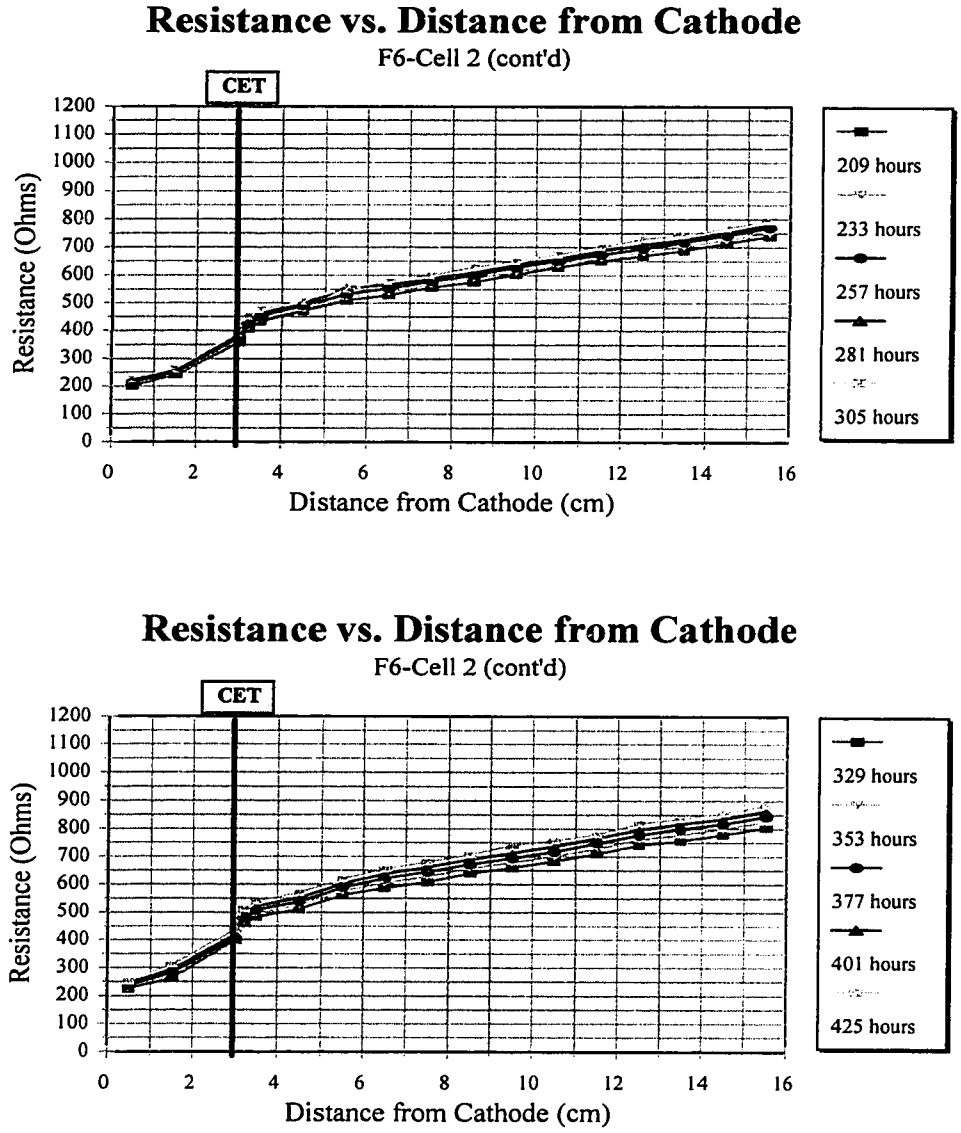

Figure 53 Resistance distribution versus distance from the cathode (F6C2) (cont'd)

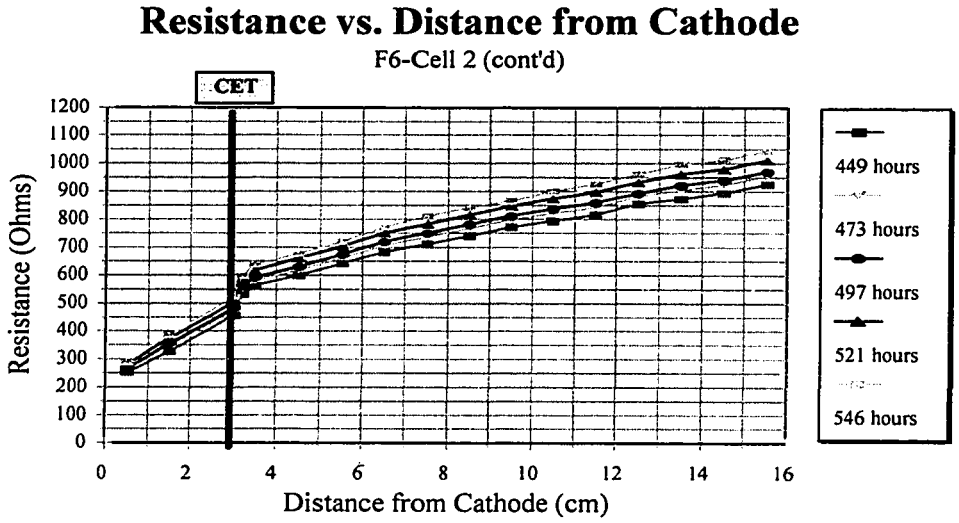

Figure 53 Resistance distribution versus distance from the cathode (F6C2) (cont'd)

The temporal increase in F6C1 and F6C2 can be attributed to the increasing resistance in the anode region created by the oxidation and release of ferric ions into this area. The ferric ions in the soil environment were transformed into slightly soluble species and readily formed precipitates, even under neutral conditions. The resistance at each probe location increased steadily with time due to the decreasing current within both cells. Their distributions are similar and both show this general increase in resistance. The current in cell F6C1 decreased from 8.47 mA at the beginning of the experiment, to 4.53 mA (53 % of the original) after 546 hours. In F6C2, the initial current was 8.57 and the final current measured after 546 hours was 4.63 (54 % of the original current). During this time period, the potential did not vary appreciably and as a result, the resistance increased accordingly.

12.1.2. Cell 1 (F6C1) and Cell 2 (F6C2): Resistance at Textile

The resistance distribution at the location of the IET within F6C1 and F6C2 showed pronounced differences than within the soil. The gradient in F6C2, at the textile location was more pronounced that in cell F6C1 with an average value of 750 Ohms/cm. Cell F6C1 showed a gradient of 200 Ohms/cm in the textile region. This is an indication of the presence of cations exchanged on the CET of F6C2. The absence of EDTA resulted in no EDTA-complexation and therefore lower exchange of anionic complexes on the AET of F6C1. As a result, a significantly lower resistance gradient resulted in the AET of F6C1 in comparison to the CET of F6C2.

Figure 59 and Figure 60 show the initial and final (after 546 hours) soil resistance distributions for cell F6C1 and cell F6C2 respectively. The presence of IETs in both cells created a discontinuity and as a result necessitated the fitting of two curves (before and after the IET) for each time. A comparison of the average spatial resistance in cell F6C1 and F6C2, as displayed in Figure 54 and Figure 55 respectively, shows similar distributions except at the textile location. A higher gradient was observed in F6C2 than in cell F6C1. As with all cells, the distribution for cell F6C1 and F6C2 seems to correlate to a power model. R^2 values for cell F6C1 and F6C2 ranged from 0.9811-0.9985 and 0.9735-0.9971 respectively, which represents an excellent fit. Although the coefficients of the power model changed, the degree of correlation remained relatively constant from the beginning to the end of the experiment. Therefore a general model would be dependent on determining suitable coefficients for the power model, for the entire EK duration. It should be noted that a 6^{th} degree polynomial had similar (sometimes higher) correlation coefficients, but the power model was chosen due to its simplicity.

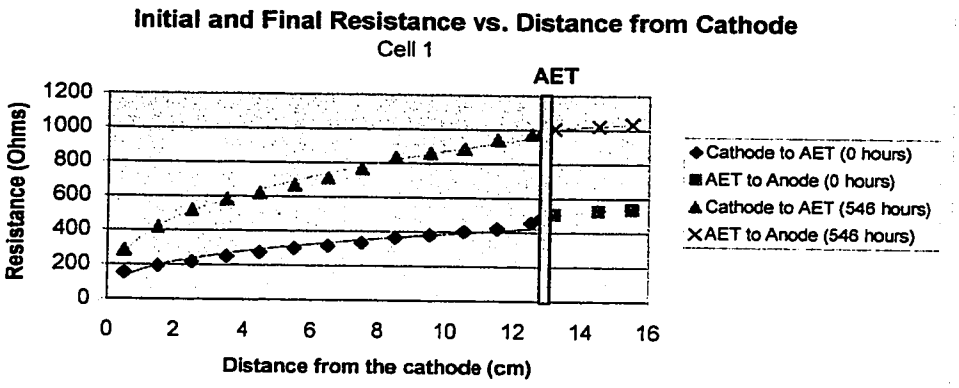

$$r(x) = \begin{cases} 171x^{0.36} & 0 < x \le 12.8 \quad R^2 = 0.9511 \\ 177x^{0.41} & 12.8 < x < 16.0 \quad R^2 = 0.9923 \end{cases} \quad t=0\ h$$

$$r(x) = \begin{cases} 360x^{0.38} & 0 < x \le 12.8 \quad R^2 = 0.9951 \\ 645x^{0.17} & 12.8 < x < 16.0 \quad R^2 = 0.9985 \end{cases} \quad t=546\ h$$

Figure 54 Initial and final resistance vs. distance from cathode (F6C1)

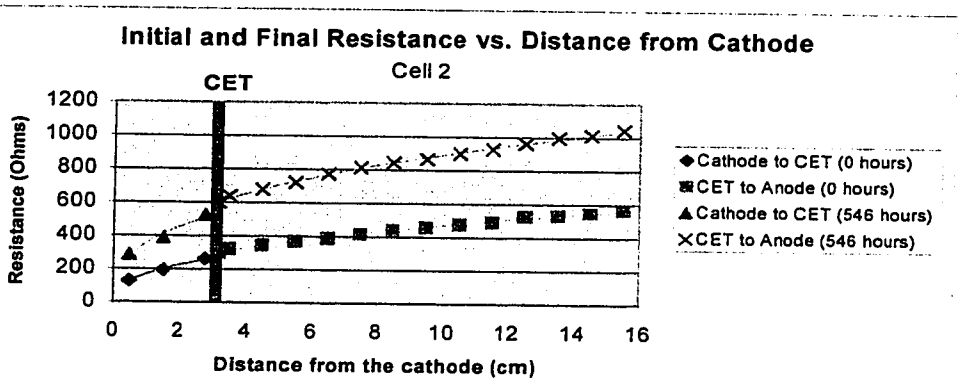

$$r(x) = \begin{cases} 170x^{0.40} & 0 < x \le 3.0 \quad R^2 = 0.9959 \\ 190x^{0.39} & 3.0 < x < 16.0 \quad R^2 = 0.9937 \end{cases} \quad t=0\ h$$

$$r(x) = \begin{cases} 356x^{0.34} & 0 < x \le 12.8 \quad R^2 = 0.9735 \\ 407x^{0.34} & 12.8 < x < 16 \quad R^2 = 0.9971 \end{cases} \quad t=546\ h$$

Figure 55 Initial and final resistance vs. distance from cathode (F6C2)

r = resistance (Ohms)
x = distance from cathode

12.1.3. Cell 3 (F6C3) and Cell 4 (F6C4): Resistance in Soil

The resistance distributions for F6C3 and F6C4 and their variance with distance is shown in Figure 56 and Figure 57 respectively. Both cells show relatively constant resistance gradients with distance, but the gradients tend to increase with time.

The resistance gradient within the soil showed small changes with distance. As the time increased, the resistance gradient increased accordingly, due to a decrease in the current from 8.51 mA (beginning of the experiment) to 4.49 mA (at the end of the experiment) in F6C3. F6C4 experienced a similar cell current reduction from 8.44 mA to 4.50 mA. The calculated gradients for F6C3 and F6C4 at the beginning of the experiment were 22 ohms/cm and 24 ohms/cm respectively. After 281 hours, the gradients were 26 ohms/cm and 40 ohms/cm respectively. At the end of the experiment (546 hours), the gradients increased to 30 ohms/cm and 56 ohms/cm respectively.

12.1.4. Cell 3 (F6C3) and Cell 4 (F6C4): Resistance at Textile

The highest gradients for F6C3 (EDTA-EK-CET) and F6C4 (EDTA-EK-AET) were in the location of the textile. Similar to cell F6C1 and F6C2, the CET of F6C3 had larger effect on the resistance gradient than the AET of F6C4. The maximum gradients in the area of the textile for F6C3 and F6C4 were 650 ohms/cm and 300 ohms/cm respectively. The gradients near the textile in both cells increased slightly with time due to fouling of the textiles by soil particles. The increase was higher in F6C3, where the gradient increased from 400 ohms/cm at the beginning of the experiment to 650 ohms/cm after 546 hours.

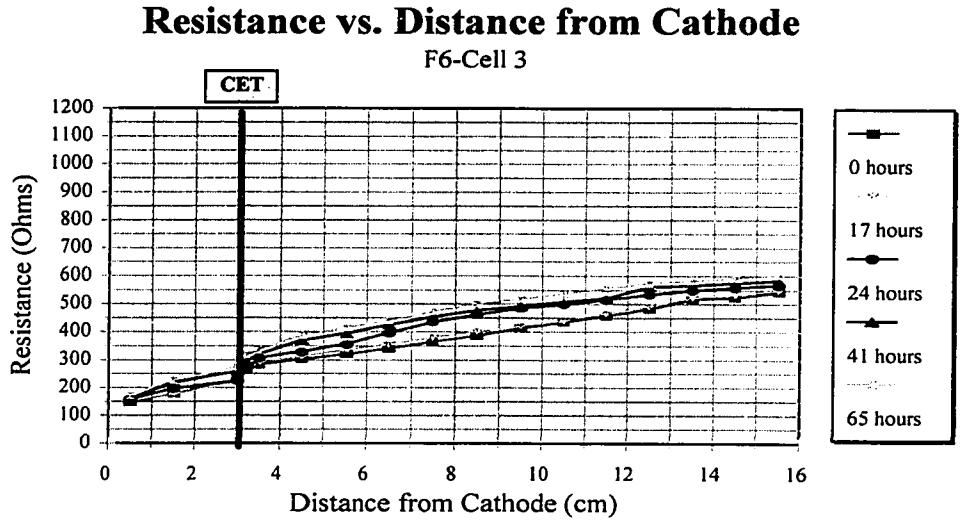

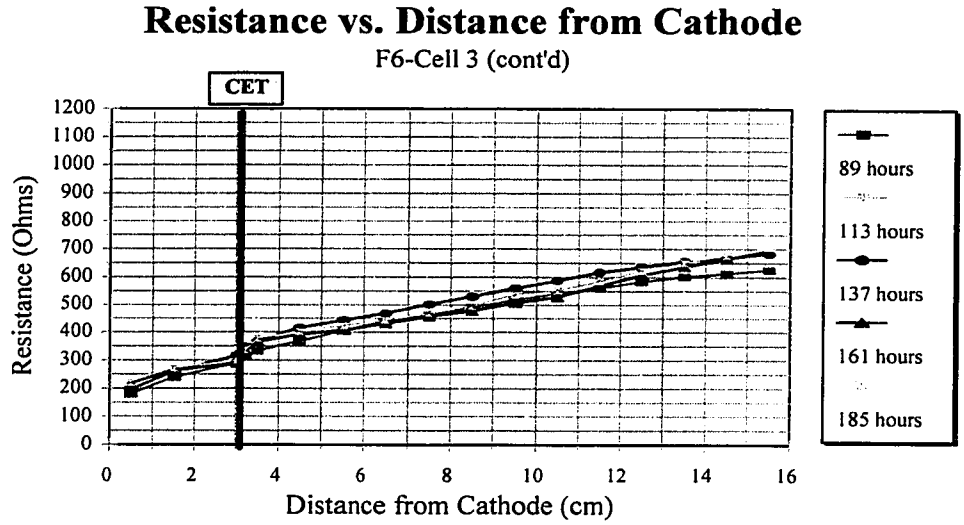

Figure 56 Resistance distribution versus distance from the cathode (F6C3)

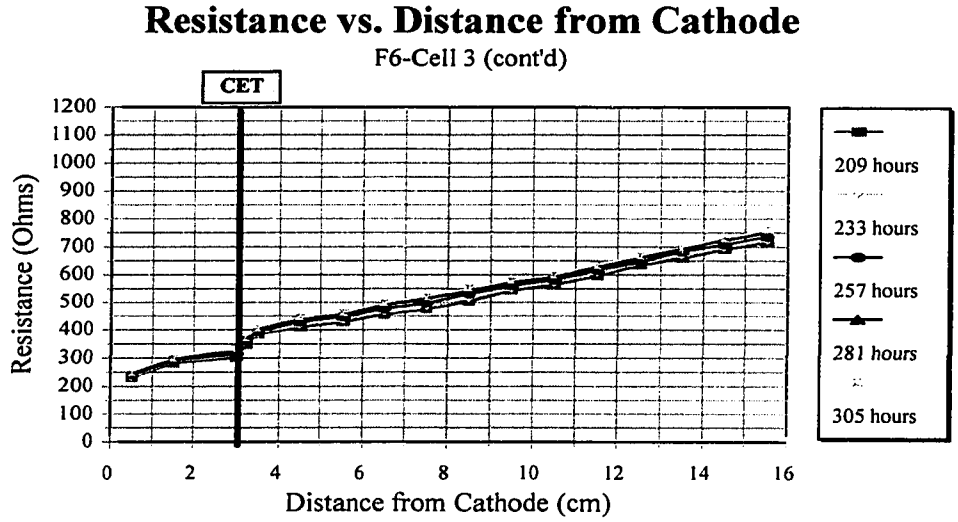

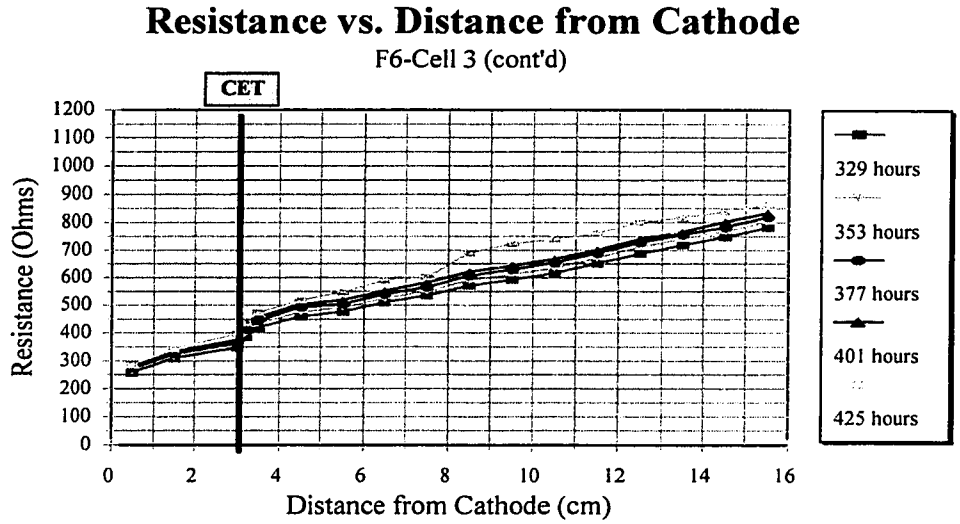

Figure 56 Resistance distribution versus distance from the cathode (F6C3) (cont'd)

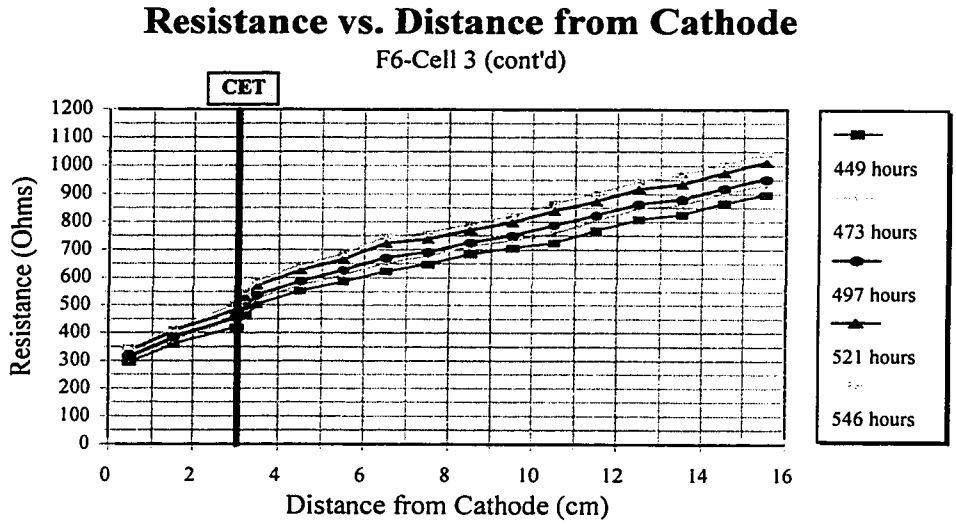

Figure 56 Resistance distribution versus distance from the cathode (F6C3) (cont'd)

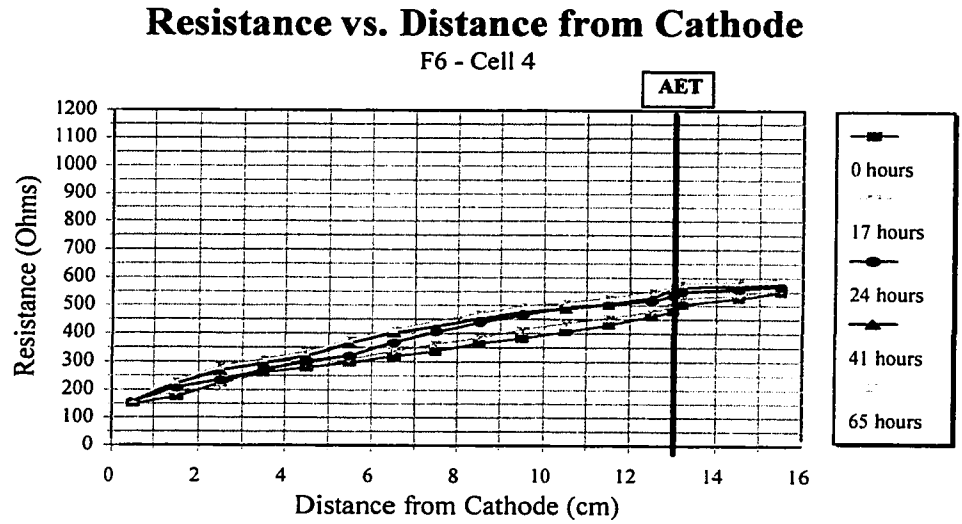

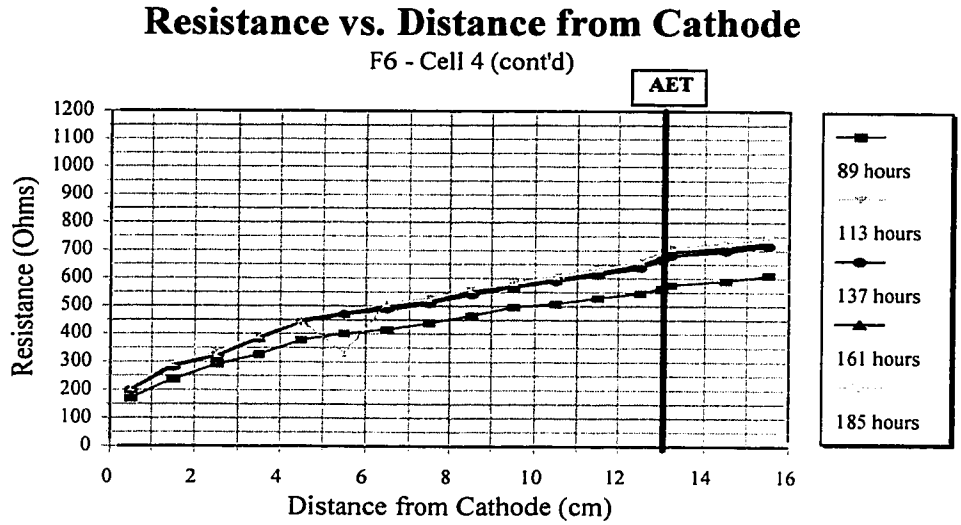

Figure 57 Resistance distribution versus distance from the cathode (F6C4)

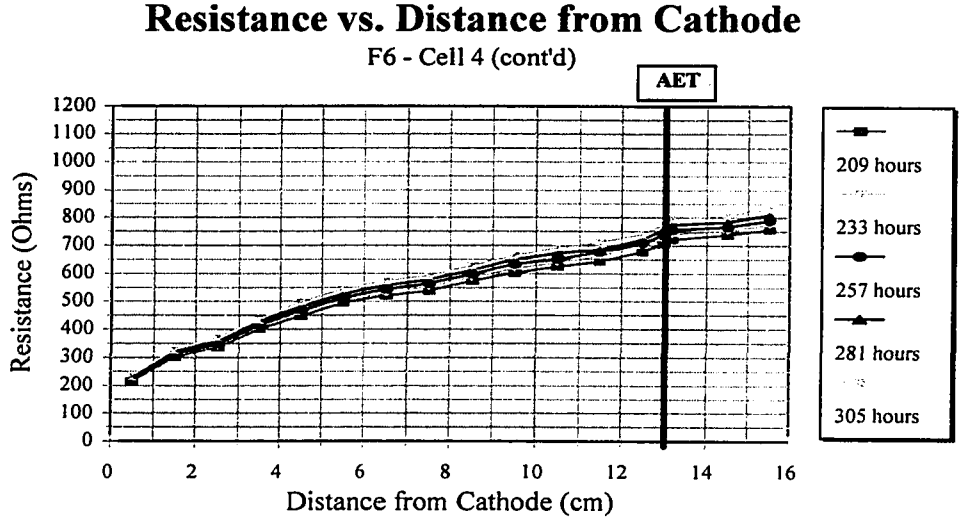

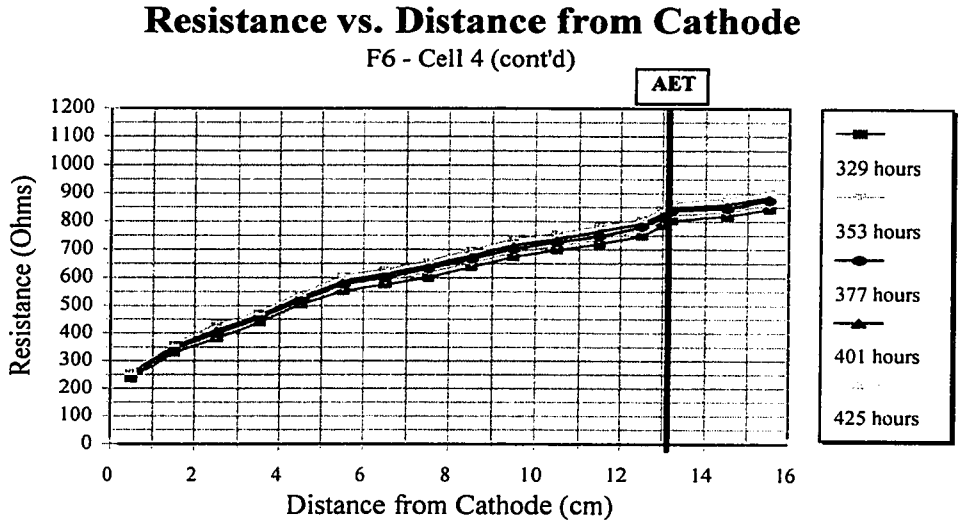

Figure 57 Resistance distribution versus distance from the cathode (F6C4) (cont'd)

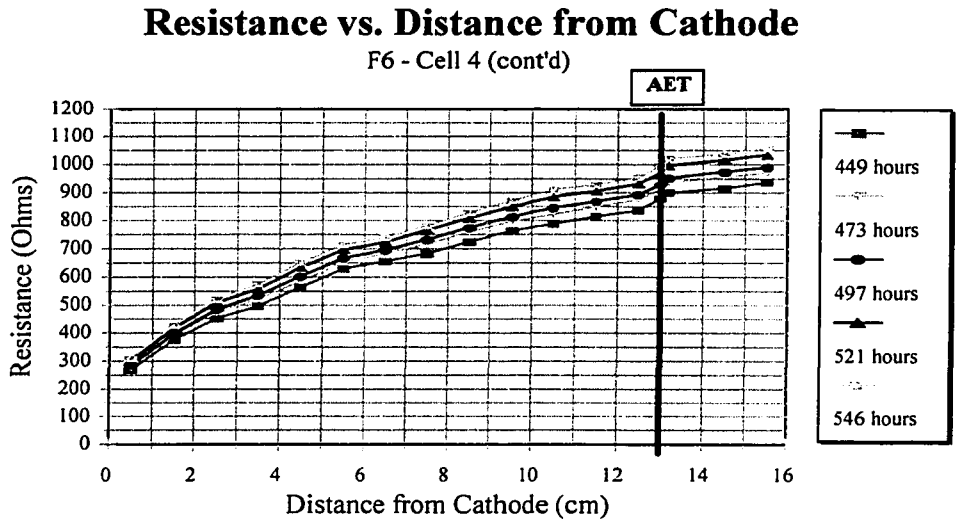

Figure 57 Resistance distribution versus distance from the cathode (F6C4) (cont'd)

The cells utilizing AETs (i.e. cell F6C1 and F6C4), had a moderate effect on the resistance gradient in the proximity of the textile. However, the gradients in the remaining area of these cells showed greater increases with time than the cells that used CETs (F6C2 and F6C3). For cell F6C3 and cell F6C4, the resistance gradient at the IET location increased with time. This demonstrated the ability of the IETs to exchange heavy metals from the soil and retain them. Although the gradient at the CET of F6C4 was greater than the AET of F6C3, the difference was 100 Ohms/cm which was significantly lower than the difference observed in F6C1 and F6C2. In addition, the resistance gradient for the CET of F6C2 (EK-CET) was higher than at the CET in F6C3. The resistance gradient at the AET of F6C1 (EK-AET) was 150 Ohms/cm lower that at the AET of F6C4. The reason for this phenomenon is due to the presence of EDTA and

its effect in complexing heavy metals. The anionic complexes that formed, were transported to the anode region. The more anionic complexes formed, the greater the transport of ions to the anode area. Also, the more complexes that are formed, the lower the amount of free cationic species remaining within the system. Therefore, with the use of EDTA, more ions are transported to the anode area than the cathode area. This resulted in the resistance gradients discussed above.

A comparison of initial and final resistance versus the distance from the cathode for F6C3 and F6C4 (Figure 58 and Figure 59 respectively), show similar distributions with the exception of the zone where the textile is located. Due to the IETs in both cells, a discontinuity resulted within each cell. This necessitated the fitting of curves separately (before and after the IETs). F6C3 shows a higher resistance gradient at the CET than at the AET in F6C4. Both cells correlate well to a power function at all locations of the cell, with correlation coefficients of 0.94. Comparing between initial and final curves shows that the correlations did not change appreciably. This shows that resistance distribution can be mathematically modeled, which would be desirable, particularly in field applications.

12.1.5. Cell 5 (F6C5) and Cell 6 (F6C6) : Resistance in Soil

The resistance distributions for F6C5 (EDTA-EK) and F6C6 (EDTA-EK-CET & AET) and their variance with distance is shown in Figure 60 and Figure 61 respectively. A comparison of F6C5 and F6C6 clearly shows the effect of IET utilization on the resistance gradient. In the absence of a textile, as in F6C5, the resistance gradient is approximately constant with distance from the cathode.

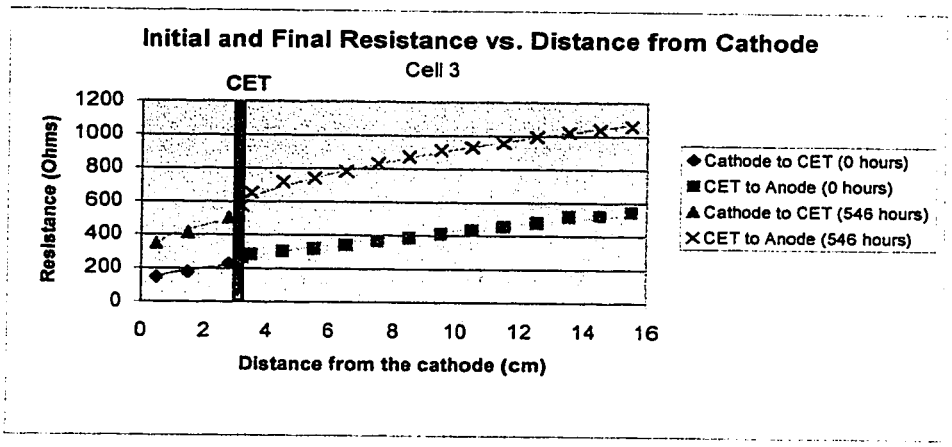

$$r(x) = \begin{cases} 172x^{0.24} & 0 < x \le 3.0 \quad R^2 = 0.9469 \\ 153x^{0.45} & 3.0 < x < 16.0 \quad R^2 = 0.9820 \end{cases} \quad t=0\ h$$

$$r(x) = \begin{cases} 397x^{0.21} & 0 < x \le 12.8 \quad R^2 = 0.9589 \\ 405x^{0.34} & 12.8 < x < 16 \quad R^2 = 0.9851 \end{cases} \quad t=546\ h$$

Figure 58 Mathematical analysis of average spatial resistance (F6C3)

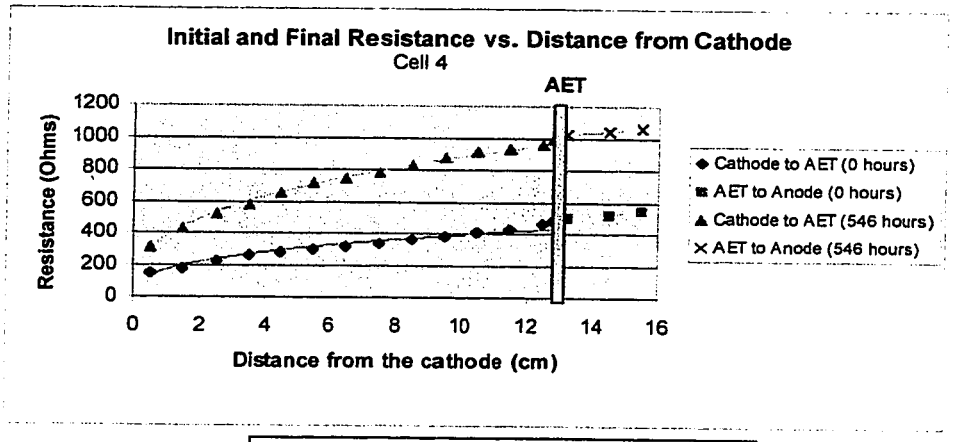

$$r(x) = \begin{cases} 167x^{0.37} & 0 < x \le 12.8 \quad R^2 = 0.9579 \\ 135x^{0.51} & 12.8 < x < 16.0 \quad R^2 = 0.9898 \end{cases} \quad t=0\ h$$

$$r(x) = \begin{cases} 380x^{0.36} & 0 < x \le 12.8 \quad R^2 = 0.9950 \\ 594x^{0.21} & 12.8 < x < 16.0 \quad R^2 = 0.9731 \end{cases} \quad t=546\ h$$

Figure 59 Mathematical analysis of average spatial resistance (F6C4)

r = resistance (Ohms)
x = distance from cathode (cm)

In F6C6, three distinct zones of resistance gradients are observed with distance, throughout the duration of the experiment. These gradients are:

1. A high gradient at the location of the CET.
2. The gradient at the location of the AET
3. Small gradients in the remaining parts of the cell.

The resistance gradient at the AET was lower than that of the CET in F6C6. This was the same to that displayed in the AET of cell F6C1 and cell F6C4 versus the CET in cells F6C2 and F6C3, where the CET gradients were higher than the AET gradients.

12.1.6. Cell 6 (F6C6): Resistance at Textiles

As with all cells containing IETs, the magnitude of the resistance gradients in the IET locations of F6C6 increased with time. At the beginning of the experiment, the AET and CET gradients in F6C6 were 250 ohms/cm and 300 ohms/cm respectively. After 281 hours, the resistance gradients were 300 ohms/cm and 500 ohms/cm respectively. At 546 hours (the end of the experiment), the AET and CET resistance gradients increased to 350 ohms/cm and 750 ohms/cm respectively. The gradients in the zones without the textile at 0 hours, 281 hours and 546 hours were 20 ohms/cm, 26 ohms/cm and 47 ohms/cm respectively. In F6C5, the gradients at 0 hours, 281 hours and 546 hours were 25 ohms/cm, 30 ohms/cm and 46 ohms/cm respectively.

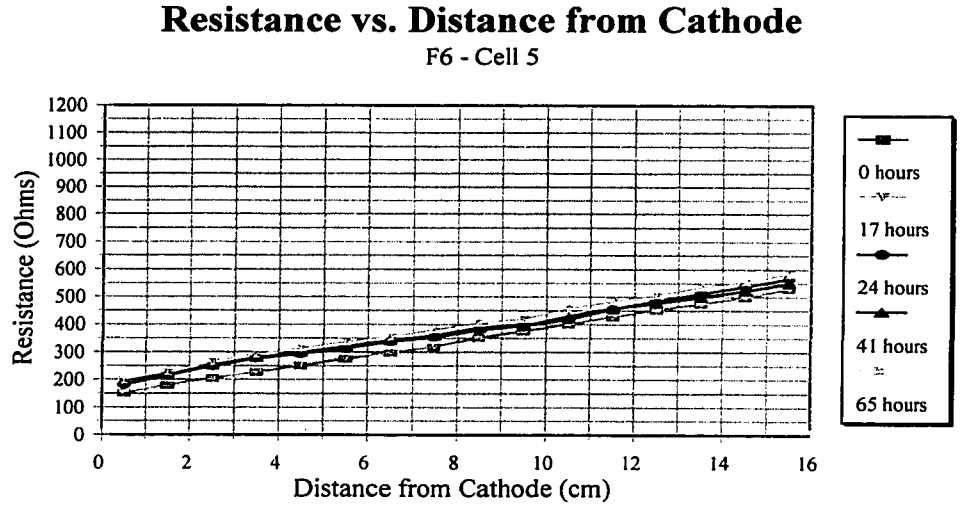

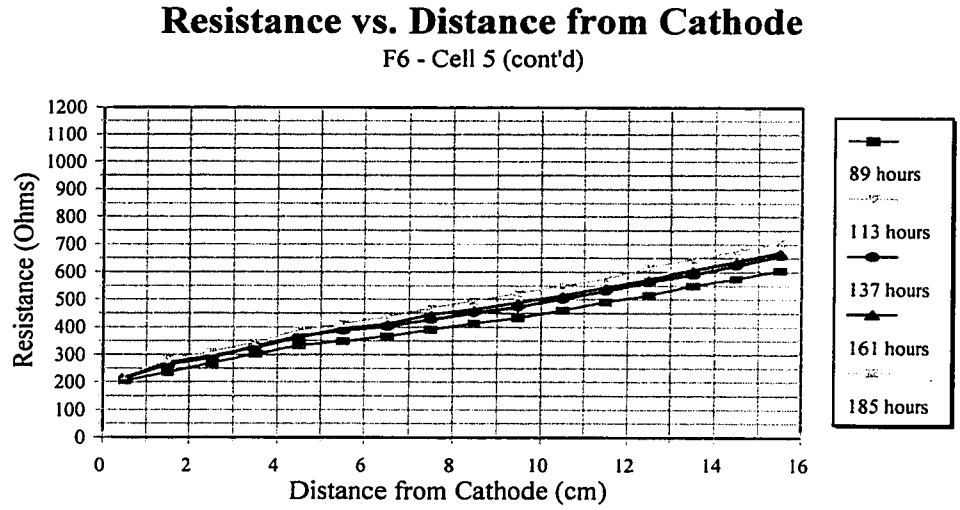

Figure 60 Resistance distribution versus distance from the cathode (F6C5)

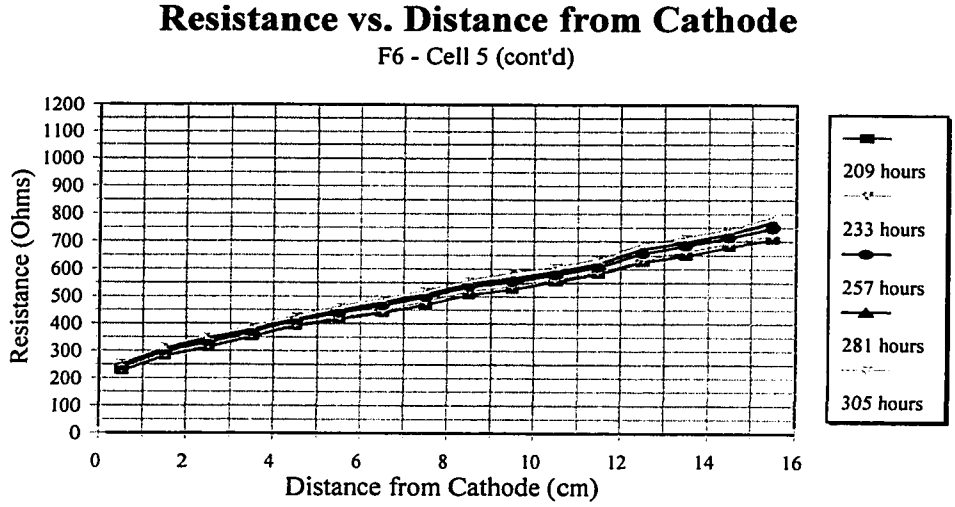

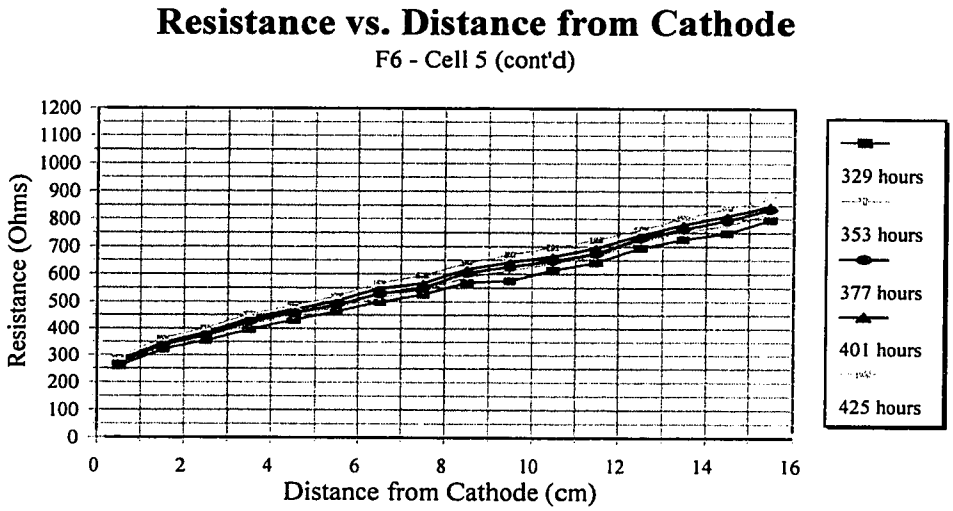

Figure 60 Resistance distribution versus distance from the cathode (F6C5) (cont'd)

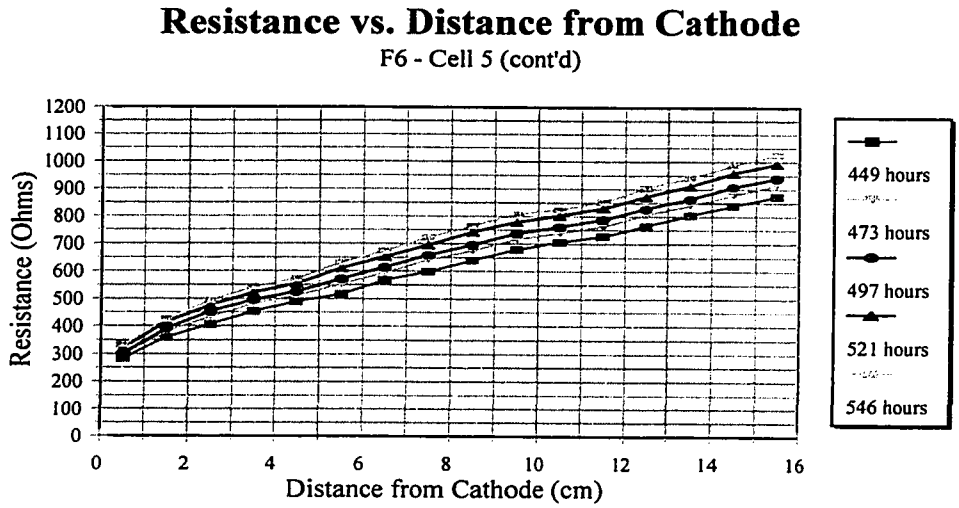

Figure 60 Resistance distribution versus distance from the cathode (F6C5) (cont'd)

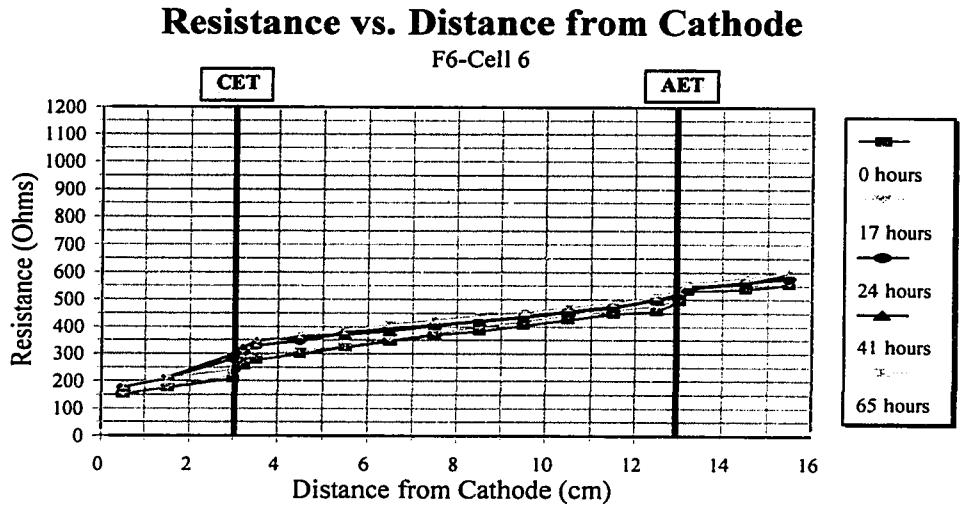

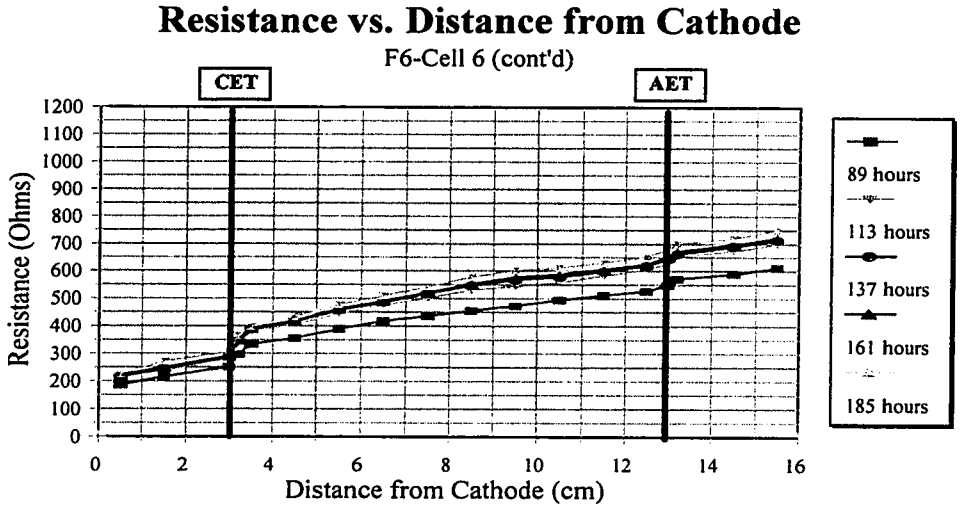

Figure 61 Resistance distribution versus distance from the cathode (F6C6)

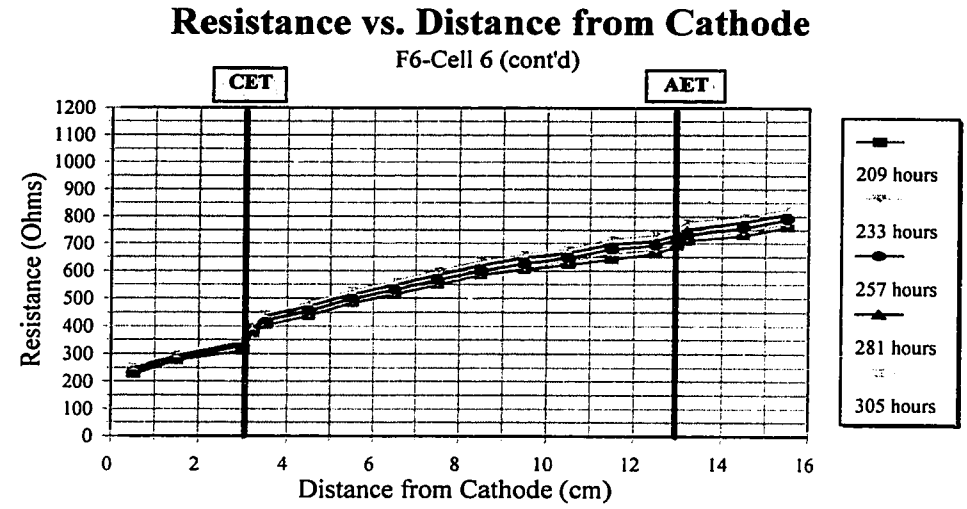

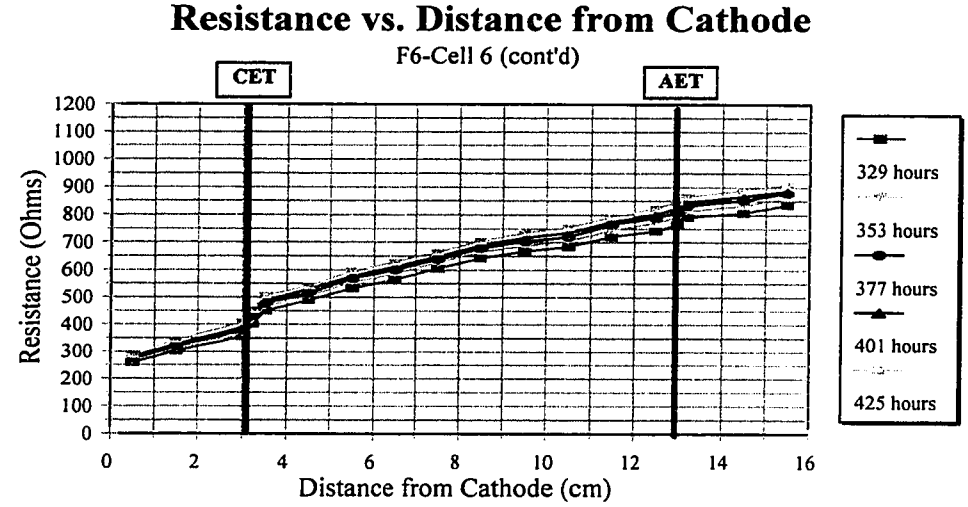

Figure 61 Resistance distribution versus distance from the cathode (F6C6) (cont'd)

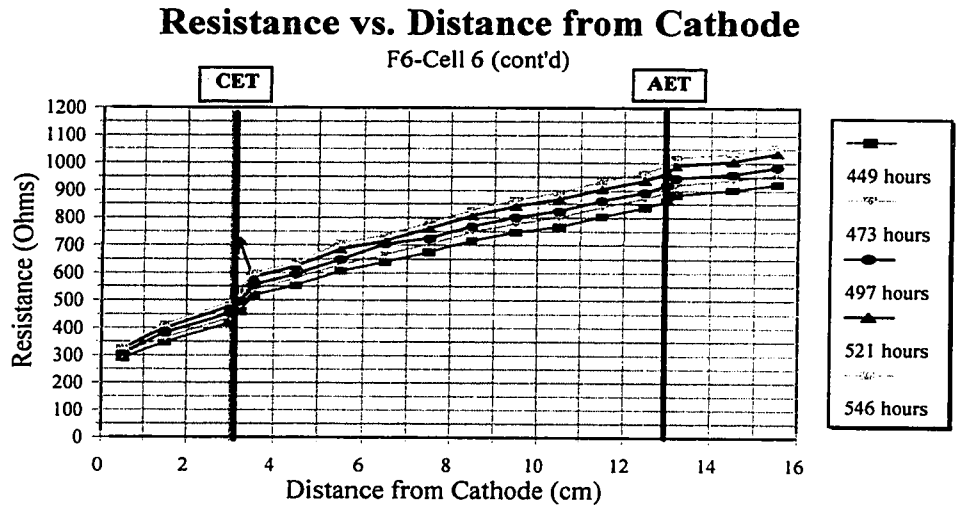

Figure 61 Resistance distribution versus distance from the cathode (F6C6) (cont'd)

Figure 62 and Figure 63 show a comparison of the initial and final resistance distributions for F6C5 and F6C6 respectively. As can be seen in both cells the resistance of the soil at each probe location approximately doubled from the initial value. However, the shape of the curve remained similar. Similar to F6C1 to F6C4, a power model was fit to both F6C5 and F6C6 for all locations and times, with correlations in the range 0.9212-0.9716 and 0.8363-0.9906 for F6C5 and F6C6 respectively. The fact that the best curve fit that was employed did not change with time shows that the power model can possibly be applied for mathematical representation of resistance distribution. This can be useful in scaling-up procedures during EDTA-EK-IET remediation.

12.1.7. Summary and Comparison of Cells

The resistance distribution and gradients were independent on whether a chelating agent was employed. The use of textiles also affected the distribution and gradients appreciably. The effect of textiles on the resistance distribution, specifically the gradients are two-fold:

1. The resistance of the cell increases with time as textile fouling occurs and as heavy metals exchange onto the textile. This has an effect on the entire cell, where the resistance and therefore, the impedance to EK transport increases with time and for all locations within the cell. This is evidenced by the sharp gradient that occurred in the textile locations.

2. The use of a CET produced gradients in the remaining locations of the cell that were 1.1 to 2.0 times higher (other than in the location of the textile), than those cells that employed AETs. This could be attributed to higher textile fouling in the CET than in the AET.

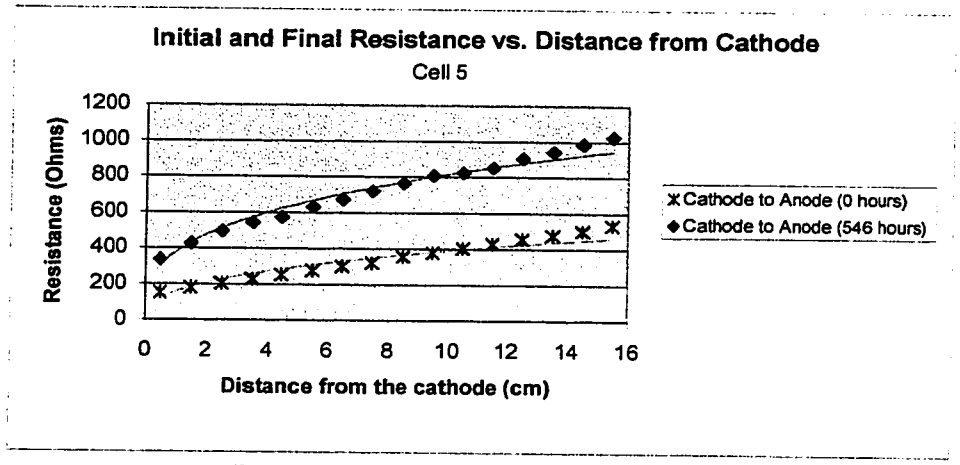

$r(x) = 158x^{0.39}$ $0 < x < 16.0$ $R^2 = 0.9212$ t=0 h

$r(x) = 376x^{0.34}$ $0 < x \leq 16.0$ $R^2 = 0.9950$ t=546 h

Figure 62 Mathematical analysis of average spatial resistance (F6C5)

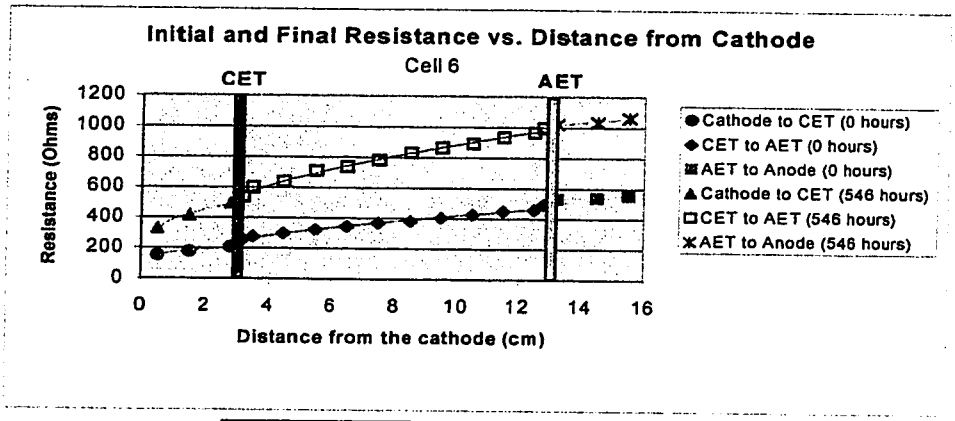

$r(x) = \begin{cases} 170x^{0.18} & 0 < x \leq 3.0 \quad R^2 = 0.9469 \\ 156x^{0.40} & 3.0 < x \leq 12.8 \quad R^2 = 0.9820 \\ 280x^{0.25} & 12.8 < x < 16.0 \quad R^2 = 0.8363 \end{cases}$ t=0 h

$r(x) = \begin{cases} 384x^{0.23} & 0 < x \leq 3.0 \quad R^2 = 0.9469 \\ 347x^{0.40} & 3.0 < x \leq 12.8 \quad R^2 = 0.9820 \\ 555x^{0.23} & 12.8 < x < 16.0 \quad R^2 = 0.8363 \end{cases}$ t=546

Figure 63 Mathematical analysis of average spatial resistance (F6C6)

r = resistance (Ohms)
x = distance from cathode (cm)

Table 39 shows a comparison of cells and the effect of textile on the resistance. A detailed table of data related to the resistance values on both sides IET, from 0 to 546 hours is shown Appendix D, Table D-1.

Table 39 Change in Resistance at IETs: Comparison of the Cells

Cell	*Final Change in Resistance at AET (from Cathode side to Anode side) (Ohms)*	*Final Change in Resistance at CET (from Cathode side to Anode side) (Ohms)*
F6C1	14	-
F6C2	-	65
F6C3	-	45
F6C4	26	-
F6C5	-	-
F6C6	24	43

The effect of the CET on the resistance distribution is evident when comparing those cells containing IETs (F6C1, F6C2, F6C3, F6C4, F6C6) with F6C5. With the retention of heavy metals or heavy metal complexes by the IETs, the resistance gradient increased accordingly. Without a textile (F6C5), there are no sharp deviations in the resistance. Comparing all cells reveals that the CET has a more pronounced effect on the resistance distribution than an AET. Although the difference in the resistance gradient for the CET and AET in those cells employing EDTA (F6C3 and F6C4) was lower than those cell not employing EDTA (F6C1 and F6C2). The exception to this rule is observed in F6C6, where both textiles were used. As shown in Table 39, the difference in the resistance gradient for the CET and the AET was 400 ohms/cm.

12.2. Volume and pH of the Cathode Liquids

12.2.1. Cell 1 (F6C1) and Cell 2 (F6C2)

The daily volume of the cathode liquids extracted from cell F6C1 and F6C2 is shown in Figure 64. Maximum and minimum values for cell F6C1 are 14.2 mL (24 hours) and 0.0 (65 hours). Maximum and minimum values for F6C2 are 12.6 (24 hours) and 0.0 (65 hours). The total and average volumes extracted in cell F6C1 were 180.7 mL and 7.5 mL respectively. Comparative values for F6C2 were 167.7 mL and 7.0 mL respectively.

The pH of the liquids extracted from the cathode in cell F6C1 and F6C2 are shown in Figure 65. Maximum and minimum pH values observed in cell F6C1 were 12.4 (257 hours) and 8.5 (21 hours) respectively. Comparative maximum and minimum values for F6C2 were 12.7 (257 hours) and 8.3 (17 hours). Cell F6C1 and F6C2 show similar pH distributions, except pH values in cell F6C1 were consistently 0.1-0.5 units lower than comparative values in F6C2. For both cells, two distinct temporal pH zones were observed. From 17 to 161 hours (pH-zone 1), rapid pH increases can be seen, with rates of increase of 0.45 pH units/d and 0.48 pH units/d for cell F6C1 and F6C2 respectively. During this time period, the pH in both cells was maintained below 11.2. The pH during this time period, particularly from 17 to 41 hours was lower than for the remaining duration of the experiment because the formation of hydroxide ions at the cathode was not enough to change the pH significantly. Changes in pH values were time dependent and the lower pH values for both F6C1 and F6C2 during this time period can be attributed to this fact. As the EK experiment progressed, the continued hydroxide formation raised the pH to as high as 12.4 and 12.7 for F6C1 and F6C2 respectively.

In pH-zone 2, from 185 hours to 546 hours, the pH was relatively constant and consistently above 11.5 in both cells. After 257 hours, small pH decreases of 0.083 pH units/day (F6C1) and 0.075 pH units/day (F6C2). The pH increase in zone 1 (from 17 to 161 hours) and the relatively small decreases in pH-zone 2 (161 to 546 hours), were as expected in the cathode area, particularly without the use of EDTA. The results can be attributed to the following phenomena:

1. This increasing high pH is indicative of extensive OH^- formation in the cathode region, which tends to increase the pH.

2. The increasing pH in pH-zone 1 for both cells was due to the constant formation of OH^- ions. The pH of the cathode liquids during this time period was lower due to the initially lower pH and the time required for OH^- formation and subsequent pH increases.

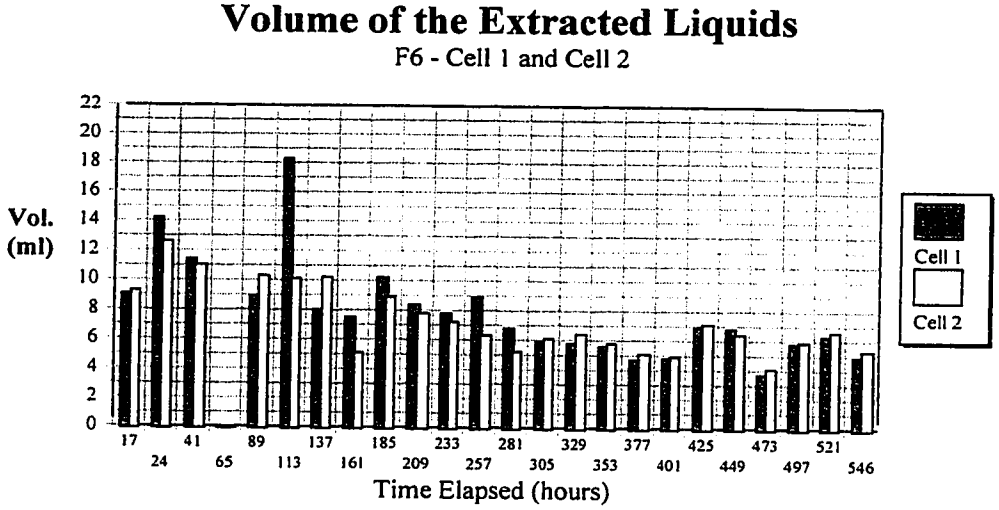

Figure 64 Volume of the liquids extracted daily (F6C1 and F6C2)

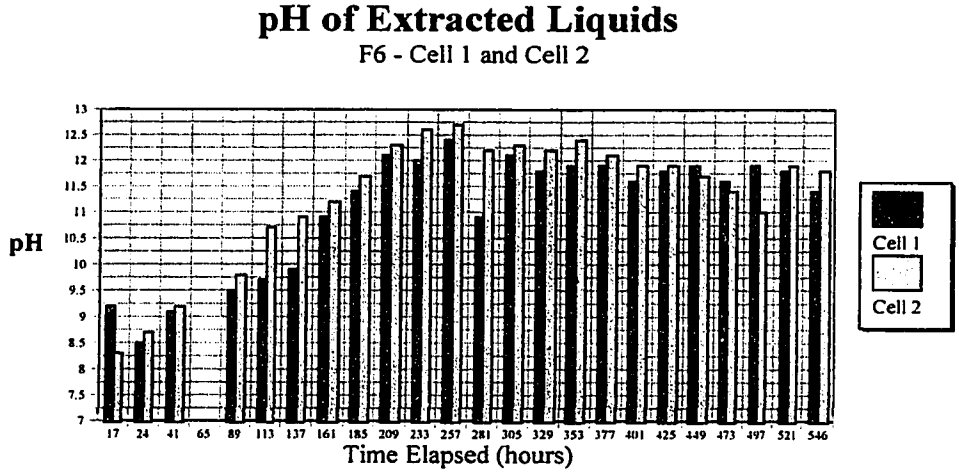

Figure 65 pH of the liquids extracted daily (F6C1 and F6C2)

3. The pH values observed from 161 to 546 hours can be attributed to the decreasing current within both cells. The sharpest decreases for all cells occurred after 161 hours and resulted in a lower rate of hydroxide formation.

4. The increase in pH in F6C1 and F6C2 from 0 to 257 hours can be attributed to the following chemical reactions, due to the presence of calcium and potassium in the soil:

$$K^+ + 1e^- \rightarrow K^0 \quad [12.1]$$
$$2K + 2H_2O \rightarrow 2KOH + H_2\uparrow \quad [12.2]$$
$$KOH \rightarrow K^+ + OH^- \quad [12.3]$$
$$Ca + 2e^- \rightarrow Ca^0 \quad [12.4]$$
$$Ca + 2H_2O \Leftrightarrow Ca(OH)_2 + H_2\uparrow \quad [12.5]$$
$$Ca(OH)_2 \Leftrightarrow Ca^{2+} + 2OH^- \quad [12.6]$$

The formation of OH^- as shown in equations [12.3] and [12.6] caused the pH to increase. After 257 hours, the reduction reaction (equations [12.1] and [12.4]) had completed, ceasing the formation of OH^- ions.

The use of anion or cation exchange textiles did not have an effect on the pH of the extracted liquids, as reflected by similar distibutions obtained in F6C1, F6C2 and F6C5 (Figure 69, no IET used).

As stated previously, the pH values in F6C1 were consistently lower (0.1-0.5) than those in F6C2 for the same time period. The difference is due to the relative electrokinetic efficiency of F6C1 and F6C2. Daily current measurements showed that the current to F6C2 was consistently higher than in F6C1 (0.05-0.50 mA). Due to a higher current, the amount of OH^- ions produced at the cathode in F6C2 via reduction, was higher than in F6C1, which in turn resulted in a lower pH.

12.2.2. Cell 3 (F6C3) and Cell 4 (F6C4)

The volume of the cathode liquids extracted daily for F6C3 (EDTA-EK-CET and F6C4 (EDTA-EK-AET) is shown in Figure 66. The maximum value for F6C3 was 12.4 mL (185 hours). The comparative value for F6C4 was 8.4 mL (497 hours). Total volumes extracted for F6C3 and F6C4 were 112.5 mL and 108.7 mL respectively. Average volumes for F6C3 and F6C4 were 4.7 mL and 4.5 mL respectively.

For F6C3 and F6C4, two temporal pH zones were observed. A pH-Zone 1, where rapid pH increases are depicted and pH-zone 2, where constant, but high pH values (11.5-13.0) are observed. The use of EDTA in F6C3 and F6C4 prevented the movement of acid front from anode to cathode, thereby preventing any pH decrease in the cathode liquids.

The pH distribution of the liquids extracted, versus time from F6C3 and F6C4 is shown in Figure 67. Maximum and minimum pH values for F6C3 were 12.6 (256 hours) and 7.9 (17 hours). Maximum and minimum values for F6C4 were 13.0 (209 hours) and 7.9 (17 hours). As with F6C1 and F6C2, F6C3 shows two temporal pH zones. Zone 1, from 17 to 161 hours represents the increasing pH zone due to the reasons outlined in section 5.2.1. The rate of increase during this time was 0.67 units/day. In pH-Zone 2,

from 161 hours to 546 hours, which can be seen in both F6C3 and F6C4, represents an area of high and relatively constant pH of the extracted liquids. This phenomenon was similar to that seen in F6C1 and F6C2.

Comparing F6C2 (EK-CET) and F6C3 (EDTA-EK-CET), reveals the effect of the use of EDTA on the overall pH of the extracted liquids. The use of EDTA did not effect the pH of the extracted liquids, except during the early stages of the experiment, that was observed at 17 hours. The pH of the liquids extracted from F6C2 and F6C3 were 8.3 and 7.9 respectively. However, from 161 hours to 546 hours, there was no discernable decrease in pH in F6C3, as there was in F6C2. The use of EDTA and the negative complexes formed in F6C3, induced an electrolytic migration that was from cathode to anode. This flow was in the opposite direction of the acid front and therefore inhibited the movement of the acid front. This prevented the pH from decreasing as time progressed. F6C4 displayed similar phenomena, with an absence of a pH decrease in pH-zone 2, which can be attributed to the use of EDTA. Comparing Figure 67 to Figure 69 (F6C5, no IET), the use of a cation exchange textile (F6C3) or an anion exchange textile (F6C4) did not effect the pH of the extracted liquids.

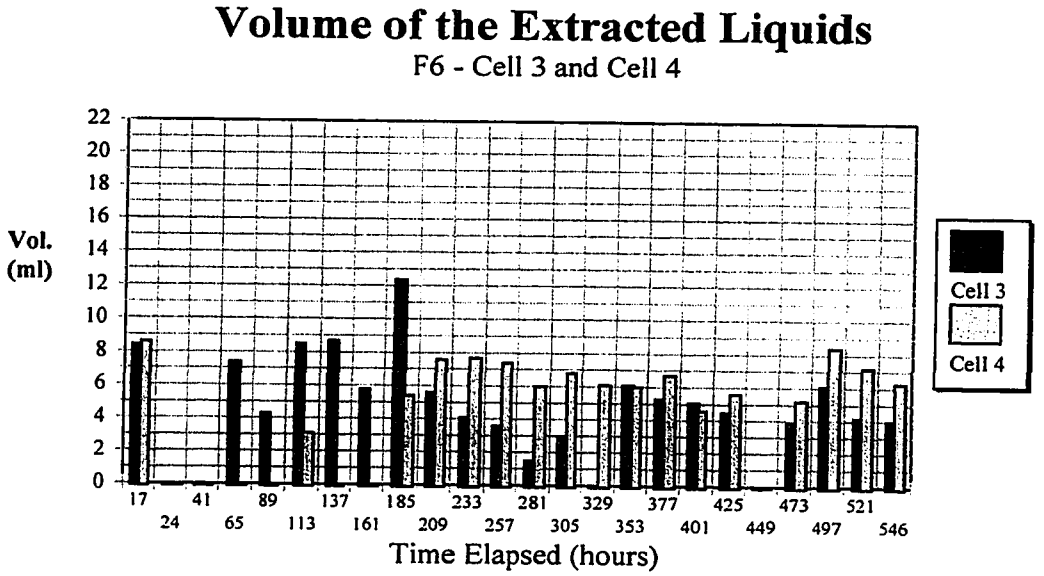

Figure 66 Volume of the liquids extracted daily (F6C3 and F6C4)

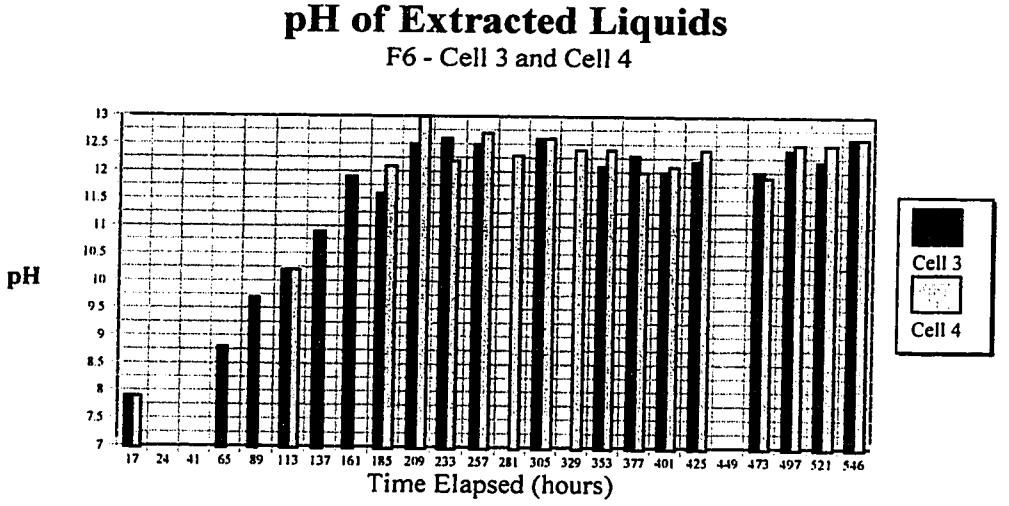

Figure 67 pH of the liquids extracted daily (F6C3 and F6C4)

12.2.3. Cell 5 (F6C5) and Cell 6 (F6C6)

The volume of the cathode liquids extracted daily for F6C5 (EDTA-EK) and F6C6 (EDTA-EK-CET & AET) is shown in Figure 68. The maximum value for F6C5 was 20.5 mL (137 hours). The comparative value for F6C6 was 8.2 mL (17 hours) and 0.0 mL (24, 41 and 65 hours). Total volumes extracted from F6C5 and F6C6 were 137.4 mL and 139.3 mL respectively. Average volumes for F6C5 and F6C6 were 5.7 mL and 5.8 mL respectively.

The temporal pH distribution of the liquids extracted from F6C5 and F6C6 is shown in Figure 69. Maximum and minimum pH values for F6C5 were 12.8 (305 hours) and 8.6 (17 hours). Maximum and minimum values for F6C6 were 12.8 (281 hours) and 8.4 (17 hours). F6C5 and F6C6 show two temporal pH zones. The first zone, pH-zone 1, from 17 to 161 hours, represents the increasing pH zone. The rate of increase is difficult to calculate due to the absence of values from 24 hours to 65 hours. However an increasing trend, similar to that of cells 1 to 4 is observed. The second zone, pH-Zone 2, from 161 hours to 546 hours, which can be seen in both F6C5 and F6C6, represents an area of high and relatively constant pH. Values were consistently above 12.0 and were similar to previous cells. The only difference between F6C5 and F6C6 was the use of textiles in F6C6. Although the pH in F6C6 was 0.1-0.2 units lower than comparative values in F6C5, it is no reason to attribute this to the use of textiles. Based on the small differences in pH within this zone, and similar temporal distributions within all cells utilizing EDTA (F6C3 to F6C6), it can be seen that the textiles have no effect on the use pH of the extracted liquids.

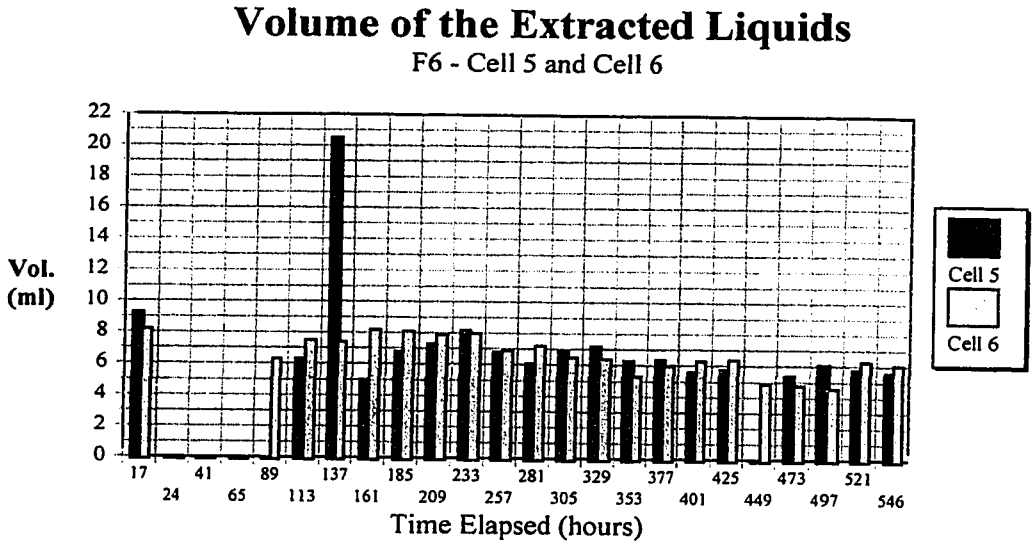

Figure 68 Volume of the liquids extracted daily (F6C5 and F6C6)

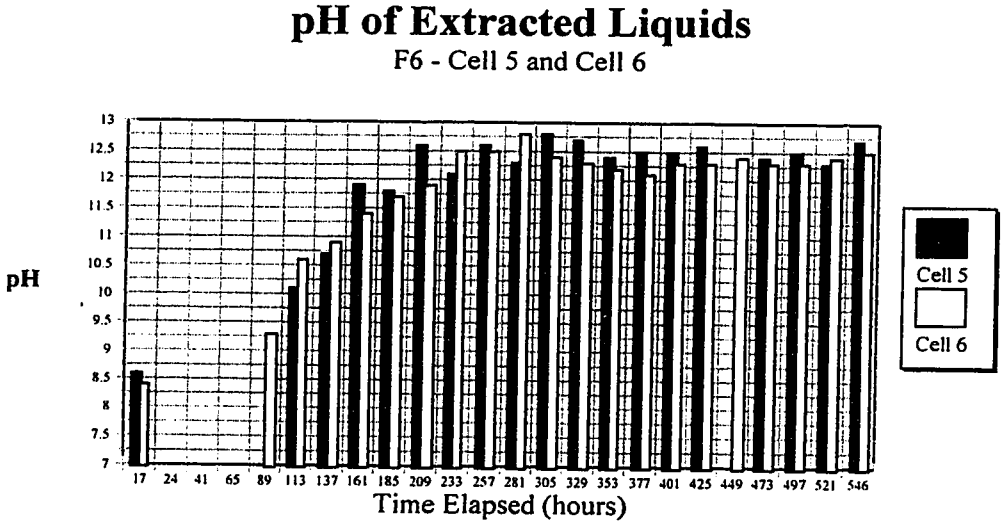

Figure 69 pH of the liquids extracted daily (F6C5 and F6C6)

12.3. Soil pH

With respect to the soil pH, it can be observed that for all cells, a prevailing trend existed, with some degree of variation. All cells show high pH values in the cathode region (due to OH^- formation) and lower pH values in the anode region; at or below the initial value of 7.6 (due to hydrogen ion formation at the anode).

Proceeding from cathode to anode, three distinct pH zones were observed relative to the initial pH. This phenomenon was observed in all cells in this experiment and in experiment F5 (see Chapter 11) and can be used as a model for electrokinetic experiments employing natural clayey soil. It should be noted that these zones differ in length and extent due to the presence or absence of the chelation agent EDTA. From anode to cathode, the zones observed were as follows:

1. **Zone 1: Final pH >> Initial pH, High pH Gradient.** Zone 1 was located in the proximity of the cathode and represented an area of high pH values and gradients. For all cells the gradients were similar, and their spatial extent was similar ranging from 4.0 to 5.0 cm in length. Typically, zone 1 began at the cathode (16.0 cm from the anode) and ended 10.0 to 11.0 cm from the anode. The pH gradients were independent of the use of EDTA and are in the range of -0.42 to -0.53 pH units/cm for F6C1 to F6C5. The pH gradient in F6C6 was -0.36 pH units/cm.

2. **Zone 2: Final pH > Initial pH, Low pH gradient.** Zone 2 is located in the central portion of all cells. In this zone, the final pH is higher than the initial, approximately 0.1 to 1.0 pH units above the initial. The extent of this zone was dependent on the presence of EDTA within the cell. For F6C1 (EK-AET) and F6C2 (EK-CET), the zone extended from the edge of zone 3 (approximately 11.0 cm from anode) to approximately 3.5 to 7.5 cm from the anode. Therefore the zone extends for 3.5-7.5 cm. In F6C3 to F6C6, where EDTA was utilized, the zone was significantly shorter, in the range of 2.0-4.0 cm. The pH gradient in zone 2 was similar for F6C1 to F6C5 and in the range of -0.11 pH units/cm to -0.15 pH units/cm. F6C6 deviated from this trend with a gradient of -0.26 pH units/cm.

3. **Zone 3: Final pH < Initial pH, Low pH gradient.** This zone began at a maximum of 7.5 cm from the anode and extended to the anode. For those cells not employing EDTA (F6C1 and F6C2), this zone extended only 3.0-4.0 cm. The decrease in pH can be attributed to the constant formation of hydrogen ions due to the oxidation of the anode according to electrochemical theory. The pH gradient in this zone is low and independent on the use of chelation agent, in the magnitude of -0.040 to -0.080 pH units/cm.

Table 40 shows a comparison of results related to the pH distribution at the end of the experiment within each cell.

Table 40 Soil pH: Distribution at the End of Experiment

Parameter	*Cell 1 (F6C1)*	*Cell 2 (F6C2)*	*Cell 3 (F6C3)*	*Cell 4 (F6C4)*	*Cell 5 (F6C5)*	*Cell 6 (F6C6)*
Min. pH	7.02	7.16	6.99	7.09	7.06	7.05
Max. pH	11.23	11.03	10.38	10.51	10.29	10.37
ZONE 1						
pH Grad. [units/cm]	-0.53	-0.43	-0.42	-0.49	-0.43	-0.36
Length [cm]	5.0	5.0	4.0	4.0	4.0	4.0
ZONE 2						
pH Grad. [units/cm]	-0.12	-0.15	-0.14	-0.11	-0.15	-0.26
Length [cm]	6.5	7.5	5.0	5.0	5.0	5.0
ZONE 3						
pH Grad. [units/cm]	-0.04	-0.07	-0.08	-0.05	-0.04	-0.05
Length [cm]	4.5	3.5	7.0	7.0	7.0	7.0

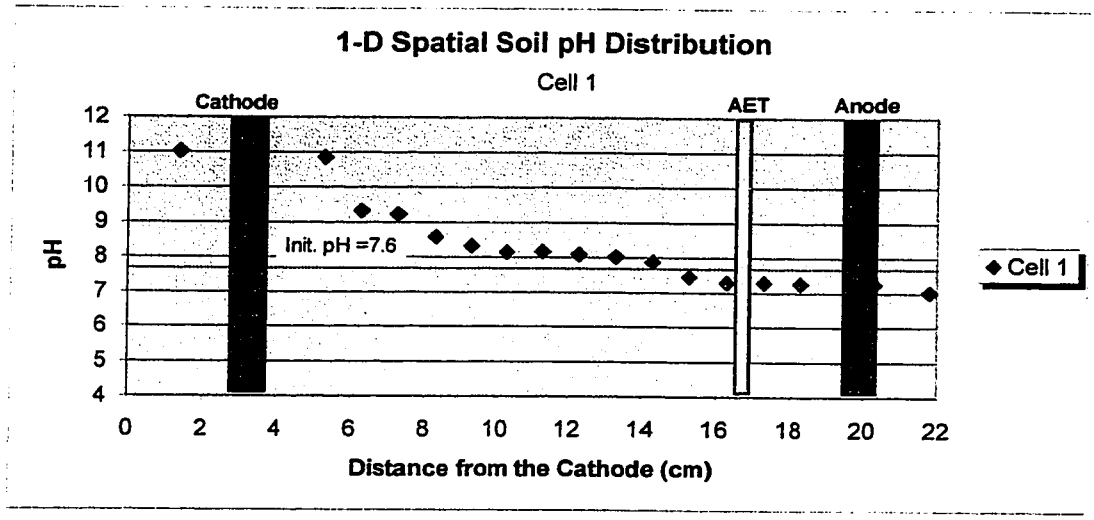

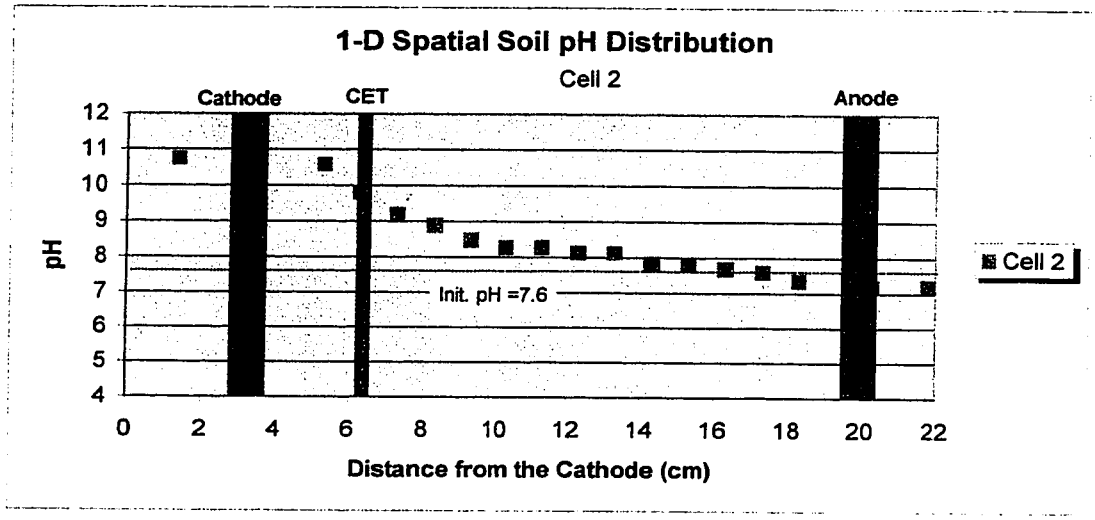

Figure 70 pH of the soil (F6C1 and F6C2)

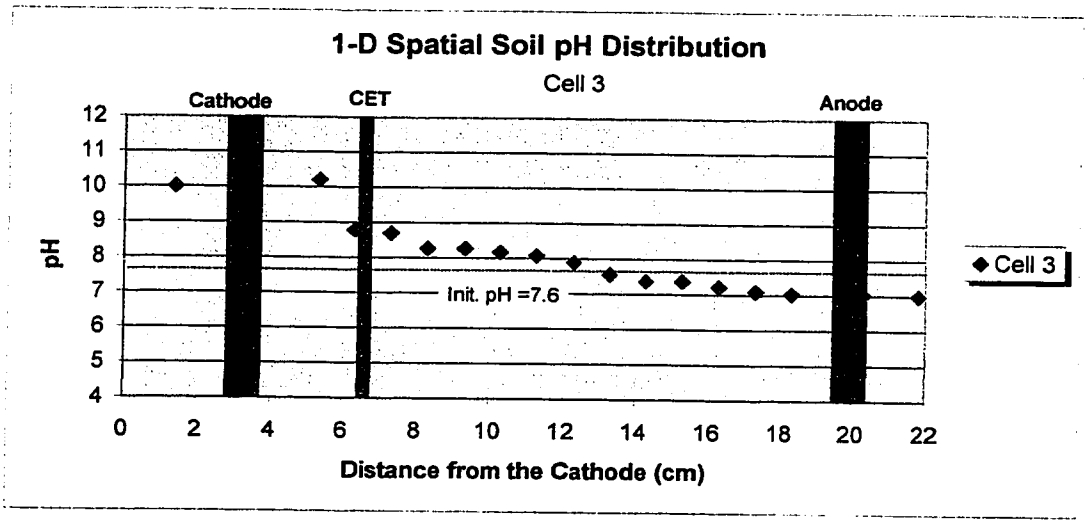

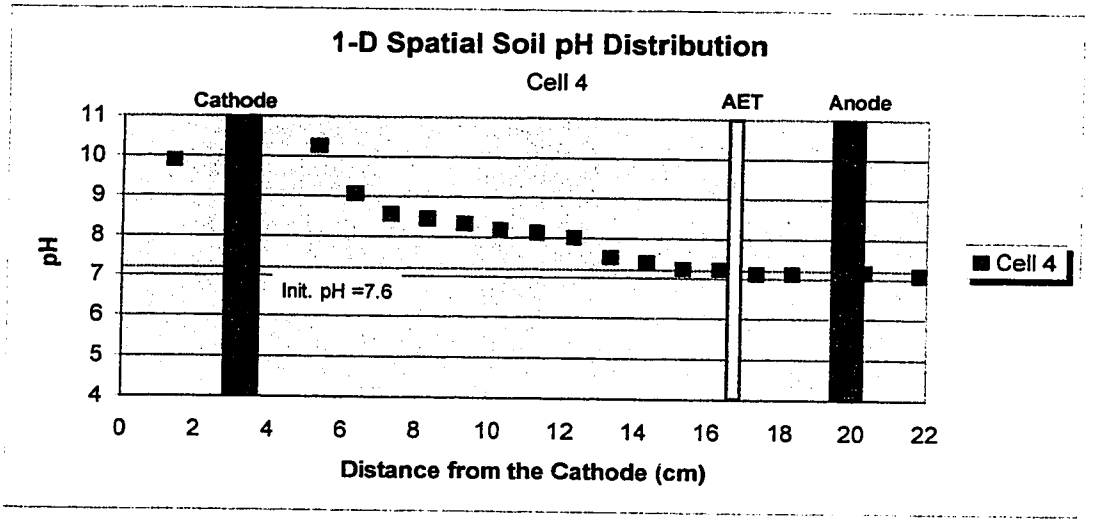

Figure 71 pH of the soil (F6C3 and F6C4)

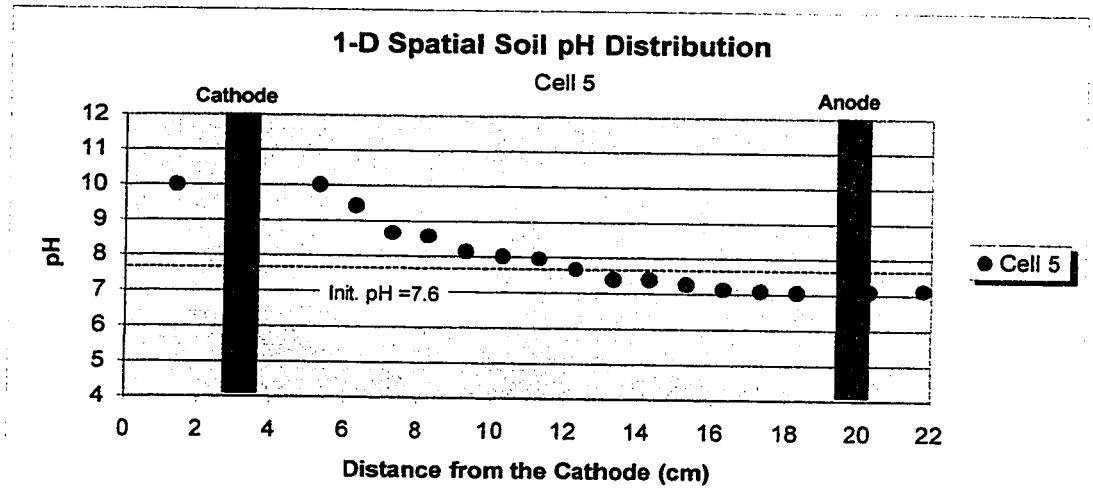

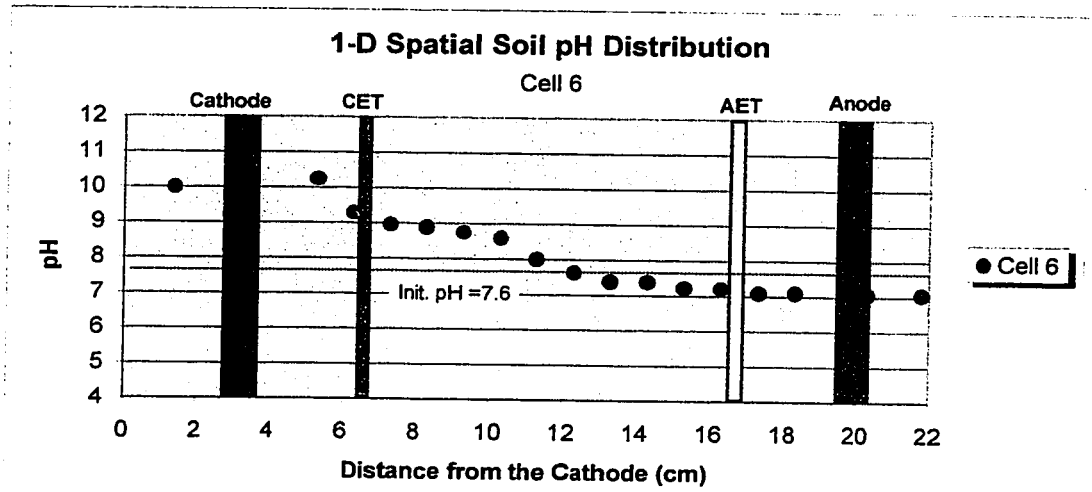

Figure 72 pH of the soil (F6C5 and F6C6)

From a comparison of F6C5 with cells F6C1, F6C2, F6C3, F6C4, and F6C6 it can be concluded that the presence of anion and cation exchange textiles had a moderate effect on the pH distribution within the soil. The CETs seemed to raise the pH in the area just before the textile (between the textile and the anode). This is evidenced with a comparison of F6C6 to those cells in experiment F5 (F5C1 and F5C2). The pH values in this area are 0.25-0.50 pH units higher in F6C6 than in F5C1 and F5C2. In F6C2 (EK-CET) and F6C3 (EK-EDTA-CET), the pH values were slightly higher than F5C1 and F5C2 in this area. Comparing the cells utilizing AET (F6C1, F6C4 and F6C6) to F5C1 (EDTA-EK), F5C2 (EDTA-EK), and F6C5 (EDTA-EK) shows that the AETs had minimal effects on the pH distribution.

As stated previously, the use of EDTA had a large effect on the pH distribution by spatially extending zone 1 (the area of low pH, less than the initial pH) and decreasing the length zone 2. In addition, the pH in the cathode region of those cells utilizing EDTA was approximately 0.50-1.00 units lower than those not employing EDTA. EDTA therefore produced more favorable conditions for heavy metal mobilization, and overall accessibility to EK transport. It can be seen from a comparison of all cells employed in experiment F5 and F6 that the trends are similar, which shows that accurate correlations can be made.

12.4. Metal Concentration

The concentration of lead, nickel, iron and calcium in the soil and retained on the textile was measured using the methods outlined in chapter 9. This section deals with a discussion of the metal concentration in the soil, the soil in the proximity of the textile and on the textile itself.

12.4.1. Nickel and Lead

12.4.1.1 Nickel and Lead Concentration in the Soil

The nickel and lead concentration distributions in soil between electrodes for F6C1 to F6C6 are shown in Figure 73 to Figure 78 respectively. The initial lead and nickel soil concentrations were 31 mg/kg and 9.3 mg/kg respectively. The soil in F6C1 and F6C2 contained very low concentrations of nickel and lead, since these cells were not contaminated with $PbCl_2$ and $NiCl_2$. The initial nickel and lead concentrations were 31 mg/kg and 9.3 mg/kg respectively (SFE-AAS methodology). Both nickel and lead concentrations in F6C1 were higher in the cathode region. This is an indication that electrolytic migration and electroosmosis occurred from anode to cathode, as is typical of an EK cell without the use of a modifier. Nickel and lead ions were transported via electrolytic migration toward the cathode until the high pH barrier (see Figure 73) was reached. At this point, the metal ions were no longer mobile and formed precipitates beginning 3.5 cm from the cathode, as indicated by the sharp increase in the soil nickel concentration. Therefore, electrolytic migration of metals was directly affected by the pH within the soil, as it effects the solubility of metals and consequently their availability to EK transport. Maximum and minimum nickel concentrations were 28.8 mg/kg and undetectable respectively. Corresponding values for lead were 19.9 mg/kg and undetectable respectively. The anion exchange textile did not play a role in the localization of nickel in F6C1. With a net surplus of cations in the system, the EK flow was from anode to cathode.

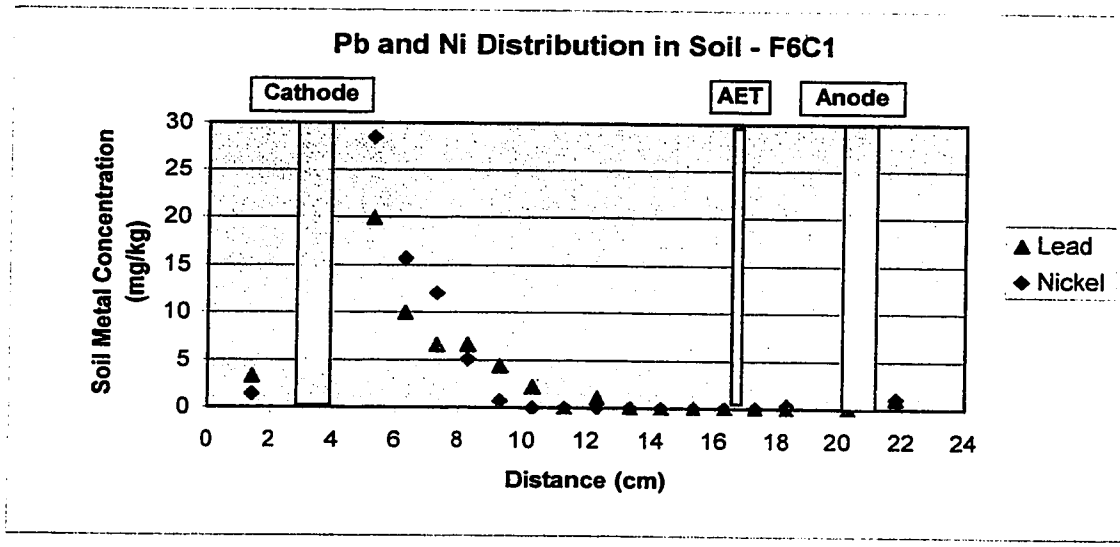

Figure 73 Pb and Ni soil concentration at the end of the experiment (F6C1)

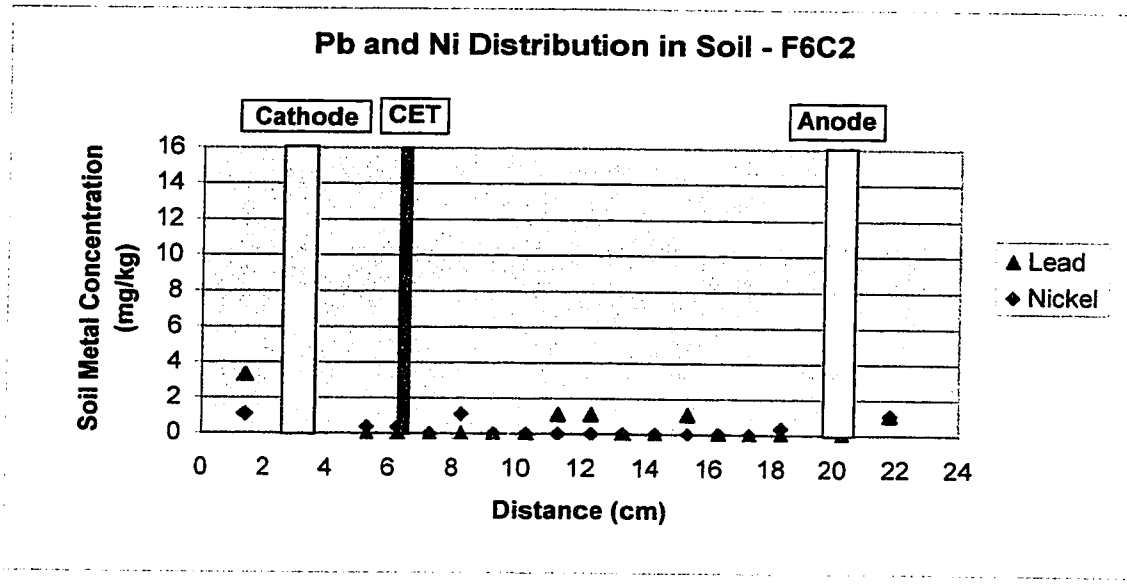

Figure 74 Pb and Ni soil concentration at the end of the experiment (F6C2)

Initial Ni concentration: 31 mg/kg
Initial Pb concentration: 9.3 mg/kg

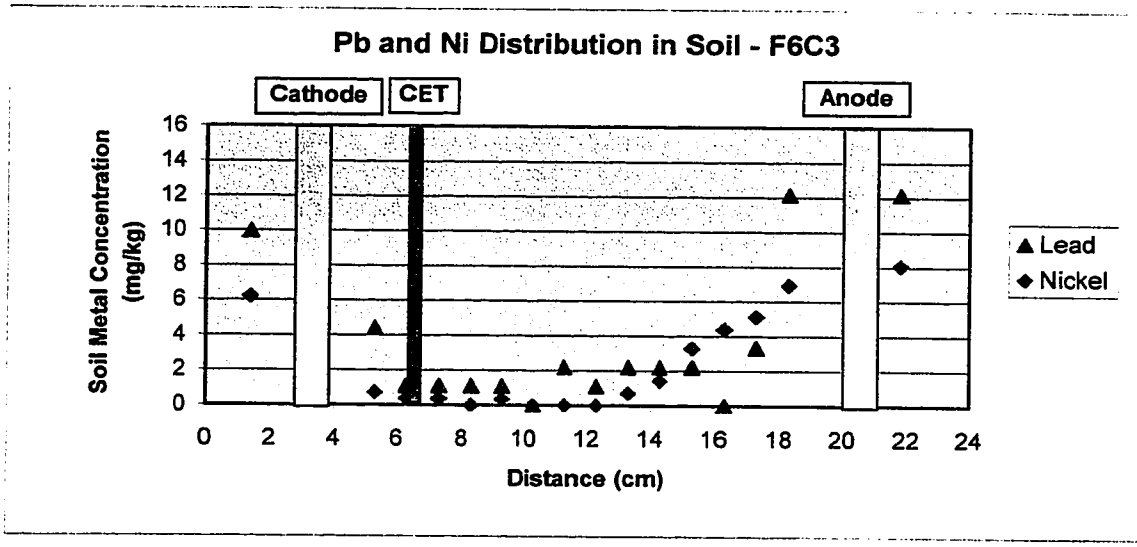

Figure 75 Pb and Ni soil concentration at the end of the experiment (F6C3)

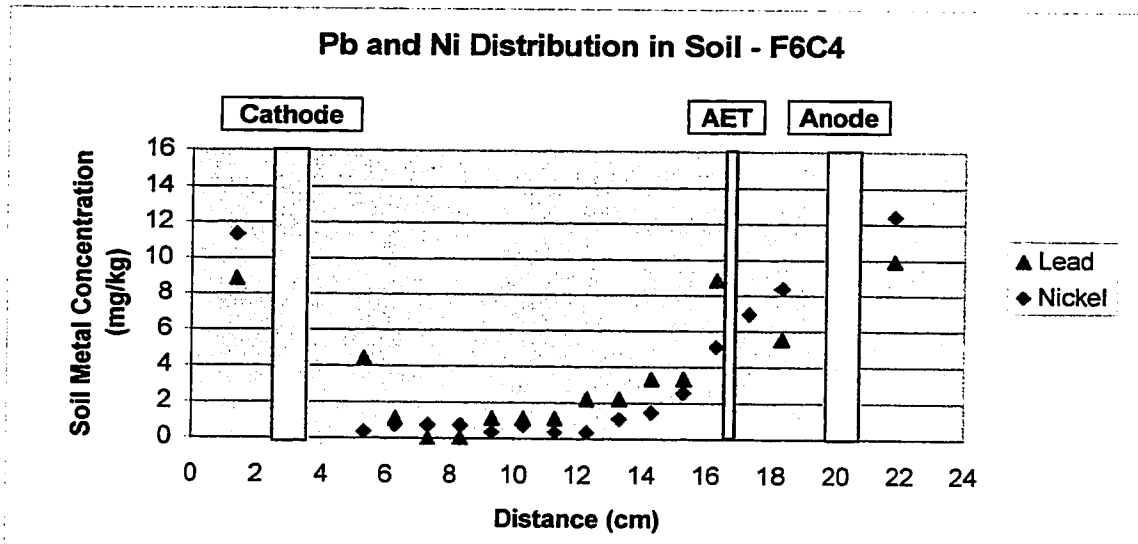

Figure 76 Pb and Ni soil concentration at the end of the experiment (F6C4)

Initial Ni concentration: 31 mg/kg
Initial Pb concentration: 9.3 mg/kg

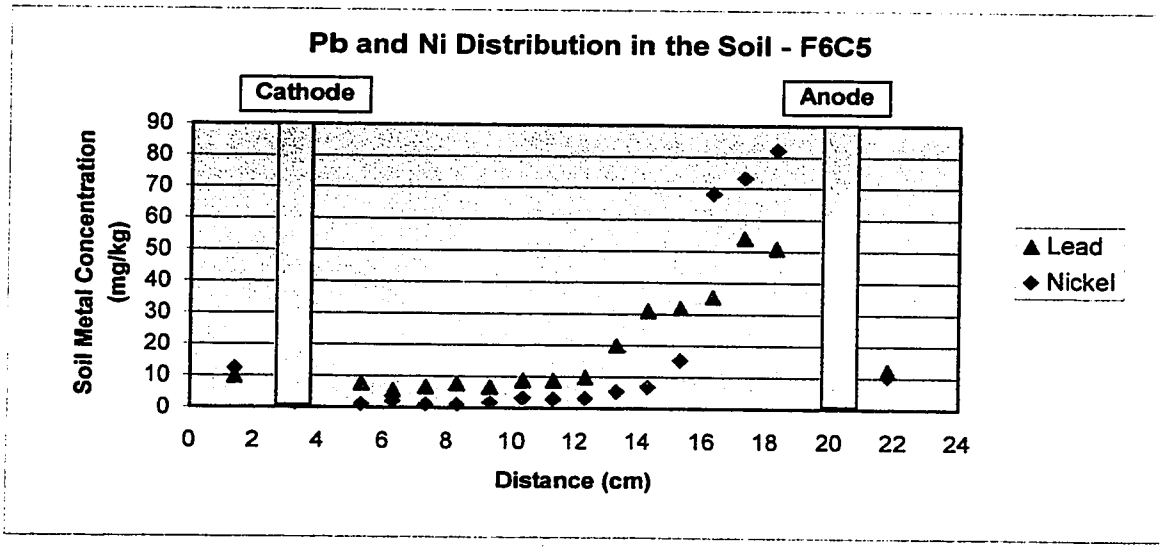

Figure 77 Pb and Ni soil concentration at the end of the experiment (F6C5)

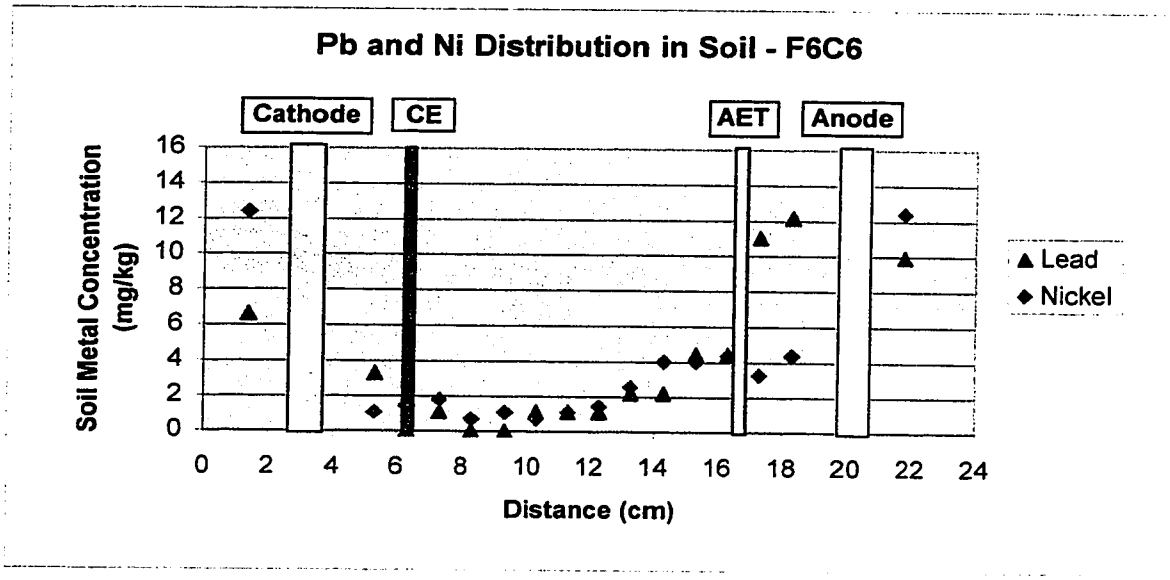

Figure 78 Pb and Ni soil concentration at the end of the experiment (F6C6)

Initial Ni concentration: 31 mg/kg
Initial Pb concentration: 9.3 mg/kg

F6C2 was characterized by low nickel and lead concentrations in the entire cell. This indicates that electrokinetic transport occurred and localized on the CET. As in F6C1, net electroosmotic flow and electrolytic migration was in the anode to cathode direction. The transport of lead and nickel occurred in this direction and the location of the CET (3.0 cm from the cathode, in the high pH cathodic zone), allowed for the exchange of lead and nickel before they could form immobile precipitates. As a result, lead and nickel concentrations below 1.0 mg/kg of soil resulted throughout the soil. The metals were essentially localized on the textile.

Table 41 summarizes the "two zone" phenomenon that occurred in both cells. The nickel and lead distribution in F6C3, F6C4, F6C5 and F6C6 show generally two zones of concentration. Conc.-Zone 1, 0.0 to 8.5 cm from the cathode, consists of low lead and nickel (below 4.0 mg/kg dry soil) concentrations. Conc.-Zone 2 is beyond 8.5 cm from the cathode, where both the lead and nickel concentrations in F6C3, F6C4, F6C5 and F6C6 increase consistently while approaching the anode. The concentrations in areas not subjected to the electrical field were significantly higher.

The effect of EDTA can be seen from a comparison of the distributions between cells. In F6C3 to F6C6, significant electrolytic migration of anionic complexes occurred from cathode to anode, resulting in movement of Pb-EDTA and Ni-EDTA complexes, and an increased ionic concentration within Conc.-Zone 2. Both F6C3 and F6C4 showed lead concentrations within the soil to be 1.3 and 1.6 times higher than nickel within Conc.-Zone 2. In F6C6, lead concentrations were 3.5-4.0 times higher than nickel, in the proximity of the anode. However, significant transport of lead and nickel complexes to the anode region was achieved. The high stability of lead and nickel EDTA (Chapter 7,

Table 26) complexes allowed for these heavy metals to remain in ionic form, thereby being accessible to EK transport to the anode region. The order of metal-EDTA complex formation according to the stability constants is as follows:

$$Fe(III)\text{-}EDTA^{-} > Ni\text{-}EDTA^{2-} > Pb\text{-}EDTA^{2-} > Fe(II)\text{-}EDTA^{2-} > Ca\text{-}EDTA^{2-}$$

Table 41 Characteristics of Pb and Ni Concentration After Enhanced EK Treatment

Cell	*Max. and Min. Lead Conc. (mg/kg)*	*Max. and Min. Nickel Conc. (mg/kg)*	*Lead Conc. Gradient (mg/kg/cm)*	*Nickel Conc. Gradient (mg/kg/cm)*
F6C3				
Zone 1: up to 8.5 cm from cathode	4.4 and undetectable	1.5 and undetectable	~ 0.0	~ 0.0
Zone 2: 8.5 cm extending to anode	12.2 and undetectable	6.9 and undetectable	~ 2.0	~ 1.2
F6C4				
Zone 1: up to 8.5 cm from cathode	4.4 and undetectable	0.7 and 0.4	~ 0.0	~ 0.0
Zone 2: 8.5 cm extending to anode	16.6 and 2.2	8.4 and 1.1	~ 2.8	~ 1.3
F6C6				
Zone 1: up to 8.5 cm from cathode	3.3 and undetectable	1.8 and 0.7	~ 0.0	~ 0.0
Zone 2: 8.5 cm extending to A	12.2 and 2.2	4.4 and 1.5	~ 1.8	~ 0.5

F6C5 shows a distribution similar to that of experiment F5 described in chapter 11. The presence of EDTA resulted in an abundance of anionic metal complexes within the system, thereby resulting in net electrolytic migration from cathode to anode. The

low concentrations observed from the cathode to 8.5 cm from the cathode, coupled with significantly higher concentrations in the anode region, indicate the occurrence of three distinct phenomena in F6C5, as well as F6C3, F6C4 and F6C6:

1. The formation of Ni-EDTA and Pb-EDTA complexes, thereby creating an abundance of anionic species within the cell.
2. The Ni-EDTA and Pb-EDTA complexes were transported from cathode to anode. This resulted in a zone of low concentration and a zone of concentrated lead and nickel, as shown in Figure 77.
3. It is speculated that the lower pH and the presence of ligands such as PO_4^{3-}, CO_3^{2-}, Cl^- and OH^-, in the anode region promoted the precipitation of these forms of lead and nickel, thereby causing their immobilization in the proximity of the anode.

These results and distributions are similar to those presented in experiment F5 and they show the effectiveness of EDTA as a chelating agent for the enhancing the solubility of accessibility of lead and nickel during electrokinetic treatment. Without the use of a textile, moderate localization was achieved with 87% of nickel localized within 1/5th of the cell and 71% of lead localized within 1/4th of the cell. This is comparable to the localization achieved in experiment F5. The use of a textile would allow for increased localization (onto a 2 mm thick textile) and this was examined in the sections to follow.

12.4.1.2. Lead and Nickel Concentration for the Soil in the Proximity of the Textile

The lead concentration for the soil in the proximity of the textile for F6C1 to cell F6C4 and F6C6 are shown in Figure 79 to Figure 84. F6C1, with no additional lead and nickel contamination showed low concentrations on both anode and cathode sides.

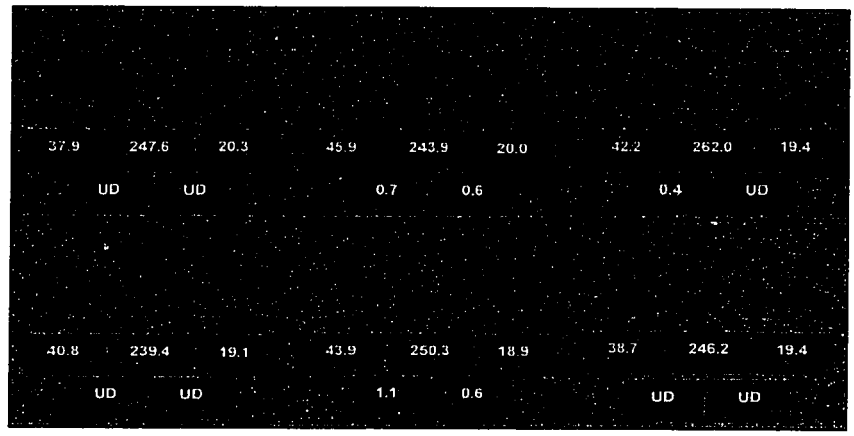

Facing the Cathode

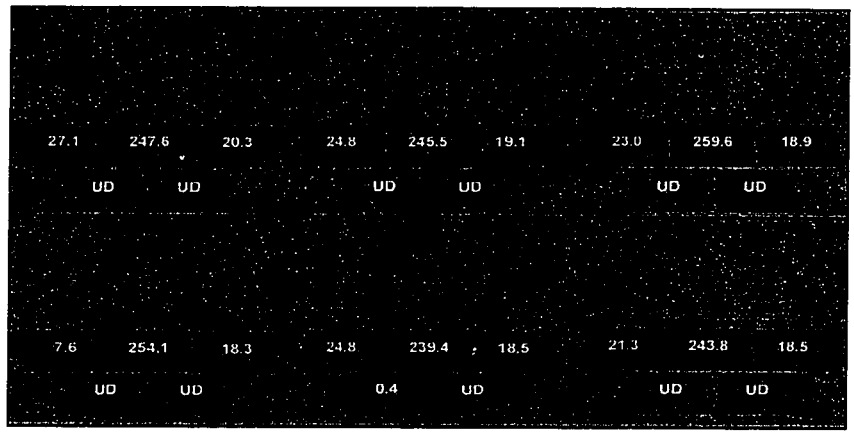

Facing the Anode

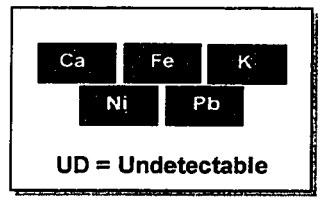

LEGEND

Figure 79 Concentration of calcium, iron, potassium, nickel and lead (mg/kg) in soil adjacent to the AET (F6C1)

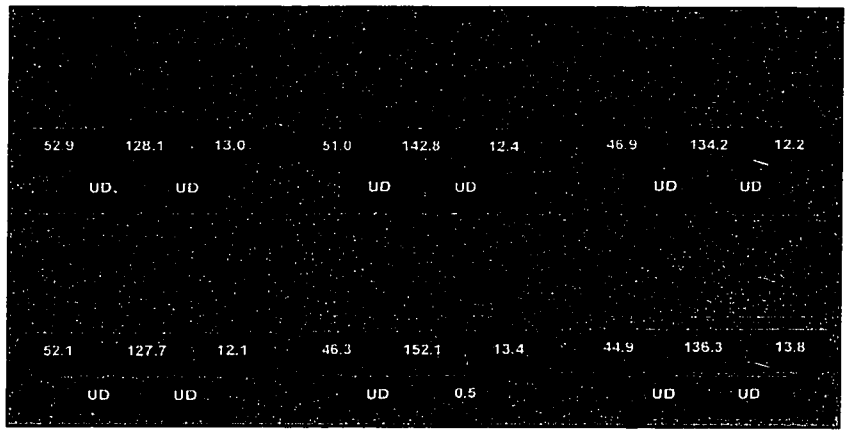

Facing the Cathode

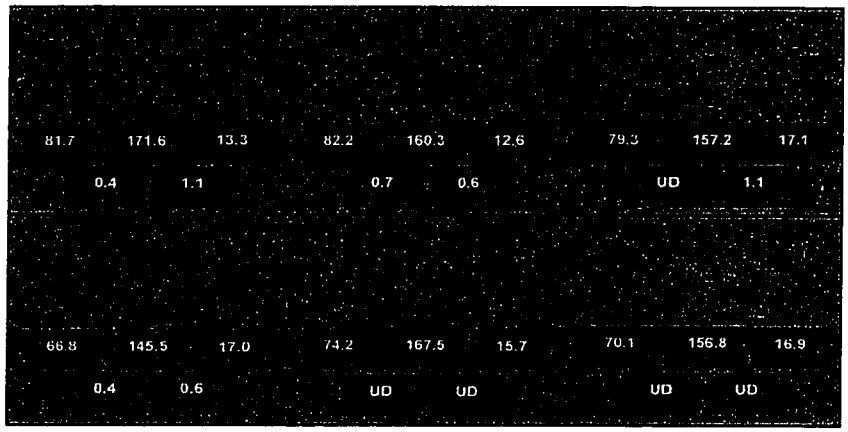

Facing the Anode

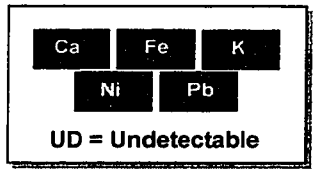

LEGEND

Figure 80 Concentration of calcium, iron, potassium, nickel and lead (mg/kg) in soil adjacent to the CET (F6C2)

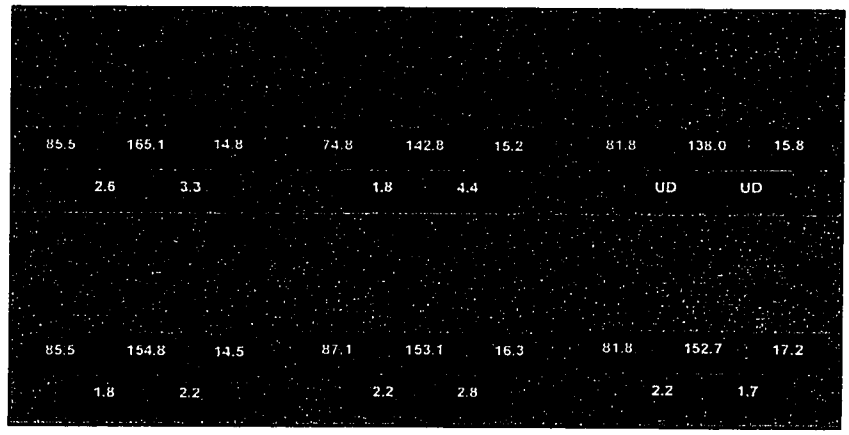

Facing the Cathode

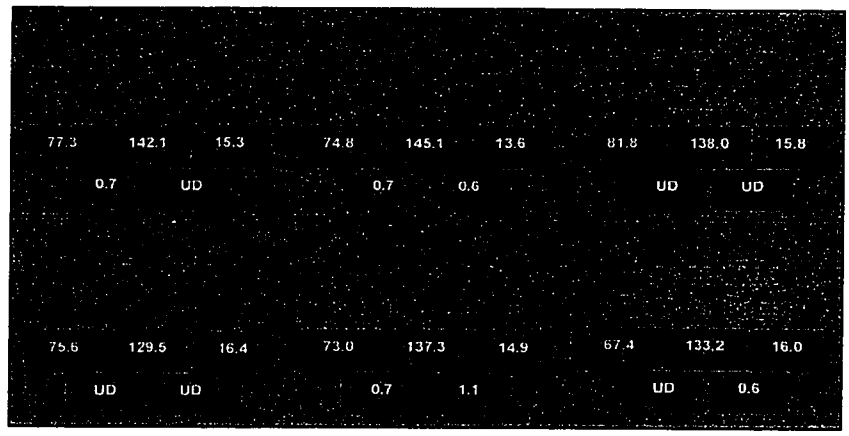

Facing the Anode

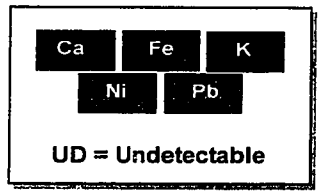

LEGEND

Figure 81 Concentration of calcium, iron, potassium, nickel and lead (mg/kg) in soil adjacent to the CET (F6C3)

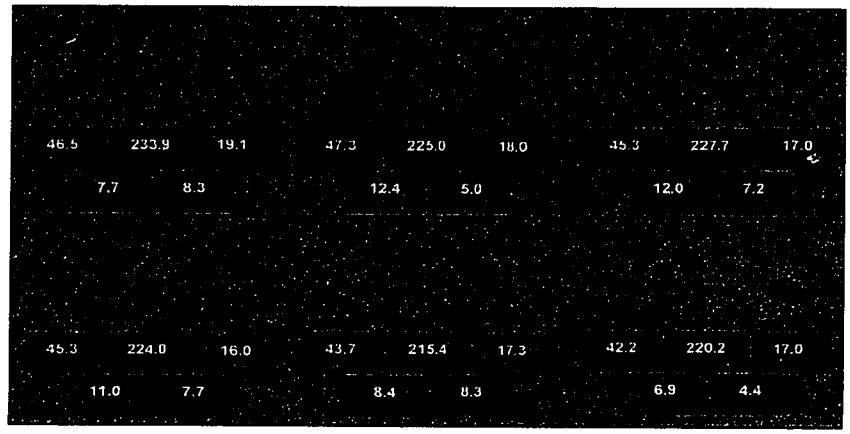

Facing the Cathode

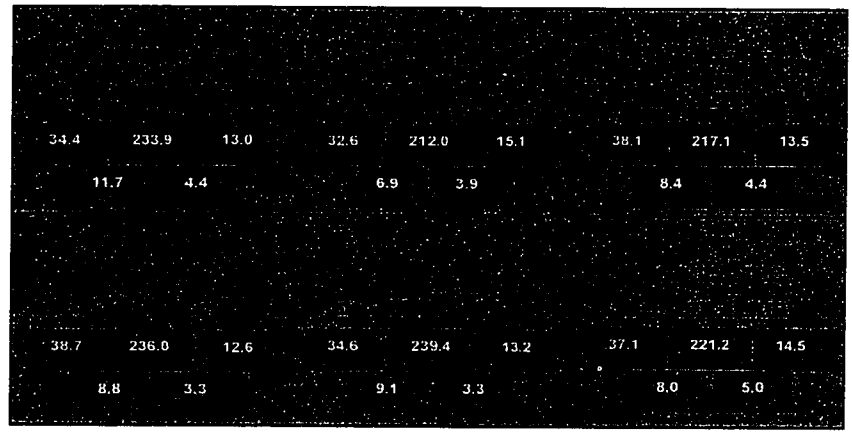

Facing the Anode

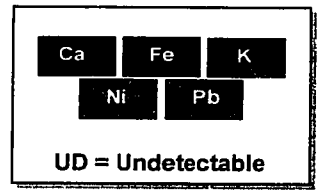

LEGEND

Figure 82 Concentration of calcium, iron, potassium, nickel and lead (mg/kg) in soil adjacent to the AET (F6C4)

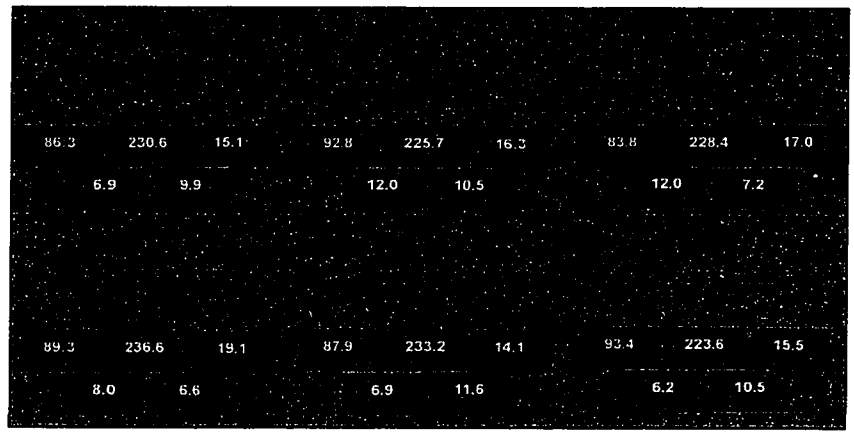

Facing the Cathode

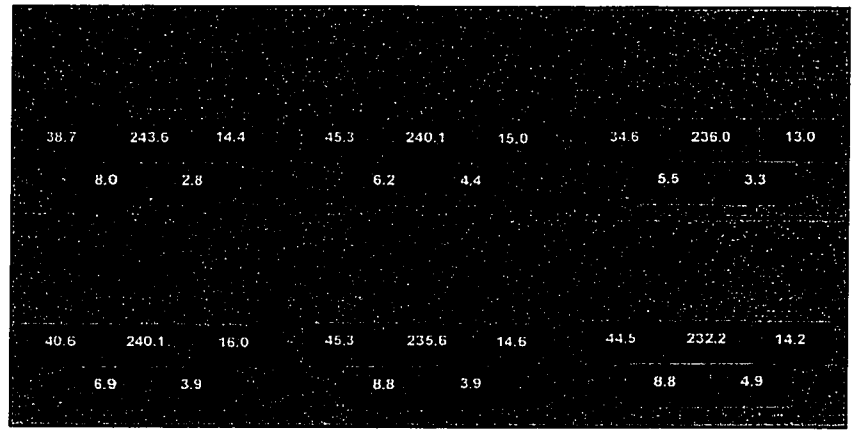

Facing the Anode

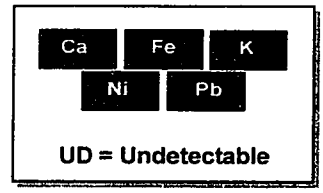

LEGEND

Figure 83 Concentration of calcium, iron, potassium, nickel and lead (mg/kg) in soil adjacent to the AET (F6C6)

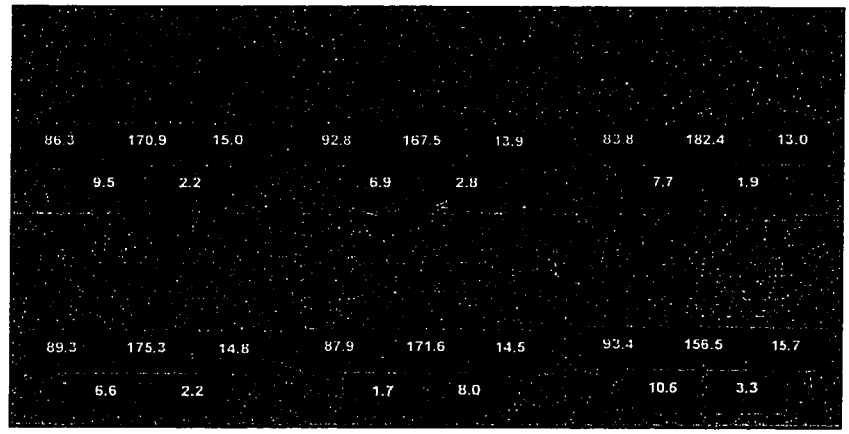

Facing the Cathode

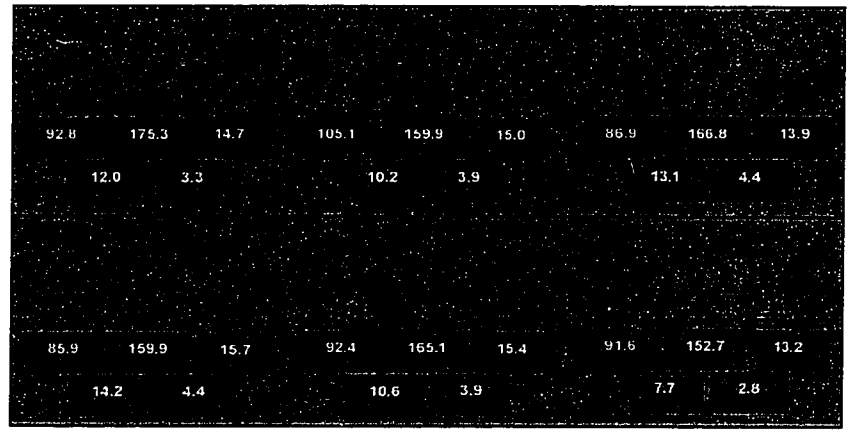

Facing the Anode

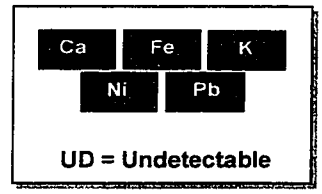

LEGEND

Figure 84 Concentration of calcium, iron, potassium, nickel and lead (mg/kg) in soil adjacent to the CET (F6C6)

The cathode side of the AET in F6C1 showed a slightly higher nickel and lead concentration. The higher concentrations observed on the cathode side can be attributed to the presence of lead and nickel on the cathode side of the AET, due to electrolytic migration from anode to cathode. Without EDTA, the ions existed in their cationic state and therefore passed through the AET. Maximum lead concentration observed was 0.552 mg/kg. A comparative value for nickel was 1.094 mg/kg. The highest concentrations were observed in the central locations, as this is where the intensity of the applied electrical field was at its highest.

For F6C2 (EK-CET, Figure 80), where the soil was the same to that of F6C1 (EK-AET), higher lead and nickel concentrations were observed on the anode side of the CET. This can be attributed to the following phenomenon:

1. Since EDTA was not employed in F6C2, net migration was from anode to cathode. Lead and nickel ions were transported towards the cathode.
2. Upon reaching the proximity of the CET, some lead and nickel ions exchanged onto the textile. As a result, a lower concentration of lead and nickel was observed on the cathode side. The lead and nickel ions located between the CET and the cathode were transported to the cathode where they were collected in the pore liquid at the cathode.

Unlike F6C1, there was no discernable concentration of ions spatially.

F6C3 (EDTA-EK-CET) and F6C6 (EDTA-EK-CET & AET) showed different results related to nickel and lead concentration. F6C6 showed significantly higher lead and nickel concentrations in all locations. More lead and nickel ions were complexed with EDTA in F6C3, than in F6C6. These complexed ions passed through the CET and continued their migration toward the anode. This is shown in Figure 75 (Ni and Pb soil

concentrations) where the highest concentrations of lead and nickel were observed in the anode region, due to the migration of Pb-EDTA and Ni-EDTA complexes from anode to cathode. In F6C6, it is probable that there was an abundance of uncomplexed lead and nickel ions, which were transported towards the cathode, and uncomplexed (non-EDTA complex) ions existing between the cathode and the CET. Nevertheless, these values are consistent with the lead and nickel distribution in the soil as shown in Figure 78. The concentration in the cathode region was similar to those observed for the soil in the proximity of the textile.

Comparing the soil in the proximity of the AET for F6C4 and F6C6 shows striking similar trends. Concentrations on the cathode side were 10-25% higher than on the anode side, which is an indication that negative complexes were possibly exchanged onto the AET. The appreciable concentrations in on the anode side can be attributed to the initially contaminated soil and addition of EDTA. The negative complexes formed would attempt to flow in the cathode to anode direction. However, these ions were already in the anode region and therefore remained stagnant. This is further evidenced in Figure 76 and 78 (Ni and Pb soil concentration), where the Pb and Ni concentrations are 5-7 times higher in the anode region than in any other part of F6C4 and F6C6.

12.4.1.3. Lead and Nickel Concentration on the Textile

The nickel retained on the textile was determined in order to obtain its overall removal efficiency and degree of localization. The concentrations of lead and nickel at specified locations on the textiles in F6C1 to F6C6 are shown in Figure 85 to Figure 90 respectively.

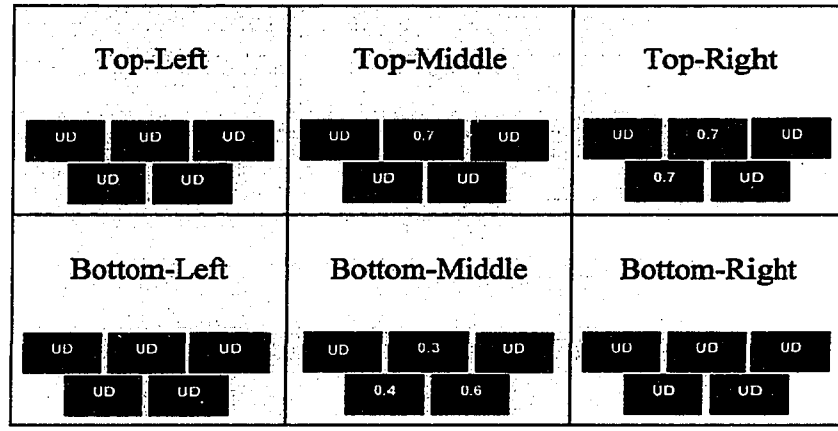

Figure 85 Concentration of metals (mg/L) retained on the textile (F6C1 EK-AET)

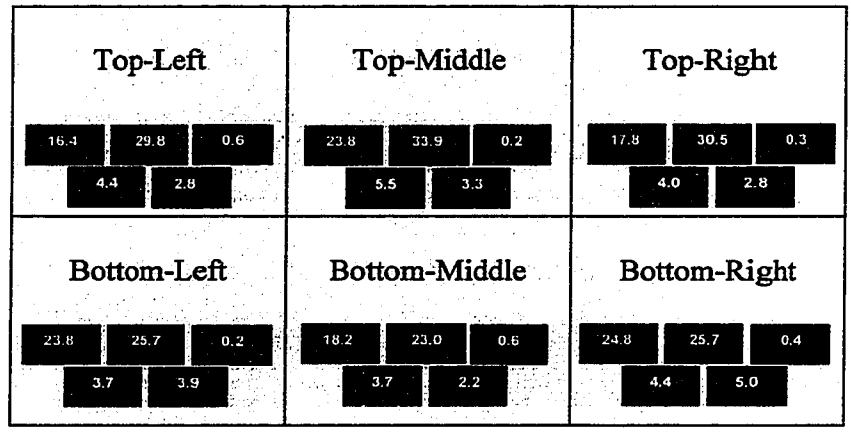

Figure 86 Concentration of metals (mg/L) retained on the textile (F6C2 EK-CET)

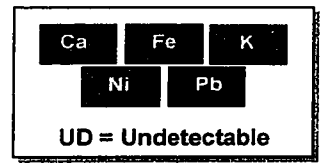

LEGEND

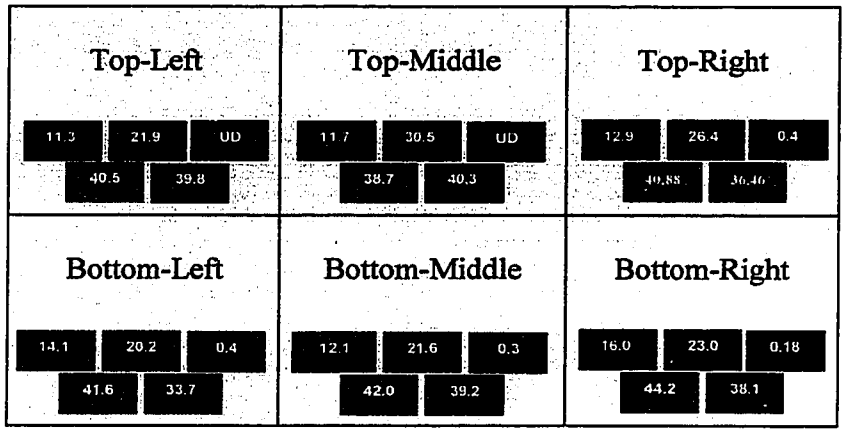

Figure 87 Concentration of metals (mg/L) retained on the textile (F6C3 EK-EDTA-CET)

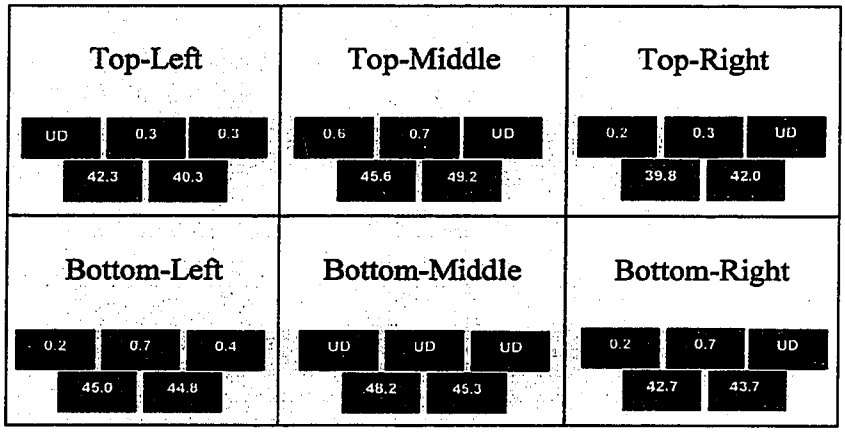

Figure 88 Concentration of metals (mg/L) retained on the textile (F6C4 EK-EDTA-AET)

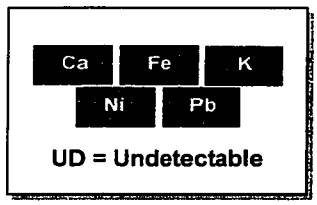

LEGEND

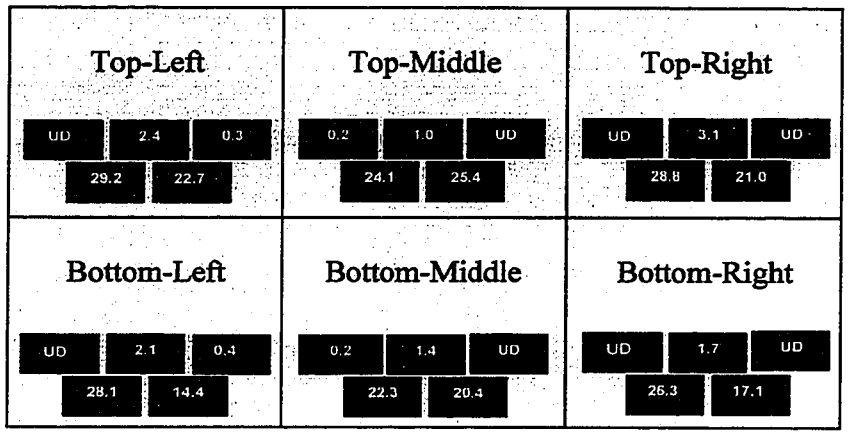

Figure 89 Concentration of metals (mg/L) retained on the textile (F6C6 EDTA-EK-AET)

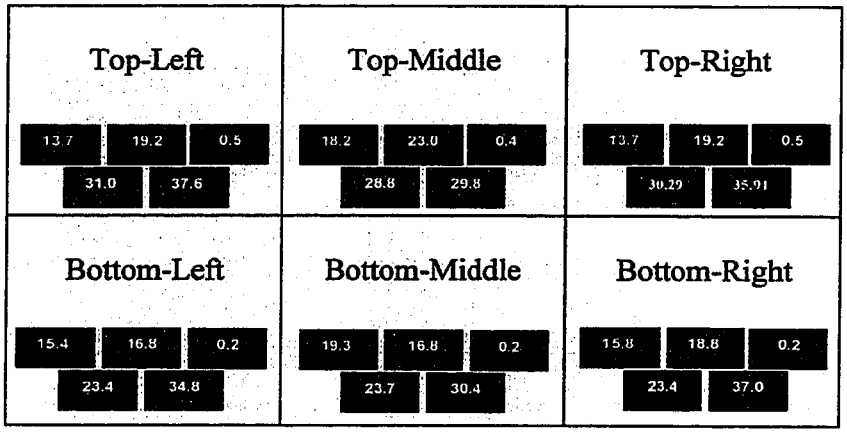

Figure 90 Concentration of metals (mg/L) retained on the textile (F6C6 EDTA-EK-CET)

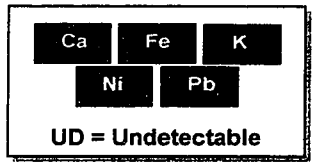

LEGEND

F6C1, with no additional contamination and an AET, showed negligible exchange of cations, as expected. Theoretically, the AET should not have exchanged any cationic species. The values obtained can be attributed to the presence of metal being enmeshed in the textile (physical process), rather than by ion exchange. The absence of EDTA resulted in a lack of metallic-EDTA complexes and therefore negligible concentrations of lead and nickel exchanged onto the AET.

In F6C2, both lead and nickel were exchanged on the cation exchange textile. In the absence of EDTA, there was an abundance of cationic species, including lead and nickel within the cell. Therefore, electrolytic migration and electroosmosis was from anode to cathode, which resulted in a flow of nickel and lead from anode to cathode where they exchanged onto the textile before they could form precipitates in the high pH zone. Removal efficiencies for lead and nickel by the CET were 213% and 82% respectively. The absence of EDTA within the cell still resulted in high removal efficiencies. The erroneous value obtained for lead can be attributed to perfectly uniform distribution of lead in the initial soil or errors related to experimental procedures and analysis.

Comparing the removal efficiencies of the textiles in F6C3, F6C4, and F6C6 with that of F6C5 (no textile) displays the improvements that resulted with respect to the use of EDTA, one type of textile and both textile types (AET and CET). A comparison of lead and nickel removal efficiencies by AETs and CETs in F6C3, F6C4 and F6C6 are shown in Table 42. There is a marked improvement in the cells which utilized textiles, in comparison to F6C5. Localization was higher, particularly in F6C6, where both textile types were employed.

Table 42 Lead and Nickel Removal Efficiencies by IETs

Cell	*Pb Removal Efficiency (CET)*	*Pb Removal Efficiency (AET)*	*Ni Removal Efficiency (CET)*	*Ni Removal Efficiency (AET)*	*Total Pb Removal Efficiency Textile*	*Total Ni Removal Efficiency Textile*
F6C3	64%	-	66%	-	**64%**	**66%**
F6C4	-	74%	69%	-	**74%**	**69%**
F6C6	33%	57%	42%	43%	**90%**	**85%**

The CET in F6C3 (EDTA-EK-CET) removed approximately equal amounts of lead and nickel, but the removal efficiency was only moderate (64% for Pb and 66% for Ni). The exchange of these metals on the CET is an indication that significant amounts of lead and nickel ion were not complexed and remained in their cationic forms. It is most likely that a countercurrent flow existed with some cationic forms of lead and nickel being transported to the cathode. The addition of EDTA resulted in an abundance of anionic species, typically in the form of Pb-EDTA and Ni-EDTA complexes, thereby shifting the net flow in the cathode to anode direction (although cationic species were still transported towards the cathode). As a result, those complexes that were transported to the anode region remained in the soil, since no AET was present. This is shown in the lead and nickel concentration distribution (Figure 75), where the concentration of these metals in the soil was significantly higher in the anode region than in other location within the cell. The lead concentrations are 10-15 times higher on the textile for F6C3, F6C4 and F6C6. This is an indication that the most of the lead and nickel ions that were

transported to the proximity of the textile by electrokinetic processes, were exchanged on the textile.

Table 43 shows the augmentation in removal efficiency that occurred with the addition of one and/or two textiles. F6C5, which did not contain textiles, showed moderate localization, with 77 % of nickel localized within 18% of the cell and 71% of lead localized within 27% of the cell. The use of EDTA showed that increased mobilization and EK transport occurred, which allowed for moderate localization. The principal disadvantage of not utilizing textiles was that a very high degree of localization was difficult to achieve. In addition, from a practical standpoint, approximately 15-30% of the soil remains contaminated.

The use of both anion and cation exchange textiles improved the removal efficiency and the overall localization during electrokinetic treatment. Table 58 shows a comparison of the degree of localization achieved with and without the use of textile. Both Table 57 and Table 58 provide a summary of the efficiency of EDTA and ion exchange textiles for the localization and removal of lead and nickel from natural clayey soil.

Table 58 shows the augmentation achieved related to the use of textiles during EK methodology. In F6C5, the use of only EDTA resulted in 50% of lead and 79% of nickel localized in 20% of the soil. The use of a CET in F6C3 resulted in a 27% improvement in lead and localization within 20% of the soil. Comparing F6C5 to F6C4, where an AET was utilized, an additional 43% of lead and 21% of nickel was localized within 10% of the cell. The use of both types of textile augmented the remediation process significantly,

where 95% of lead and 91% of nickel were localized within 10% of the soil. This represented a large improvement over F6C5 where no textile was employed.

Table 43 Comparison of Enhanced Electrokinetic Localization

Cell	*AET Utilized?*	*CET Utilized?*	*Degree of Pb and Ni Localization within 10 % of Soil*	*Degree of Pb and Ni Localization within 20 % of Soil*
F6C3		✓	73% (Pb)	77% (Pb)
			72% (Ni)	74% (Ni)
F6C4	✓		82% (Pb)	86% (Pb)
			83% (Ni)	86% (Ni)
F6C5			39% (Pb)	50% (Pb)
			62% (Ni)	79% (Ni)
F6C6	✓	✓	95% (Pb)	99% (Pb)
			91% (Ni)	99% (Ni)

The presence of iron represented a problem with respect to the use of cation exchange textiles. As shown in Figures 87, 88 and 90, high concentrations of iron exchanged onto the textile, despite the fact that these textiles were manufactured to be selective to lead and nickel. The high concentrations of iron (220-250 mg/kg) were also observed on the soil in the proximity of the AET and CET in F6C3, F6C4 and F6C6. However, high concentrations were observed only on the CETs, not the AETs. Therefore, Fe-EDTA complexes were transported to the proximity of the AETs in F6C4 and F6C6, but they did not exchange on the AET itself. These are desirable results since

Fe-EDTA complexes did not compete with Pb-EDTA and Ni-EDTA for exchange sites on the AETs. Calcium and potassium were present in low concentrations on the textile and tended not to cause any problems related to competition for exchange sites on the textiles.

12.4.2. Calcium

12.4.2.1. Calcium Concentration in the Soil

The concentration of calcium in soil and its variance from anode to cathode is shown in Figure 91 to Figure 96 for cells F6C1 to F6C6 respectively. The initial calcium concentration in the soil was 250 mg/kg. All cells show similar concentration distributions, with calcium concentrations approximately 25% higher in the cathode region than in the anode. The concentration is a reflection of the soil pH in all cells. Since the solubility of calcium is highly dependent of pH, and since the pH distribution for F6C1 to F6C6 was relatively similar, a similar calcium concentration distribution resulted. In F6C1, the pH of the soil in the cathode area increased from 8.6-11.3, and the calcium concentration in this area did increases substantially from other locations in the soil. At high pH values, calcium forms insoluble precipitates, particularly $Ca(OH)_2$, and takes part in the formation of OH^- ions in the cathode area.

The use to EDTA in F6C3 to F6C6 resulted in a lower pH in the cathode region that in F6C1 and F6C2. This did not correspond to lower calcium concentration in this area. In F6C5, the calcium concentration was higher in the cathode region. The maximum value observed was 118 mg/kg. Therefore, the presence of EDTA did not minimize the calcium concentration. The use of a CET in F6C2, F6C3 and F6C6 resulted in a calcium soil distribution that was similar to F6C1 and F6C4, where a CET was not

employed. This is an indication that the CET did not exchange calcium. This is favorable, since competition between Ca with the Pb and Ni ions probably did not occur.

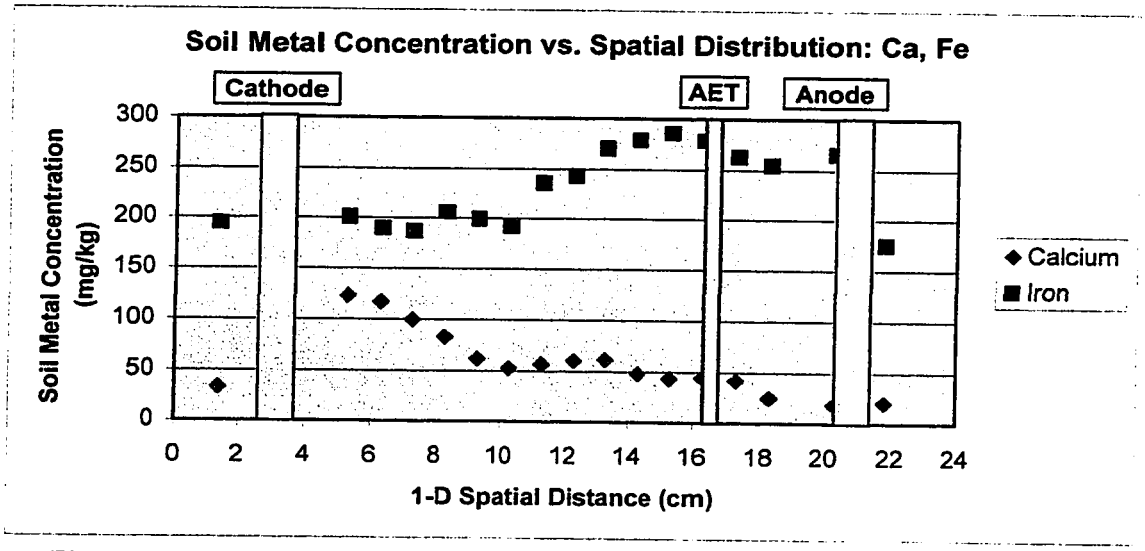

Figure 91 Ca and Fe concentration at the end of the experiment (F6C1 EK-AET)

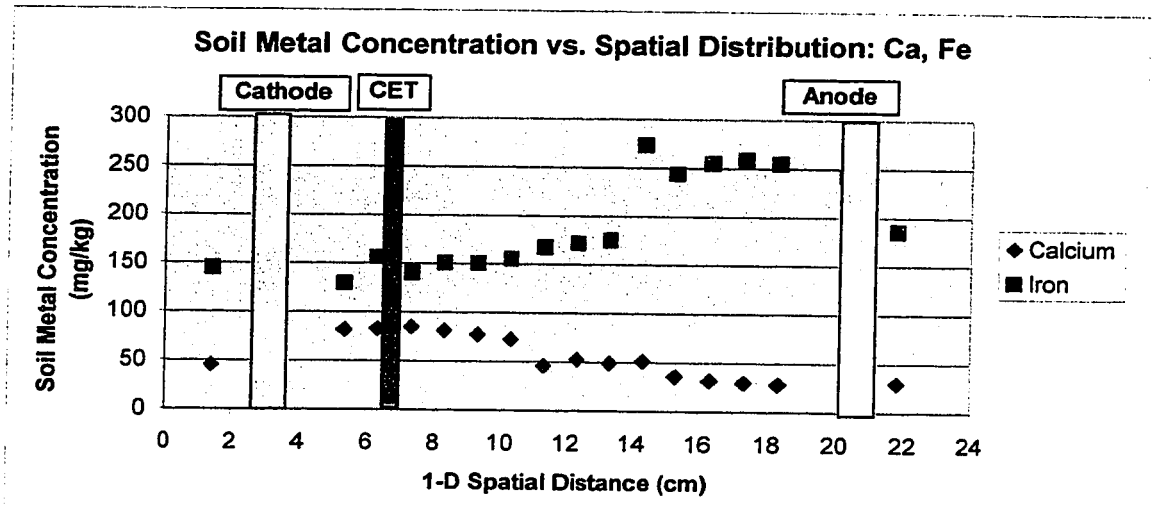

Figure 92 Ca and Fe concentration at the end of the experiment (F6C2 EK-CET)

Initial Ca concentration: 250 mg/kg
Initial Fe concentration: 273 mg/kg

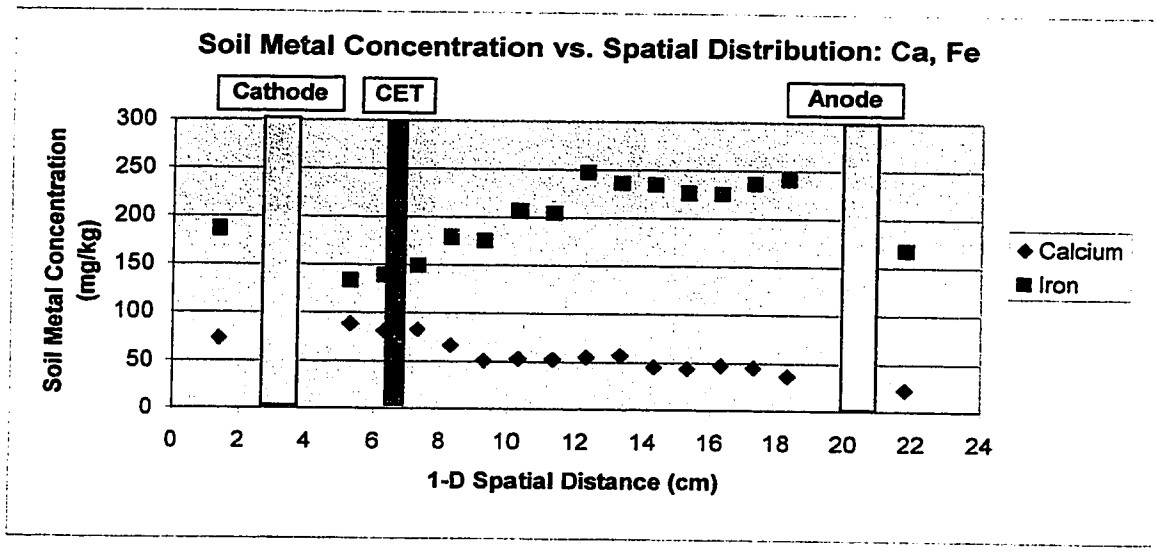

Figure 93 Ca and Fe concentration at the end of the experiment (F6C3 EDTA-EK-CET)

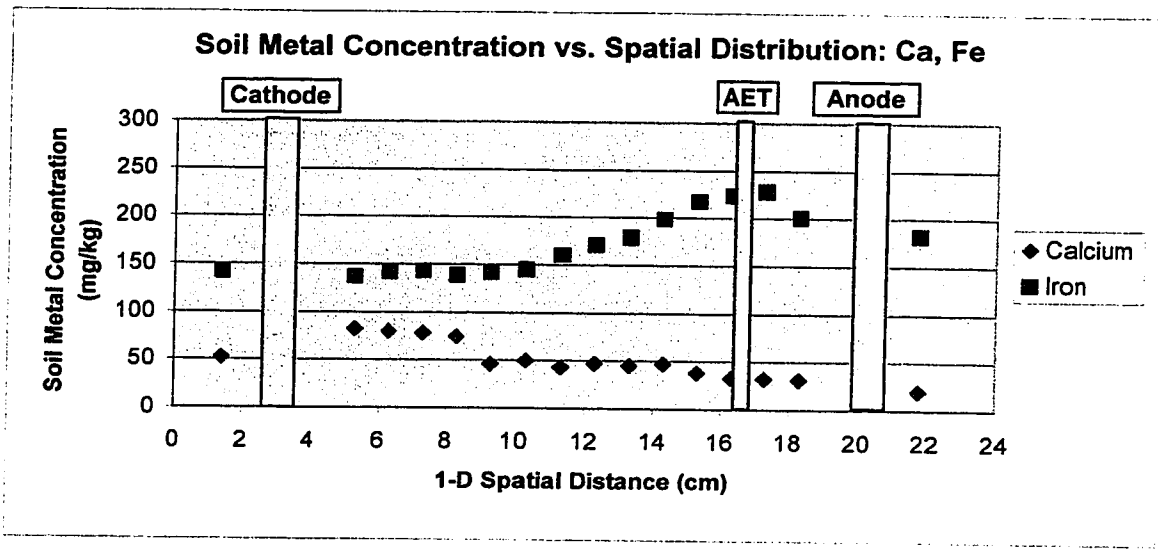

Figure 94 Ca and Fe concentration at the end of the experiment (F6C4 EDTA-EK-AET)

Initial Ca concentration: 250 mg/kg
Initial Fe concentration: 273 mg/kg

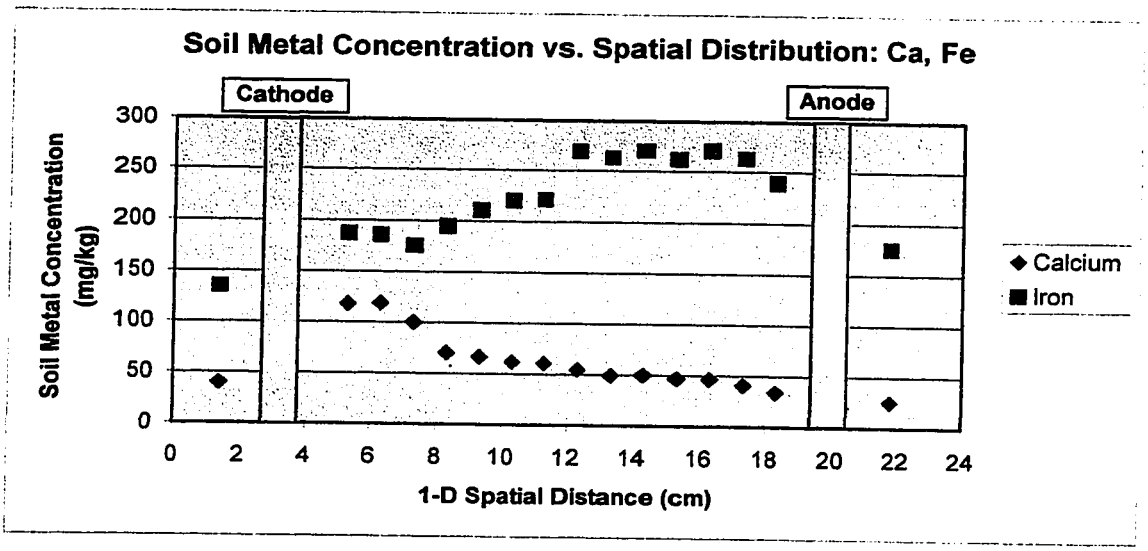

Figure 95 Ca and Fe concentration at the end of the experiment (F6C5 EDTA-EK)

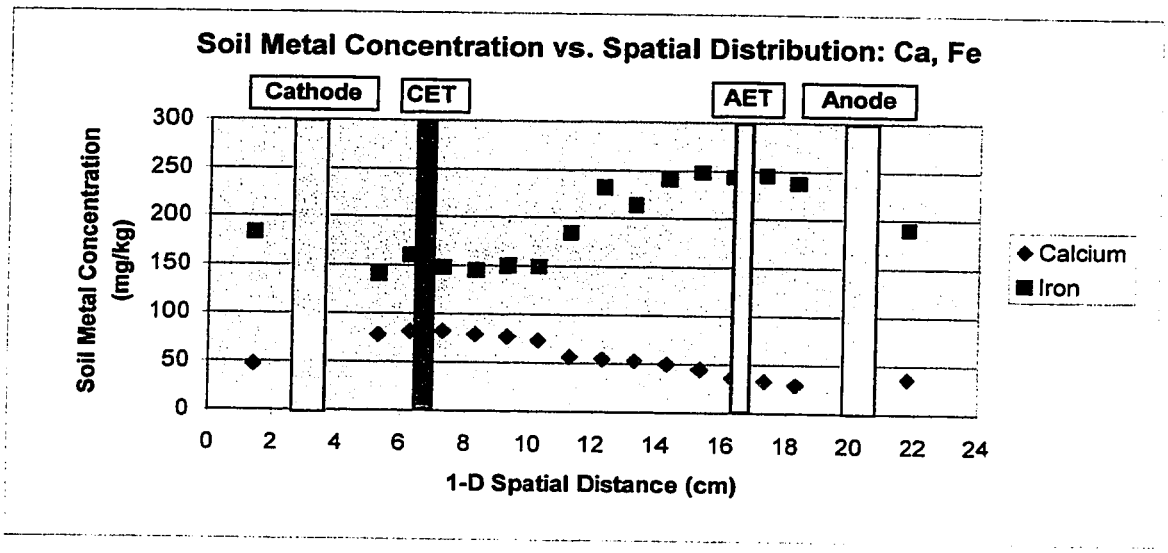

Figure 96 Ca and Fe concentration at the end of the experiment (F6C6 EDTA-EK AET & CET)

Initial Ca concentration: 250 mg/kg
Initial Fe concentration: 273 mg/kg

12.4.2.2. Calcium Concentration: Soil in the Proximity of the Textile

The calcium concentration for the soil in the proximity of the textiles in F6C1 to F6C4 and F6C6 are shown in Figure 79 to Figure 84 respectively. The calcium concentrations observed are directly related to the pH and location of the textile. For F6C1, F6C4 and the AET in F6C6, the calcium concentrations were one-third to one-half those of F6C2, F6C3 and the CET in F6C6. This is not due to the textile being used, but rather the location and the pH distribution in the corresponding area. The location of the AETs were in an area of low pH (7.3-7.8) and typically, calcium ions are relatively soluble. In the cathode region, where the CETs were located, the pH was in the range of 8.5-11.0 due to the constant production of OH^- ions. At this pH, calcium forms $Ca(OH)_2$, which is then reduced to Ca^{2+} and OH^- ions. The calcium ion then forms $Ca(OH)_2$ once again. Similar concentrations were observed on the middle and adjacent sections of the textile. It seems that the calcium concentration is a product of electrochemical processes. In order to minimize the formation of calcium, the system chemistry has to be optimized, by lowering the overall pH within the system.

12.4.2.3. Calcium concentration on the Textile

The total calcium concentration located on the textiles of F6C1 and F6C2 is shown in Figure 85 and Figure 86 respectively. The total amount of calcium retained on the textile for F6C1 and F6C2 was 20.00 mg/L and 25.69 mg/L respectively. For both cells, this concentration was relatively low, which indicated that the presence of calcium did not impede the exchange of the target compounds significantly, namely lead and nickel. Superimposing these results with those of the soil further evidences this fact. It

can be seen in both cells that the calcium concentration of the soil samples adjacent to the textile was 2-3 times higher for F6C1 and 3-4 times higher for F6C2, than on the textile. This indicates that the textile allowed for the passage of calcium ions. However, the presence of calcium indicates that the textile also acts as a filter, which is undesirable, since many nickel and lead exchange sites are used by calcium ions. This phenomenon must be taken into consideration in any comparable field operation. However, based on the results obtained, the presence of calcium does not represent problem related to the tested textile efficiency.

12.4.3. Iron

12.4.3.1. Iron Concentration in the Soil

The iron concentration in the soil for F6C1 to F6C6 is shown in Figures 91 to 96 respectively. The initial iron concentration in the soil was 273 mg/kg. The iron concentration in F6C1 to F6C6 was comparable and they represented the highest metal concentration of the ones analyzed. The high concentration was most likely due to the extensive oxidation of the anode and the initial iron already present within the soil. All cells showed higher concentrations observed in the anode regions than in the cathode regions. This phenomenon can be attributed to the following:

1. The formation of iron ions due to anode oxidation occurred in this area.
2. The formation of Fe-EDTA complexes resulted in their transport from cathode to anode. Once these complexes reached the lower pH zone in the anode region, they exchanged onto the anion exchange textile or formed precipitates in the anode region.

Table 44 shows a comparison of the maximum and minimum iron concentration in the soil for each cell. It shows similar values of iron in all cells. The high iron concentration in the cathode region shows that EK transport of ferrous ions in soil was high. This transport was countercurrent to the transport of lead and nickel complexes. Once these ions were transported to the cathode, the hydroxide ions produced at the cathode formed ferrous and ferric hydroxide precipitates, which caused high soil concentrations. All cells were subjected to anode oxidation, which introduced these levels of iron into the soil.

Table 44 Maximum and Minimum Iron Concentrations in the Soil

Cell	*Maximum Iron Concentration (mg/kg)*	*Minimum Iron Concentration (mg/kg)*
F6C1	286	175
F6C2	273	129
F6C3	247	133
F6C4	228	134
F6C5	271	134
F6C6	248	136

12.4.3.2. Iron Concentration for the Soil in the Proximity of the Textile

The concentration of iron for the soil in the proximity of the textile in F6C1 to F6C4 and F6C6 are shown in Figure 79 to Figure 84. For F6C1 and F6C4, where AET were used, the iron concentration on both the anode and cathode sides were similar to those observed in the soil. This is an indication that the iron ions formed on the anode

side of the AET did not exchange on the textile. Without the presence of EDTA to form negative complexes, the ions formed due to the oxidation of the steel anode and mesh could not exchange on the AET. In addition, the two-dimensional spatial variation was negligible in both cells with maximum and minimum values of 262.0 mg/kg and 239.4 mg/kg and 239.4 mg/kg and 212.0 mg/kg for F6C1 and F6C4 respectively. The high iron concentration can be attributed to the high initial iron content of the soil and oxidation occurring at the anode.

In F6C2, where a CET was used, the iron concentration was appreciably lower than in F6C1, due to the location of the textile (in the cathode region). Maximum and minimum values for the CET in F6C2 were 171.6 mg/kg and 134.2 mg/kg respectively. The concentration on the cathode side was 20-50 mg/kg lower than on the anode side for each location of the textile. Some iron ions were exchanged onto the textile, therefore resulting in a lower concentration on the cathode side.

The opposite phenomenon was observed in F6C3 where a CET was also used. The iron concentration on the cathode side of the textile was 15-25 mg/kg higher than on the anode side. This is due to the presence and effect of EDTA. In F6C3, net electrolytic migration was from cathode to anode, due to the abundance of Fe-EDTA anionic complexes. It is possible, that some complexes, particularly those between the cathode and the CET may have become immobile in the high pH zone and remained in this location (in the proximity of the textile). It is possible that most Fe^{2+} ions, as a result of the dissociation of $FeCO_3$, did not form complexes and therefore remained in their location. The ions that came into contact with the textile readily exchanged.

For the AET in F6C6, the iron concentration was similar to F6C4. The variation from anode side to cathode side was negligible. Maximum and minimum values observed were 243.6 mg/kg and 223.6 mg/kg respectively. It is possible, that iron complexes were not exchanged onto the textile or that the constant formation of Fe^{2+} ions (non-EDTA complex) due to the oxidation of the anode and anode mesh offset those ions exchanged onto the textile, by passing through the AET. This resulted in a similar concentration on both sides of the soil in the proximity of the textile.

Iron concentration values were consistently 7-10 times higher than the corresponding values for calcium. These high values are expected due to the extensive oxidation that occurred during the electrokinetic experiment, which released ferrous ions into the soil. The oxidation of ferrous ions to insoluble ferric ions resulted in precipitation to $Fe(OH)_3$. This accounted for the iron concentration in this area. The amount of iron in the proximity of the textile is of concern to the ion-selective textile because iron ions may acquire the exchange sites that are delineated for the target heavy metals.

12.4.3.3. Iron Concentration on the Textile

The iron concentration on the textile for both F6C1 (EK-AET) and F6C2 (EK-CET) is shown in Figure 85 and Figure 86 respectively. In order to facilitate a proper comparison, the nickel concentration detected on the textile is also shown. In F6C1, the top-middle sample (see Figure 85) contained approximately equal amounts of iron and nickel. This is detrimental to the electrokinetic removal of heavy metals since increased removal of nickel was prevented by the retention of iron on the textile. In the bottom-right sample of F6C1, a higher concentration of iron was retained. For F6C2, the bottom-

right (see Figure 85) sample retained 2.5 times more iron than nickel, which is undesirable. As stated previously, the amount of iron present in the cell can be attributed to the high levels of oxidation at the anode. In other locations of the textile, the amount of nickel retained was substantially higher, but the amount of iron was appreciable and definitely poses a problem related to the use of exchange sites that could be used for the removal of target heavy metals. Total iron on the textile, consisted of a summation of all textile samples, for F6C1 and F6C2, was 187.5 mg/L and 281.2 mg/L respectively.

Based on the pH distribution, the locations of the textiles were appropriate. The cation exchange textiles were located either just before and just at the beginning of the high pH gradients. This allowed for the removal of heavy metals (non-complexed) just before entering the high pH zone, thereby preventing precipitation and immobilization. At the same time, significant localization is achieved. Ideally, the location of the AET should be just before the pH decreases significantly, since the lower the pH the greater the tendency of anions to form precipitates. However, sharp pH decreases were not observed in zone 1 for any of the cell and the pH in this area was close to neutral or above. Therefore, the location of the AET was not as critical as that of the CETs.

12.4.4. Potassium

Based on the concentration of potassium in the proximity of textile and those retained on the textile in all cells, it can be seen that potassium did not play a major role in the EK-EDTA-IET system. Observing all cells, the maximum concentration for the soil in the proximity of the textile was 20.3 mg/kg (F6C1). The highest potassium concentration retained by any textile was less than 1.0 mg/L. The concentration on the CET and in the soil in the proximity of these CETs for cells F6C2, F6C3 and F6C6 were

very low compared to the other metals that were analyzed. This indicates that potassium did not enter in competition with lead, nickel and iron for exchange sites. With respect to the AETs and the soil in the proximity of the AETs for cells F6C1, F6C4, and F6C6, the concentrations were also very low, which indicated that potassium ions did form complexes with EDTA. Therefore, competition for EDTA ligands between potassium and the target heavy metals (Pb and Ni ions), was not prevalent.

13. CONCLUSIONS AND RECOMMENDATIONS

This thesis dealt with the improvement of standard electrokinetic methodology for the remediation of natural clayey soil contaminated with lead and nickel. Technology improvements, to eliminate the inherent problems with standard EK methods, namely precipitation and immobilization in the high pH zone, and the inherently low solubility of lead and nickel compounds, were examined. Experiments dealing with the sole use of EDTA coupled with EK methods showed improved solubility of lead and nickel and moderate degrees of localization in the anode area. The presence of EDTA promoted the formation of Pb-EDTA and Ni-EDTA anionic complexes, which where transported via electrolytic migration to the anode region. Results showed that an average of 85% of nickel ions localized within $1/4^{th}$ of the cell and 75% of the lead ion localized within $1/3^{rd}$ of the cell.

The experiments utilizing EDTA, electrokinetics and textiles (experiment F6) provided a detailed four-point analysis related to:

1. Electrical parameters (current, potential and resistance)
2. System chemistry (soil pH, soil metal concentration, cathode liquids)
3. Enhanced mobilization and transport by EDTA and EK methods only, and
4. The overall localization and removal efficiency of EDTA-EK-IET systems.

This thesis also provided a detailed comparison of the relative improvement that the use of textiles, in combination with EDTA and EK methodology, provided. The use of EDTA–EK methods, without textiles, produced enhanced solubility and transport of lead

and nickel. Using all three techniques (EDTA-EK-textiles), solubility was enhanced and the localization and removal achieved was improved, with 90-95% of lead and nickel ions localized within $1/10^{th}$ of the cell. In addition, the use of textiles allowed for the simple removal of lead and nickel contamination. This represented a significant improvement over standard EK methods (which typically have been applied only to low pH soil) and represents a possible remediation technique in natural clayey soil. To summarize, and with respect to the objectives of this thesis, the following statements and observations can be made related to all experiments performed and the results obtained:

1. **The utilization of EDTA, electrokinetic methods and IETs improved the overall localization and removal of lead and nickel from natural clayey soil.** The use of EDTA for enhanced mobilization, EK methods for the transport of ionic species and textiles for the localization of lead and nickel showed significant improvements over standard EK and combined EK-EDTA methods. The hybrid method combining all three techniques produced high lead and nickel removal efficiencies and a localization of 90-95% within 10% of the cell. The localization of EDTA-EK cells, produced a nickel localization of 84% in $1/4^{th}$ of the cells and 75% lead localization within $1/3^{rd}$ of the cells (Chapter 12).

2. **The use of EDTA enhanced the solubility of lead and nickel in natural clayey soil.** The lead and nickel concentration was highest in the anode region, which is an indication that electrolytic migration from cathode to anode was high, as a direct result of the abundance of Ni-EDTA and Pb-EDTA complexes. The enhanced solubility of Pb and Ni increased the amount of metals that were accessible to electrokinetic transport (Chapter 11 and Chapter 12).

3. **The pH distribution was generally typical of an electrokinetic cell.** High pH values developed at the cathode in response to the production of OH^- ions in that area. The use of EDTA tended to maintain a lower pH (0.5-1.0 units lower) in the cathode area. Based on the pH distribution, the cation exchange textiles were well placed (i.e. just before the sharp pH increase in the cathode area). The distributions shown previously can be useful in the determination of the best location of the textile (Chapter 11 and Chapter 12).

4. **The spatial resistance distribution in all cells showed similar trends.** The use of textiles tends to increase the resistance in that area, thereby reducing the electrokinetic transport efficiency. The use of EDTA did not have a major impact on the resistance distribution, with the exception of local potential and resistance gradients occurring at the location of the textile. All cells correlated to a power function with R^2 values generally above 0.9. The generally similar distributions, with or without the use of textiles and EDTA, lend themselves to the possibility of mathematically modeling the spatial resistance distribution. Although the use of a textile creates a discontinuity and must be considered during mathematical modeling (Chapter 11 and Chapter 12).

5. **Conclusions related to the use of IETs:**

   5a. The placement of the textile in an area just before the high pH zone (cathode region) alleviated the problem of extensive carbonate and hydroxide precipitation. The textile readily exchanged nickel and lead before they formed precipitates in the high pH zone. This localized these heavy metals, rather than forming insoluble or low solubility precipitates, as is prevalent with standard electrokinetic techniques.

   5b. The textiles did not have a drastic effect on the resistance distribution. In all cells, the textiles caused local gradients at the location of the textile, which were higher for CETs than AETs. Nevertheless, the improvement in the localization and removal of lead and nickel achieved with the introduction of textiles.

   5c. The use of EDTA lowered the overall pH within the soil. This was shown in a comparison of F6C1 and F6C2 with F6C3 to F6C6.

   5d. The textiles did not significantly effect the pH distribution in the soil. The different locations of the textile in F6C1 and F6C2 did not effect the pH. This is significant since the pH is a controlling factor over mechanisms such as mobilization, sorption, ion exchange and precipitation.

   5e. The textile can be made to be ion-selective, thereby allowing for the selective removal of heavy metal contamination. Therefore, lead and nickel can be removed selectively.

   5f. Textiles improved the localization of lead and nickel. Using EDTA for enhanced mobilization, in combination with EK methodology for transport to the textiles, allowed for high concentration of target heavy metals to be localized in a small area of the EK cell.

5g. The textiles allow for simple removal, recovery and possible recycling of lead and nickel. By localizing the target heavy metal on a textile, their removal and recovery represents a relatively simple procedure. Comparing this to F6C5 where lead and nickel were localized within the soil, removal and recovery of lead and nickel is more difficult. In addition, if recovery is not desired, disposal still presents a problem.

5h. Textiles alleviate the inherent problems related to standard electrokinetic processes. The high pH gradients occurring during EK processes create problematic conditions related to the immobilization/precipitation of cations in the cathode region (high pH) and anions in the anode region (low pH). The placement of a CET just before the high pH zone and an AET just before the low pH zone allowed for the exchange of target species before they become immobilized in the soil via precipitation or sorption.

6. **SFE techniques, using EDTA as a modifier, proved to be effective in the extraction of lead, nickel, calcium and potassium from natural clayey soils and those metals bound to textiles.** SFE-AAS techniques showed 2-3 times the extraction efficiency as the standard acid digestion technique and represented a faster, safer and more efficient method of metal extraction (Chapter 10).

Based on the results presented in this thesis, the use of this hybrid technique, namely electrokinetics (transport of ionic species in soils having a low coefficient of permeability), in combination with EDTA (solubility enhancer) and ion exchange textiles (localization and removal), represents a promising technological innovation for the remediation of natural clayey soils. Some obstacles must be overcome in order to strengthen the viability of this technique:

1. **The presence of iron within the soil.** Its ability to form highly stable complexes with EDTA creates a competition with Pb and Ni for EDTA complexation sites. In addition, iron ions tended to also compete with Pb and Ni for exchange sites on CETs. The method of supplying EDTA, as studied in experiment F5 seems to be effective in distributing of EDTA throughout the soil, as evidenced by the cathode-anode direction of transport and the localization achieved. However, scale-up procedures pose a significant obstacle.

2. **Establishing the time required for EDTA-EK-IET treatment.** This may be limited by the exchange capacity of the textiles or the efficiency related to the current supply.

3. **Scaling up procedures.** This presents a significant obstacle with respect to determining the amount of EDTA required, since this will be dependent on the metal content of the soil, and the speciation.

In order to alleviate or minimize some of these problems the following implementations and aspects that require further research are recommended:

1. **Obtain a better characterization of the soil with respect to metal concentration and speciation.** This is particularly important in field applications. Other metals such as copper, have high stability constants and can compete with Pb and Ni for EDTA complexation sites.

2. **Determine the speciation of metal complexes formed in the anode region of the cell.** It is possible that many strong ligands, such as PO_4^{3-} can promote immobilization, thereby rendering these metals immobile and preventing their exchange onto an AET. Knowing the speciation of these ligands before treatment and the complexes formed during treatment would be desirable.

3. **Determine the amount of EDTA required for the treatment of a given soil.** The presence of metals other than lead and nickel will increase the stoichiometric amount of EDTA required.

REFERENCES

Acar, Y. B., A. N. Alshawabkeh, R. J. Gale, 1992, "Fundamentals of Extracting Species from Soils by Electrokinetics", Waste Management, Vol. 13, pp. 141-151.

Acar, Y. B., A.N. Alshabwabkeh, 1993, "Principles of Electrokinetic Remediation", Environmental Science and Technology, Vol. 27, No. 13, pp. 2638-2647.

Acar, Y. B., A.N. Alshabwabkeh, 1996, "Electrokinetic Remediation I: Pilot-Scale Tests with Lead-Spiked Kaolinite", Journal of Geotechnical Engineering, Vol. 122, No. 3, pp. 173.

Allen, H. E., P. Chen, 1993, "Remediation of Metal Contaminated Soil by Incorporating Electrochemical Recovery of Metal and EDTA", Environmental Progress, Vol. 12, No. 4, pp. 284-293.

Alshawabkeh, A. N., Y.B. Acar, 1996, "Electrokinetic Remediation II: Theoretical Model", Journal of Geotechnical Engineering, Vol. 122, No. 3, pp. 186-196.

Chen, T., E. Macauley, A. Hong, 1995, "Selection and Test of Effective Chelators for Removal of Heavy Metals from Contaminated Soils", Canadian Journal of Civil Engineering, pp. 1185-1197.

Choudhury, A., Elektorowicz, M., 1997, "Enhanced Electrokinetic Methods for Lead and Nickel Removal from Natural Clayey Soil", 32nd Central Symposium on Water Pollution Research, February 1997, Burlington, ON.

Clifford, D., Z. Zhang, 1994, "Modifying Ion Exchange for Combined Removal of Uranium and Radium", Journal of the American Water Works Association, Vol. 12, No. 4, pp. 214-227.

D'Avila, J. S., C. M. Matos, M. R. Cavalcanti, 1992, "Heavy Metals Removal from Wastewater by Using Activated Peat", Journal of Water Science and Technology, Vol. 26, No. 9, pp. 2309-2312.

Das, B. M., 1994, Principles of Geotechnical Engineering, 3rd ed. PWS Publishing Company, Boston, 672 pages.

Drioli, E., 1992, "Membrane Operations for the Rationalization of Industrial Productions", Water Science and Technology, Vol. 25, No. 10, pp. 107-125.

Elektorowicz, M., 1996, CIVI 690V: Engineering Aspects of Soil Bioremediation, Class Notes, Concordia University, Montréal, Canada.

Elektorowicz, M., Boeva, V., 1996, "Electrokinetic Supply of Nutrients in Soil Bioremediation", Environmental Technology, Vol. 17, pp. 1339-1349.

Elektorowicz, M., Chifrina, R., Kozak, M., Hatim, J., 1996a, "The Behaviour of Ion Exchange Membranes in the Process of Heavy Metals Removal from Contaminated Soil", '96 CSCE-4th Environmental Engineering Specialty Conference, May, Edmonton, Canada.

Elektorowicz, M., Jahanbakhshi, P., Chifrina, R., Hatim, J., Lombardi, G., 1996b, "Phenol Removal from Groundwater using Electrokinetics", International Conference on Municipal and Rural Water Supply and Water Quality, Vol. 2, pp. 105-116, June, Poznan, Poland.

Elektorowicz, M., 1995, "Technical Requirements Related to the Electrokinetic Removal of Contaminants from Soil", ASCE/CSCE Joint Conference on Environmental Engineering, July 1995, Pittsburgh, U.S.A.

Elektorowicz, M., Chifrina, R., Konyukhov, B., 1995, "Enhanced Removal of Diesel Fuel from Soil by Electrokinetic Method", 30th Annual Central Canadian Symposium on Water Pollution Research, February 1995, Burlington, ON.

Elektorowicz, M., 1993, CIVI 469: Geo-Environmental Engineering, Class Notes, Concordia University, Montréal, Canada.

Evans, L. J., 1989, "Chemistry of Metal Retention by Soils", Environmental Science and Technology, Vol. 23, No. 9, pp. 1046-1056.

Eykholt, G. R., D. E. Daniel, 1994, "Impact of System Chemistry on Electroosmosis in Contaminated Soil", Journal of Geotechnical Engineering, Vol. 120, No.5, pp. 797-815.

Fane, A. G., A.R. Awang, M. Bolko, R. Macoun, R. Schofield, Y. R. Shen, F. Zha, 1992, "Metal Recovery from Wastewater Using Membranes", Journal of Water Science and Technology, Vol. 25, No. 10, pp. 5-18.

Ferguson, J. E., 1990, The Heavy Elements: Chemistry, Environmental Impact, and Health Effects, Pergamon Press, New York, 614 pages.

Guha, A. K., C. H. Yun, R. Basu, K. K. Sirkar, 1994, "Heavy Metal Removal and Recovery by Contained Liquid Membrane Permeator", AIChE Journal, Vol. 40, No. 7, pp. 1223-1237.

Hamblin, W. K., 1992, Earth's Dynamic Systems, 6th ed., Maxwell Macmillan Canada, Toronto, Canada, pp. 202-206.

Hamed, J., Y. B. Acar, R. J. Gale, 1991, "Pb(II) Removal from Kaolinite by Electrokinetics", Journal of Geotechnical Engineering, Vol. 117, No. 2, pp. 214-267.
Harland, C. E., 1994, Ion Exchange: Theory & Practice, 2nd ed., Royal Society of Chemistry, Cambridge, 285 pages.

Harter, D. R., 1983, "Effect of Soil pH on Adsorption of Lead, Copper, Zinc, and Nickel", Soil Science Society American Journal, Vol. 47, pp. 47-52.

Kotz, J. C., K. F. Purcell, Chemistry and Chemical Reactivity, 1987, Saunders College Publishing, Montreal, 1020 pages and Appendices.

Lageman, R., 1989, "Electrokinetic Reclamation: State-of-the-Art", Demonstration of Remedial Action Technologies for Contaminated Land and Groundwater, Geokinetics, Poortweg, the Netherlands.

LaGrega, M. D., P. L. Buckingham, J. C. Evans, 1994, Hazardous Waste Management, McGraw-Hill, Inc., New York, 1146 pages.

Laintz, K. E., C. M. Wai, 1992, Extraction of Metal Ions from Liquid and Solid Materials by Supercritical Carbon Dioxide", Analytical Chemistry, Vol. 64, No. 22, pp. 2875-2878.

Legret, M., Raimbault, G., "Etude de la modélisation des fonctions assurées par une décharge Caractérisation Hydrodynamique et étude du devenir des métaux lourds dans un déchet-type", Bulletin Liason Physique et Chimique, Vol. 175, pp. 77-91.

Li, M., J. B. Schlenoff, 1994, "Ion Exchange Using a Scintillating Polymer with a Charged Surface", Analytical Chemistry, Vol. 66, No. 6, pp. 824-829.

Lin, Y, R. D. Brauer, K. E. Laintz, C. M. Wai, 1993, "Supercritical Fluid Extraction of Lanthanides and Actinides from Solid Materials with a Fluorinated β-Diketone", Analytical Chemistry, Vol. 65, No. 18, pp. 2549-2551.

Maliou, E., M. Malamis, P. O. Sakellarides, 1992, "Lead and Cadmium Removal by Ion Exchange", Journal of Water Science and Technology, Vol. 25, No. 1 pp. 133-138.

McNeff, C., P. W. Carr, 1995, "Synthesis and Use of Quartenized Polyethlenamine-Coated Zirconia for High-Performance Anion-Exchange Chromatography", Analytical Chemistry, Vol. 67, No. 21, pp. 3886-3892.

Merian, P. D., 1991, Metals and their Compounds in the Environment: Occurrence, Analysis and Biological Relevance, VCH Publishing, New York, 1438 pages.

Muraviev, D., A. Gonzalo, M. Valiente, 1995, "Ion Exchange on Resins with Temperature-Responsive Selectivity. 1. Ion-Exchange Equilibrium of Cu^{2+} and Zn^{2+} on Iminodiacetic and Aminomethylphosphonic Resins", Analytical Chemistry, Vol. 67, No. 17, pp. 3028-3035.

O'Brien, R. W., "Electroosmosis in Porous Media", 1986, Journal of Colloid and Interface Science, Vol. 110, No. 2, pp. 477-487.

Pamukcu, S, J. K. Wittle, 1992, "Electrokinetic Removal of Selected Heavy Metals from Soil", Environmental Progress, Vol. 11, No. 3, pp. 241-250.

Peavy, H. S., D. R. Rowe, G. Tchobanoglous, 1985, Environmental Engineering, McGraw-Hill, New York, pp. 162-164.

Pesavento, M. R Biesuz, M. Gallorini, A. Profumo, 1993, "sorption Mechanism of Trace Amounts of Divalent Metal Ions on a Chelating Resin Containing Iminodiacetate Groups", Analytical Chemistry, Vol. 65, No. 18, pp. 2522-2527.

Pulles, W., G. J. G., Juby, R. W. Busby, 1992, "Development of the Slurry Precipitation and Recycle Reverse Osmosis (SPARRO) Technology for Desalinating Scaling Mine Waters", Water Science and Technology, Vol. 25, No. 10, pp. 177-192.

Reed, B. E., M. T. Berg, J. C. Thompson, J. H. Hatfield, 1995, "Chemical Conditioning of Electrode Reservoirs During Electrokinetic Soil Flushing of Pb-Contaminated Silt Loam", Journal of Environmental Engineering, Vol. 121, No. 11, pp. 805-815.

Rump, H. H., H. Krist, 1988, Laboratory Manual for the Examination of Water, Wastewater and Soil, Lewis Publishers: Michigan, 190 pages.

Sata, T., 1993, "Properties of Composite Membranes Formed from Ion-Exchange Membranes and Conducting Polymers. 4. Change in Membrane Resistance during Electrodialysis in the Presence of Surface-Active Agents", Journal of Physical Chemistry, Vol. 97, No. 26, pp. 6920-6923.

Segall, B. A., C. J. Bruell, 1992, "Electroosmotic Contaminant-Removal Processes", Journal of Environmental Engineering, Vol. 118, No. 1, pp. 84-100.

Sethi, S., M. R. Wiesner, 1995, "Performance and Cost Modelling of Ultrafiltration", Journal of Environmental Engineering, Vol. 121, No. 12, pp. 874-883.

Stathakis, C., R. M. Cassidy, "Cationic Polymers for Selectivity Control in the Capillary Electrophoretic Separation of Inorganic Anions", Analytical Chemistry, Vol. 66, No. 13, pp. 2110-2115.

Veerapaneni, S., D. Brejchova, D. C. Schmelling, F. F. Nazzal, M. R. Wiesner, 1992, "Pilot Evaluation of Ceramic Membranes in Surface Water Treatment with Coagulant Pretreatment", Journal of Water Science and Technology, Vol. 26, No. 11, pp. 2285-2288.

Wang, J., W. D. Marshall, 1994, "Metal Speciation by Supercritical Fluid Extraction with On-Line Detection by Atomic Absorption Spectrometry", Analytical Chemistry, Vol. 66, No. 22, pp. 3900-3907.

Wenzel, T. J., K. J. Townsend, D. E. Frederique, A. G. Baker, 1993, "Supercritical Fluid Extraction of Metal-Containing Selective Sorbents", Journal of Chromatography, No. 637, pp. 187-194.

Yang, J. H. K., J. H. Burban, E. L. Cussler, 1995, "Copper Selective Adsorption with a Microemulsion-Based Resin, AIChE Journal, Vol. 41, No. 5, pp. 1165-1170.
Yeung, A. T., R. M. Menon, 1996, "EDTA-Enhanced Electrokinetic Extraction of Lead", Journal of Geotechnical Engineering, Vol. 122, No. 8, pp. 666-673.

Yong, R. N., A. M. O. Mohamed, B. P. Warkentin, 1992, Principles of Contaminant Transport in Soils, Elsevier Publishing, New York, 327 pages.

APPENDIX A:

Ecological Impacts of Heavy Metals

A. ECOLOGICAL IMPACTS OF HEAVY METALS

A.1. Accumulation of Metals in the Food Chain

Although some metals have nutritional importance to microorganisms (e.g. nickel) and members of the food chain, others, such as lead, calcium, mercury, arsenic have no nutritional importance, and their presence can have adverse human health effects. Concentration is the most important factor due its influence of potential toxicity. Essential elements produce their intended effects within a specified concentration range. The behaviour and potential toxicity of these metals can be altered if these values are outside a specified concentration range.

Heavy metals can reach the food chain via water, soil, plants, animals, and humans. Accumulation takes place in certain target tissues, the extent being dependent on the duration of exposure, and the existing concentration of the metal in the organism's environment. Differing reactivities of the heavy metals promote deposition, through the binding of ionized metals to storage structures. Adsorption and distribution depend considerably upon the lipid solubility of the individual compound. Corresponding to their ability to penetrate lipid membranes, organic compounds are more likely to enter and accumulate in an organism than are inorganic ones. Since individual heavy metals exhibit different behaviour, a differentiated description of each is necessary.

A.1.1. Accumulation of Lead in the Food Chain

Lead found in food and animal feed comes mainly from external sources, for example, lead-containing dust can adhere to the surfaces of edible plants. Transfer of lead from the soil to plants takes place only when the lead concentration of the soil is

extremely high (more than 5000 mg/kg of dry matter). Plant feed and food have lead contents ranging from less than 0.1 mg/kg up to 5 or 10 mg/kg of dry matter. Industrial pollution can cause values of between 100 and 1000 mg/kg in certain areas (Merian, (1991)). In general, plant foodstuffs contain more lead than foodstuffs of animal origin. The lead content of animal tissues is caused mainly by the uptake of contaminated feed. About 10 to 70 % of the total burden is caused by the inhalation of lead containing dust. Lead shows different accumulation rates in tissue. No more than 0.1 mg/kg lead is found in the skeletal muscle of farm animals, even if the animals have been exposed to massive levels. In liver, however, concentrations can reach more than 0.1 mg/kg, and in exceptional cases even 10 mg/kg in animals from polluted areas. Similar concentrations are found in the kidneys. Lead concentrations in the muscle, liver, and kidney of wild boars are higher than those of domestic pigs, which corresponds to the more polluted feed of wild animals. To avoid accumulation, animal drinking water should not contain more than 0.1 mg lead per liter (Merian, (1991)).

Within an organism, lead is most likely present in the form of organic compounds. It is bound to certain protein fractions of the protoplasm in liver and kidney cells. Highest accumulation takes place in bone. Domestic animal feed with a lead content of no more than 30 mg/kg dry matter will result in liver levels of less than 1 mg/kg, although swine feed should not contain more than 5 mg/kg lead.

Lead does not play a major role in aquatic food chains. Lead levels in fish depend upon the amount of lead pollution in the environmental water. Levels of 0.01-0.03 mg/kg and 0.04-0.15 mg/kg have been determined in fish muscle and liver, respectively, but these values may increase to 0.08 and 0.09 mg/kg in fish from polluted water. There is

wide variation in the investigative data, in particular among different species of fish. Fish can contain up to 0.5 mg/kg lead, oysters up to 1 mg/kg. Accumulation in the aquatic food chain is limited (Merian, (1991)).

Human intake of lead through food is about 0.3 to 1.0 mg lead per week, with single cases of up to 2.5 mg/week. A weekly uptake of 3.0 to 4.0 mg is accepted as toxicologically harmless. About half of human lead intake is through food, of which more than half originates from plants. The normal food chain from soil to plant to animal to man causes a dilution, rather than an accumulation, of the metal. The dilution factor is about 1000, and in polluted industrial areas the factor is approximately 100. No acute hazard from lead in the food chain has been determined, although it should be kept in mind that lead content is higher in the liver and kidneys of animals kept near industrial emission sources. If these organs contain more than 3 mg/kg, they are considered unfit for human consumption (Fergusson, (1990)).

A.1.2. Accumulation of Nickel in the Food Chain

Food of plant origin shows normal nickel concentrations of about 0.3 mg/kg. Uptake into plants occurs mainly through the soil, but is also possible from the atmosphere. Animals show a very slow absorption, but very high excretion rate for nickel which together result in zero-accumulation in animals, with the exception of some marine organisms.

A.1.3. Lead in the Food Chain: Observations

Lead in food can result from various sources: 1) lead uptake of plants growing on high lead soils or treated with lead arsenate pesticides, 2) surface deposition of lead on plants consumed by food-producing animals or man, 3) inadvertent addition of lead

during food processing, and 4) leaching of lead from cans with lead soldered seams or from improperly glazed pottery used as food storage or dining utensils. Furthermore, home food preparation practices may be potential sources of additional lead residues in food. Lead in cooking water may also become part of the diet.

Numerous estimates and investigations exist of the lead content of individual foods. Large-scale market basket surveys have been conducted in the UK, the Federal Republic of Germany, and several other countries. Studies on wheat and potatoes show they contain on the average about 0.04 to 0.09 ppm Pb, meat contains approximately 0.01 to 0.06 ppm, and liver about 0.3 ppm (Merian, (1991)). Although there is a large variability of lead concentrations in individual foods depending on various factors including the geographic location in which the food was grown, the following generalizations can be made:

1. **Vegetables:** the lead concentrations are highest in the roots, lower in stems and leaves, and lowest in flowers or seeds. Exception are leafy vegetables that may retain surface dust or dirt that is not readily removed by washing.

2. **Fruits:** the highest lead levels are found in the peel and stem. - Foods of animal origin: muscle meat, unprocessed milk, and eggs have a relatively low lead content, whereas organ meat, particularly kidney and to a lesser extent liver, is substantially higher in lead concentrations.

3. **Alcoholic beverages:** wine may contain substantial amounts of lead with mean values between 50 and 100 μg/L and individual samples ranging up to several hundred μg/L (Merian, (1991)) depending on the bottle sealing. High lead concentrations have also been found in illegally distilled whisky (moonshine whisky). Lead contamination of the latter may occur from lead-soldered joints of the distilling apparatus.

The total daily intake of lead varies widely among populations and individuals. It is difficult to measure the dietary uptake accurately.

Within the past 15 years, attention has been directed to the lead content of com-

mercial infant foods. A number of studies suggest that infants and young children, on a body weight basis, may have a significantly higher lead intake than adults. Regarding bottle fed infants the lead content of drinking water may be of significant importance.

A.1.4. Lead in Drinking Water

Lead in drinking water may result from contamination of the water source or from the use of lead materials in the water distribution system. Lead entry into drinking water from the latter is increased in water supplies with soft water and pH values below 6.5. Human exposure may occur through direct ingestion of the water or via food preparation in such water. The lead concentrations normally found in drinking water are of the range of 2 - 25 mg/L (Merian, (1991)).

Numerous studies indicate that the major source of lead contamination of drinking water is the distribution system itself, particularly in older urban areas with old houses frequently equipped with lead water pipes. The highest lead levels are encountered in "first-draw" samples, i.e., water sitting in the piping system for an extended period of time.

A.1.5. History of Global Lead Pollution

The history of global lead pollution has been assembled from chronological records of the deposition of lead in polar snow and ice strata, marine and freshwater sediments, and the annual rings of trees. These records aid in establishing natural background levels of lead in environmental and biological media and document the sudden increase of atmospheric lead emissions at the time of the industrial revolution, with a later burst during the 1920s when lead alkyls were first added to gasoline. Pond sediment analyses have shown a 20-fold increase in lead deposition during the last 150

years, documenting not only the increasing use of lead since the beginning of the industrial revolution, but also the relative fraction of natural versus anthropogenic lead inputs. Perhaps the best chronological record is that of the polar ice strata, which extends nearly three thousand years back in time. The authors found an about 10-fold increase between 1750 and 1940 and an accelerated increase after 1940, which was attributed to the increasing lead emissions since the beginning of the industrial revolution and the increased use of lead alkyls in gasoline in the 1920s. At the South Pole, Merian, (1991) found a 4-fold increase of lead in snow from 1957 to 1977 but no increase from 1927 to 1957. The author concluded that the extensive atmospheric lead pollution, which began in the 1920s and primarily was located in the Northern hemisphere did not reach the South Pole until the mid-1950s.

The history of human lead exposure has been estimated on the basis of lead analyses of ancient teeth and bones. Overall, the available studies show a significant increase of the lead concentrations in historical and modern human bones and teeth compared with prehistorical remains of members of premetallurgical societies. It should be noted, however, that the use of results from such studies, as a basis for comparison with modern findings requires special caution if erroneous conclusions are to be avoided. Lead concentrations in human bones markedly increase with the introduction of metallurgical processes. The amount of lead in organs and bones which may be potentially active toxicologically in terms of being available to biological sites of action can be estimated by the measurement of plumburesis in response to administration of a chelating agent, specifically $CaNa_2EDTA$. The chelatable amount of lead probably consists of the mobile fraction of lead in soft tissues and the exchangeable bone fraction.

Dietary lead in humans and animals that is not absorbed passes through the gastrointestinal tract and is eliminated with the feces. The same applies to air lead that is swallowed and not absorbed. Absorbed lead is excreted primarily in urine. The mechanism of urinary excretion appears to be essentially glomular filtration. Other excretion routes are gastrointestinal secretion, and nails and sweat. The rate of biliary excretion in humans is not known. Lead is also excreted in human milk in concentrations up to 10 μg/L (Merian, (1991)).

A.2. Effects of Lead on Plants, Animals, and Humans

A.2.1. Effects on Microorganisms and Plants

With respect to the effects of lead on the terrestrial microbiota it appears that microorganisms are more sensitive to soil lead pollution than plants. Changes in the composition of bacterial populations may be an early indication of lead effects. These changes, with the more resistant organisms dominating, may be very drastic at certain locations. Delayed composition may occur at 750 μg Pb/g soil and vitrification. inhibition at 1000 μg/g (Fergusson, (1990)). Usually, the effects are smaller in clay and peat soils compared to sandy soils.

Since most of the physiologically active tissues of plants are involved in growth, maintenance, and photosynthesis, it can be expected that lead might interfere with one or more of these processes. Such interferences have been observed in laboratory experiments at lead concentrations greater than those normally found in the field, except near smelters or mines. Studies of lead effects on other plant processes, especially maintenance, flowering, and hormone development, have not been conducted, and no conclusions can be drawn concerning these processes.

Lead in soil is strongly immobilized by the humic fraction. The uptake of lead via the root system depends on the amount of available lead in soil moisture. The literature of experimental studies reviewed by the U.S. EPA in 1986, supports the conclusion that inhibition of plant growth begins at lead concentrations of less than 1 mg/kg soil moisture and becomes completely inhibitory at levels between 3 and 10 mg/kg. Plant populations that are genetically adapted to high-lead soils may achieve 50 % of their normal root growth at lead concentrations above 3 mg/kg. Plants that absorb nutrients from deeper soil layers may receive less lead. A few species of plants have the genetic capability to adapt to high lead soils. Plant communities near smelter sites, therefore, may experience a shift toward lead-tolerant plant populations.

A.2.2. Miscellaneous Biochemical Effects

Lead has many diverse physiological and biochemical effects, which generally are of a deleterious nature. No evidence has been presented for an essential function of lead in the metabolism of humans and animals. A review of the subcellular effects of lead have been presented by the US EPA (1986). The effects of lead on energy metabolism and the neurochemical and neurophysiological correlations of lead toxicity have been documented by Merian, (1991). Lead interferes with several enzymes that participate in the heme synthesis pathway. The most important effects are (1) stimulation of the mitochondrial enzyme b-aminolevulinic acid synthetase (ALA-S), which mediates the formation of oiaminolevulinic acid; (2) direct inhibition of the cytosolic enzyme o;-aminolevulinic acid dehydratase (ALA-D), which catalyzes the formation of porphobilinogen from two molecules of d-aminolevulinic acid (ALA), and (3) inhibition of ferrochelatase (heme synthetase), which mediates the insertion of iron(III) into

protoporphyrin IX to form heme.

The PbB threshold value, at which loch of persons exhibit decreased ALA-D activity is about 10 μg/100 mL (Merian, (1991)). As far as is known, ALA-D activity is without functional importance in the mature erythrocyte, in which heme synthesis no longer occurs. For this reason, inhibition of ALA-D activity is considered a subcritical effect of no direct biological importance. Inhibition of ALA-D activity by lead is reflected by elevated levels of its substrate, ALA, in blood, urine, and soft tissues. Urinary ALA (ALA-U) is frequently employed as an indicator of excessive lead exposure in lead exposed workers. The diagnostic value of this measurement in pediatric screening is limited, however, when only spot urine samples are collected. More satisfactory results can be obtained with 24 h urine samples. Numerous studies indicate that there is a direct correlation between PbB and log ALA-U in human adults and children. The PbB threshold for increases of ALA-U is about 40 μg/100 mL (Merian, (1991)).

Inhibition of ferrochelatase by lead results in an accumulation of protoporphyrin IX in erythrocytes. In lead exposure, the porphyrin acquires a zinc ion in lieu of iron, thus forming zinc protoporphyrin (ZPP). Elevation of free erythrocyte protoporphyrin (FEP) or erythrocyte ZPP is closely correlated with PbB and is generally accepted as a true critical effect of undue lead exposure. In adults, the PbB threshold for ZPP elevation is about 20-30 μg/100 mL, females being more sensitive than males. In children the threshold is below 20 μg/100 mL. According to one study, the no-response level seems to be below 10 μg/100 mL (Merian, (1991)).

Anemia is a well-known manifestation of clinical lead poisoning. Although there are conflicting results in the literature it appears that there is a negative correlation

between hemoglobin (Hb) and blood lead at higher PbB concentrations. The effects of lead on Hb production involve disturbances of both heme and globin synthesis. Iron deficiency as a potential confounding factor, the non-specificity of the Hb parameter as well as the great inter-individual variation in its sensitivity may give rise to many difficulties in finding a significant relationship between PbHb and PbB. The PbHb threshold for reduced hemoglobin content appears to be about 50 μg/100 ml in adults and 40 μg/100 mg in children. The hemolytic component of lead-induced anemia appears to be attributed to a decreased erythrocyte survival time resulting from increased cell fragility and increased osmotic resistance.

A.2.3. Effects on Domestic Animals and Wildlife

Although the incidence of lead poisoning among animals is difficult to evaluate accurately, it has been suggested that lead is one of the most frequent single sources of accidental poisoning in domestic animals. The most important sources of lead are lead containing dust fall-out on pastures near lead smelters or lead mines, lead-based paint and improperly disposed wastes such as oil wastes and storage battery casings. Fall-out from automotive exhausts has been shown to increase the lead intake, but has not yet been demonstrated to account for reported cases of lead poisoning. Various groups of wild living animals, e.g., rats, rabbits, and birds, have been studied as indicators of environmental lead pollution.

Hazards for lead poisoning may exist for grazing cattle near lead smelters or lead mines, where lead fall-out or soil lead is extremely high. Numerous fatal intoxications have been reported from such areas. The acute signs characteristic for lead poisoning include central nervous system disorders, excitement, stupor or depression, motor

abnormalities, and blindness. Some animals may die without showing any of these signs. Clinical signs frequently found in lead-poisoned horses include difficulty in breathing, which leads to a characteristic roaring sound, stiffness, clumsiness, enlarged joints, facial paralysis, muscular weakness, and poor appetite. Lead intoxications in dogs have been reported from areas where lead paint is common in dwelling houses and seem to result from ingestion of peeling or flaking lead paint. It is also known that pellet wedges in wild birds (ducks and other water fowl) paralyze muscles, and the birds may die of starvation. Merian, (1991) demonstrated, for instance, that lead impairs selective behavioral functions of feeding (e.g., manipulation of fish) in young fowl.

A.2.4. Effects of Inorganic Lead on Experimental Animals and Humans

A.2.4.1. Clinical Diagnosis and Sequelae of Lead Intoxications in Humans

The clinical diagnosis of lead poisoning is not always easy. It is made partly on the basis of subjective and objective symptoms, a variety of signs, biochemical analyses indicating an accumulation or increased excretion of metabolic products, and evidence of lead exposure. Individuals may be asymptomatic or symptomatic, presenting a wide variety of symptoms and being in different states of the disease. Usually, the onset of lead poisoning, even in cases of acute intoxications, is not a sharply defined event but rather a continuum of changes from normality to illness.

In adults, the most important symptoms of severe lead poisoning are (in descending order of frequency): abdominal pain (colic), constipation, vomiting, non-abdominal pain, asthenia, psychological symptoms, and diarrhea. Mild symptoms and signs include: tiredness, lassitude, constipation, slight abdominal discomfort or pain, anorexia, sleep

disturbances, irritability, anemia, paleness, and less frequently diarrhea and nausea (Merian, (1991)). The signs and symptoms in children are somewhat different than in adults. For example, peripheral neuropathy is more common in adults, while encephalopathy is much more common in children. The most important symptoms of pediatric lead poisoning (in descending order of frequency) are: drowsiness, irritability, vomiting, gastrointestinal symptoms, ataxia, stupor, and fatigue. Further signs may include behavioral changes, speech disturbances, fever and dehydration

A.2.4.2 Effects of Lead on the Peripheral Nervous System

It is a well known fact that peripheral paresis occurs in severe lead poisoning, but such cases are extremely rare today. In recent times, attention has been directed mainly to electrophysiologically detectable functional abnormalities that occur in the peripheral nerves in the absence of clinical neurological signs. The most important neurophysiological abnormalities recorded consist of slowing of the nervous motor conduction velocity, especially that of the slower fibers, and electromyographic abnormalities, such as fibrillations and a diminished number of motor units in maximal contraction. Dose-effect relationships for some conduction velocities (maximum conduction velocity of the median and ulnar nerves, sensory conduction velocity and conduction velocity of the slower motor fibers), especially of the arm nerves, have been reported to occur in the PbB range of 30-70 μg/100 mL. PbB levels in excess of 50 μg/100 mL are associated with an increasing frequency of abnormal conduction velocities among occupationally exposed workers (Merian, (1991)).

A.2.4.3. Effects of Lead on the Central Nervous System (CNS)

Numerous cases have been documented in which heavy lead exposure caused encephalopathy in children and adults. The major symptoms were dullness, restlessness, irritability, headache, muscular tremor, hallucinations, and loss of memory and ability to concentrate. The signs and symptoms may progress to delirium, mania, convulsions, paralysis, and coma. Severe and potentially fatal encephalopathic conditions have been reported to occur markedly more often in children than in adults. Prior to the introduction of chelation therapy as a standard medical practice the mortality rate for lead encephalopathy cases among children was approximately 65%. Following the introduction of chelation therapy the mortality could be reduced substantially (Merian, (1991)). Children who survive lead encephalopathy may be left with permanent neurological sequelae such as recurrent seizures and mental retardation. It should be noted that there is an enormous variation in individual susceptibility. Some children suffer from irreversible brain damage or even death at PbB levels of about 100 μg/L, whereas others appear to show no effects at levels double this.

In the past 20 years, studies have been undertaken to determine whether lower intensities of exposure that do not give rise to overt signs of lead toxicity, can still cause impairments of CNS functions. To study such effects different psychological performance tests and symptom questionnaires have been applied. Several studies consistently show some impairment in the performance of different psychological functions and an excess of subjective central nervous symptoms among workers with comparatively low lead exposures (PbB levels between 60 and 80 μg/100 mL). Tests

measuring visual motor functions and visual intelligence seem to be the most sensitive indicators of such effects. Impairments of a wider area of psychological functions appear to be detectable when the exposure range is somewhat higher.

Children as a risk group for CNS effects have received particular attention in studies dealing with lead-induced neuropsychological deficits at PbB levels between 10 and 50 μg/100 mL. More recent studies, however, give rise to extend the range of concern down to lower PbB levels. In a critical review of these studies by Merian, (1991). came to the following conclusions:

1. The effect of lead on intelligence and cognitive functioning, if it exists at all within the range of lead burdens currently experienced by the general population of children, is small. Most studies point to differences of up to 5 to 6 IQ points with data suggesting that lead accounts for no more than 2 or 3910 of the variance in cognitive performance. This is much less than is accounted for by genetic and many other environmental factors. However, small is a relative term, and a population shift of 5 IQ points up or down is not negligible.

2. Recent epidemiological studies conducted in Britain, West Germany, and in the USA consistently suggest that lead is causally related to deficits in cognitive functioning.

3. There is no convincing consistent evidence for an association between moderate levels of lead exposure and behavioral patterns in general.

4. The question of a possible threshold PbB level is still open and may be difficult to answer, possibly because the notion of a clear cut-off point is questionable.

For detailed information on the results of the most recent studies the reader is referred to the proceedings of a workshop on lead exposure and child development which was held at the University of Edinburgh in September 1986. Motor activity and learning of tasks of various difficulty and complexity are behavioral dimensions that have

received particular attention. These studies show that lead can be considered causative for certain neurobehavioral deficits at moderate or even low exposure levels, which are not associated with overt signs of toxicity. Some of these neurobehavioral deficits resemble cognitive deficits in man.

Generally, learning of visual discrimination has proved to be most sensitive to the effects of lead. In contrast, increased motor activity (hyperactivity) appears to be only secondarily related to lead exposure, and primarily to lead-induced undernutrition during early stages of brain development. Many of these effects seem to be irreversible, particularly if lead exposure occurs maternally and/or in early life.

A.3. Accumulation of Heavy Metals in the Food Chain

A.3.1. Cadmium

Cadmium is a relatively mobile heavy metal that enters the food chain beginning with soil. The concentrations of this heavy metal have been shown to be dependent on soil type. These levels can be increased considerably through the application of phosphate fertilizers as well as sewage sludge or compost on cultivated fields. Uptake of cadmium by plant roots differs depending on the pH of the soil. Due to a short vegetation period, however, only small-scale accumulation is observed in plants. Cadmium-containing dust can also increase the concentration of cadmium in plants since resorption via the leaves is possible in some cases. Thus, the cadmium contents of vegetable feeds vary from 0.005 to 0.1 mg/kg, and in certain cases up to 1.0 mg/kg. These levels may increase to 50 mg/kg in cases of atmospheric cadmium contamination by industry. Levels of up to 10 mg/kg have been observed after application of cadmium-containing phosphate fertilizers.

In rice, concentrations of up to 1.0 mg/kg cadmium have been found, originating from the water used for cultivation (Evans, 1989).

Due to facilitated resorption, leafy vegetables, with their large surface areas, and root crops such as potatoes, carrots, and radishes, contain higher cadmium levels than foods from other parts of the plant. Fruits such as grapes barely take up cadmium. Some species of edible mushrooms concentrate the metal to a considerable extent in their mycelia and surficial parts resulting in cadmium concentrations of about 0.4 mg/kg.

As a result of contaminated animal feed, cadmium is ubiquitous in animal product foodstuffs. Since the rate of oral uptake exceeds excretion, accumulation results in some animal tissues. Apparently, the constant presence of cadmium in foodstuffs is sufficient to cause a slowly increasing concentration in the kidneys. Slaughtered animals more than 10 years old showed concentrations of up to 40 mg/kg, whereas young animals had only trace amounts of about 0.5 mg/kg. Besides the kidneys (especially the renal cortex), the other target organ is the liver, with levels of 0.08 mg/kg in young animals and from 0.3 to 1.0 rng/kg in older ones. Values of only 0.001 to 0.002 mg/kg have been measured in meat (corresponding to those amounts found in plants), less in milk, but more in fish, especially oysters. As with lead, cadmium concentrations are higher in wild boars than in domestic pigs (Merian, (1991)).

An accumulation of cadmium in the meat and milk of domestic animals is unlikely. A critical concentration in the kidneys should not occur before the age of three years if the animal's feed contains less than 0.5 mg cadmium per kg dry matter. On the basis of this level in feed, however, the kidneys of animals older than three years may contain I mg/kg and more. Cadmium concentrations in swine kidney may reach the same

values as in feed, in liver about half that. The same applies to sheep, for which a concentration of 6 mg/kg in feed can lead to 10 mg/kg in the renal cortex. Accumulation can be avoided if the feed concentration does not exceed 0.6 mg/kg, and drinking water should not contain more than 0.05 mg/liter (Merian, (1991)). Kidneys used for human consumption should not contain more than 1 mg/kg cadmium.

In living tissue, cadmium is bound to certain digestible protein fragments. In organic forms, cadmium is biologically disposable. Among marine organisms, concentrations ranging from 0.02 mg/kg in fish from unpolluted waters to 2.0 mg/kg in oysters and 12 mg/kg in crabs have been found. Levels of 10 to 100 mg/kg have been reported in squid. Cadmium apparently accumulates in marine organisms, but information is still controversial (Merian, (1991)). Fresh water fish and shellfish from the Elbe estuary in Germany show cadmium levels of about 0.03 mg/kg due to their contaminated environment. Liver of fish from polluted water may contain 10 to 50 mg cadmium/kg, whereas normal fish liver contains about 1 mg/kg.

In humans, about one-third of the total cadmium burden originates from animal products and two-thirds from plant products. Taken together, cadmium intake from these sources approaches the toxicological limit of 0.525 mg per week as established by the World Health Organization. Actual weekly uptake should be about 0.10 to 0.25 mg cadmium, in extreme cases 0.50 mg. These amounts do not result from meat, dairy products, kidneys or plants which are produced far away from industrially contaminated areas, but may be found in leafy vegetables, root crops, kidney and liver, and uncultivated mushrooms.

A.3.2. Chromium

Chromium is an essential trace element that does not accumulate in organisms. Concentrations of 0.05 to 0.2 mg/kg have been measured in meat, and these levels do not increase in liver (0.4 mg/kg) or kidney (0.2 mg/kg). Merian, (1991) found only about 0.1 mg/kg in bovine liver. The chromium content of animal drinking water should not exceed 1.0 mg/L.

A.3.3. Copper

Copper is an essential element and it accumulates in the liver resulting in concentrations of 20 to 100 mg/kg (the mean is about 50 mg/kg). Merian, (1991) found as much as 190 mg/kg copper in bovine liver. Kidneys normally contain about 3 mg/kg copper, and meat from 0.3 to 5.0 mg/kg. Oysters, which are supposedly storage animals for copper, can contain up to 137 mg/kg. Aquatic organisms accumulate copper far more easily than mercury, lead, or cadmium. Foodstuffs normally contain 2 to 4 mg Cu/kg. Levels in animal feed should not exceed 10 mg/kg. In animal drinking water, levels should be no higher than 0.5 mg/L (Merian, (1991)).

A.3.4. Zinc

Zinc is an essential metal that is typically absorbed by plants through the soil or from industrial dusts. Zinc can be phytotoxic. Normal values in plants are between 1 and 40 mg/kg of dry matter. Cereals sometimes show concentrations of over 100 mg/kg. Farm animals continuously receive zinc with their feed, and the excess is immediately excreted. An accumulation in animal tissues does not occur. Normal levels in meat, fish, and poultry are within 10 and 200 mg/kg with a mean of 25 mg/kg. Milk products show levels of about 5 mg/kg, liver 100 to 150 mg/kg, and kidney 50 to 100 mg/kg. Since zinc

does not accumulate, it is of no health significance as an industrial pollutant in foodstuffs. Zinc contents of 200 to 500 mg/kg in animal feed, and 25 mg/L in drinking water are of no significance. Concentrations of up to 1500 mg zinc/kg have been found in oysters from estuarine areas (Merian, (1991)).

A.4. Metals as Essential Trace Elements for Plants, Animals, and Humans

Due to their potential for accumulation and toxicity in plants, animals and humans, heavy metals have become a primary health concern. Protection of the environment from toxic heavy metals, such as cadmium, lead, and nickel occupies a predominant position. As a consequence of the modern technological processes coupled with human negligence related to sustainable development, they have spread throughout the biosphere to an unprecedented degree. Table A-1 displays the trace elements and their necessity in the sustenance of biological and chemical processes.

Up to now, modern research has shown that at least 24 elements are essential to life. Reference to the Periodic Table indicates that they form three coherent blocks which almost touch each other. The *non-metals* hydrogen, carbon, nitrogen, oxygen, fluorine, silicon, phosphorus, and sulfur are the main building blocks of all organic compounds such as proteins, carbohydrates, fats, nucleic acids, and vitamins. The *metals,* on the other hand, are mainly responsible for the correct functioning of innumerable enzymatic and metabolic reactions. Sodium, magnesium, potassium, calcium, phosphorus, and chlorine are often called minerals or electrolytes, whereas vanadium, chromium, manganese, iron, cobalt, nickel, copper, zinc, selenium, molybdenum, tin, and iodine are called trace elements (citations are in the order of increasing atomic number).

In natural foodstuffs, the trace elements are present in very different

concentrations and various chemical forms, the characterization of which is a domain only at its beginnings. Sparse data only for a few elements exist in this latter respect. The bioavailability of an element is in fact strongly influenced by its chemical form. Apart from this the intestinal mucosa contains unspecific and specific transport mechanisms for the different metals. Some metals may share the same carrier. These interdependencies demonstrate the importance of equilibrium in the overall trace element content of a healthy food supply. There is still an unresolved problem in making available the complete set of essential trace elements in optimal amounts at a more or less continuous rate for all people. One of the recurring problems is the widespread use of refined foodstuffs, such as white sugar, corn syrups of all kinds, isomerized corn syrup (HFCS), pure glucose, fructose, and sugar, alcohols, refined (white) flours and refined fats and oils. For instance, iron absorption changes in many ways, baked rolls may decrease it, meat, and/or vitamin C may increase it. The interaction of ascorbic acid with the daily intake of "absorbable" iron is even quantifiable. Fasting, fiber content of the diet, and fruit juices (compared to aqueous solutions) have also an influence on the uptake of iron and of other trace elements. Cardiovascular integrity of male rats is especially impaired in case of copper deficiency, when sucrose or fructose (instead of starch) is administered. In specific concentrations, metals are essential to all life forms. Approximately 98 % of the body mass of humans are made up of 9 non-metallic elements. Another 1.89 % are formed by the 4 main electrolytes, sodium, magnesium, potassium, and calcium. The 11 typical trace elements occupy just a tiny 0.012910 or 8.6 grams of the body weight. This small fraction exerts a tremendous influence on all body functions, both adverse and advantageous. Due to extensive environmental contamination, it is necessary to study

their effects and essentiality.

Whether an element is essential for life or not depends on its participation in one or several biochemical reactions. According to the recommendations of a WHO expert committee, this expression is not optimal when it is applied to trace elements because of the mentioned difficulties in establishing an absolute essentiality. According to a new, improved definition an element is already useful to the organism and to the maintenance of health when a measurable deficit in the diet reduces the growth and vitality of humans, animals, or plants to a reproducible degree. If we start from this definition it becomes plausible that even well-known toxic elements, such as arsenic, silver, cadmium, and lead, and possibly aluminum, are needed in minute quantities for the normal functioning of cell metabolism, although they are recognized as toxic in higher concentrations. The most important biological functions of the known trace elements, taken from many different literature sources, are listed in Table A-1. The recommended daily intake of minerals and trace elements is shown in Table A-2.

In most cases, the ions of trace elements act as coordination centers for building up or stabilizing the structure of enzymes and proteins. Exceptions are iron, which is the central atom of heme in cytochromes and hemoglobin, cobalt in the center of vitamin B, and iodine, which is a constituent of the hormone thyroxine. Chromium seems to be essential for the biosynthesis of the glucose tolerance factor in man which itself seems to be chromium-free.

About 50 zinc enzymes, and as many reactions, are known. Regarding copper deficiency, it has also been observed that there may be correlations with mitochondrial changes and with a reduction of pancreatic weight and protein concentration. Food and

drinking water must contain all the essential mineral elements in adequate quantities, otherwise the continuous losses with urine, feces, and sweat would produce severe deficiency syndromes within a relatively short period of time. In some countries the desirable ranges of intakes for each element are established and published in regular intervals by semi-official national nutrition boards.

The absorption rates differ remarkably between the elements. Table A-3 shows these rates for seven trace elements. The called "Recommended Dietary Allowances". The best-known tables of this kind are those published in the USA. Table A-3 indicates the values for the electrolytes and trace elements for adults. These values consider the fact that only a certain percentage of the metal ions present in the food can be absorbed in the intestine. Table A-4 shows the interactions between trace element adsorption.

Nutrients are taken up from water and soil by plants. The minimal quantity of most trace elements that accumulate is a consequence of their genetically determined cell structure and function that can vary somewhat between the species. However, trace metals that are accidentally present in the soil for geological reasons or by human deposition as, for example, with lead from gasoline along the highways, can accumulate in grass and food crops. This can have serious ramifications on the agricultural sectors and eventually the food chain.

Table A-1 Main Functions of Trace Elements and Consequences of Their Absence (Merian, (1991))

Element	*Constituent of*	*Causes of Total Absence*
Chromium	• Needed for the biosynthesis of the glucose tolerance factor	• Diabetes Type II
Copper	• Cytochrome Oxidase	• Blocking of all respiration
	• Ceruloplasmin = laccase	• Lack of copper transport
	• Ascorbic Acid oxidase	• Disturbed Redox reactions
	• Lysine oxidase	• Stop of Cartilage formation
	• Tyrosinase	• Albinism
	• Superoxidase Dismutase, SOD	• Cell destruction by superoxide radicals
	• Monoamine Oxidase	• Lack of neurotransmitter synthesis
Iron	• Cytochromes	• Blocking of oxidative reactions, blocking of cell respiration and energy production
	• Catalase, peroxidases	• Multiple lipid peroxidation
	• Hemoglobin	• Anemia, no oxygen transport
Nickel	• Urease, glucose	• Nitrogen fixation in soil inhibited
	• Alkaline Phosphatase	• Energy metabolism compromised
	• Alcohol dehydrogenase	• Alcohol intoxication
	• Carboanhydrase	• Acidosis
	• Carboxypeptidase	• Protein biosynthesis blocked, infertility
	• Lactate dehydrogenase	• Lactate accumulation, acidosis in muscles
	• Superoxide dismutase	• Cell destruction by superoxide radicals

Table A-2 Recommended Daily Intakes of Mineral Elements (Merian, (1991))

Element	*Recommended Daily Intake (mg)*
Potassium	1850-5500
Sodium	1100-3300
Calcium	800-1200
Phosphorous	800-1200
Magesium	350-400
Iron	10 (men) 18 (women)
Zinc	15
Manganese	2.5-5.0
Copper	2.0-3.0
Molybdenum	0.15-0.50
Chromium	0.05-0.20
Selenium	0.05-0.20
Iodine	0.15

Table A-3 Adsorption Rates of Minerals and Trace Elements (Merian, (1991))

Element	*Adsorption Rate (%) (Ingestion)*
Sodium	90-95
Chlorine	95-100
Potassium	90-95
Molybdenum	70-80
Selenium	50-80
Phosphate	60-70
Calcium	25-40
Zinc	20-40
Magnesium	30-35
Copper	10-30
Iron	7-15
Magnesium	3-5
Chromium (III)	0.5-1.0

Table A-4 Interactions in Trace Element Absorption (Merian, (1991))

Element in Excess	***Produces a Deficit in...***
Cadmium	Selenium, Zinc
Calcium	Zinc
Iron	Copper, Zinc
Manganese	Magnesium
Molybedenum	Copper
Zinc	Copper, Iron

APPENDIX B:

Photographs Comprising All Experiments

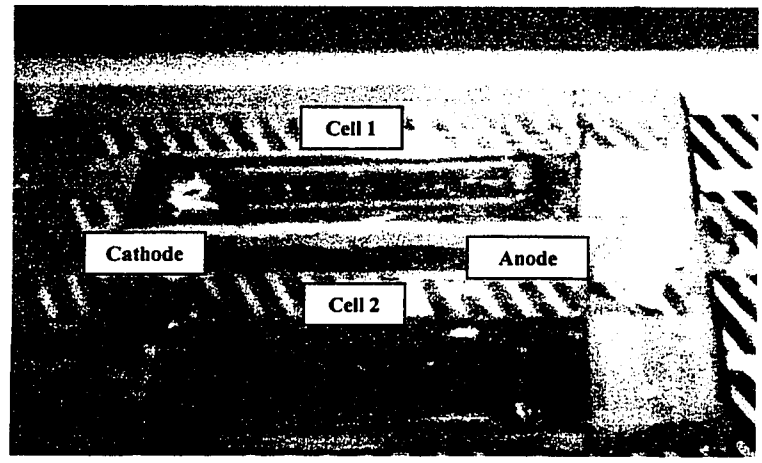

Figure B-1 F5C1 and F5C2 during experimentation (Experiment F5)

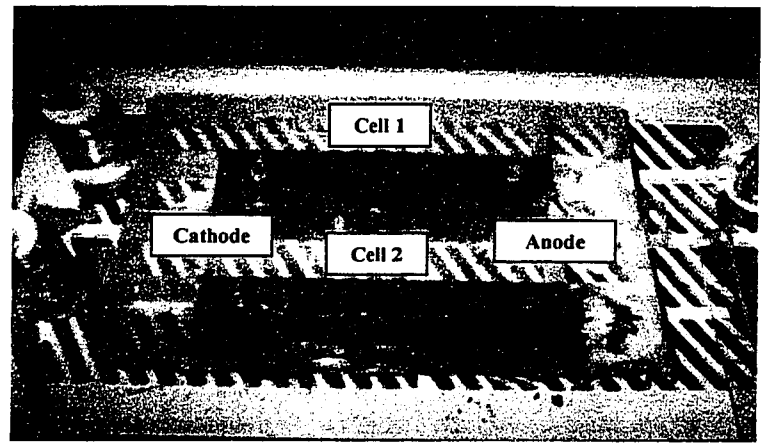

Figure B-2 F5C1 and F5C2 after experimentation (Experiment F5)

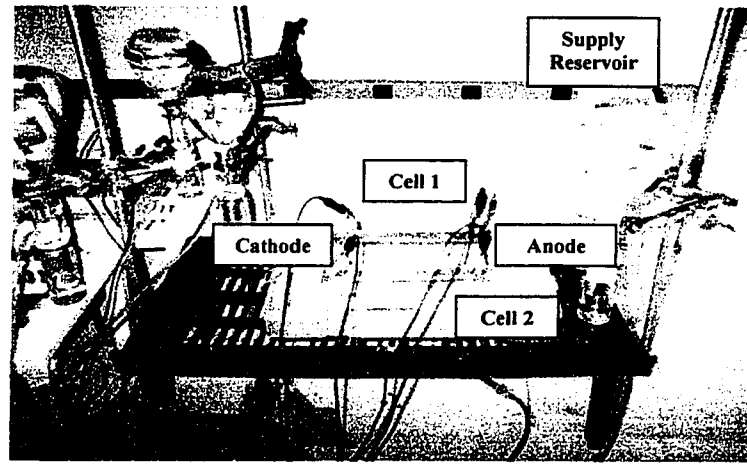

Figure B-3 F6C1 and F6C2 during experimentation (Experiment F6)

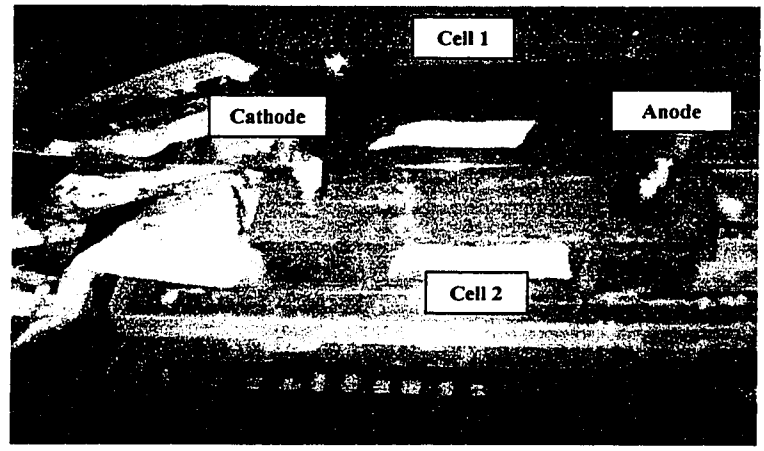

Figure B-4 F6C1 and F6C2 after experimentation (Experiment F6)

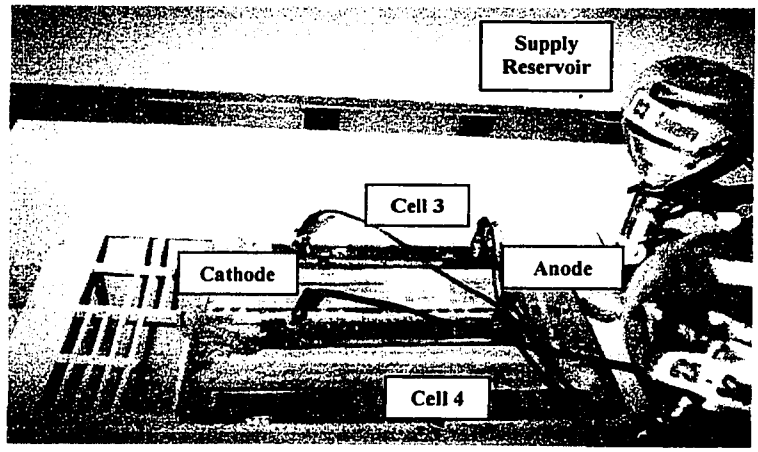

Figure B-5 F6C3 and F6C4 during experimentation (Experiment F6)

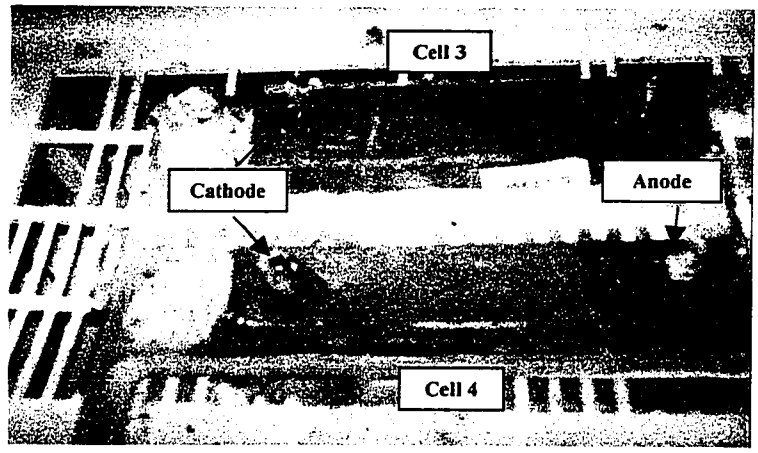

Figure B-6 F6C3 and F6C4 after experimentation (Experiment F6)

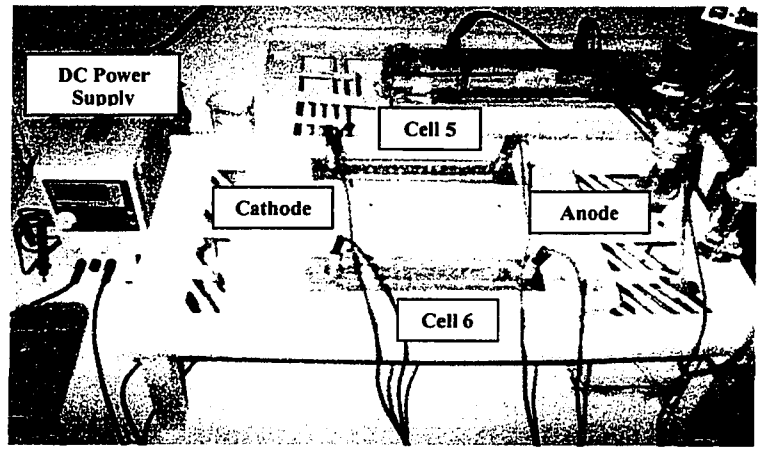

Figure B-7 F6C5 and F6C6 during experimentation (Experiment F6)

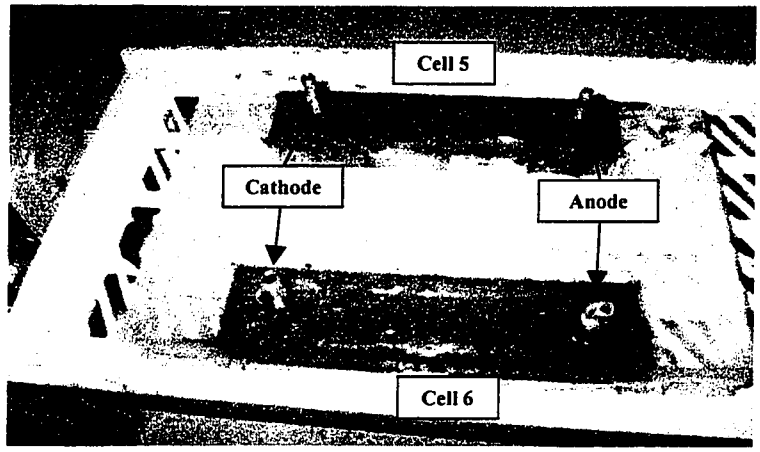

Figure B-8 F6C5 and F6C6 after termination (Experiment F6)

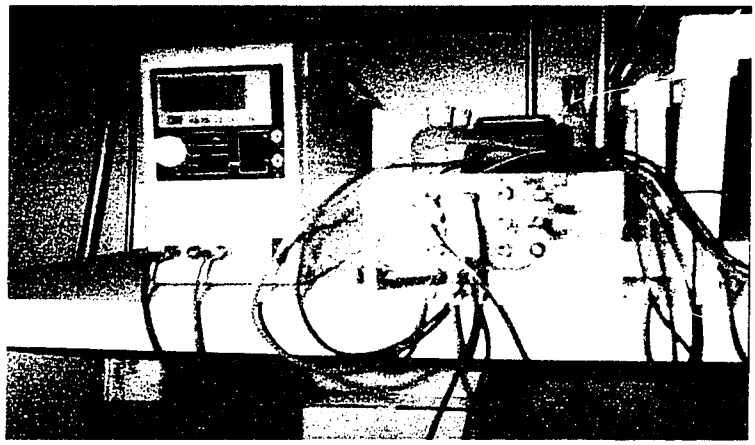

Figure B-9 DC power supply and cell connection used in all experiments

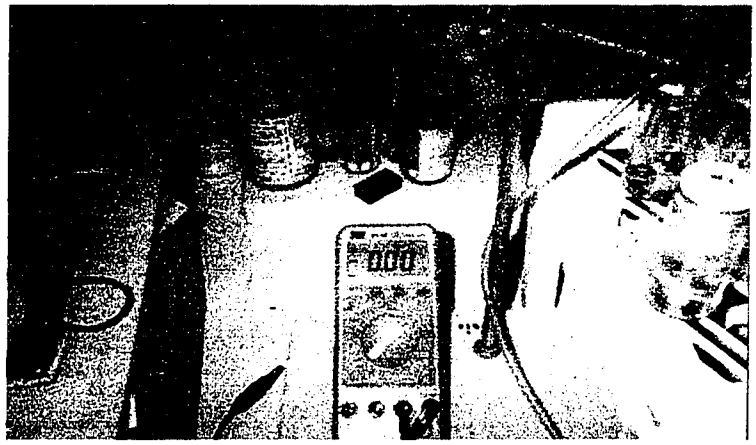

Figure B-10 TES multimeter for current and potential measurements

APPENDIX C:

EDTA-EK-IET Experiment (F6): Summary of Cells

Table C-1 Experiment F6: Cell Summary

Cell Designation	*Anion Exchange Textile (AET)?*	*Cation Exchange Textile (CET)?*	*Liquid Mixed with Cell*	*Soil*	*Notes*
Cell 1 (F6C1)	Y 3.0 cm from edge of anode		Water	Non-contaminated	To test behaviour of AET in soil Blank/Control for AET
Cell 2 (F6C2)		Y 3.0 cm from edge of cathode	Water	Non-contaminated	To test behaviour of CET in soil Blank/control for CET
Cell 3 (F6C3)		Y 3.0 cm from edge of cathode	0.1 M EDTA	Contaminated	To test CET in contaminant removal Applicability of CET and EDTA in soil for localization and removal of Pb and Ni
Cell 4 (F6C4)	Y 3.0 cm from edge of anode		0.1 M EDTA	Contaminated	AET behaviour with EDTA in the removal of Pb and Ni Testing of hybrid technique (EK, Anion exchange and complexation)
Cell 5 (F6C5)			0.1 M EDTA	Contaminated	Blank/control for EDTA
Cell 6 (F6C6)	Y 3.0 cm from edge of anode	Y 3.0 cm from edge of cathode	0.1 M EDTA	Contaminated	Behaviour of both textiles and condoning liquid in removal of Pb and Ni

APPENDIX D:

Miscellaneous Data from Experiment F5 and Experiment F6

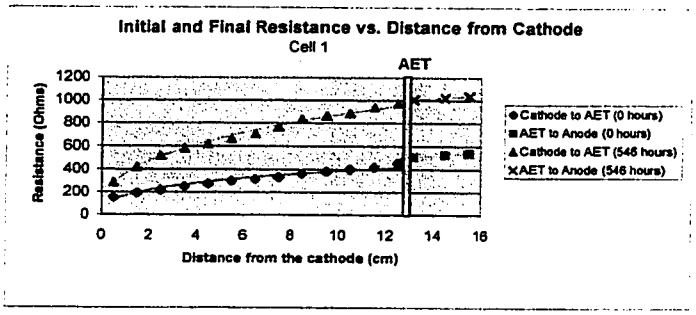

$$r(x) = \begin{cases} 171x^{0.36} & 0 < x \le 12.8 \quad R^2 = 0.9511 \\ 177x^{0.41} & 12.8 < x < 16.0 \quad R^2 = 0.9923 \end{cases} \quad t=0\ h$$

$$r(x) = \begin{cases} 360x^{0.38} & 0 < x \le 12.8 \quad R^2 = 0.9951 \\ 645x^{0.17} & 12.8 < x < 16.0 \quad R^2 = 0.9985 \end{cases} \quad t=546\ h$$

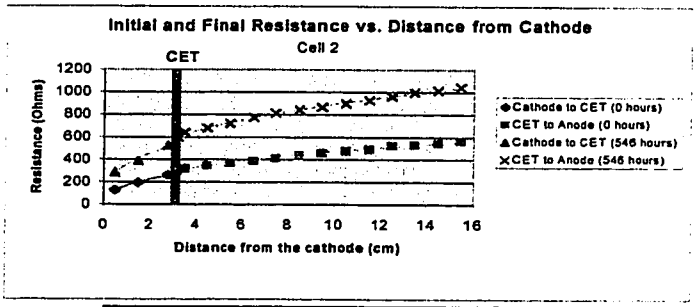

$$r(x) = \begin{cases} 170x^{0.40} & 0 < x \le 3.0 \quad R^2 = 0.9959 \\ 190x^{0.39} & 3.0 < x < 16.0 \quad R^2 = 0.9937 \end{cases} \quad t=0\ h$$

$$r(x) = \begin{cases} 356x^{0.34} & 0 < x \le 12.8 \quad R^2 = 0.9735 \\ 407x^{0.34} & 12.8 < x < 16 \quad R^2 = 0.9971 \end{cases} \quad t=546\ h$$

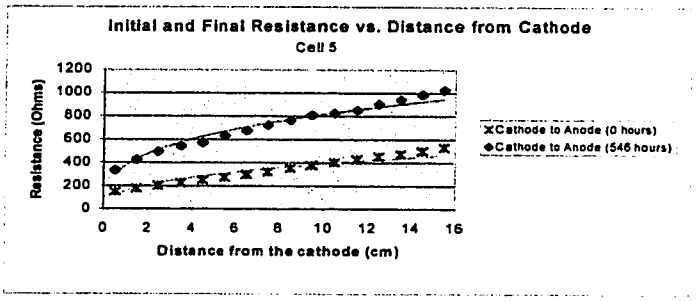

$r(x) = 158x^{0.39}$ $0 < x < 16.0$ $R^2 = 0.9212$ $t=0\ h$

$r(x) = 376x^{0.34}$ $0 < x \le 16.0$ $R^2 = 0.9950$ $t=546\ h$

r = resistance (Ohms)
x = distance from cathode (cm)

Figure D-1 Comparison of resistance distributions with and without the use of IET: Exp. F6

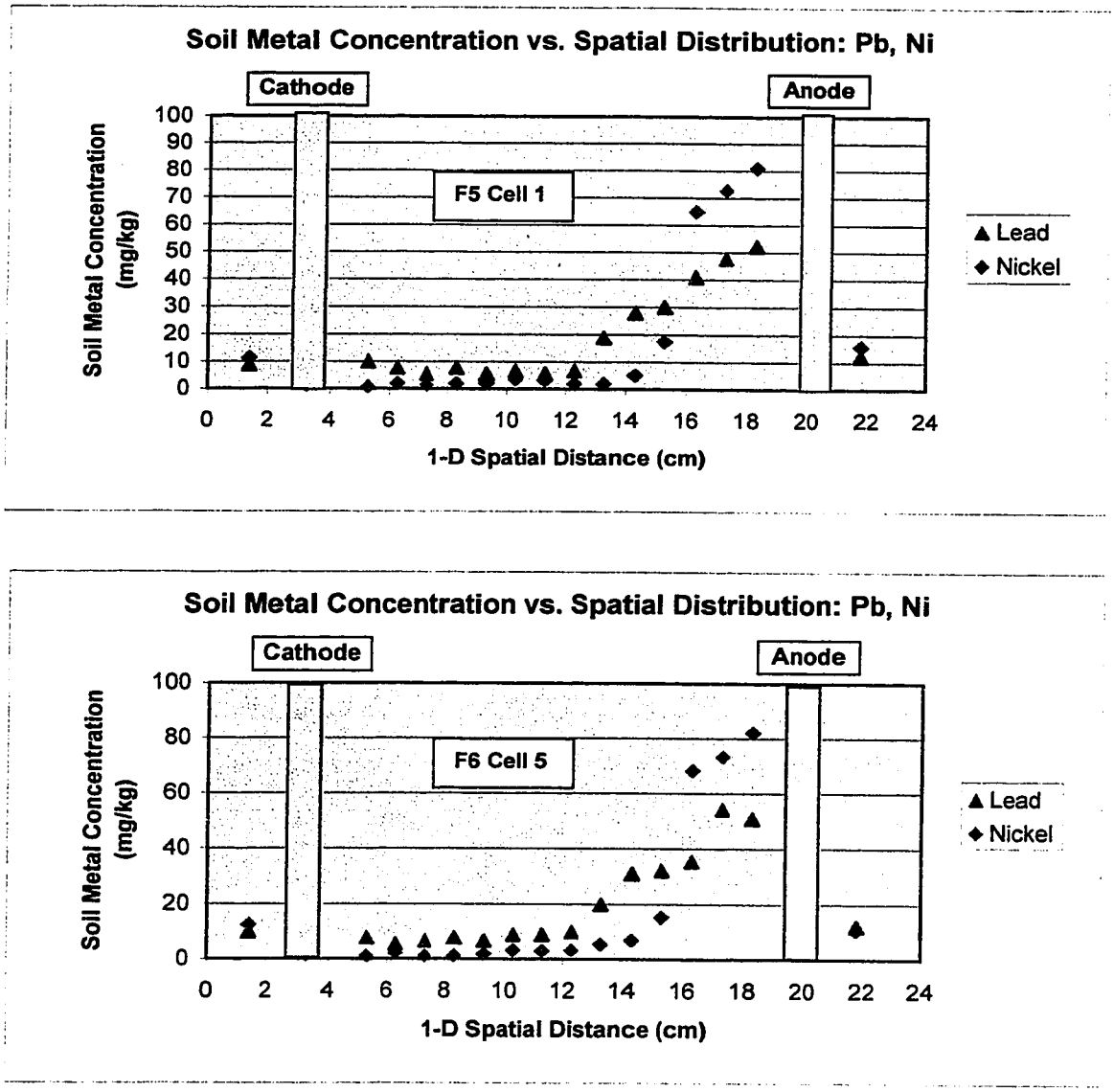

Figure D-2 Comparison of lead and nickel soil distribution between experiment F5 and F6

Initial Ni Concentration: 31 mg/kg
Initial Pb Concentration: 9.3 mg/kg

Table D-1 Resistance Values (Ohms) at Locations Adjacent to IETs

[illegible]	[illegible]		[illegible]		[illegible]		[illegible]		[illegible]	
	C	A	C	A	C	A	C	A	C	A
0	484	505	261	299	229	267	481	504	208	256	495	533
17	486	525	272	317	223	272	498	527	220	271	502	542
24	539	545	218	278	225	269	535	551	282	306	517	541
41	477	565	266	305	260	296	559	566	297	322	522	547
65	579	587	274	312	274	317	566	579	242	302	536	559
89	585	601	274	319	289	314	565	577	251	297	550	572
113	643	656	318	370	318	344	671	680	283	338	628	653
137	679	693	333	390	317	349	670	682	290	348	645	665
161	688	695	336	393	290	336	677	694	290	349	651	673
185	701	710	351	405	299	337	696	710	307	364	681	701
209	713	723	358	407	302	348	706	722	313	373	690	710
233	723	732	367	415	309	358	721	741	326	374	703	721
257	735	743	379	424	317	365	737	756	331	382	716	733
281	746	755	383	433	325	370	758	775	340	390	733	752
305	765	775	392	452	336	375	777	796	351	398	757	782
329	769	777	401	460	348	385	787	804	356	401	766	792
353	790	798	401	469	358	401	805	823	368	416	793	813
377	802	809	410	480	365	414	815	839	380	431	811	833
401	817	830	422	491	375	423	828	848	388	437	824	844
425	847	856	438	511	398	436	846	867	409	453	848	866
449	864	874	458	534	420	464	878	900	421	460	862	883
473	903	915	475	553	447	489	914	937	439	484	897	921
497	929	941	484	564	456	499	929	954	455	497	921	946
521	974	987	504	590	484	531	972	998	479	717	965	991
546	993	1007	523	598	504	549	996	1022	493	536	996	1020

C = cathode side of IET
A = anode side of IET